UNIVERSIDADE FEDERAL DE MINAS GERAIS
Instituto de Ciências Biológicas
Programa de Pós-Graduação em Neurociências

MOSTAFA ABDELLATIF ABDELSALAM ABDELRHEEM

# AVALIAÇÃO DO PEPTÍDEO SINTÉTICO LyeTx I-b DERIVADO DO VENENO DE ARANHA COMO UM POTENCIAL PROTÓTIPO ANTITUMORAL: ESTUDOS TOXICOLÓGICOS E FARMACOLÓGICOS

Tese apresentada ao Programa de Pós-Graduação em Neurociências, do Instituto de Ciências Biológicas da Universidade Federal de Minas Gerais, como requisito parcial à obtenção do título de Doutor em Neurociências.

Orientadora: Prof. Dra. Elaine Maria de Souza-Fagundes
Co-orientadoras: Prof Dra. Juliana Carvalho Tavares e
Prof Dra. Maria Elena de Lima Perez Garcia.

Belo Horizonte

2018

UNIVERSIDADE FEDERAL DE MINAS GERAIS
Instituto de Ciências Biológicas
Programa de Pós-Graduação em Neurociências

MOSTAFA ABDELLATIF ABDELSALAM ABDELRHEEM

# EVALUATION OF THE LyeTx I-b SYNTHETIC PEPTIDE DERIVED FROM SPIDER VENOM AS A POTENTIAL ANTITUMORAL PROTOTYPE: PHARMACOLOGICAL AND TOXICOLOGICAL STUDIES

Tese apresentada ao Programa de Pós-Graduação em Neurociências, do Instituto de Ciências Biológicas da Universidade Federal de Minas Gerais, como requisito parcial à obtenção do título de Doutor em Neurociências.

Orientadora: Prof. Dra. Elaine Maria de Souza-Fagundes
Co-orientadoras: Prof Dra. Juliana Carvalho Tavares e
Prof Dra. Maria Elena de Lima Perez Garcia.

Belo Horizonte

2018

**ACKNOWLEDGEMENTS**

First of all thanks to GOD, by grace whom this work was accomplished. I would like to express my great appreciation and sincere gratitude to my supervisors Dr. Elaine Maria de Souza Fagundes, Dr. Juliana Carvalho Tavares, and Dr. Maria Elena de Lima Perez Garcia for giving the opportunity to undertake this study such an exciting project besides the continuous help during the course of the present study and in writing the thesis.

Since taking the leap to move to Belo Horizonte. I have made some good friends here at ICB-UFMG, I would particularly to thank Jonas and Bárbara for all the fun times we had in the lab together.

Deep thanks are also expressed to Dr. Geovanni Dantas Cassali, General Pathology department, ICB-UFMG for his valuable cooperation in the anticancer experiments *in vivo*.

Finally I would like to mention my collaborators during this project, Dr. Gregory Kitten, Morphology department, Dr. Lilian Bueno, Parasitology department, and Dr. Andréa Teixeira, Fiocruz, who help me with experiments and scientific advice.

Thankful to CAPES, CNPq, Fapemig and Humboldt foundations for the financial support

## DEDICATION

**I dedicate this thesis to my Mother, Father, Sisters and Brothers for all the support lovely offered during my post-graduate studies and always they believed in my abilities.**

## ABSTRACT

Antimicrobial peptides present a broad spectrum of therapeutic applications, including their use as anticancer peptides. These peptides have as a target microbial, normal and cancerous cells. In this work we demonstrate for the first time the cytotoxic effects of the cationic alpha-helical antimicrobial peptide LyeTx I-b on glioblastoma lineage U87-MG. The anticancer property of this peptide was associated with a membranolytic mechanism in U87- MG. Loss of membrane integrity occurred after incubation with the peptide for 15 minutes, as shown by trypan blue uptake, reduction of calcein-AM conversion and LDH release. Morphological studies using scanning electron microscopy demonstrated disruption of the plasma membrane from cells treated with LyeTx I-b, including the formation of holes or pores. Transmission electron microscopy analyses showed swollen nuclei with mild DNA condensation, cell volume increase with an electron-lucent cytoplasm and organelle vacuolization, but without the rupture of nuclear or plasmatic membranes. Morphometric analyses revealed a high percentage of cells in necroptosis stage, followed by necrosis and apoptosis at lower levels. Necrostatin-1, a known inhibitor of necroptosis, partially protected the cells from the toxicity of the peptide in a concentration-dependent manner. Imaging flow cytometry confirmed that, 59% of the cells underwent necroptosis after 3-hour incubation with the peptide. In addition, LyeTx I-b showed cytotoxicity for non-tumor cell lines derived from kidney epithelial cells (Vero), Lung fibroblast (GM637), brain (Luhmes), PBMC and hemolytic activity in human erythrocytes. Additionally, other *in vitro* data also demonstrated cytotoxicity of this cationic peptide against human and mouse breast cancer cell lines (MCF-7, MDA-MB-231 and 4T1, respectively), at low micro molar concentration (<10 μM). The peptide induced death by apoptosis in 4T1 cells, observed by the increase of DNA fragmentation and annexin-V labeling, besides to reducing the clonogenic survival of this lineage. Considering this finding, all data pointed out the antitumor potential of this peptide, which was evaluated using the 4T1 breast cancer model in mice regarding it toxicity and antineoplastic effect. Sub-acute toxicity of LyeTx I_b peptide *in vivo* was assessed, and BALB/c mice treated with LyeTx I_b peptide showed no lesion or significant alterations in lung, kidney, spleen, heart, brain, and liver conducted by histopathological analysis. Moreover, LyeTx I-b peptide decreased tumor's volume and weight, size and number of metastatic foci in the 4T1 tumor-bearing animals. In addition, the peptide reduced the circulating neutrophils, eosinophils and monocytes. By using intravital microscopy, we found a remarkable increase of leukocytes rolling and reduction of leukocytes adhesion after treating with LyeTx I-b peptide into the spinal cord and tumor vessels in 4T1 tumor-bearing animals. Quantification of cytokines and tumor growth factors by ELISA revealed that LyeTx I-b and carboplatin groups showed a significant reduction in TGF-β expression in tumor and spleen, and suppression of IL-1 β in the lung and tumor. Further, LyeTx I-b peptide induced an increase of the anti-inflammatory IL-10 cytokine in the tumor. In summary, our *in vivo* and *in vitro* data suggested that LyeTx-I-b peptide could be an interesting prototype to develop an antitumor chemotherapeutic agent, with a potential immunomodulatory effect.



Key words: LyeTx I-b peptide, Glioblastoma multiform, Breast cancer, Necroptosis and Immunomodulation.

**RESUMO**

Os peptídeos antimicrobianos apresentam um amplo espectro de aplicações terapêuticas, incluindo seu uso como peptídeos anticâncer. Estes peptídeos têm como alvo células microbianas, normais e cancerígenas. Neste trabalho, demonstramos pela primeira vez os efeitos citotóxicos do peptídeo antimicrobiano catiônico alfa-helicoidal, LyeTx I-b, sobre a linhagem de glioblastoma U87-MG, que está associado a um mecanismo membranolítico. A perda de integridade da membrana ocorreu após a incubação com o peptídeo por 15 minutos, observado pela captação de azul de tripan, redução da conversão de calceina-AM e liberação de LDH. Estudos morfológicos utilizando microscopia eletrônica de varredura demonstraram uma rápida ruptura da membrana plasmática de células tratadas com LyeTx I-b, incluindo a formação de orifícios ou poros. Análises por microscopia eletrônica de transmissão mostraram núcleos inchados com leve condensação de DNA, aumento do volume celular com citoplasma eletron-lucente e vacuolização de organelos, mas sem a ruptura de membranas nucleares ou plasmáticas. Análises morfométricas revelaram uma alta porcentagem de células em estágios de necroptose, seguidas de necrose e apoptose em níveis mais baixos. A necrostatina-1, um inibidor especifico de necroptose, protegeu parcialmente as células da toxicidade do péptido de um modo dependente da concentração. Estudos de citometria de fluxo por imagem confirmou que 59% das células tratadas com o peptide estavam em necroptose após 3 horas de incubação com o peptídeo. Ademais, o LyeTx I-b apresentou citotoxicidade para linhagens celulares não tumorais derivadas de rim embrionário humano (HEK293), fibroblasto (GM637), cérebro (Luhmes), PBMC e atividade hemolítica em eritrócitos humanos. Outros dados *in vitro* também demonstraram a citotoxicidade deste peptídeo catiônico contra linhagens de células de câncer de mama de humanos e camundongos (MCF-7, MDA-MB-231 e 4T1, respectivamente) em baixa concentração micromolar (<10 μM). O peptideo induziu morte por apoptose em células 4T1, observado pelo aumento de fragmentação do DNA e marcação com anexina-V, além de reduzir a sobrevivencia clonogenica das mesmas. Considerando estes achados, avaliou-se o efeito *in vivo* deste peptídeo utilizando o modelo de câncer de mama triplo-negativo 4T1 em camundongos, quanto à toxicidade e potencial antineoplásico. Avaliou-se a toxicidade sub-aguda do péptido LyeTx I_b *in vivo*, e os camundongos BALB/c tratados com o péptideo LyeTxI_b não apresentaram lesão ou alterações significativas no pulmão, rim, baço, coração, cérebro e fígado, após análise histopatológica. No entanto, o peptideo LyeTx I-b diminuiu o volume e o peso do tumor, o tamanho e numero de focos metastáticos nos animais portadores de tumor 4T1. Adicionalmente, após tratamento dos animais com o péptideo LyeTx I-b foi observada uma redução significativa de neutrófilos, eosinófilos e monócitos circulantes. Usando microscopia intravital, encontramos um aumento notável de leucócitos rolando e redução da adesão de leucócitos após o tratamento com o peptídeo LyeTx I-b na medula espinhal e vasos tumorais de animais portadores de tumor 4T1. A quantificação de citocinas e dos fatores de crescimento tumoral por ELISA revelaram que os grupos tratados com LyeTx I-b e carboplatina apresentaram uma redução significativa na expressão de TGF-β no tumor e no baço, e supressão de IL-1 β no pulmão e tumor. Além disso, o peptídeo LyeTx I-b induziu um aumento da citocina anti-inflamatória IL-10 no tumor. Em resumo, nossos dados *in vitro e in vivo* sugerem que o peptídeo LyeTx-I-b pode ser um protótipo interessante para o desenvolvimento de um quimioterápico antitumoral, com um potencial imunomodulador.

**Palavras-chave:** peptídeo LyeTx I-b, Glioblastoma multiforme, Cancer de mama, Necroptose e Imunomodulação.

## COLLABORATORS

Prof. Dr. Geovanni Cassali, Departamento de Patologia Geral, ICB/UFMG

Prof. Dr. Andréa Teixeira de Carvalho, Fiocruz Minas

Prof. Dr. Gregory Kitten, Departamento de Morfologia, ICB/UFMG

Prof. Dr. Marcel Leist, Konstanz University, Germany

**Financial Support**

Fundação de Amparo a Pesquisa do Estado de Minas Gerais - Fapemig

Conselho Nacional de Desenvolvimento Científico e Tecnológico - CNPq

Coordenação de Aperfeiçoamento de Pessoal de Nível Superior – Capes

Fundação Alexander von Humboldt, Germany

**List of Abbreviations**

**AKT:** Protein kinase B

**AMPs:** Antimicrobial Peptides

**ATP:** Adenosine Triphosphate

**ATG:** Autophagy-related protein

**AVOs:** acidic vesicles organelles

**BBB:** Blood Brain Barrier

**BBTB:** Blood Brain Tumor Barrier

**BRCA:** Tumor Suppressor Genes

**CYLD:** Cylindromatosis, turban tumor syndrome

**CTLA-4:** Cytotoxic T-lymphocyte Antigen

**CPPs:** Cell-penetrating Peptides

**CSF:** Cerebrospinal Fluid

**DOX:** Doxorubicin

**EGFR:** Epidermal Growth Factor Receptor

**ECM:** Extracellular Matrix

**ER:** Estrogen Receptor

**FGFR:** Fibroblast Growth Factor Receptor

**GBM:** Glioblastoma Multiforme

**GM637:** Human Lung Fibroblasts

**GSH:** Glutathione

**HER2**: Human Epidermal growth factor Receptor

**HL60:** Human Promyelocytic Leukemia

**HT-29:** Human Colorectal Adenocarcinoma cell line

**IL-6:** Interleukin 6

**IL-10:** Interleukin 10

**IL-1β:** Interleukin 1 Beta

**JURKAT:** Acute T-cell Leukemia Lymphocyte

**LDH:** Lactate Dehydrogenase

**Luhmes cells:** Lund Human Mesencephalic

**MCF-7:** Human Breast Adenocarcinoma cell line

**MDA-MB-231:** Human Breast Adenocarcinoma cell line

**MLKL:** Mixed lineage Kinase Domain-like Protein

**MMP:** Matrix Metallopeptidase

**MOMP:** Mitochondrial Outer Membrane Permeabilization

**NEC-1:** Necrostatin-1, Necroptosis Inhibitor

**NK:** Natural Killer cells

**PDGFR:** Platelet-derived Growth Factor Receptor

**PDL-1:** Programmed Death Ligand

**PI:** Propidium Iodide

**PIK3CA:** Phosphatidylinositol-4,5-bisphosphate 3-kinase catalytic subunit alpha

**PBMC:** Peripheral Blood Mononuclear Cells

**PMNs:** Polymorphonuclear cells

**PTEN:** Phosphatase and Tensin Homolog

**PS:** Phosphatidylserine

**RIP1:** Receptor-interacting Protein Kinase 1

**RIP3:** Receptor-interacting Protein Kinase 3

**SEM:** Scanning Electron Microscopy

**SHSY5Y:** Neuroblastoma cell line

**TEM:** Transmission Electron Microscopy

**TGF-β:** Transforming growth factor

**THP-1:** human Leukemic monocyte

**TK:** Tyrosine Kinase

**TNF:** Tumor necrosis factor

**TP53:** Tumor protein p53

**U-373 MG:** Human Astrocytoma cell line

**U-87MG:** Human glioblastoma cell line

**Vero:** African Green Monkey Kidney

**VGFR:** Vascular Endothelial Growth Factor Receptor

# Table of contents

**List of Figures**

**Review literature**



**Chapter 1**



**Chapter 2**

## List of Tables

### Chapter 1



### Chapter 2



### Chapter 3

## 1. Introduction

Cancer is currently in the spotlight due to their designation of death in both developed and non-developing countries. It's expected to rank as the main cause of mortality and decreasing life expectancy around the world in the 21st century (Bray, F. et al., 2018). The number of cases and deaths by cancer projected for the next 20 to 40 years will be the double of the current numbers, although cancer incidence varies significantly from one continent to another. The incidence is fast increasing in developing countries (Pillai and Jayasree. 2017). Precisely, the registration of cancer cases in different regions around the world is necessary part of surveillance and plays vital role in cancer prevention. Brazilian registers system informed that rate of cancer incidence and death are lower than Western Europe and North America countries, while the rate is still similar to developing countries (Barbosa, de Souza. et al., 2015).

Cancerous tumors are characterized by the uncontrolled growth of mutated stem cells or undifferentiated pericytes, which can emigrate through the lymphatic and vascular circulation systems, causing high morbidity and mortality rates. For this reasons, the cancer research becomes a major focus of medical research (Kumar, V. et al., 2014).

Glioblastoma multiforme (GBM) becomes the most deadly brain cancers with poor survival rate, less than one year because of drug resistance and tumor recurrence after surgery and radiotherapy as well (Cheng, Zhao et al. 2014, Tivnan, H. et al., 2017). Regardless of powerful treatment with surgery, radiotherapy and chemotherapy, tumors definitely recurred as an immediate finding of the infiltrative way of GBM. In addition, poor prognosis of patients with GBM underscores the clear and dire requirement for more precise and powerful treatments (Swartz, B. et al., 2015).

Breast cancer becomes the first cancer incidence in the women around the world because of many factors, like changes in lifestyle, delayed first child born and the short time of breastfeeding (Rivera-Franco & Leon-Rodriguez, 2018). Previous study using a World Health Organization (WHO) database have analysed trends in breast cancer mortality over the period 1970-2014 for 37 European countries, and predicted a 10% decline in mortality to 2020 in the European Community. According to National cancer institute (INCA) database in Brazil, breast cancer is the most common type among women in Brazil, after non-melanoma skin, accounting for about 25% of new cases each year. Estimation of 59,700 new cases of breast cancer is expected in Brazil. It is the most frequent in women in the South, Southeast, Midwest and Northeast regions. Breast cancer

also affects men, but it is rare, accounting for only 1% of all cases of the disease (INCA, 2018). The majority of breast cancer patients survived less 10 years due to metastasis and resistance to chemotherapy and radiotherapy. The process of metastasis and sites of secondary tumors is nowadays better understood, but the trigger mechanism associated to initial steps towards metastasis is still unclear (Heerboth, S. et al., 2015).

Several of chemotherapeutic agents were accepted in clinical practices and their side effects were commonly observed in cancer patients like neurological problems, including, loss of memory and mood disorder, once these agents are able to induce hippocampal dysfunction and neuronal damage (Yang and Moon. 2013). Neuropathy is a term that refers to general diseases or malfunctions of the nerves, resulted in painful during patient's chemotherapy with various anticancer drugs like Taxol, Cisplatin, oxaliplatin, vincristine and vinblastine. Chemotherapy leads to the chronic syndromes accompanied by neurological symptoms such as severing pain, tingling and numbness. Thereby, pharmacological management of chemotherapy-induced neuropathy remains largely ineffective. Subsequently, it is necessary to find out a new strategy for optimization of novel anticancer drugs (Di Cesare Mannelli, L. et al. 2017).

In the last decades, anticancer drug discovery field presented many antitumor agents from different natural sources like animals, microorganisms, plants and others (Xiao, M.N. et al., 2016). Human innate immune system contains many natural antimicrobial peptides, which are able to fight against infectious diseases and cancer cell, when used alone or in combination with other anticancer agent. (Gaspar, V. et al. 2013). In addition, other antimicrobial peptides can be widely found in the nature, such as animal venoms and plant toxins.

Cancer treatment based on peptides have been gained much attention due to their advantages, such as affinity to bind with receptors, selectivity and specificity to tumor cells with low toxicity in normal tissues. The structure of peptides developed for tumor targeting moieties and increasing of cell penetration, binding, and permeability in malignant tissue, via targeting for specific cell surface receptors (Lau, L. et al., 2018). In scenario thesis one antimicrobial cationic peptide derived of spider venom was investigated regarding it potential as a prototype to develop new drugs to treat glioblastoma and breast tumor.

## 2. Review of literature

### 2.1. Recent challenges of Glioblastoma Multiform (GBM) treatment:

Regardless, a great efforts extended, and also the knowledge about glioma invasiveness molecular pathways, GBM still considered as a difficult challenge in clinical oncology. Nowadays, novel drugs and techniques contributed to improve the quality of life and surviving rate in the patients with GBM. For instance, the scientific progress in surgical operations, clinical practices of radiotherapy and chemotherapy. Nevertheless, glioblastoma (GBM) still remains as the most deadly cancer, and GBM patients usually cannot survive more than one year after diagnosed with tumor grade IV (Di Carlo, D. et al., 2017).

Currently, more significant strides are prerequisite to make positive outcomes, compared to successful treatment seen in certain other cancers. To investigate the safety, efficacy and toxicity of the anticancer agent, it is necessary a large cohort of patients which are difficult to achieve with cancer disease. Preclinical studies in the neuro-oncology field require a great effort from collaborators to make efficient of the novel drugs rapidly for improving clinical outcomes in the patients (Mrugala, N. 2013). The dark side in glioblastoma treatment is the unsuccessful drug test procedures during pre-clinical experiments and clinical trials due to lack of drugs that able to cross through blood brain tumor barrier (BBTB). In addition, extensive hypoxic regions in glioblastomas contribute to the highly malignant phenotype of these tumors, in order to increase metabolic rate and angiogenesis, which enhances migration, invasion and BBTB dysfunction. BBTB was viewed as ‘leaky’ membrane in the core part of glioblastomas, in low tumor grade. Although, the BBTB more nearly look like the intact blood brain barrier (BBB), however it bans efficient cross of cancer therapeutics, such as small molecules and antibodies (Van Tellingen, Y.A. et al., 2015).

### 2.2. Promising approach of GBM therapy:

Novel therapeutic approaches are intensely being investigated. Glioblastoma therapy based on targeting epidermal growth factor receptor EGFRvIII, especially the abundant active form, which leads to enhancing cell proliferation via PI3K-AKT pathway (Wei, C. et al., 2017). Furthermore, at least 50% of high grade glioblastoma patients have HER1/EGFR overexpression and irregular molecular pathway.Consequently, the

oncologists used different inhibitors such as tyrosine kinase (TK) inhibitors that makes down-regulation of over-expressed EGFR receptor through these mechanisms as follow: (1) the combination between EGFR inhibitor and anti-apoptotic agent might defeat cross-resistance of high grade of gliomas. (2) Intra-tumoral diversity within GBM tumors may drive resistance to single based anti-EGFR agents due to RTK co-activation, PTEN deletion/mutations, and tumor cell-tumor cell interactions via secreted molecules. (3) Efflux of EGFR TKIs and increased genetic stability may lead to tumor relapse. (4) Enhanced immunosuppression mediated by circulating growth factors, cytokines and suppressor T cells can antagonize the systemic immune responses generated by anti-EGFR immunotherapies. Additionally, circulating IL-6 in the tumor microenvironment can facilitate resistance intracellular via activation of the JAK/STAT3/$Bcl_2$ pathway (Taylor, F. et al., 2012 & Karpel-Massler, S. et al., 2009).

Cyclic peptide (Cilengitide) showed anti-angiogenesis effect through targeting integrin's proteins αvβ3 and αvβ5 in different glioma models *in vitro* and *in vivo*. In addition, evaluation of cilengitide in clinical trial phases demonstrated that peptide was effective in recurrent glioma patients (Gilbert, M. R. et al., 2012). Chlorotoxin (CTX) is also cyclic peptide, which consist of 36 amino-acid extracted and purified from venom of the scorpion (*Leiurus quinquestriatus*) and has been used as a good agent to characterize chloride channels. Recent studies showed that chlorotoxin was able to bind with chloride channels and targeting malignant tissues, in particular glioma, medulloblastoma and neuroblastoma (Dardevet, R. et al., 2015). Also, conjugated CTX-Onc (Chlorotoxin-Conjugated Onconase) showed promising results *in vivo*, as a good model of drug delivery in clinical practice of glioma because conjugated CTX-Onc can be injected through the cerebrospinal fluid, avoiding blood-brain barrier (BBB), resulted in identification of malignant gliomas region (Wang and Guo. 2015). Drug resistance still remains the main obstacle and redundant hurdle to overcome, and therefore the development of anticancer agents required with unclassical mechanisms of action. The peptides could be able to destroy and eliminate cancer cells obviously because of positive charges that can bind with negative charges on the cell membrane, causing cell membrane disruption (Liu, Q. et al., 2016).

For decades, it has been supposed that the most anticancer drugs could cross the blood–brain barrier during glioblastoma chemotherapy regimen course using methotrexate, cisplatin, carmustine, etoposide and paclitaxel. The recent studies reported that glioblastoma cells secrete cytokines, which causing BBB disruption (Oberoi, R. K., et al. 2016). In addition, many studies have suggested that nearly all chemotherapeutic agents can cause disorders of the central nervous system (CNS), including encephalopathy, leukoencephalopathy, ototoxicity and cerebellar symptoms (Verstappen, H. et al., 2003, Puduvalli, C. et al., 2017). Peptide-based drug delivery is one of the best strategies to overcome drug failure during conventional therapy, once peptides are able to deliver adequate and effective amounts of drugs to glioblastoma cells. For instance, the AngioPep-2 peptide (ANG1005) increased significantly the delivery of paclitaxel *in vivo* and also in recurrent malignant glioma clinical trials by targeting low-density lipoprotein receptor in glioma cells (Drappatz, J., et al., 2013). In a similar study, SynB1 peptide conjugated with doxorubicin increased cellular uptake in brain tumor compared with doxorubicin alone (Agarwal, S. et al., 2013). BBB is composed of cell layer from endothelial cells, no fenestrated basal lamina, pericytes, and astrocytes tied together. This complex barrier regulate and restrict passage of the systemic drug delivery into the central nervous system (CNS). BBB and drug resistance are the main obstacles for glioblastoma therapy, because of BBB limits drug transport to tumor region (Bhowmik, A. et al., 2017). Drugs delivery of hydrophilic drugs or even macromolecules to CNS is difficult, due to presence of tight junctions and microvessels that control drug diffusion, and also the barrier integrity play a crucial role in efflux transportion into tumor cells (Agarwal, S. et al., 2011).

### 2.3. The Cellular Origin of Breast Cancer:

One of the key questions in cancer cell biology is to recognize the mechanisms that control tumor and to explore, which tumor heterogeneity effects on clinical outcome. Breast cancer is the most frequent cancer type diagnosed in women over the world (Ghoncheh, M. et al., 2016). It is characterized by neoplastic transformation which is caused by mutant genes such as BRCA1, BRCA2, DNA repairing genes, AKT, FGFR, and PIK3CA, in mammary epithelial stem cells. The mutations leading to uncontrolled cell division, invasiveness, and metastatic capability and ultimately death, if not treated (Ghoncheh, M. et al., 2016 & Zhang, M. et al., 2017). In previous study, Van Keymeulen and colleagues discovered that overexpression of oncogenic gene PIK3CA

stimulates a multilineage differentiation program in adult stem cells, followed by induction of luminal estrogen receptor (ER)-positive/progesterone receptor (PR), leading to tumor formation in the primary breast cancer (Van Keymeulen, et al., 2015). Interestingly both mutations in phosphatidylinositol-4, 5-bisphosphate 3-kinase catalytic subunit alpha (PI3KCA) and Phosphatase and Tensin homolog (PTEN) are involved in the phosphoinositide 3-kinase (PI3K) signaling axis suggesting dis-regulation of this pathway has a particularly strong role during oncogenesis in breast carcinoma. Positioned downstream of both receptor tyrosine kinases (RTK) and G-protein coupled receptors (GPCR), the PI3K lipid kinases act as major downstream effector pathway in regulating multiple cellular processes, including proliferation (Kandula, M. et al., 2013). In addition, the women who have certain gene mutations, such as a BRCA1 or BRCA2, have an increased risk of breast cancer incidence (Girardi, F. et al., 2018).

Douglas Hanahan and Robert Weinberg have been described the biological hallmark of cancer in a multi-step process including arising from evading growth suppressors, preventing immune destruction, modifying cellular energetics regulation, inflammation, genetic alterations (mutations), promoting angiogenesis, sustaining proliferative signaling, enhancing proliferation metastasis, and increasing cell death resistance (Hanahan, & Weinberg, 2018).

### 2.4. Metastatic Breast Cancer

The process of metastasis is the final and fatal step during cancer progression and is defined as the stage IV of cancer caused by spreading breast cancer cells into other organs, most often lung, liver, bone and brain. The spread of breast cancer cells from primary tumor involves a multi-step process known as the invasion metastasis cascade. This cascade of events includes the local invasion of primary cancer cells into nearby normal cell or lymph nodes entrance and survival into blood circulation and lymphatic system, arrest and extravasation through vascular wall, migration to distant tissue, and eventually, the growing of new cells (colonization mechanism) to form micrometastases (Inoue, K., & Fry, E., 2016 & Lambert, A.W., 2017).

Metastatic breast cancer usually happens due to changing of estrogen receptor alpha (ERα), progesterone receptor (PR), and epidermal growth factor receptor (EGFR or HER 2) status (Schrijver, W. et al., 2018). HER 2 receptor has been extensively studied, about 20 to 30% of breast cancer patients who exhibited HER 2 overexpression have a high prediction and prognostic of tumor invasion, recurrence, and increased mortality rates (Mitri, Z. et al., 2012). In the other

hand, find estrogen receptor (ER)-positive means an increased proliferation of progenitor cells in breast tissues that facilitates the metastatic process (Zhang, M. et al., 2014) .The common types of invasive breast cancer are ductal adenocarcinoma and lobular carcinoma. The etiology is multifactorial, involves diet, reproductive factors, hormonal imbalance and genetic mutation (BRCA1, BRCA2, BRCA3, CDH1, and TP53) (National Cancer Institute, 2016). Positive BRCA2 mutation in breast cancer patient associated with tumor recurrence and metastasis (Rizvi, W. et al., 2017).

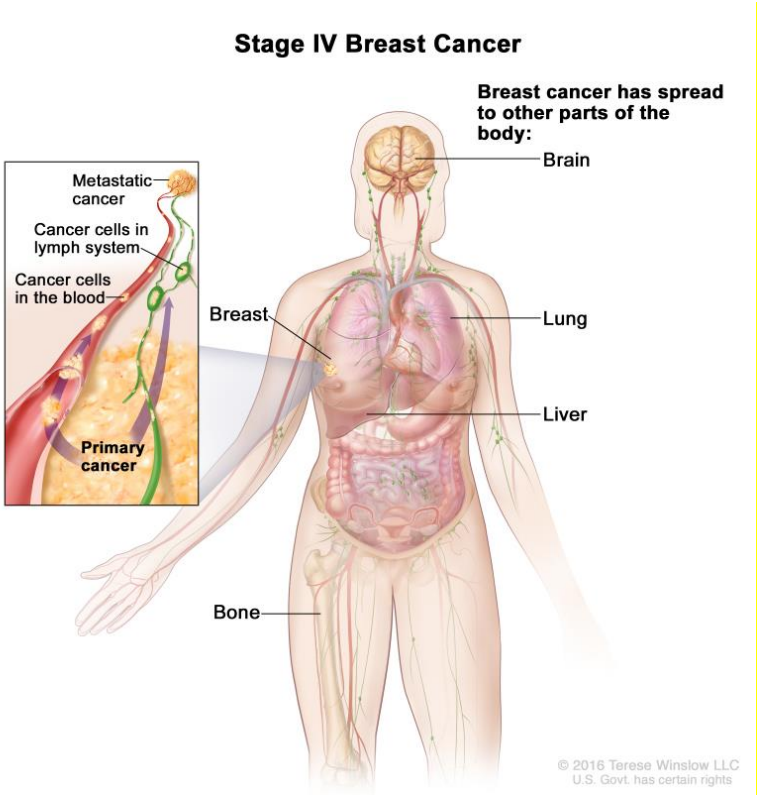


Figure 1. Stage IV breast cancer. The cancer has spread to other parts of the body, such as the brain, lung, liver, and bone (National Cancer Institute, 2016).

Clinical data from breast cancer patients also support the metastasis concept that it is an inefficient process throughout its progression since only a small percentage of breast cancer patients with bone marrow micro-metastasis at the time of diagnosis eventually developed clinically detectable macro-metastasis. However, cancer patients who underwent surgical resection of their primary tumors presented recurrent metastatic disease many years after the initial diagnosis (Tjensvoll, K. et al., 2012).

### 2.5. Angiogenesis: Physiological feature of Breast cancer

Angiogenesis is a natural event associated to embryonic development and wound healing. Furthermore, angiogenesis occurs once breast tumor has formed and is more a tumor physiology feature of cancer rather than a cellular feature. Breast tumors obviously contain areas of severe hypoxia and in order for the residing cancer cells to receive nutrients and oxygen, angiogenesis should initiate (Castañeda-Gill & Vishwanatha, J. 2016). The formation of new vessels in cancer tissues is a process that involves also blood vessel maturation and survival via activation of angiopoietin protein (Longatto, F. et al., 2010). Breast carcinoma cells initiate angiogenesis by releasing different angiogenic factors, such as vascular endothelial growth factors (VEGF), interleukins (IL-1β, IL-8, and IL-6), and matrix metalloproteinases (MMP-1, MMP-3, MMP9 and MMP-12). Moreover, transforming growth factor like TGF-β also induces angiogenesis through mediating signals of apoptosis cell death mechanism (Ferrari, G.et al., 2009).

### 2.6. Molecular mediators of Breast cancer

#### 2.6.1. Vascular endothelial growth factors (VEGFs)

VEGFs have roused much interest because of their roles in various physiological process such as endothelial and epidermal cell proliferation, macrophages migration and cancer cells progression. The highly expressed VEGFR receptor (R1, R2 and R3 ligands) in breast tumor endothelial cells is the key modulator of angiogenesis due to the vital role in development, invasiveness, and aggressiveness. Consequently, targeting VEGF receptor is a proper therapy of breast cancer patients due to its functional relevance in neovascularization process (Sa-nguanraksa, D., & O-charoenrat, P., 2012). In addition, high expression of VEGFR receptor in hypoxic tumor lesions leading to up-regulation of hypoxia-inducible factors (HIF1α, that play a crucial role in maintaining breast cancer stem cells, due its ability to avoid eradication by macrophages (Zhang, H. et al., 2015).

#### 2.6.2. Interleukins

All interleukins have dual functions in tumor microenvironment, although their roles during metastasis are not clear yet. Interleukins are secreted proteins and signal transduction molecules expressed by T- lymphocytes, monocytes, macrophages and endothelial cells to regulate immune response during inflammation, tumor initiation and malignant conversion (Grivennikov, S. et al.,

2010). The majority of all cancers has been associated to inflammatory environment factors in somatic cells, and, a dysregulation of interleukins in this chronic inflammatory context leading to tumor progression and development. (Aggarwal, B. et al., 2009& Esquivel-Velázquez et al., 2015). The inflammatory process in a tumor microenvironment encompasses the infiltrated and circulating leukocytes, which lead to the increase of interleukins, and growth factors secretions (Grivennikov, S. et al., 2010). IL-6, TNF-α, and IL-1β are critical inflammatory mediators for breast cancer development and migration. Previous data showed that treatment with inhibitors of these mediators could be increase breast cancer survive rate (Goldberg & Schwertfeger, 2010).

The high levels of IL-1β cytokine have been correlated with carcinogenesis and the maintenance of tumor of microenvironments, it means, IL-1β level is a predictable biomarker of cancer risk and prognosis (Idris, A. et al., 2015).The interleukin-6 (IL-6) levels in serum of breast cancer patients related with tumor grade and poor surviving rate. In addition, it is well know that IL-6 induces breast cancer metastasis due to impairment of E-cadherin expression and increasing epithelial-mesenchymal transition (Sullivan, N. et al., 2009). Furthermore, the IL-6 levels in ER- estrogen negative breast cancer cells is lower than ER-alpha-positive human breast cancer (MDA-MB-231 and MCF-7), and may lead to enhance tumor cell growth and proliferation (Sasser, A.et al., 2007).

Tumor necrosis factor alpha (TNF-α) is an inflammatory cytokine plays a crucial role in breast cancer by activation of nuclear factor kappa B (NF-κB transcript factor, resulting in enhancing malignancies in the tumor microenvironment, formation of covalent protein-DNA adducts and tumor invasion (Kamel, M. et al., 2012). By contrast, local administration of high doses of TNF-α inhibitors have been demonstrated potent antitumor and antiangiogenic effects in early metastatic breast cancer patients (Hamed, E. et al., 2012). *In vitro* study was showed that TNF alpha-induced down-regulation of ER alpha, inhibited cell proliferation that mediated by a PI3K/Akt signaling pathway in MCF-7 cells (Lee, S. & Nam, H., 2008).

Many studies suggested that IL-10 has dual functions in cancer pathogenesis, inhibition and stimulation of breast tumor growth (Hamidullah, B. & Konwar, R., 2012). Although interleukin-10 (IL-10) exhibits anti-inflammatory and immunosuppressive effects in breast cancer, it also facilitates tumor escape against immune surveillance. The elevated serum levels of IL-10 in breast cancer patients have been linked to immunosuppression (Bhattacharjee, H. et al., 2016). Tian and his colleagues found that IL-10 associated with activation of tumor microenvironment factors leads

to breast cancer prognosis (Tian, K. et al., 2017). On the other hand, IL-10 and IL-6 overexpression can inhibit migration and proliferation in early stage of breast cancer (Ahmad, N. et al., 2018). Furthermore the high level of IL-10 in breast cancer tissues correlated with down regulation of VEGF, TNF-α, IL-1β, and thereby IL-10 could be inhibits tumorgensis and angiogenesis (Sheikhpour E et al., 2018).

### 2.6.3. Transforming growth factor-β (TGF-β)

The transforming growth factor-beta (TGFβ) superfamily including more than 40 different family members. Three distinct isoforms have been identified (TGFβ-1, -2, -3) in the TGFβ subfamily. TGF-β is multifunctional and signaling cytokines secreted by leukocytes for differentiation, chemotaxis, and TGF-β receptor binds to serine/threonine kinase complex (Massagué, J. 2012). The importance of TGF-β in non-tumoral cells is blocking cell cycle (G1 phase) through the signaling pathway that leads to apoptosis induction.

The role of TGF-β in breast cancer stages have been extensively studied. TGF-β plays dual context-dependent roles in cancer: in the early stages of tumor development TGF-β primarily functions as a tumor suppressor, while in the later stages of cancer TGF-β function as tumor promoter of metastasis (Xie, F. et al, 2018). TGF-β to stimulate epithelial-to-mesenchymal transition (EMT), through upregulation of a transcription factor of EMT morphology (TF3) and dysregulation of Tight Junction Proteins claudin-3 and E-cadherin, that allows breast cancer stem cells to migrate and invade (Yin, X. et al., 2010). In cancer cells, TGF-β receptor becomes mutated (Zu, X. et al., 2012). Mutant signaling pathway enhances proliferation of epithelial, stromal and immune cells leading to tumor progression and invasion (Hanahan, D. & Weinberg, R. 2000).Although TGF-β contributes to breast cancer metastasis, it is also able to inhibit proliferation in the early stage of breast tumorigenesis caused by inhibiting cyclin-dependent kinases in G1 phase (Caja, F. & Vannucci, L. 2015).

## 2.7. Breast Cancer and the Immune System

Immune systems including innate and adaptive play vital role in breast cancer recurrence and tumor relapse. Lymphocytes, natural killer cells, monocytes, neutrophils, macrophages, and dendritic cells activate the transcription of genes encoding inflammatory mediators, such as cytokines and chemokines thus initiating the immune response (Standish, L. et al., 2008).

Neutrophils or polymorphonuclear cells (PMNs) are the most abundant leukocyte in humans, comprising 70% of the white blood cell compartment and also defined as multi-lobed nuclei and ability to retain neutral dyes (Amulic, B. et al., 2012). Although it is apparent from the literature that neutrophils actually play a key role in the efficacy of numerous immunotherapeutic agents, their role in cancer is often overshadowed in favour of the lymphocytes (Carroll, C., 2016).

Neutropenia is a low neutrophil count in the blood. The occurrence of neutropenia in breast cancer patients associated with adjuvant chemotherapy have been explained due to the influence of antineoplastic drugs like etiposide to induce myelosuppression (Do Nascimento, T. et al., 2014). Fifteen studies comprising 8563 patients have been proved that the high-level ratio between neutrophils and lymphocytes correlated with increasing of breast cancer mortality rate in both early and metastatic stage.Thus neutrophil/lymphocyte ratio could be used to determine the prognostic value in breast cancer patients (Ethier, J. et al., 2017).NLR= (Neutrophil percent / lymphocyte percent)X100.

Monocytes can differentiate into macrophages and dendritic cells. Macrophages are the main cellular component of the tumor stroma used for breast cancer prognosis because macrophage can be able to stimulate stem cell pro-tumorigenic activity. Macrophages are also able to infiltrate into high-grade breast cancer tumors like MCF7 and MDA-MB-231, resulting from migration and progression of cancer cells (Ward, R. et al., 2015). Monocytes contribute in breast cancer aggressiveness via producing TNF-α in stromal cells, which is associated with inflammation localized surround of the tumor, give rise to promote resistant towards the apoptotic action (Blot, E. et al., 2003).

Eosinophils or arise from hematopoietic $CD34^{+}$ stem cells in the bone marrow and represented 1-3% of the total count of leukocytes. Eosinophils are responsible for allergy and inflammation of tumor stroma (Uhm, T. et al., 2012). Eosinophils could be able to infiltrate into tumor stroma and induce tumor angiogenesis by activating heparin-like molecules that allow forming of neovascularization (Amini, R. et al., 2007).

The lymphocyte is a type of white blood cell including natural killer cells (NK cells), T-cells, and B-cells, located mainly in lymph nodes. NK functions are cytotoxic innate immunity, T-cells are responsible for cytotoxic adaptive and Cell-mediated immunity, and B cells are responsible for humoral, antibody-driven adaptive immunity (Golovtchenko, A. & Raichvarg, D. 1975).The

importance of the lymphocytes in breast cancer has been described in many studies. Tumor-infiltrating lymphocytes are using as a predictive tool to determine the efficacy of adjuvant and neoadjuvant chemotherapy. Despite, in early stage of breast cancer, immunosurveillance-related lymphocytes $CD8^+$, $CD4^+$, T-helper cells, and natural killer cells could able to recognize and destroying malignant cells. Unfortunately, in late stage, lymphocytes couldn't recognize cancer cells, due to the decrease of surface cancer antigens expression and an overexpression of immune-checkpoint molecules, such as programmed cell death ligand-1(PD-L1), giving rise to invisible cancer cells (Ravelli, A. et al., 2017).

**2.8. Chemotherapy induced Neurotoxicity:**

Despite, chemotherapy is a common and the most basic therapeutic module for brain cancers and is often administered concomitantly with radiotherapy. It is usually recommended for children having disease progression after surgery included alkylating agents like Temozolomide, derivatives of platinum, nitrosoureas, topoisomerases, angiogenesis inhibitors and cytomegalovirus. However, chemotherapy leads to resistance, toxicity and poor clinical outcome like low survival rate in pediatric glioma patients. Based on this information, there is an urgent need to find out a novel high effective anticancer agent to overcome nerve damage problems (Zhang, L. et al., 2017). Intrathecal administration of methotrexate drug caused chronic leukoencephalopathy as the most common complaint from chemotherapy of lymphoblastic leukemia in pediatric patients in order to it highly penetrates in the central nervous system (Duffner, A. et al., 2014). Furthermore, posterior reversible encephalopathy syndrome (PRES) has been developed and notified after the adjusted dose (etoposide, prednisone, vincristine, cyclophosphamide, and doxorubicin) of intrathecal chemotherapy regime. After treatment, neuroimaging requested by neurologists for diagnosis, almost all cases had severe neurotoxicity, CNS infection and hypertension (Floeter, P. et al., 2017). The intrathecal methotrexate becomes related to appearance of clinical neurotoxicity in all documented cases with symptoms of leukoencephalopathy and posterior reversible encephalopathy syndrome (Bhojwani, S. et al., 2014). Despite chemotherapy agents are necessary to achieve cure often have undesirable toxicities, which remain after treatment is over. In addition, a frequent side effect of pediatric cancer

treatment, named chemotherapy-induced peripheral neuropathy (CIPN), may cause functional impact and affect the quality of life of survivors (Gilchrist, T. et al., 2017).

Although etoposide is a potent chemotherapeutic agent act as inhibitor of topoisomerase enzyme to induce apoptosis cascade in some childhood cancers, accumulative doses of etoposide can cause peripheral neurotoxicity, predominantly sensory axonal neuropathy (Grisold, C. et al., 2012). Furthermore a long-term adverse effect of vincristine has been described. There was preferential involvement of motor nerves with relative sparing of sensory nerves in the children exposed to vincristine (Jain, G. et al., 2014).

Cisplatin is always the first choice used in treatment of all most cancer types, it capable to ameliorate levels of cleaved caspase-3, and pro-apoptotic Bax of p53, but it also can induce neurotoxicity, thereby it's necessary to limit dosage and usage (Huang, M. et al., 2017). Doxorubicin (Adriamycin) is a successful drug in majority of cancerous tumors such as gliomas and breast adenocarcinomas. Long-term use of this drug to treat breast cancer patients resulting in cognitive and memory loss complications (Ramalingayya, C. et al., 2017).

**2.9. Current statues of therapeutic peptides in the pharmaceutical market:**

Nowadays, therapeutic peptides are showing signs of future success to treat cancer diseases. In order to their advantages like low toxicity, low accumulation in tissues, selectivity, and specificity, but still there are some limitations to use therapeutic peptides in large scales, such as low stability and rapid clearance (Marqus, S et al., 2017). Various therapeutic peptides alone or in combination with other conventional chemotherapeutic agents have been shown well tolerance and high efficacy in clinical trials to treat cancer patients (Le Joncour, V. & Laakkonen, P. 2017).

For last decades, 60 peptides have been produced by pharmaceutical companies. In addition, about 500 novel peptides still in clinical trial phases (Fosgerau and Hoffmann. 2015). According to the drug market, several peptides have been used successfully due to their features like low toxicity with high efficacy and specificity. The peptides research field focusing on chemical and physical properties of these peptides via improving rational design and biotechnological tools. Furthermore, therapeutic targeting peptides such as cell penetrating and dual target or multifunctional peptides could be utilized in a lot of clinical applications. Also, Protein and peptides biotechnology could

be overcome poor oral bioavailability and toxicity by synthetize conjugated peptide for drug delivery purposes (Fosgerau and Hoffmann. 2015& Lau and Dunn, 2018).

### 2.10. Cationic Antimicrobial Peptides

Although Antimicrobial Peptides (AMPs) have been examined basically to inhibit or killing the pathogenic microorganisms. In addition, they have been shown a potent cytotoxic effect and selectivity against many types of malignant tumors like carcinoma, adenoma, sarcoma, and leukemias. (Gaspar, V. et al., 2013). Four synthesized enantiomeric 9-mer peptides were showed various extents of growth inhibitory activity against different cancer cell lines like U-251 human glioma cells (Iwasaki, I. et al., 2009). Liu et al. reported in another study that Magainin II (MG2) is a potent anticancer cationic peptide with high selectivity toward glioma cells (C6) and human skin malignant melanoma cells (A375) *in vitro*. Cationic anticancer peptides induced rapid cell membrane disruption effect, thus might be reducing drug resistance in cancer cells (Liu, Y. et al., 2013).

Transferrin receptor lytic hybrid peptide (TfR-lytic) showed cytotoxic activity in 12 cancer cell lines such as SN-19, and U251 glioblastoma cell lines. In vitro and in vivo studies have been demonstrated that TfR-lytic hybrid peptide was able to inhibit tumor progression, based on the level of cell-surface TfR expression in cancer cells compared with normal cells (Kawamoto, H. et al., 2011). The TfR-lytic peptide also exhibited ability to induce mitochondrial collapse through activation of caspase 3 and 7. Lytic peptides disintegrated the cell membrane like a detergent. Furthermore, high selectivity and specificity of the peptide diastereoisomeros, in order to electrostatic attraction between their positive charges and negative charges of phosphatidylserine (PS) and O-glycosylation of mucin on surface of cell membrane (Papo and Shai. 2003& Kohno, H. et al., 2011).

### 2.11. Cytotoxic peptides and mechanism of Action:

#### (A) Disruption of plasma and mitochondrial membrane selectivity.

The cell surface content is different between cancer and healthy cells, represented in a high level of negative charge in the cell membrane that leads to attraction with positive charge of antimicrobial peptides, thereby showing their high selectivity to cancer cells. Furthermore,

the peptide positive charge could be bind to a high content of the negative charge of lipids and phosphatidylserine, causing pore forming in mitochondria membrane and cytosol translocation (Schweizer. 2009). Also, the cancer cells have susceptibility toward anticancer peptide based on numbers of microvilli and amount of fluids found in cancer cells. (Schweizer. 2009, Riedl, Z. et al., 2011). Chu et al reported that bacterial membrane is similar to cancer cells membrane, due to negative charge of glycosaminoglicans and bulky β-naphthylalanine residues. Therefore hydrophobic interaction between cationic peptide and cancer cell membrane, its can penetrate deeper than normal cells, that might leads to cell membrane disruption rapidly, followed by distortion of the mitochondrial membrane after uptake into the cytoplasm (Chu, Y. et al., 2015 & Jäkel, C. E., et al., 2012).

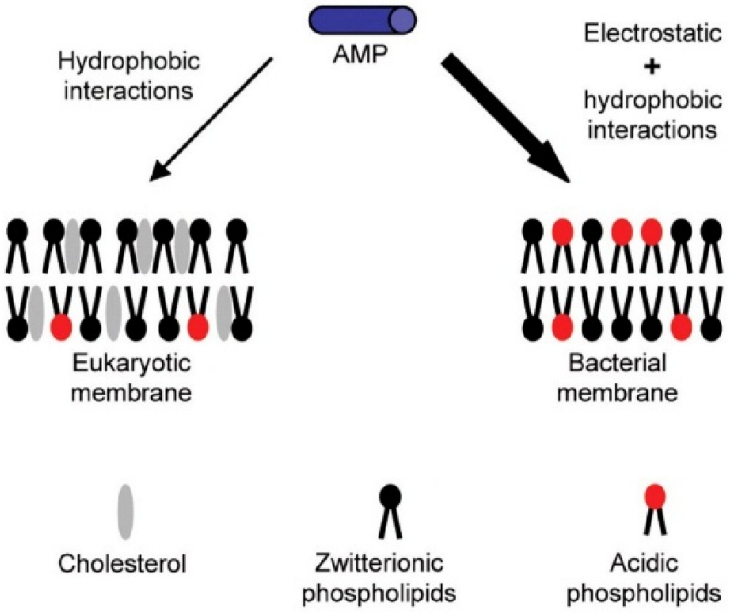


Figure 2. Effect of cationic antimicrobial peptides on cancer cell membrane and Bacterial membrane *in vivo*. Jäkel CE et al. (2012).

**(B) Apoptosis.**

One of the most important hallmarks of different types of cancers is their ability to evade cell death and apoptosis. Apoptosis-programmed cell death has been typically characterized by DNA fragmentation, chromatin condensation, and blebbing of the plasma membrane (Figure 3).

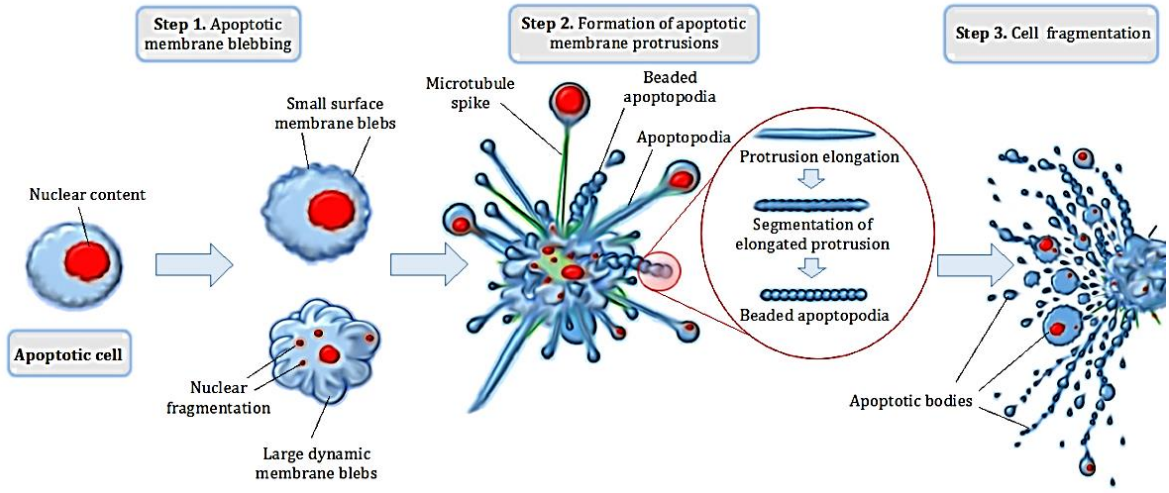


Figure 3: Apoptotic cell death mechanism: a multistep cascade events. (Extracted from Smith, A. et al., 2017).

Through activation of apoptosis, a dying cell causes minimal damage to its surrounding environment. However, many cancer cells have the ability to elude this process, because of imbalance between pro-apoptotic and anti-apoptotic proteins and their corresponding signals in cancer cells (Kandoth, C, et al., 2013). Apoptosis is a physiological mechanism occurred in a wide range of human diseases. Thus, a deregulation of apoptosis can lead to an accumulation of mutated or unwanted cells as well as an excessive depletion of a particular cell type. Numerous pro-apoptotic signal transducing molecules and pathological stimuli converge on mitochondria to induce mitochondrial outer membrane permeabilization (MOMP), followed by activation of pro-apoptotic proteins like Bcl-2 for regulation of the permeability transition pore leads to Apaf-1 activation and trigger the apoptotic caspases (Bhatti, K. et al., 2017). Apoptosis divided into two pathways (intrinsic and extrinsic), intrinsic pathway is initiated by the release of cytochrome C into the cytoplasm from the mitochondria, followed by activation caspase 9 as a result of that activating caspase 3. While the extrinsic pathway initiated by death receptors (DRs), followed by activation caspase 8 and 10 (Repsold, L. et al., 2017). Many anticancer peptides showed ability to induce apoptosis via targeting mitochondria for apoptosis modulation (Jacotot, D. et al., 2006). K4R-Nal2-SI peptide demonstrated apoptosis induction in different cancer cells and apoptosis hallmarks have been confirmed *in vitro* and *in vivo* as well by using xenograft mouse model (Chu, Y. et al., 2015).

**(C) Necroptosis.**

Necroptosis is programmed or regulated necrosis cell death through activation of independent caspase as a new strategy to treat cancer. The signaling pathway of necroptosis based on the cooperation between (RIP1 and RIP3) receptor-interacting protein kinase and MLKL, mixed lineage kinase domain-like protein to form necrosomes, which give rise to caspase 8 inhibition (Su, Z. et al., 2016). Tumor necrosis factor (TNF) also mediates and regulates necroptosis process through recruitment of RIP1, thus TNF can regulates signal transduction to promote mitochondria generation followed by typical events of necrosis (Galluzzi, L., et al., 2011). RIPK1 is an important kinase-dependent receptor, in order to it can inhibits or stimulates necroptosis through scaffolding function. RIPK1 and RIPK3 are able to make auto-transphosphorylation to each other in absence of active form of Caspase 8, resulted in eviction of cellular contents into the extracellular (Pasparakis, M. and Vandenabeele, P. 2015).

Necroptosis is an alternative cell death mechanism induced after treatment with chemotherapeutic agent to overcome obstacle of drug resistance (Chen, Y. et al., 2016). TAT-RasGAP317-326 is a cell permeable peptide, inducing necroptosis in different malignant cell lines in vitro and also showed the ability to prevent metastatic progression *in vivo* (Heulot, C. et al., 2016). TAT-RasGAP317-326 cell death mechanism based on loss integrity of cell membrane, because of the peptide could be a bind or interact with signaling necroptosis proteins like RIP in the inner side of the membrane (Poon, B. et al., 2014).

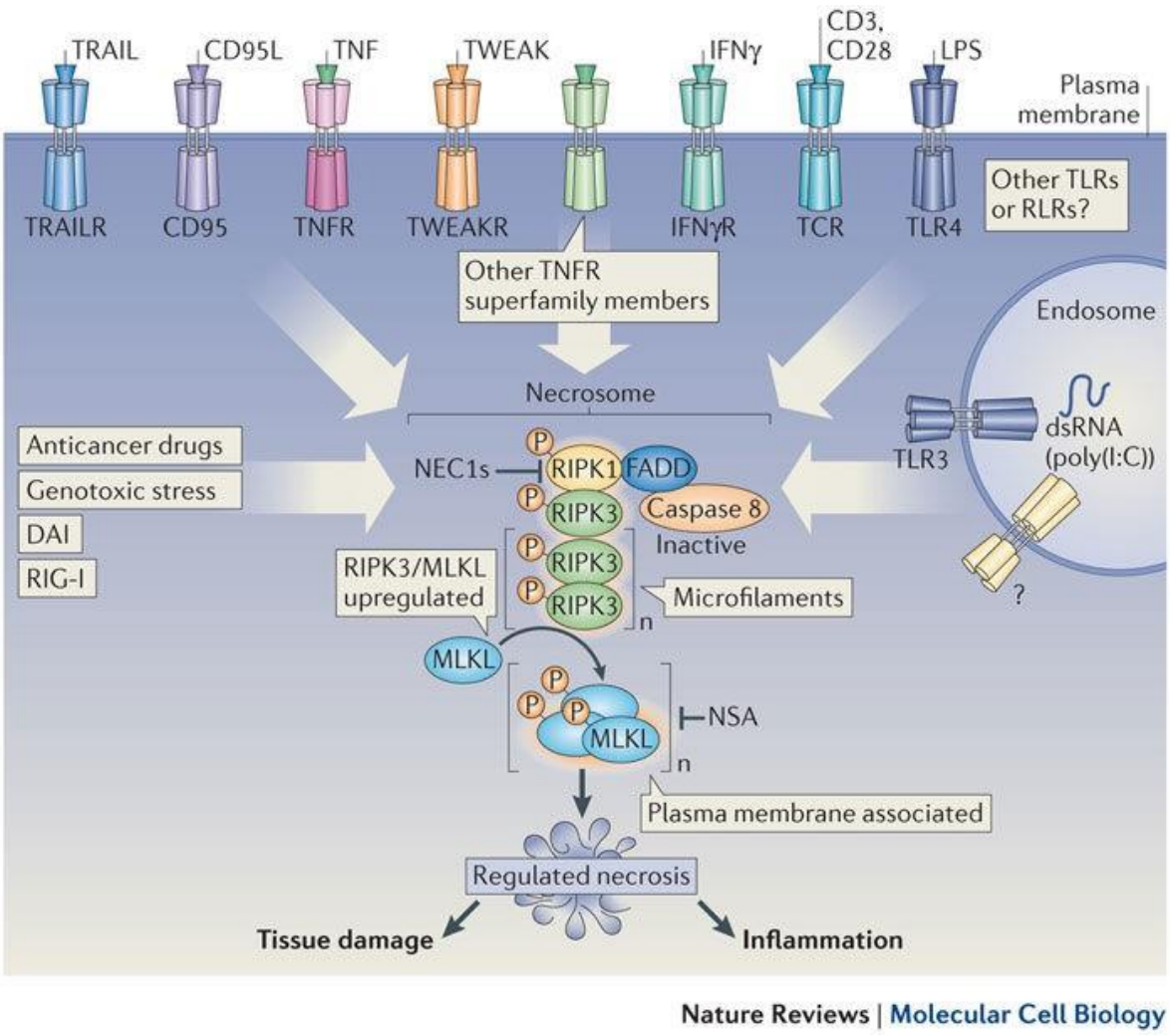


Figure 4. Necroptosis molecular pathway, Pasparakis and Vandenabeele (2015)

**(D) Necrosis.**

Necrosis is kind of cell death mechanism caused by toxins and pathogenic microorganisms infection, which resulted in unregulated elimination of cell components and then leads to immune response. Morphology of necrosis is characterized by cell membrane disruption followed by swelling of organelles, and eventually release of intracellular signals to initiate inflammation in the surrounding tissue (He, W. et al., 2009). AMPs were demonstrated ability to induce necrosis cell death in many types of cancer cells via alteration membrane fluidity and surface of cancer cell (Chu, Y. et al., 2015). DK6L9 is lytic peptide induced necrosis and antiangiogenic effect through cell membrane disruption and diminished tumor

vessels thickness (Papo, S. et al., 2006). MPI-1 peptide triggers to cancer cells, resulting in a necrosis through swelling of cell membrane followed by rupture (Zhang, L. et al., 2010).

**(E) Autophagy**

Autophagy is self-eating process happens in almost organisms, also known as regulated and destructive mechanism of unnecessary cellular components, caused by ATG proteins of signaling cascades to form autophagosome, which surround unnecessary organelles for degradation by acidic hydrolases released from lysosome. Autophagy plays a vital role in starvation and cellular stress through utilizing degradable proteins for biosynthesis of necessary and essential protein for bioenergetics, surviving and recovery process (Oberst, A. 2013).

**(F) Autophagy and Necroptosis.**

Defects in necroptosis related genes contributed to the pathological process of human malignancies. Deubiquitination of RIP1 by CYLD is important for the formation of complex II, leading to either apoptosis or necroptosis (Alameda, J.P et al., 2010). Several chemotherapeutic agents like alkylating agents induce necroptosis and DNA damage that leads to overcome cancer cell resistance (Mourtada, R. et al., 2013). Naphthoquinone compound (Shikonin) is a natural plant product that showed ability to induce necroptosis in different cancer cells *in vivo* and *in vitro* (Han, W. et al., 2007).

The opposite correlation between both cell mechanisms, through inhibition of necroptosis using necrostatin-1 leads to activation of caspase-8 and RIP1 cleavage, give rise to stimulate autophagy process, which cause restoration of cell division and increased cancer cell survival (Bell B.D. et al. 2008). Moreover, inhibition of autophagy process using 3-MA inhibitor, leads to enhancing of necroptosis signaling RIP1 activity, resulting in cell death (YuL. et al. 2004). TAT-RasGAP317-326 peptide is an antimicrobial peptide and also potent anticancer peptide induced cytotoxic effect in different cancer cells. It was able to mediated tumor cell death by autophagy activation in human neuroblastoma cells (NB1) and Burkitt's Lymphoma cells (Raji), followed by inhibition of apoptosis and necroptosis signaling pathway (Heulot, M. et al., 2016). By contrast, FK-16 peptide demonstrated induction of two cell mechanism in parallel in HCT116 colon carcinoma cells through autophagy

induction by overexpression LC3 protein, and also activation of caspase-independent apoptosis via p53-Bcl2/Bax pathway (Ren, S. et al., 2013).

### 2.12. Wolf spider venom as source of natural products to anticancer drug discovery

Spider venoms are a rich source for a novel antimicrobial peptides (Wang, Y. et al., 2016). LyeTx I, an antimicrobial peptide identified and isolated from the venom of wolf spider *(Lycosa erythrognatha)*. LyeTx I has been shown to be an active antimicrobial agent against pathogenic fungi and like *C. krusei* and *C. neoformans* and also pathogenic bacteria like *E. coli* and *S. aureus* (Santos, D. M et al. 2010). The microbiological test exerted that N-terminal modification did not affect on bacterial growth, while, the C-terminal modification exhibited a high bacterial growth inhibition, with low MIC. For example, S. aureus MIC was 5.05 $\mu mol.L^{-1}$ and E. coli MIC was10.10 $\mu mol.L^{-1}$ (Fuscaldi, L. et al., 2016). The secondary structure of LyeTx I shows a small random-coil region at the N-terminus followed by an alpha-helix that reached the imitated C-terminus, which might favor the peptide-membrane interaction. The high activity against bacteria together with the moderate activity against fungi and the low hemolytic activity have indicated LyeTx I as a good prototype for developing new antibiotic peptides (Reis, P. et al., 2018).

LyeTx I_b is a potent antimicrobial effect against Gram-positive and Gram-negative bacteria. LyeTx I_b exhibited more efficiency in killing of bacteria than the LyeTx I original peptide formulated tested by Consuegra et al. (2013). In mouse septic arthritis's model induced by *S. aureus*, LyeTx I_b decreased the bacterial load compared to control and Clindamycin groups, and also exhibited a high efficacy through decreasing the number of mononuclear cells and neutrophils, accompanied by reducing of the cytokine IL-1β and chemokine CXCL-1 levels and prevented cartilage damage as well in treated group (Dos Reis, P.M.V. et al., 2018).

**Cell penetrating peptides role in treatment of Glioblastoma**:

Treatment of malignant tumors is usually followed by poor prognosis and relapse due to the existence of extravascular core regions of the tumor. Cell-penetrating peptides (CPPs) have gained interest because of promising properties in drug delivery field, which could be used as a noninvasive method and targeting malignant tumor specifically in a tumor origin-

dependent manner (Kondo, Saito et al. 2012). The importance of new strategies for chemotherapy of glioma patients by crossing of various chemotherapeutic agents through blood brain barrier (BBB) that leads to increase survival rate (Gao, Y. et al., 2014).

Although cell penetrating peptides are used broadly for neoplasm drug delivery, but there is a limit application, due to the non-selectivity between tumor and healthy cells (Guo, Z. et al., 2016). R8-dGR is an effective cell penetrating and dual target peptide trigger to glioma tissues by intratumoral diffusion route of administration (Liu, M. et al., 2016). In a similar study, cell penetrating transferrin peptide is multifunctional peptide conjugated with liposome contain doxorubicin anticancer agent for delivery (Transferrin/TAT-Liposome-DOX) this formulation increased cellular uptake from doxorubicin in the brain through blood brain barrier in C6 glioma rat model. Transferrin/TAT-Liposome-DOX formula also showed potent anti-proliferative effect against glioma cells and besides a good bio-distribution. Thus, Transferrin/TAT-Liposome could be used as a promising anticancer drug delivery during glioma treatment (Zheng, M. et al., 2015). The R3V6 peptide is a cell penetrating peptide that can carry antisense oligodeoxynucleotide into glioma cells in animal C6 glioma model. It was induced apoptosis cell death, in order to the peptide and antisense were able to inhibit miR-21 gene expression of tumor-promoting genes in glioma cells. Subsequently, the R3V6 peptide might be efficient to deliver of antisense into glioma cells (Oh, S. et al., 2017). Using peptides in targeted personalized therapy would be one step forward and may offer new avenues for glioma therapeutics (Wanjale and Kumar. 2016).

### 2.13. Therapeutic peptides for breast cancer treatment

Chemotherapy is based on cytotoxic drugs use, which may be administered in both advanced and early-stage breast cancer, and can be useful after or before surgery (Hassan, M. et al., 2010). The most common drugs used after or before surgery (adjuvant and neoadjuvant) are paclitaxel, doxorubicin, cyclophosphamide, 5-fluorouracil, carboplatin and cisplatin to kill cancer cells that might have been left behind (Ejlertsen, B. 2016). Even though, chemotherapy outcomes continue to improve, but still there are long side effects of chemotherapy for many patients like menstrual changes, cardiotoxicity, neuropathy, neurotoxicity, cognitive function and eventually increasing of leukemia risk. It is relevant to identify the patients who may get benefit from cytotoxic drugs (Tao, J. et al., 2015). Although hormonal therapy based on estrogen receptor (ER) inhibitors such

as Tamoxifen, raloxifene and aromatase inhibitors might be effective to prevent breast cancer, it also has shown serious side effects like stroke and pulmonary embolism (Jordan, V. C., 1993).

Immunotherapy has emerged as an important strategy to treat breast cancer in the last decades, due to their benefits like tolerable toxicity profile and selectivity. For instance, passive immunotherapy using anti-HER2 monoclonal antibody (Herceptin or trastuzumab), which targeting tumor-specific protein associated with forming of micrometastases, resulted in great clinical outcome in metastatic breast cancer patients (Schneble, E et al., 2015). Moreover, immunotherapy may blockade immune checkpoint via inhibiting T lymphocyte-associated protein 4 (CTLA- 4), modulates cell motility and signaling AKT/PI3 pathway (Knieke, K. et al., 2012). Monoclonal antibodies (mAb) used for programmed death-ligand 1 (PD-L1) blockade is an important strategy to fight breast cancer through suppressing T-cell inflammatory activity (Vonderheide, R. et al., 2017). On the other hand, passive immunotherapy can be causing autoimmune diseases and anaphylactic shock by activation of the host's immune system (Verma, S. et al., 2012).

There is an urgent need to find out novel chemotherapeutic agents to overcome adverse effects of conventional anticancer drugs. For instance, doxorubicin and paclitaxel are widely used to treat breast cancer but they cause cardiotoxicity, neurotoxicity and renal injury (Ponnusamy, L. et al., 2016). Moreover, drug resistance occurs in 30% of the women diagnosed with metastatic breast cancer stage, and its overcoming is still a challenge (Rivera, E., & Gomez, H. 2010).

Survivin is an inhibitor of apoptosis protein and plays a crucial role in breast cancer drug resistance, particularly late metastatic stage. It plays a role inhibiting activation of caspases and thus it can be able to downregulate cell programmable death and promotes mitosis process by interacting with tubulin (Sah, N. et al., 2018). SU18 and SU22 synthetic peptides are novel helper epitope peptides which binding with survivin protein in order to enhance apoptosis, cellular and humoral immune responses in breast cancer patients (Ohtake, J. et al., 2014).

Somatostatin (SST) is mainly localized in the central nervous system but overexpressed in breast cancer tissue, thereby targeting SST receptor gives rise to inhibiting of cell growth and proliferation by inducing apoptosis (Watt, H. et al., 2008). In addition, SST peptides are utilizing for tumor visualization of breast, bone and prostate metastatic lesions by PET/CT imaging (Cook, G. 2010). Octreotide peptide has been shown a high affinity towards the somatostatin receptor and

inhibits tumor regression in human primary colon tumor and breast tumor xenografts in vivo (Prasad, S. et al., 2006).

LyP-1 is a cyclic 9-amino-acid peptide, which is able to recognize lymph nodes contain breast cancer cells without recognizing lymph nodes in normal tissues. In addition, LyP-1 can bind with breast cancer cells effectively in triple-negative breast cancer patients, whose cells not produce or express HER-2, estrogen, and progesterone. LyP-1 peptide could be used as a contrast agent in magnetic resonance imaging (Abulrob, A. et al., 2017).

### 2.14. The 4T1 mammary adenocarcinoma model in drug discovery process

Murine models are a useful tool for researchers and oncologists in order to mimic the pathology and understand the spread of breast cancer. 4T1 murine mammary carcinoma model have been used as a non-surgical model that induces tumor metastasis spontaneously in the animal with similar human kinetics (Paschall, A. & Liu, K. 2016). Moreover, it is relevant to highlight that in 4T1 model, animals develop mammary carcinoma, which corresponds to stage IV human breast cancer (Kocatürk, B. & Versteeg, H. 2015), and making it a good model of human metastatic breast cancer.

Currently, many spontaneous breast metastatic models have been studied to understand the molecular mechanism of tumor invasion and progression for developing new anticancer agents (Kocatürk, B. & Versteeg, H. 2015). The 4T1 model is aggressive transplantable mammary adenocarcinoma induced by inoculation of 4T1 cancer cell line into BALB/c mice. It is the best model to study breast cancer metastasis, in order to similarity to lymph node drainage of human breast cancer. In addition, in this model, metastasis can be progress spontaneously and rapidly from a primary tumor to different distant organs like lung, brain, liver, kidney and lymph node (Pulaski, B. & Ostrand-Rosenberg, S. 2001). Furthermore, 4T1 model is very sensitive in quantifying proliferation and spreading of breast cancer cells to distant organs. Subsequently, it is considered an excellent model for testing anti-metastasis drugs and immunotherapeutic agents in vivo (Paschall, A. & Liu, K. 2016).

Although, many transgenic mouse models of human mammary cancer like C3(1)/Tag and c-myc are considered the best models to study mechanisms associated to metastasis *in vivo*, however these models are not suitable for testing anti-metastatic drugs due to high cost of long-term of drug

administration and also its take months for metastasis (Khanna, C. & Hunter, K. 2005). By contrast, 4T1 a transplanted breast cancer model has high capacity to metastasize efficiently in few days to get micrometastasis. Moreover, 4T1 allows tracking and quantitation of the cells in vivo easier than other models (Tao, K. et al., 2008).

### 2.15. Immunogenicity of 4T1 model

It has been reported that mammary carcinoma is an immunogenic tumor. In this immunogenic tumor the breast cancer cells could escape from immunity by down-regulation of tumor recognition or inhibiting immune surveillance process, e.g. inhibition or deletion of MHC and tumor-associated antigens. The lack of susceptibility to immune attack and immune dysfunction to promote localized immunosuppression in the tumour microenvironment (Stewart, T. & Abrams, S 2008). The overexpression of regulatory T cells (Treg), transforming growth factor (TGF-β), cytotoxic T-lymphocyte antigen (CTLA-4) and programmed death ligand (PDL-1) play an important role in tumor immunogenicity via inhibition of immune surveillance (Garcia-Lora, A. et al, 2003 & Lechner, M. et al., 2013). 4T1 transplantable tumor model has been shown a highly successful response to an immunotherapeutic agent associated with high tumor immunogenicity and enlargement of draining lymph nodes during metastasis (Abe, H. et al., 2016).

### 2.16. Leukocytosis in 4T1 model

Leukocytosis means a rising count of circulating white blood cells (neutrophils, monocytes, eosinophils, and lymphocytes) above the normal range. . Leukocytosis usually happens during infection and cancer (Rogers, K. 2011). 4T1 considered as high immunogenic mammary carcinoma model because of aggressive cancer cell growth, followed by expansion of all leukocyte populations, resulting in leukocytosis accompanying with splenomegaly due to granulocytic hyperplasia from bone marrow (Dupre, S., & Hunter, K. 2007). It has been shown undesirable side effects such as leukocytosis, thrombosis, and peripheral neuropathy via increasing of circulating leukocytes in the 4T1 murine model (Reis, D. et al., 2014).

## 2.17. Extravasation of leukocytes in tumor model

Extravasation is also known as diapedesis, a multistep process of migration of leukocytes or/and tumor cells from bloodstream into tissues through interaction between leukocytes and vascular endothelium. This process enables tumor cells to cross basement membranes, and to reach tissue parenchyma due to alterations of endothelial integrity and architecture damage (Strell, C. et al., 2008 & Madsen, C. D. et al., 2010).

The recruitment of leukocyte from microcirculation to endothelial interface is the hallmark feature of inflammatory process. It is well know that the recruitment of circulating leukocytes is a multistep cascade of events involving adhesion molecules. Leukocyte-endothelium interaction starts with leukocyte tethering and rolling along the venule before they can firmly adhere and emigrate out of the vasculature (Carvalho-Tavares, J. et al., 1999, 2000). Although, there is an equilibrium between rolling and adhered leukocytes in normal conditions, during pathological conditions, like tumorigenesis, and metastasis, the ratio of these steps is altered (Iadocicco, K. et al., 2002).

The bloodstream represents a hostile environment for CTCs, exposing them to rapid clearance by natural killer (NK) cells. Carcinoma cells gain protection through the actions of platelets, which coat CTCs. Neutrophils provide protection from NK cell attacks and contribute to extravasation of CTCs. Once into a capillary, activated platelets and carcinoma cells secrete mediators that can act on monocytes, endothelial cells, and the carcinoma cells themselves. All interactions promote the migration of tumor cells (Lambert, A. W., et al 2016). Then, metastasis is facilitated by leukocytes extravasation, since interactions between cancer cells and leukocytes/platelets lead to cancer cell adhesion. This interaction is mediated by selectin (CD62) cell adhesion glycoprotein family, which promotes tumor metastasis. In addition, P-selectin and E-selectin molecules over-expression became an indicator for poor prognosis in cancer patients (Laubli, H., & Borsig, L. 2010).

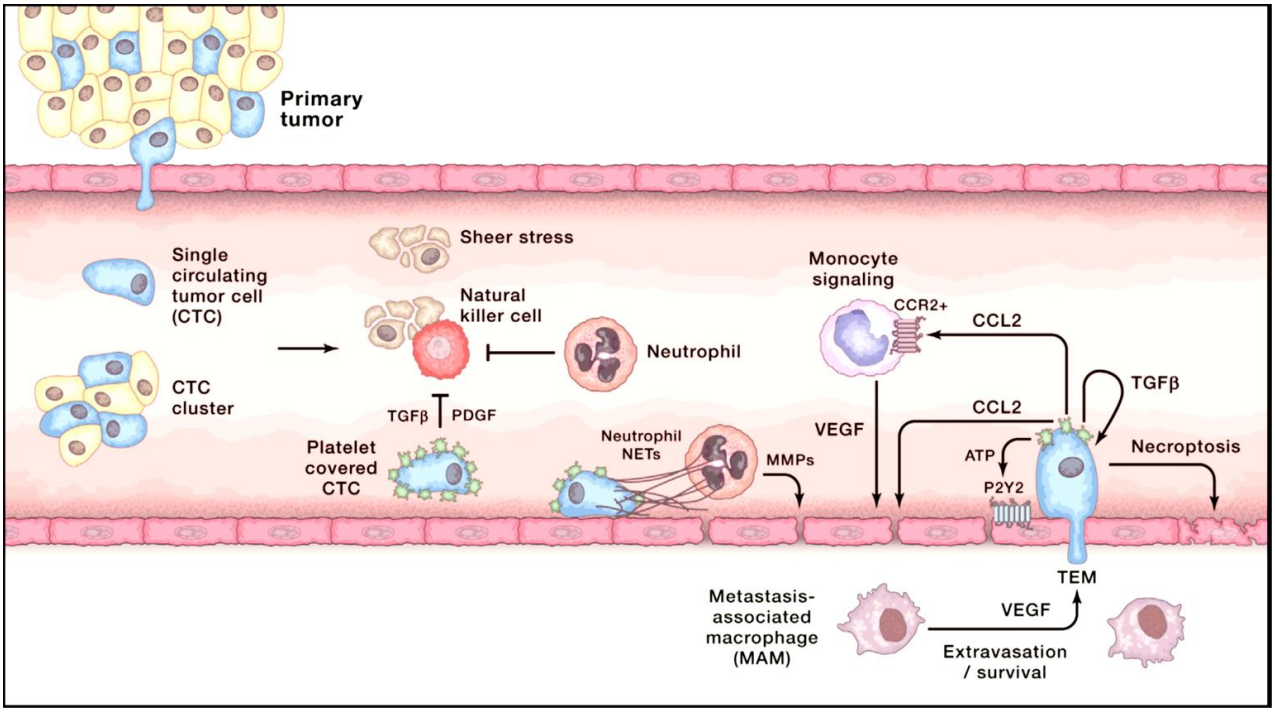


Figure 5: Intravascular interactions between circulating tumor cells (CTCs), neutrophils, endothelial cells and platelets (extracted from Lambert, A. W., et al 2016).

### 2.18. Imaging of 4T1 primary tumor and metastatic lesions by intravital microscopy

Intravital microscopy is an important experimental imaging technique, which can be able to identify various pathophysiological processes in all organs and vessels in living animals. For instance, examination of leukocytes recruitment and interactions after inducing inflammation in animal models such as experimental autoimmune encephalomyelitis (EAE) and inflammatory bowel disease (Herr, N. et al, 2015). In addition, many benefits of intravital microscopy has been demonstrated like quantifying of drug delivery and clearance, visualization of drug uptake and distribution, monitoring of tumor neovascularization, tracking of tumor progression in a live animal (Van de Ven, A. et al., 2013). Currently, targeting of primary breast tumor remains became an important goal during breast cancer treatment after resection of this tumor, resulting in an increased chance of patient survival. To achieve this goal, the intravital can be used for tracking remains of the primary tumor or even metastatic lesion through navigation of rolling leukocytes into tumor vasculature endothelium (Palomba, R. et al., 2016). On the other hand, to identify the underlying mechanism of tumor invasion might help in controlling and prevention of breast cancer metastasis. Intravital microscope provides high resolution and time-lapse images of breast tumor

microenvironment. This technique could be used to detect glycolysis in breast cancer remaining lesions, increased glucose uptake, decreased ATP production, and also oxygenated hemoglobin saturation in tumor vessels (Rasul, R. et al., 2018). Furthermore, intravital microscopy is using for measurement of mitochondria membrane potential in living 4T1 tumor-bearing mice. (Zhu, C. et al., 2017).

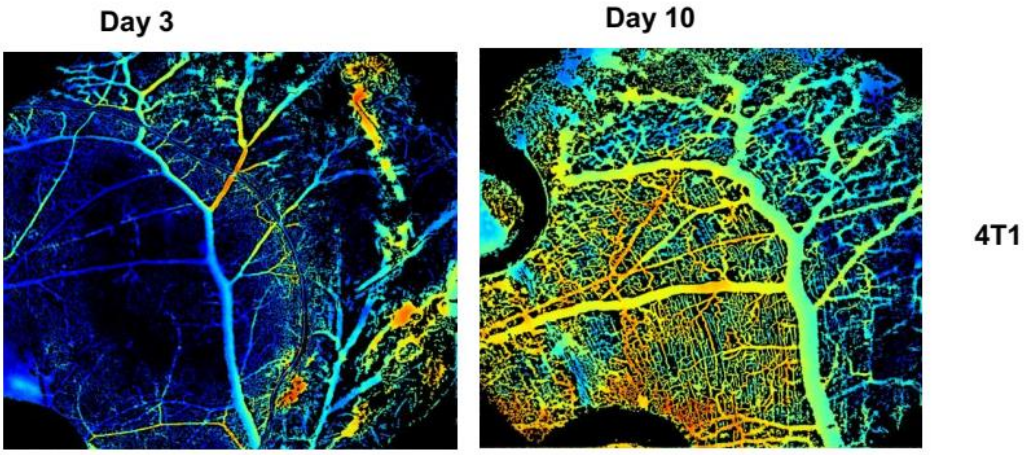


Figure 6. Intravital vascular images of hemoglobin oxygen saturation of 4T1 metastatic tumors on days 3 and 10 in thin and thick vessels (Rasul, R. et al., 2018).

### 2.19. Therapeutic peptides absorption by Subcutaneous Administration

Subcutaneous injection is a method to delivering bio pharmaceutics. Usually, subcutaneous injection is applied into the fatty layer beneath the skin. As subcutaneous tissue has few blood vessels, the injected drug is diffused very slowly at a sustained rate of absorption, i.e. distributing the drug over a long period of time (Kim, H. et al., 2017). Currently, subcutaneous route is a viable and favored method to deliver drugs alternative to intravenous administration. For example, subcutaneous injection achieved a successful outcome in the oncology field (Jones, G. et al., 2017).

In the last decades, the subcutaneous (SC) route of administration gained much interest for several biotherapeutics treatment like immunoglobulins, insulin, erythropoietin, growth hormone and fusion proteins, because the increaseof the bioavailability, voiding degradation by proteases (Richter, W. et al., 2012). Subcutaneous injection is an important route to deliver therapeutic proteins and peptide into systemic circulation by lymphatic system and blood capillaries depended

on molecular size and weight.For example, peptide presenting low molecular size or weight may cross through blood capillaries, whereas the high molecular size may be absorbed by lymphatic vessels and lymph nodes (Kagan, L. 2014).

Subcutaneous injection of anticancer drugs demonstrated low absorption and high bioavailability more than intravenous injection. For example, methotrexate, cladribine, omacetaxine, cytarabine, and bleomycin have been approved to inject subcutaneously in Europe (Leveque, D. 2014).

The chemotherapeutic agents administered subcutaneously and distributed by lymphatic vessels, lymph nodes, and blood circulation, have been shown efficacy and less toxicity than administered intravenously because of the crucial role of the lymphatic system in tumor microenvironment. Subsequently, anticancer drug delivery by targeting lymphatic tissues might be able to prevent migration of cancer cell and lymphatic metastasis (Zhang, X. & Lu, W. 2014).

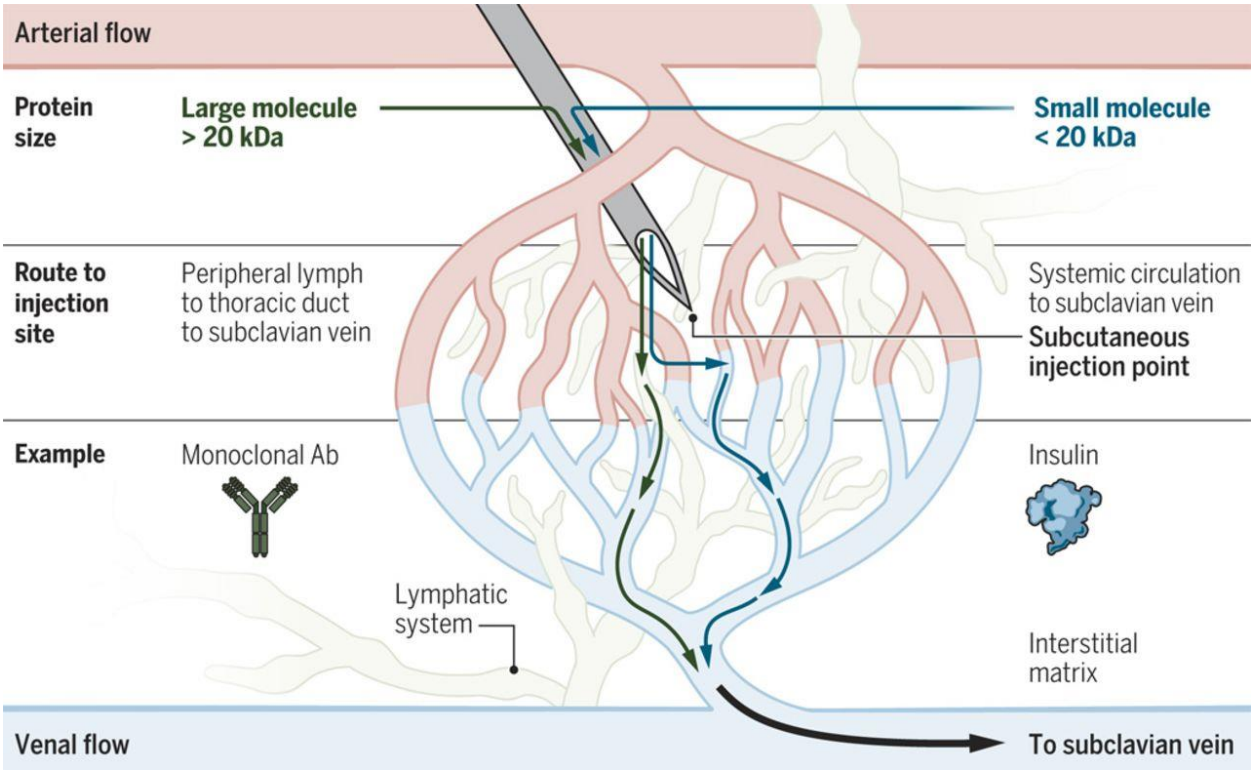


Figure 7. Protein size determines the choice of subcutaneous injection of drugs (Jones, G. et al., 2017).

## 2.20. Cationic peptide and selective for breast cancer cells

The cationic peptides are a type of s broad-spectrum antimicrobial peptides produced by different organisms. The relationship between structure and function of cationic peptide have been studied through the influence of peptide on mammalian and bacterial subcellular structures. Cationic peptides can interact with phospholipid bilayer to form pores or membrane disruption, resulted in cell lysis as shown in figure 4 (Huang, Y. et al., 2010).

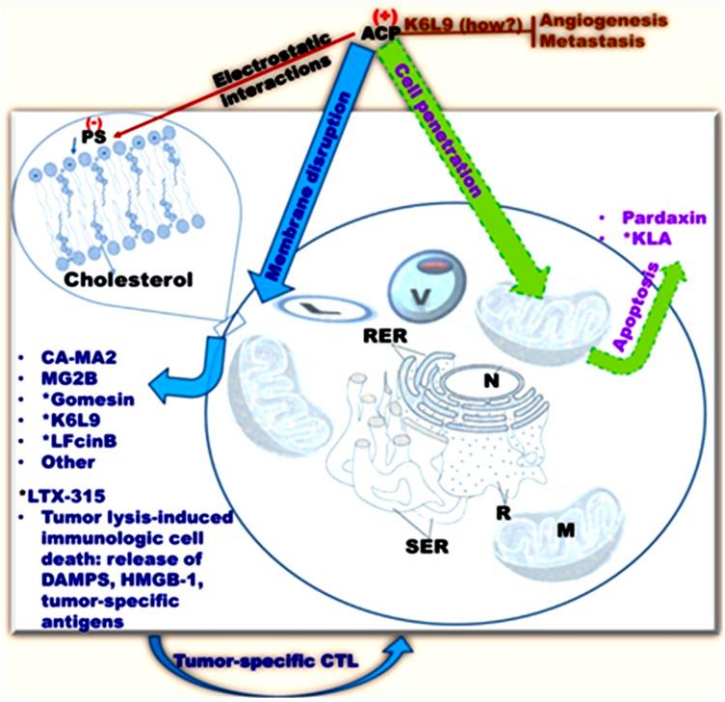


Figure 8. Anticancer mechanisms of cationic antimicrobial peptides (Deslouches, B. & Di, Y. 2017).

Breast cancer cell membrane surface contains a high proportion of negative charges from phospholipids (phosphatidylethanolamine and phosphatidylserine). Cationic peptides characterized by net positive charges from amino acids residues, and the attraction between positive and negative charges make electrostatic interactions, that facilitates penetration and membranolytic effects (Deslouches, B. & Di, Y. 2017).

K6L9 peptide is a cationic peptide induce cell membrane disruption in several cancer cell line in vitro. In addition, intratumoral injection of K6L9 peptide into B16-F10 murine melanoma and C26 colon carcinoma tumors, inhibited tumor growth and tumor reoccurrence in different in vivo models by necrosis induction (Cichoń, T. et al., 2014). Similar study showed that cationic peptide

LTX-315 induced cell membrane disruption and permeabilized mitochondrial membranes in the human osteosarcoma U2OS cell line. Furthermore, LTX-315 injected intratumorally into B16-F10 murine melanoma, stimulated an immune response by increasing of tumor-specific antigens, cytotoxic T-lymphocytes and large necrosis area in melanoma tissues (Zhou, H. et al., 2016).

A magainin II (MG2B) peptide is a cationic peptide isolated from skin secretion of African frog, which has been shown high affinity and selectivity toward several cancer cells with mild effect on normal cells *in vitro*. MG2B have been tested in MCF-7 breast cancer xenograft model, and have induced a remarkable reduction in tumor volume and weight, after intratumoral injection (Liu, S. et al., 2011).

## 3. Rationale of research:

Despite significant advances in the discovery of new strategies for cancer treatment, drug resistance is the second of the leading causes of death worldwide. There is an urgent need for the development of novel anticancer strategies. Among cancers, glioblastoma comprises the most common malignant brain tumor and patients presenting such tumor survive for less than two years (Mellinghoff, L. et al., 2017). Surgery, radiotherapy and chemotherapy are the main treatments but many patients are not cured and suffer with incapacitating pain. Therefore, new drugs to treat this class of tumors still are very important. Besides brain tumors, breast cancer is the most common women cancer over the world and the second leading cause of female cancer-related deaths. Long-term survival rates for patients with breast cancer are rising. Several studies have reported that increasing of survival rate in young women diagnosed with metastatic breast cancer than old ages, because of chemo and immunotherapy improvements (Mariotto, AB. et al., 2017). However, the fundamental issue is the challenge that patients with breast cancer have to deal with multiple long-term side effects of treatment protocol.

Nowadays peptides drugs emerge as a new class of promising anticancer reagents owing to their lytic nature and ability to avoid drug resistance (Szczepanski, C. et al., 2014). Peptides are an important class of therapeutics, with over 60 peptide drugs now approved in the US and other major markets (Fosgerau and Hoffmann. 2015). Cationic antimicrobial peptides also exhibit anticancer function, displaying advantages such as low toxicity (Dalzini, A. et al., 2016). These anticancer peptides have many features such as mild toxicity without accumulation in different tissues and eventually a possible selectivity and specificity for cancer targets and receptors. However, peptides have some limitations to apply in clinical scale like poor oral bio-availability and metabolism, fast clearance, besides value of manufacturing process is still very costly. Thus it is necessary to find new strategies to overcome these limitations through increasing of therapeutic activity compared to other conventional chemotherapy (Marqus, S. et al., 2017).

In this context, our group synthetized a cationic peptide named LyeTx-I, first isolated from the venom of the spider *Lycosa erythrognatha* that displayed an interesting antimicrobial activity (REIS, P. 2015). The peptide consists of 25 amino acid residues and carries a natural carboxylterminal (C-terminal) carboxyamide (HIWLTALKFLGKNLGKHLAKQQLAKL-NH2).

Considering the great challenge to treat tumors in the central nervous system (CNS), as well to treat metastatic breast cancer, we hypothesize that LyeTx I-b antimicrobial synthetic peptide is a potential prototype to develop a new anticancer agent. To verify this hypothesis, we performed an initial screening to evaluate the cytotoxicity of this peptide against human cancer cells representative of solid tumors and leukemia. Cells from brain and breast tumors were used (including the murine 4T1) to predict antitumor potential *in vitro*. Unspecific cytotoxicity was evaluated using non-tumoral cells. Once we focused in brain tumors, the human Glioblastoma lineage U87 MG was selected to study the type of cell death triggered by peptide to get insights regarding probable cellular targets, *in vitro*. Neurotoxicity using the lineage Luhmes was also investigated. Once the *in vivo* model of brain tumor was not available, studies to confirm the in *vitro* findings with U87 MG cells were not performed.

The second focus was to investigate the anticancer potential of peptide in *vivo* using the 4T1 metastatic murine model of triple-negative breast cancer to evaluate the potential of LyeTx-I to be used to develop new chemotherapic to treat tumors. For that, subacude toxicity, assessment of tumor growth and volume, animal weight, immunological parameters and growth factors were investigated. All these strategies allowed to propose the potential of LyeTx-I as a prototype useful to develop drugs to glioblastoma and metastatic breast cancer treatment.

For a better understanding, this thesis was divided into three chapters:

**Chapter 1:** Cytotoxicity studies evaluating the effect of peptide on viability of some tumor and non tumoral cell lines, including cells from brain and breast tumors. In this chapter some insights on the cytotoxic effect of peptide against murine 4T1 breast cancer cells were performed to predict the prospective efficacy *in vivo*.

**Chapter 2:** Characterization of the type of cell death induced by peptide against glioblastoma cells, U87 MG, through biochemical and morphological studies. These studies were carried out considering the importance to discover new drugs to treat brain tumors.

**Chapter 3:** *in vivo* studies to evaluate the safety of the peptide by assessment of sub-acute toxicity and antitumor activity using the 4T1 triple-negative breast cancer mouse model.

## 4. General objective:

The overall aim is to evaluate the *in vitro* cytotoxic cellular mechanism of a synthetic cationic peptide LyeTx I_b and its potential anticancer effect *in vivo*.

**Specific objectives:**

I. To evaluate the cytotoxicity of synthetic peptide (LyeTx I_b) against tumor cell lines from brain tumors (glioblastoma, astrocytoma, and neuroblastoma), breast (MCF-7, MDA-MB-231,and 4T1), colon (HT-29), leukemia (HL60, Jurkat and THP-1), as well as against non-tumor cells (Vero, GM637 and human PBMC).

II. To evaluate the neurotoxicity of the peptide using as a model the Human Mesencephalic (LUHMES) cell line comparing it with other anticancer agent used in clinic.

III. To investigate if the cytotoxicity of peptide against glioblastoma lineage U87-MG is associated with alteration in cell cycle and induction of cell death by apoptosis, autophagy, necrosis and necroptosis.

IV. To investigate the cell death induced by the peptide in U87-MG cells through determination of molecular, biochemical and morphological alterations.

V. To verify whether the cytotoxicity of LyeTx I-b is associated with the induction of apoptosis in 4T1 cells and its effect on the clonogenic survival of these cells to expect the possible efficacy during *in vivo* studies.

VI. Evaluate the systemic sub-acute toxicity and tolerance of LyeTx I-b peptide in BALB/c mice.

VII. To assess the antitumor effect of LyeTx I-b peptide using the murine model of triple negative breast cancer 4T1, after administration intra-tumor and subcutaneous, through evaluation of:

- Growth of tumor (weight and volume) and metastasis in lung.
- Impact in immune cells (neutrophils, lymphocytes, monocytes and eosinophils).

VIII. Investigate the role of LyeTx I-b peptide on inflammation specifically leukocyte recruitment (rolling and adhesion) and production of their cytokines and growth factors such as VEGF, TGF-β, TNF-α, IL-1β, IL-10 and IL-6 .

# Chapter 1

## Cytotoxic effect of the cationic peptide LyeTx I_b against tumoral and non tumoral cell lines.

## Hypothesis

The cationic antimicrobial peptide LyeTx I-b peptide possess cytotoxicity against tumoral and non-tumoral human cell lines from human and mice.

## 1. Materials and Methods

### 1.1. Peptide

Peptide LyeTX I_b sequence is (IWLTALKFLGKNLGKLAKQQLAKL), it was synthesized by GenOne (Rio de Janeiro, RJ, Brazil) and purification grade by using HPLC was 98%. The samples were maintained at -80° C and solubilized in PBS immediately before the experiments.

### 1.2. Cell lines

Human glioblastoma U-87 MG, Neuroblastoma SHSY5Y and Colorectal Adenocarcinoma HT29 cells were kindly donated by Dr. Marcel Leist/University of Konstanz, Germany. Astrocytoma U-373 cells were donated by Dr. Rodrigo Resende/ICB/UFMG. Cells were maintained in culture in DMEM high glucose medium, supplemented with 10% fetal bovine serum and incubated at 37°C in atmosphere of 5% CO2 enriched with 2 mM L-Glutamine (GIBCO UK, Grand Island, NY), 1% antibiotic solution (100 IU / ml penicillin and 100 µg / ml streptomycin (GIBCO BRL, Grand Island, NY). The GM-637cells (donated by Dr. Adriana Abalen, ICB/UFMG) were used a model of normal human lung fibroblasts cells from School of Medicine, New York University. USA. This lineage was maintained in the logarithmic phase of growth in DMEM supplemented with 100 IU/mL penicillin and 100 µg/mL streptomycin (GIBCO BRL, Grand Island, NY) enriched with 10% fetal bovine serum. VERO (African green monkey kidney cells) lineage was used as a model of normal cells and was kindly provided by Dr. Erna Kroon (Universidade Federal de Minas Gerais, UFMG). This lineage was maintained in the logarithmic phase of growth in DMEM supplemented with 100 IU/mL penicillin and 100 µg/mL streptomycin (GIBCO BRL, Grand Island, NY) enriched with 5% fetal bovine serum. VERO cells were maintained at 37 °C in a humidified incubator with 5% CO2 and 95% air. Leukemia cells HL60 (human promyelocytic leukemia) THP-1 (human monocytic leukemia) and Jurkat (human lymphocytic leukemia) were donated by Dr. Gustavo Amarante-Mendes (University of São Paulo). The MCF-7 and MDA-MB-231 (human breast carcinoma) lineages were kindly donated by Prof. Dr. Alfredo Goes

(Department of Biochemistry - UFMG). Leukemia cells were maintained in RPMI medium (Sigma Aldrich, USA), containing 10% fetal bovine serum (GIBCO BRL, Grand Island, NY), enriched with 2 mM L-Glutamine (GIBCO UK, Grand Island, NY), 1% antibiotic solution (100 IU / ml penicillin and 100µg / ml streptomycin (GIBCO BRL, Grand Island, NY). For all lineages, cells were splitting twice weekly, and the cells were regularly examined and used until 15 passages.

The mice 4T1 mammary adenocarcinoma cells were kindly donated by Dr Miriam Teresa Paz Lopes, from Department of Pharmacology, Federal University of Minas Gerais (UFMG. The cells lines were cultured in DMEM medium supplemented with 10% fetal bovine serum, 1% antibiotic solution (100 IU/ml penicillin and 100 µg/ml streptomycin) (GIBCO BRL, Grand Island, NY), and incubated at 37°C, in 5% $CO_2$.

All of the cell lines used were examined by PCR to check mycoplasma, the experiments were done between 5 to 15 passages for avoiding changes of the phenotype. All cells were cryogenically preserved using 45% of fetal bovine serum plus 45% DMEM or RPMI and 10% DMSO.

### 1.3. Human Peripheral Blood Cells

Human peripheral blood mononuclear cells (PBMC) were obtained from six healthy donors. About 30 mL of blood was collected from each individual and added in heparinized tubes. This project was approved by COEP, under protocol number 666.658/2016. All healthy donors provided written consent.

### 1.4. Cytotoxicity of LyeTx I_b peptide in tumoral and non-tumoral cell lines

#### 1.4.1. Screening using tumor and non-tumor cell lines.

Nine human lineages including: U-87 MG, U373, GM637, SHSY5Y, MCF-7, MDA-MB-231, HT29, VERO, GM-637 and one murine breast cancer (4T1 cells) were used at the density of 10.000 Cells per well (96-well plate) the viability of cells was checked by exclusion with Trypan blue (> 90% viable), which stains only dead cells. The viable cells number was determined by using a Newbauer chamber. Leukemia cells were seeded at densities of 50,000 (HL60) and 100.000 cells/well (Jurkat and THP-1). All lineages were incubated overnight for recovery and adherence in order to reach exponential growth phase. After stabilization, all cells were incubated for 48 hours in presence of different concentrations of the peptide (1.5 to 100µM), in order to

determine the concentration that inhibits 50% of viability (IC50), for each lineage. Three experiments in triplicate were performed and solvent PBS diluted in culture medium was used as a control.

### 1.4.2. Evaluation of cell viability and proliferation assay, MTT method.

MTT assay is a standard colorimetric assay, in which mitochondrial activity is measured based on the metabolic reduction of 3- (4,5-dimethylthiazol-2-yl) -2,5-diphenyltetrazolium bromide (MTT) to formazan by mitochondrial dehydrogenases in viable cells only and allows to evaluate both cell proliferation and viability as described by Monks, S. et al. 1991 and Mosmann, L. 1983, with modifications. After treatment of the various lineages for 48h in presence of the peptide, 2.5 mg/mL of MTT (Sigma® Co., USA) (30µl/well) were added. The plates were incubated for 4 h at 37 ºC with an atmosphere of 5% CO2 until getting formazan crystals, the supernatant was removed by syringe needle coupled with suction pump to preserve crystals, 200µl from solution of 0.04 HCL isopropanol were added. Stringing gently for 5 min at room temperature, absorbance of solubilized MTT formazan product was spectrophotometrically measured at 595 nm, on an ELISA reader (Spectramax-Molecular Devices®). The results were expressed as percentage of the viable cell and the y-axis values relative to the control (PBS) considered as having 100% viability. The IC50 values were calculated by nonlinear or linear regression using GraphPad Prism® Version 5.01 software (GraphPad Software Inc., La Jolla, CA, USA) and data were analyzed with sigmoidal dose response. The results were expressed as percent of inhibition of cell viability over the negative control (PBS or DMSO), calculated as follows:

Inhibition of cell viability = 100- [(sample x100)/ PBS]

Interactions between peptide and medium were estimated based on the differences between the medium containing the peptide and the medium free of substances to avoid false-positive and false negative. No interference was observed.

### 1.5. Evaluation of cytotoxic activity in human peripheral blood mononuclear cells.

PBMC from 6 healthy individuals (4 females and 2 men) were isolated by Ficoll paque (sodium diatriazoate) gradient separation solution centrifugation (LSM; Organon Teknica, Charlesnton, S.C.) as previously described (Gomes, B. et al., 2003). The cells were washed in RPMI 1640 medium and cultured in flatbottom 96-well plates (Nunc Brand Products). Proliferative responses were evaluated by incubating 2.5 ×105 cells/well in presence or not of the peptide or phytohemaglutinin (2.5µg/mL), to stimulate the cells in a final volume of 200 µL of complete RPMI-1640 (10% FBS, 2mM L-glutamine, 100 IU / ml penicillin and 100 µg / ml streptomycin). Incubation was carried out in a humidified 5 % CO2 incubator at 37 °C for 3 days for PHA-stimulated cultures. Peptide was evaluated using eight serial dilutions 1: 2 (100-1.56 µM) for determination of the IC50.The cell viability was evaluated by the resazurin assay (O'Brien, W. et al., 2000).The concentration-response curves were obtained through non-linear regression using GraphPad Prism® Version 5.01 software.

### 1.6. Evaluation of cell viability of human PBMC by the resazurin assay.

The cell viability assay was performed according to (O'Brien, W. et al., 2000) with modifications. The resazurin is blue and when added to the cell culture is converted to the reduced form called resofurin, pink and fluorescent, which can be measured by colorimetric or fluorimetric. In the experiment, in each well, after treatment time, 20 µL of 0.6 mM resazurin solution. The plates were incubated in a CO2 incubator at 37 ° C for 48 hours. The spectrophotometric reading of the absorbance was performed in two wavelengths 570 and 600nm in the plate reader (Spectramax-Molecular Devices®). The number of viable cells correlated with the percentage reduction of resazurin and were expressed as % inhibition as follows:

$$\% \text{ inhibition} = 100 - \frac{(\text{Abs of Samples } 570\text{nm} - \text{Abs of samples } 600\text{nm})}{(\text{Abs of Control } 570\text{nm} - \text{Abs of Control } 600\text{nm})}$$

In this formula, all absorbance values must all be decreased by the absorbance value of the corresponding blank.

### 1.7. Determination of hemolytic activity.

The effect of LyeTx1_b peptide on human red blood cells (RBCs) was evaluated by a hemolysis assay (Yu, M. et al., 2011). Briefly, 1ml of fresh peripheral blood from 5 healthy volunteers was added with 400µl of heparin (5000 IU/ml) and centrifuged at 1200 rpm for 10 minutes at room temperature. The RBCs were further washed three times with sterile PBS and prepared in 1% (v/v) suspension of erythrocytes in PBS. 190 µl of diluted RBCs were seeded in a 96-well plate with 10µl of LyeTx I_b peptide in range of 100 to 1.56 µM in the experimental groups, with 100µl of 2% (v/v) Triton X-100 in positive control group, or with 10µl of PBS in negative control group. After incubation at 37 °C for 1 hour, samples were centrifuged at 1200 rpm for 5 minutes, and then 150 µL were transferred from each well to new 96 well/ plate and the absorbance was measured at 450 nm using a microplate reader (Spectramax-Molecular Devices®). The percent of hemolysis was calculated as:

Hemolysis %= [(Sample absorbance – negative control)/ (positive control – negative control)] X100.

The scheme below summarizes the methodological strategies used in cytotoxicity studies for tumor and non-tumor cells and hemolysis.

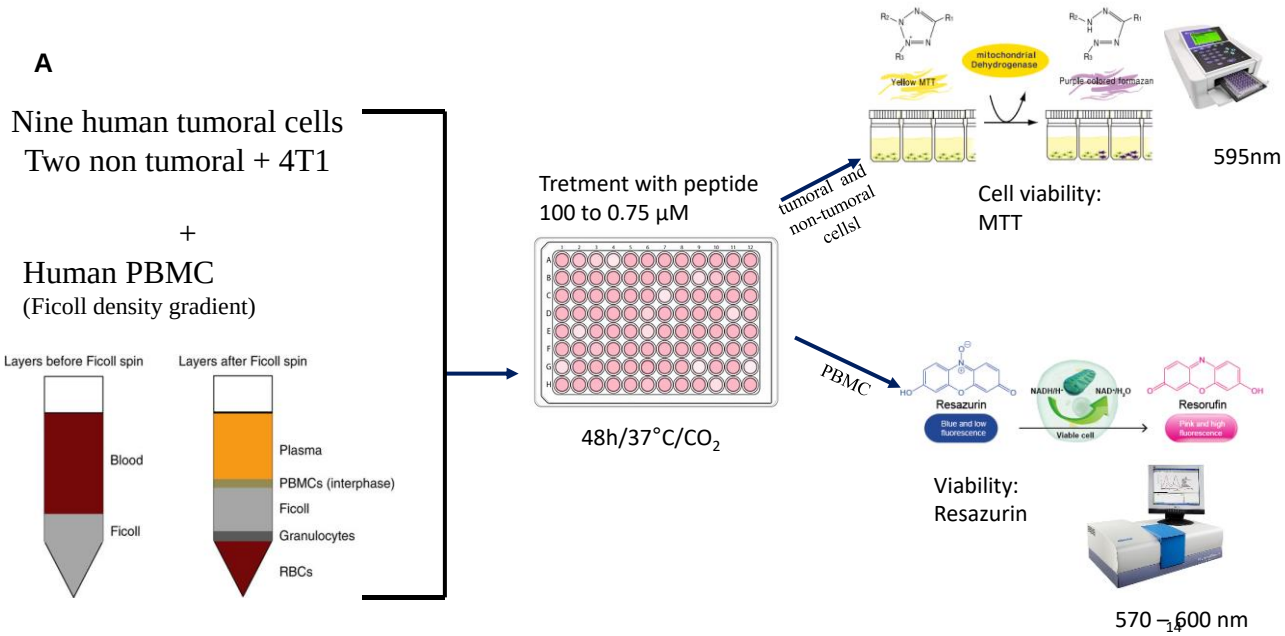


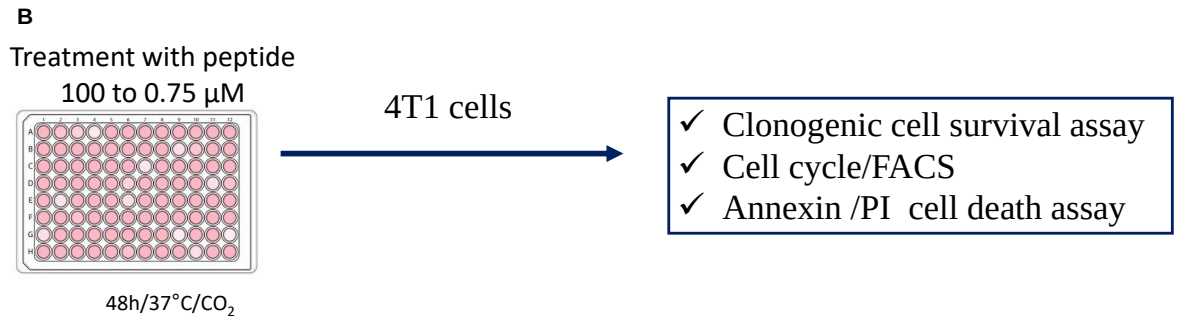


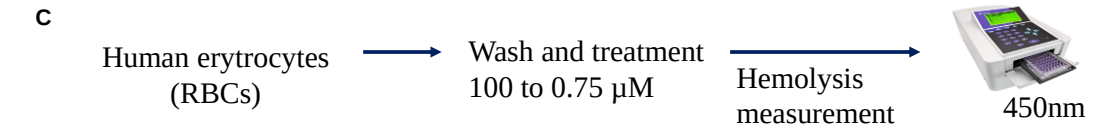


Scheme 1. Methodological strategy for the cytotoxicity assays using tumoral and non tumoral cell lines: (A) studies with all lineages and PBMC; (B) studies with 4T1 cells and (C) evaluation of hemolysis. Three independent experiments were performed in triplicate.

### 1.8. Evaluation of the clonogenic survival of 4T1 cells after treatment with peptide

Clonogenic assays were used to evaluate a potential efficacy of peptide in vitro that can correlate with a potential anticancer activity *in vivo*. 4T1 model used for those studies as a murine breast cancer model. The 4T1 cells were seeded at density of 200 cells/well (6 well plates, SARSTED, Germany) and incubated for 24h. Then cells were treated with 6.5 µM ($IC_{50}$) and 25 µM ($IC_{80}$) of

LyeTxI-b peptide for 12 hours at 37 ° C, 5% $CO_2$. In the next day, the medium was removed, rinsed carefully with PBS and fresh medium was added and the cells kept to grow for 10 days at 37 ° C, 5% $CO_2$. Plates were fixed with ethanol 70% for 40 minutes and stained with 0.5% crystal violet for 15 minutes. The ethanol and crystal violet mixture removed carefully and rinsed with water (Rafehi, et al. 2011). The plating efficiency surviving fraction was calculated. The $IC_{50}$ and $IC_{80}$ values were calculated using Prism 5.0® (GraphPad Software Inc.).

### 1.9. Quantitation of cell death using Annexin V and PI after treatment of 4T1 cells with peptide

Detection of Apoptosis and Necrosis by Annexin V Binding and Propidium Iodide uptake, according to the specifications of the supplier. Briefly, the 4T1 cells were maintained in the DMEM culture medium, supplemented with 10% fetal bovine serum. Cells were harvested and seeded in 24-well plates (SARSTED, Germany) at density of 200.000 and incubated overnight at 37 ° C, 5% $CO_2$ for stabilization. Then 4T1 cells were incubated with 6.5 µM LyeTxI-b for 24 hours. Next day, the cells were transferred into 1 ml tubes and centrifuged at 10,000 rpm for 5 min (Denver Instrument Company, USA). The supernatant was discharged, treated and untreated cells were stained with 2.5 µL from Annexin V and Propidium Iodide (BD Biosciences) for 15 minutes in a dark place at room temperature. Then the samples were submitted to the FACS Calibur flow cytometry analysis. The values of FSC-H, SSC-H, were acquired for histograms and statistics analyzes in the FlowJo 7.6.4® program (Tree Star, Inc).

### 1.10. Evaluation of the neurotoxic impact of peptide through the neurite growth assay using Human neuronal precursor cells (LUHMES), LDH release, ATP and glutathione.

Scheme 2 below represents the methodologic strategies for the studies of neurotoxicity using LUHMES cells.

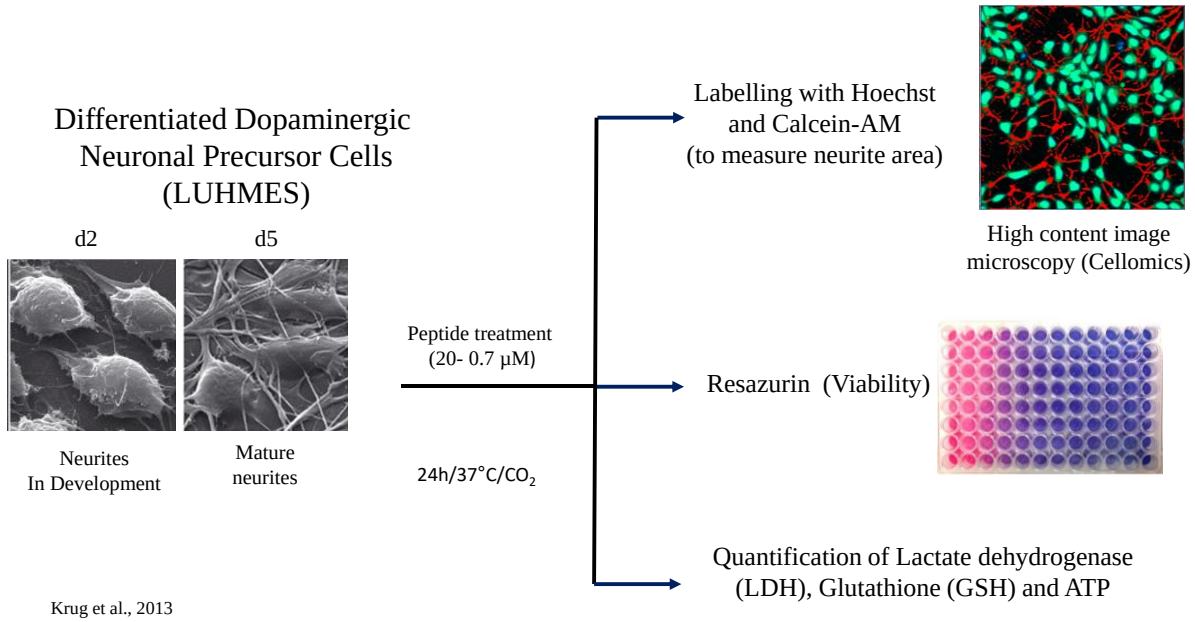


Scheme 2. Methodological strategy of evaluation of neurotoxicity.

The neurotoxic potential of the peptide was evaluated as recently described (Delp, J. et al., 2018). Lund Human Mesencephalic cells (LUHMES) were kept in proliferation medium (AdvDMEM/F12 containing 2 mM L-glutamine, 1× N2 supplement) enriched with 40 ng $ml^{-1}$ recombinant human basic fibroblast growth factor (bFGF) and cultured in 5% CO2 at 37°C. Cell culture dishes and flasks were coated with 50 µg $ml^{-1}$ poly-L-ornithine (PLO) and 1 µg $ml^{-1}$ fibronectin. Differentiation to post-mitotic neurons was performed by seeding the cells at a density of 45,000 cells $cm^{-2}$, culturing them in proliferation medium for 24 h, and then changing to differentiation medium (AdvDMEM/F12 supplemented with 2 mM L-glutamine, 1× $N^2$ supplement, 1 mM dibutyryl 3,5-cyclic adenosine monophosphate (cAMP), 1 µg $ml^{-1}$ tetracycline, and 2 ng ml-1 recombinant human glial cell-derived neurotrophic factor (GDNF). After 48 h of differentiation (day 2), cells were detached with 0.05% Trypsin/EDTA and seeded into a 96 well plates at a density of 100,000 cells $cm^{-2}$. For the assessment of developmental neurotoxicity, these cells were treated with the peptide 1 h after seeding and then incubated for 24 h. To measure neurite stability (mature neurites), cells were allowed to grow neurites for 72 h after seeding (i.e., d5 of differentiation) and subsequently treated with the peptide for 24h [37]. LyeTx I-b was added in a concentration range of 0.09 to 100 µM with 1:4 dilution steps

in DMSO added to the medium. Image acquisition was performed 22-26 h after starting peptide treatment (Stiegler, K. et al., 2011).

### 1.10.1. Image acquisition and quantification

The acquisition was performed as described previously by Stiegler, K. et al. 2011. Briefly, cells were live-stained with Hoechst H-33342 and calcein-AM for image acquisition. The neurite area was calculated as the total calcein positive area corrected for the somatic area, i.e. the Hoechst positive area, expanded by a surrounding ring of 3.2 µm representing the neuronal body. The images were used simultaneously to assess viability. Double positive cells were counted as viable; Hoechst positive objects without calcein stain were counted as dead cells. Viability was expressed as (viable cells / total cells) X 100.

Three independent experiments were performed in technical triplicates. First, data of the technical replicates were expressed as percent of solvent-treated. After that, technical replicates were averaged to reduce technical variability. Subsequently, the mean of three biological replicates was determined for neurite area and viability relative to solvent-control. Fits were calculated using a 4 parameter Hill model with constraining the baseline to max. Hundred of solvent-treated signal. The equation of the Hill model was solved for f(x) = 50 % to determine the EC50, i.e. concentration at which the neurite growth inhibiting/destabilizing effect was at 50% of the solvent control.

Evaluation of the LyeTx I_b peptide in the neurite outgrows assay was performed in three independent experiments in triplicate.

### 1.10.2. Impact of peptide in the release of Lactate dehydrogenase (LDH) in Luhmes cells, ATP assay and Glutathione determination.

LDH activity was detected separately in the supernatant and cell homogenate of LUHMES cells, treated as described in 2.6 and cells were lysed with PBS /0.5% Triton X-100 for 20 min. 10 µl of sample were added to 200 µl of reaction buffer containing NADH (100 µM) and sodium pyruvate (600 µM) in sodium phosphate buffer adjusted to pH 7.4 with 40.24 mM K2HPO4 and 9.7 mM KH2PO4 buffer. Absorption at 340 nm was detected at 37°C in 1 min intervals over a period of 20 min [39]. LDH release was expressed in percentage LDH

supernatant/LDH total. To evaluate ATP content, LUHMES cells grown in 24-well plates were lysed in PBS-buffer containing 0.5% phosphatase inhibitor cocktail 2 (Sigma) and boiled at 95°C for 10 min. Following centrifugation at 10,000 ×g for 5 min for the removal of cell debris, the protein content in the supernatant was measured and adjusted to equal amounts. Samples were then diluted 1:10 in PBS/0.5% phosphatase-inhibitor buffer. For the detection of ATP levels, a commercially available ATP assay reaction mixture (Sigma), containing luciferin and luciferase, was used. 50 µL of adjusted sample and 100 µL of assay mix were added to a white half-area 96-well plate. Standards were prepared by serial dilutions of ATP disodium salt hydrate (Sigma) to obtain concentrations ranging from 1000 nM to 7.8 nM (Stiegler, K. et al., 2011). LUMES Cells were washed twice with PBS and lysed in 200 µl of 1% sulfosalicylic acid (w/v) on ice. The lysates were collected, sonicated 3–4 times on ice and centrifuged at 12,000 ×g for 5 min at 4°C to remove cell debris. Total glutathione content (GSH and GSSG) was determined by a DTNB (5, 5′-Dithiobis (2-nitrobenzoic acid)) reduction assay. After supernatants were diluted 1:10 in H2O, a 100 µl sample was mixed with 100 µl assay mixture containing 300 µM DTNB, 1 U/ml glutathione-reductase, 400 µM NADPH, 1 mM EDTA in 100 mM sodium phosphate buffer, pH 7.5 (all reagent from Sigma). DTNB reduction was measured photometrically at 405 nm in 5 min intervals over 30 min. Total protein content of each sample was detected after neutralization of the precipitated protein pellet with 100 mM NaOH by BCA reagent (Pierce, Thermo Scientific, Rockford, IL). Oxidized glutathione (GSSG) was detected by scavenging GSH with 2-vinylpyridine for 1 h and revealed intracellular levels between 1 and 5% of total glutathione content in controls. GSH and GSSG standard curves (Sigma) were performed by serial dilutions ranging from 1000 nM to 7.8 nM (Schildknecht, P. et al., 2009).One experiment in triplicates was performed in triplicate.

## 2. Results

### 2.1. Cytotoxicity effects of LyeTx I_b peptide against tumoral and non-tumoral cell lines.

The LyeTx-I_b peptide was investigated regarding it cytotoxity against nine human tumoral cell lines, two non-tumoral and one murine mammary carcinoma lineage. LyeTx-I_b peptide showed moderate cytotoxicity against malignant tumor cells, The $IC_{50}$ values of LyeTx-I_b peptide for each cell line are shown in the table and representative dose-response curves in figure1. The aim of this experiment was to explore if LyeTx-I_b could affect cell survival of cancer cell lines compared to non-tumoral cell lines. For that, the toxicity of this new peptide was evaluated against representative models of immune cells (human PBMC, erythrocytes), neuronal precursors cells (Luhmes), fibroblast (GM637) and kidney cells (Vero). LyeTx-I_b has been demonstrated different potency against several lineages such as breast cancer cells and leukemia (except Jurkat cells) which are more susceptible ($IC_{50}$ values in the lower micromolar range, i.e, <10µM), comparing with glioma and neuroblastoma lineages (>20µM). LyeTx-I_b peptide exhibited cytotoxic effect against breast cancer cells (from human or mice), colon and two leukemic lineages (HL60 and THP-1) at lower micromolar range (<10 µM), compared with carboplatin (>100µM, data not shown) as a standard drug used in clinic. Regarding non-tumoral cells such as GMS637 and Vero cells, the peptide showed higher values of $IC_{50}$ (>100µM), differently that observed to PBMC $IC_{50}$ value was at the lower micromolar range, similar to those of the most of the tumoral cell lines, demonstrating cytotoxicity (Table 1, figure 9). Standard drugs used in clinics such as cisplatin and etoposide presented $IC_{50}$ values of 29, 78 and 116 µM, respectively (data not shown).

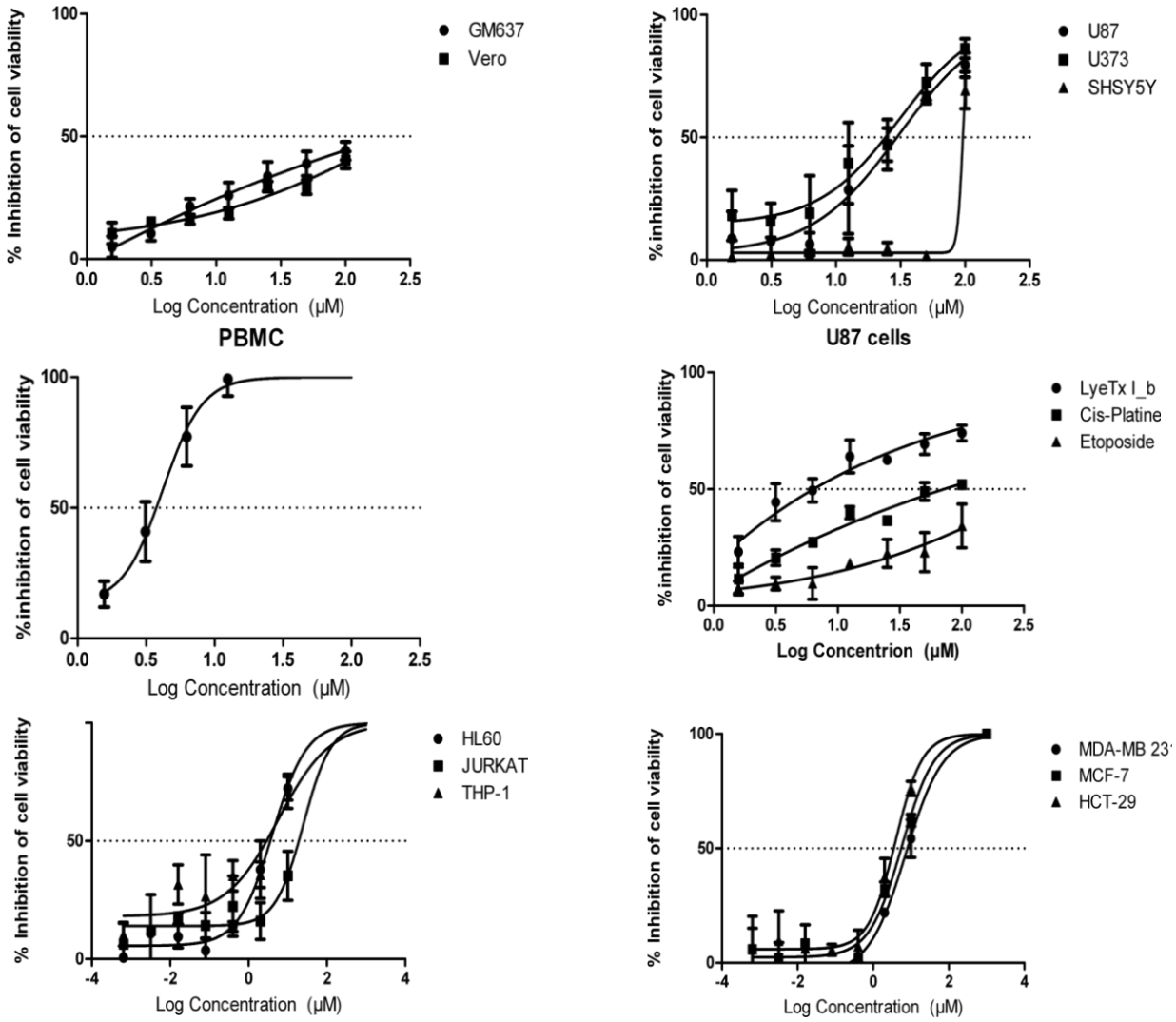


Figure 9. Representative dose-response curves of the effect of LyeTx-I_b peptide on viability of different cell lines. Tumoral and non tumoral cells were treated with LyeTx-I_b peptide at various concentrations for 48 hours and cell viability was determined by MTT assay. IC50 is the concentration of compound that inhibits cell growth by 50 % and values represent mean ± SD of three independent experiments in triplicates. IC50 values determinates to non-tumoral cells after analysis of cell viability evaluated by resazurin assay.

Table 1. $IC_{50}$ value of LyeTxI_b cytotoxicity against cancer and normal cell lines

| **Human cell line** | **LyeTx I-b $IC_{50}$ (µM)** |
|---|---|
| U-87 MG (Glioblastoma) | 29.20±7.96 |
| U-373 MG (Astrocytoma) | 20.94±5.18 |
| SHSY5Y (Neuroblastoma) | 93.80±2.17 |
| MDA-MB-231 (human breast adenocarcinoma) | 7.34±3.09 |
| MCF-7 (human breast adenocarcinoma) | 5.77±0.83 |
| HT-29 (human colorectal cancer) | 3.86±0.47 |
| HL60 (Human promyelocytic leukemia) | 4.21±0.35 |
| JURKAT (Acute T-cell Leukemia Lymphocyte) | 25.44±3.45 |
| THP-1(human Leukemic monocyte) | 5.71±4.70 |
| **Non-tumor** | |
| GM637 (human lung fibroblasts). | ≥100 |
| Vero (African green monkey kidney) | ≥100 |
| PBMC (Peripheral Blood Mononuclear Cells) | 4.161±1.94 |
| **Mouse line** | |
| 4T1 (murine breast cancer) | 6.5 ±5.30 |

$IC_{50}$ values were calculated from the linear regression of the dose-log response curves after 48 h exposure to peptide, determined by the MTT and resazurin assays. Values are mean ± S.D. of at least 3 experiments.

## 2.2. LyeTx I-b induced mild hemolytic activity.

Cytotoxicity of the peptide was also evaluated against human erythrocytes (RBCs). As observed in figure 9, the rate of hemolysis of human RBCs did not reach to 40% of hemolysis, even at higher concentration of peptide (100µM), $IC_{50}$ was 155±13.04 µM.

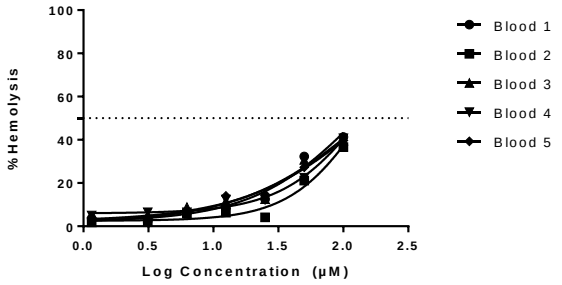


Figure 10. Relative rate of hemolysis in human RBCs upon incubation with LyeTx-I_b peptide at increased concentrations compared with the control group. Peptide was tested in erytrocytes of peripheral blood of five different donors.

## 2.3. LyeTx I-b peptide reduces neurite outgrowth, integrity and LUHMES cells viability

Since our focus was to evaluate the antitumor potential of this peptide for the treatment of tumors, it was necessary to evaluate if the peptide displayed any adverse neurotoxic effect, as often observed with chemotherapy treatments. We used neuronal precursor cells (Lund Human Mesencephalic cells, LUHMES) as a predictive model. The effect of LyeTx I-b on LUHMES cells was evaluated during different stages of differentiation as previously described by Krug et al. (2013). This methodology allows to separate compounds with unspecific toxicity against neurons (ratio between $EC_{50}$ values for viability and neurite area of <4 ($EC_{50}$ (V/NA)) from compounds with specific neurotoxic hazard ($EC_{50}$ (V/NA) ratio ≥4), meaning that the neurite area was adversely affected at compound concentrations that did not trigger cell death. As shown in Figure 11A, LyeTx I-b demonstrated unspecific cytotoxicity against neurons (at lower micro molar range) both during development (d2-3) and after maturation (d5-6), with $EC_{50}$ ratios of less than 4. Figure 11B shows representative of LUHMES cells with the neurite network, and LUHMES cells with developing (d2-3) and mature neurites (d5-6) treated with two concentrations (0.3 and 1.25µM) close to the $EC_{50}$ values of peptide. It possible observes reduction of the neurite area in a concentration-dependent way.

To further explore the relationship between neurite growth and the neurotoxicity of LyeTx I-b in LUHMES cells, general cytotoxicity was evaluated by measuring the LDH release into the medium. The effect on viability was confirmed using the resazurin viability assay. In addition, GSH and ATP concentrations were determined in cell lysates. LUHMES cells which were exposed to LyeTx I-b for 24 h (d2-3), clearly demonstrated that their viability was reduced in a concentration-dependent fashion. There was a simultaneous liberation of LDH, demonstrating loss of membrane integrity. Moreover, the intracellular ATP and GSH levels decreased in a dose-dependent manner (Figure 12).

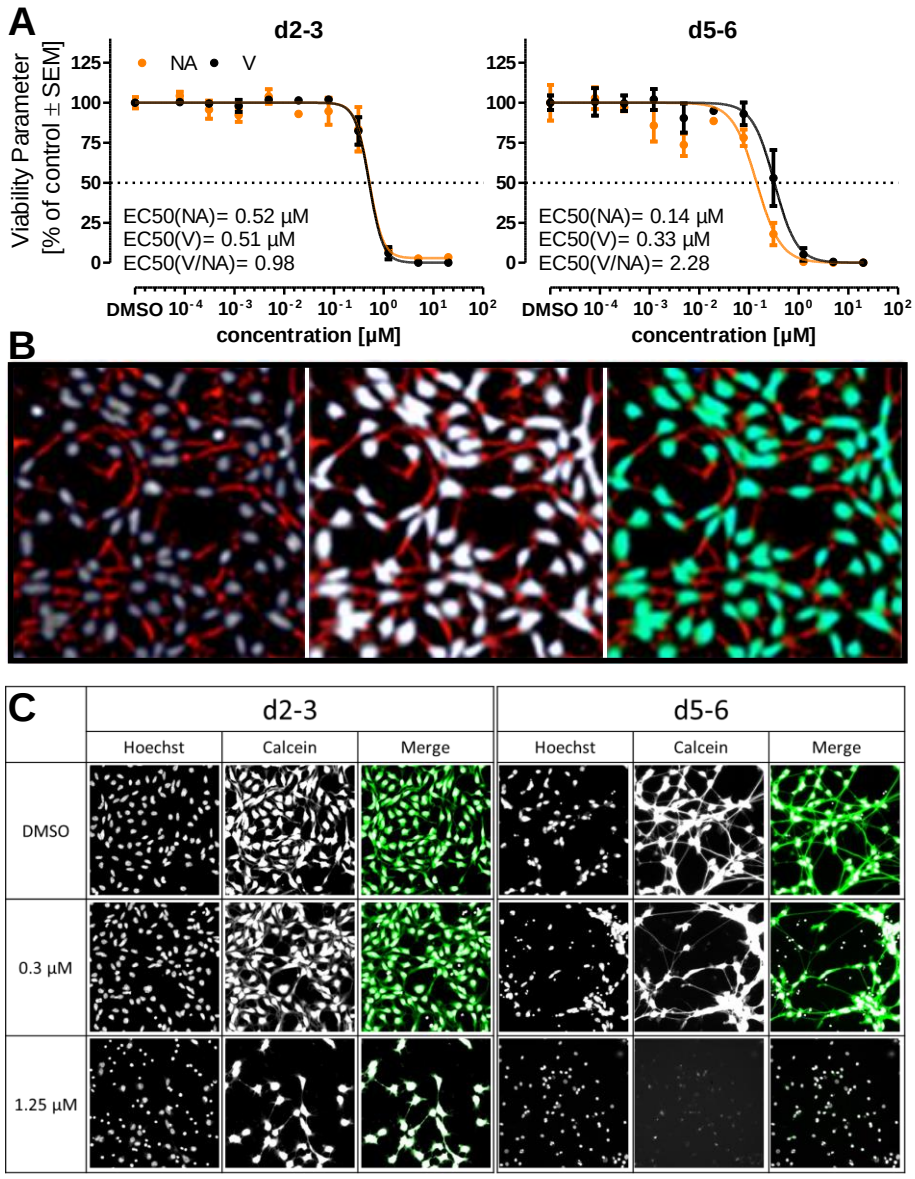


Figure 11. Effect of LyeTx I_b peptide on differentiating (d2-3) and differentiated (d5-6) LUHMES cells. Cells were seeded at day 2 (d2) into 96-well plates, and the peptide was added, either 1 h after seeding or on day 5 (d5). After 24 hours of exposure, images were acquired after staining with Hoechst H-33342 and calcein-AM to calculate the neurite area (NA) and viability (V). A) Concentration response curves and EC50 values of differentiating and differentiated LUHMES cells treated for 24 h with LyeTx I_b peptide. B) Exemplification of how the image analysis was conducted. Nuclei were identified through the Hoechst signal. Cells with calcein-positive nuclei were counted as living cells, and only Hoechst-positive cells were counted as dead cells. Neurite areas were derived by subtracting the Hoechst-positive area plus an enlargement (somatic area) from the total calcein-positive area (red). C) Representative images of LUHMES cells treated with either DMSO control, 0.3 µM or 1.25 µM of LyeTx I_b peptide ($4^{th}$ and $3^{rd}$ highest concentration, respectively). In the merge, Hoechst was colored gray and calcein green. Image size is always 330 µm. Representative data of three experiments performed in triplicate.

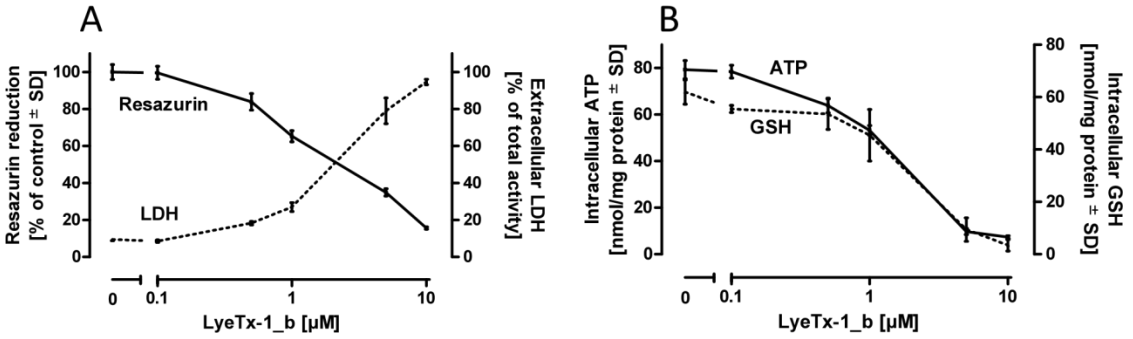


Figure 12. Toxicity assessment in LUHMES cells. LUHMES cells during day 2-3 of differentiation were treated with LyeTx I-b for 24 h. (A) Cell viability was assessed by the resazurin reduction and by lactate dehydrogenase (LDH) release assay. (B) Additional measurements of cell viability, the levels of intracellular ATP and glutathione (GSH), were also determined. Two independent experiments in triplicates were performed.

## 2.4. The LyeTx I-b peptide reduced the clonogenic survival of triple-negative 4T1 cells

Experiments to evaluate antitumor efficacy of peptide *in vitro* were performed with murine breast cancer lineage 4T1, once this cell line was used in the murine breast cancer model to investigate the anticancer potential *in vivo*. Clonogenic assays are used in drug discovery programs as a predictive model to evaluate efficacy in *vivo (*Zip, D. et al., 2005). LyeTx I-b demonstrated ability to reduce the clonogenic survival of 4T1 cells, observed by a decrease of the number of colonies, comparing with control. LyeTx I-b peptide prevented the capacity of clonogenic cells to proliferate in vitro, suggesting that LyeTx I-b peptide has tumoricidal activity (Figure 13).

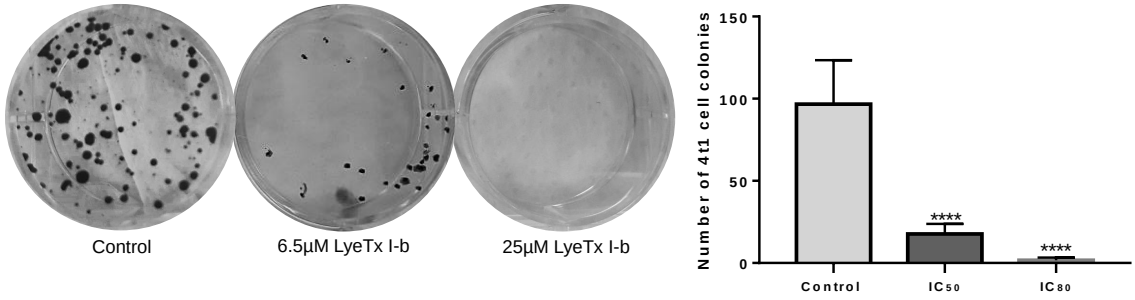


Figure 13. Quantification of 4T1 single cell survival colonies untreated (control), or treated with 6.5 µM ($IC_{50}$), or 25 µM ($IC_{80}$) of LyeTx I-b peptide. Data represent means ±SD of three independent experiments in duplicates, One-way ANOVA followed by Dunnett's comparison test, P< 0.001.

## 2.5. The LyeTx-I_b peptide increases sub-diploid DNA content in 4T1 cells

Apoptosis is a wanted mechanism to be triggered by a substance with a potential anticancer effect. To gain insights regarding *in vitro* potential of peptide to induce apoptosis in 4T1 cells, the sub-diploid DNA content was determined. Cells undergoing apoptotic cell death display an increase of sub-diploid DNA content that can be correlated with DNA fragmentation and can be evaluated by flow cytometry. After treatment of 4T1 cells for 48h with the $IC_{50}$ concentration of LyeTx I-b peptide and carboplatin a significant increase of sub-diploid (sub-G1) DNA content was observed (figure 14), when compared with with control (PBS), suggesting apoptosis or necrosis induction.

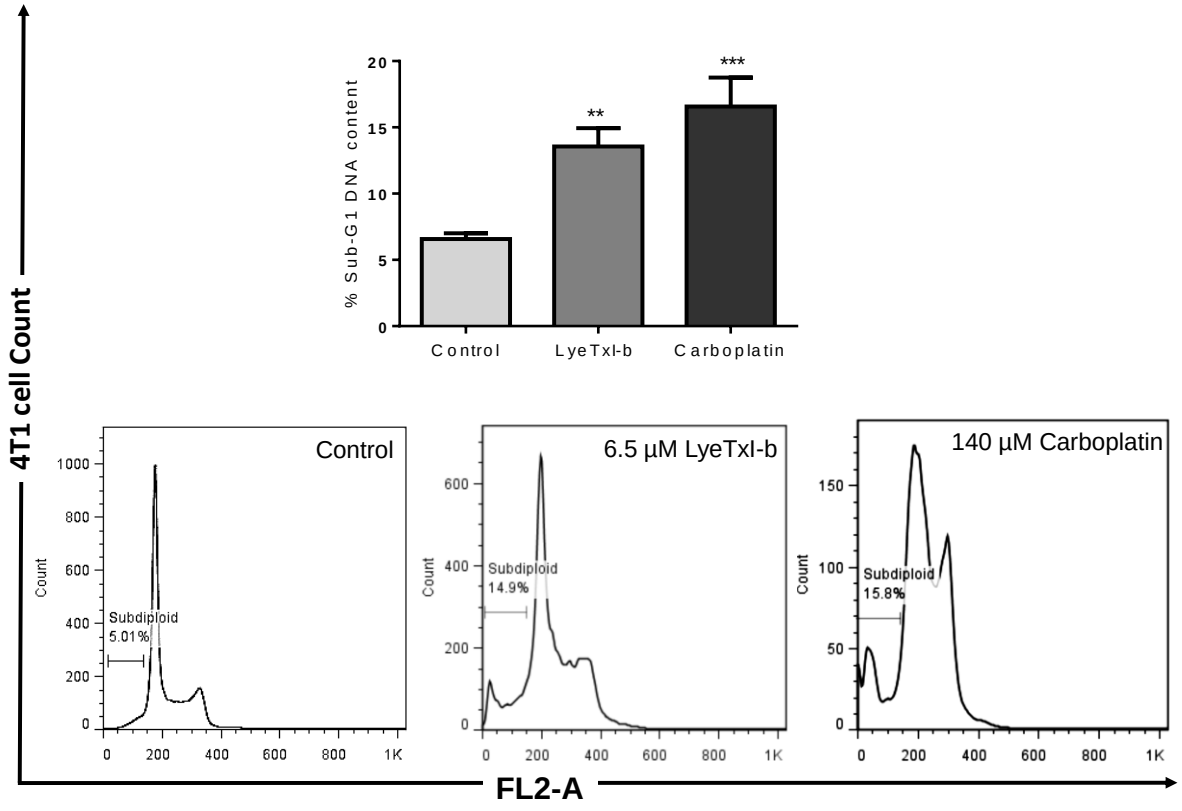


Figure 14. Representative histograms of cell cycle analysis after exposure to LyeTx-I_b peptide and carboplatin $IC_{50}$ values, for 48 hours. Data showed significant differences between the negative-control and the treated cells in terms of the G0/G1 (sub-diploid) population. Statistical analysis was One-way ANOVA followed by Dunnett's comparison test, $P< 0.001$.

## 2.6. LyeTx I-b peptide induces early events of apoptosis in 4T1 cells

To distinguish between apoptosis and necrosis, labelling with anexin-V and propidium iodide (PI) was performed using flow cytometry. After 24h treatment, an increase of cells labelled with annexin-V, an early event of apoptosis associated with the phosphatidylserine translocation from the internal to external leaflet of membrane, was observed. The flow cytometric data also demonstrated that majority of the 4T1 cells were in early apoptosis, observed by the labelling with Annexin-V only (quadrant Q3). Double positive cells (Q2, PI +ve /Annexin V+ve) were observed in minor proportion, demonstrating cells in late apoptosis. Only few cells were labelled with PI, indicating necrotic cells (Q1, figure 15).

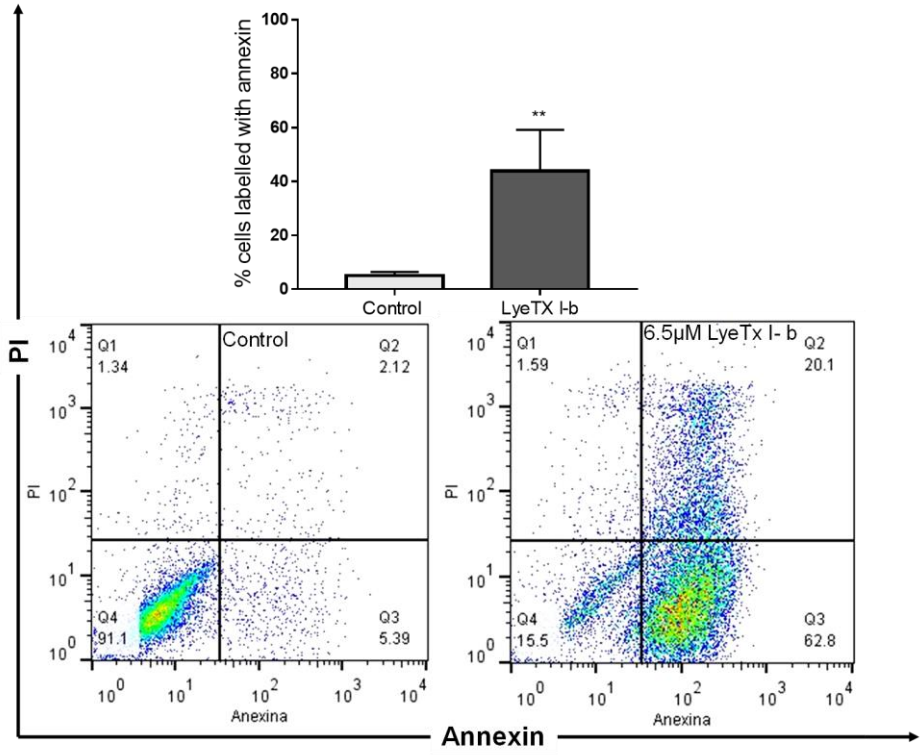


Figure 15. Illustrative histogram representing quantification of the dead and live cells proportions after 4T1 cells exposed to 6.5 µM of LyeTx I-b peptide for 24 hours and stained with Annexin V/PI. The population number of individual cells in quadrant (Q) gates can be quantified in each one as follows: Q4 = live cells (PI−ve/Annexin V−ve); Q3 =apoptotic cells (PI−ve/Annexin V+ve); Q2 = necrotic or late apoptotic cells = PI+ve/Annexin V+ve) and eventually Q1 = nuclei without plasma membrane = (PI+ve/Annexin V−ve). Three independent experiments in triplicate and unpaired t-test was performed, $P<0.001$.

These data suggested that LyeTx I-b induced apoptosis in 4T1 cells, besides reduce the survival of clonogenic cells, showing the potential of this peptide to display an anticancer effect *in vivo*.

## 3. Discussion

To characterize the cytotoxicity of LyeTx I-b peptide and it anticancer potential, we used as a predictive models tumor cells derived from nine types of tumor and non-tumoral cells (human PBMC, human fibroblast, monkey kidney cells) and human neuronal lineage (LUHMES), in order to measure the neurotoxic hazard. We found that LyeTx I-b peptide effectively inhibits the growth of some cells derived of brain cancers in a dose-dependent manner (Table 1), whereas neuroblastoma cells (SHSY5Y, $IC_{50}$ =93µM) were less susceptible, comparing with glioma cells ($IC_{50}$ = 29 and 20 µM, respectively to U-87 MG and U373-MG). The LyeTx I-b peptide induced cytotoxicity against breast cancer cells from murine mammary carcinoma (4T1) and also from human (MCF-7, MDA-MB-23). This effect was compared with carboplatin, an anticancer drug used in clinic. The $IC_{50}$ values of LyeTx I-b peptide obtained to 4T1, MCF-7 and MDA-MB-231 cells were at lower micromolar range (6.5 µM, 5.77µM and 7.34 µM, respectively), comparing with carboplatin (>100 µM). In drug discovery program, compounds considering as promising compounds are in the order of lower micromolar range (1-10 µM) up to 40 µM (Hughes, J. et al., 2011). Data obtained to carboplatin in our conditions are in agreement with Łakomska and colleagues (2014), they tested carboplatin toward 4T1 and T47D (human ductal breast carcinoma) by using MTT assay, the $IC_{50}$ values were 84 µM and 134 µM respectively.

The most of the chemotherapeutic agents in clinics also induce adverse effects such as myelosuppression, cardiotoxicity, ototoxicity, neurotoxicity and malignancies (Swartz, A.M., et al., 2015). When evaluated against representative models of non-tumoral cells, the peptide showed more cytotoxicity against human PBMC, a representative model of immunotoxicity ($IC_{50}$ = 4 µM), comparing with human fibroblast GM-637 cells and monkey kidney cells Vero ($IC_{50}$>100 µM). Fluidity of PBMC membranes play a crucial role in drug sensitivity due to high content of lipids like eicosanoid (Hon, G. et al., 2012).Considering the hemolytic effect of AMPs, we also evaluated it effect against human erythrocytes (IC50>100 µM), indicating disruption of RBC membrane (Figure 10), similar to the hemolytic effects of others alpha-helix peptides as described by Huang and co-workers (2011). Hydrophobicity is a key factor of AMPs cytotoxic efficacy against cancer cells and less hemolytic activity because of the presences of alanine residue in α-helical peptides that might help to penetrate and accumulate in cancer cell membrane, leading to disrupt cell membrane rapidly than red blood cells. V13K, K4R2-Nal2-S1 and D-K6L9 are cationic peptides,

which have been demonstrated high specificity to kill various cancer cells with less hemolytic effect (Huang, Y.P et al., 2011 & Chu, H.L. et al., 2015).

As mentioned previously, in order to investigate the anticancer effect of peptide *in vivo*, the 4T1 murine breast cancer model was selected for this purpose considering the importance of new drugs for breast cancer treatment. Viability data demonstrated that peptide was active against murine breast cancer lineage at lower concentration (< 10 µM).The MTT method is able to estimate total of surviving cells, but it is not able to determine the assessment of surviving fraction of clonogenic cells, it also predict antitumor *in vivo*. One of the goals of anticancer drugs is to kill cell death or inducing the loss of clonogenic cells (Zip, D. et al., 2005). Clonogenic assays is a predictive and an informative methology to determine effectiveness of anticancer agents and radiation (Rafehi, H. et al., 2011). We performed this assay to predict the potential tumoricidal effect of the peptide in vitro and make decision to go further to *in vivo* experiments. The LyeTx I-b peptide significantly inhibited the clonogenic survival of 4T1 cells (figure 13) at $IC_{50}$ (6.5µM), suggesting anticancer potential *in vivo*. A complete inhibition was observed at $IC_{80}$ concentration (25µM). Several studies reported that cationic peptides could be reducing colonies survival of breast cancer cells through blocking transformation of the single cell into colonies (Douglas, S. et al., 2014). In fact, reduction in viability and clonogenic survival of 4T1 cells after treatment with LyeTx I-b seems to be associated apoptosis induction and this is a desired effect to potential anticancer candidate. These data was supported by the increase of sub-diploid DNA content in treated cells with peptide or carboplatin (figure 14) and by the labelling with Annexin-V observed by flow cytometric analysis. Carboplatin is an alkylating agent, which induced and increase of sub-diploid DNA that related to apoptosis in various cancer cell lines, after 48 h of exposure (Wang, S. et al., 2010 & Darzynkiewicz, Z. 2010). Overexpression of Protein kinas C in metastatic cells like 4T1 resulting in resistance to apoptosis and enhancing cell survival (Hong, S. et al., 2012).

Cultures of 4T1 cells treated with LyeTx I-b peptide showed the majority of cells stained only with by Annexin-V comparing with control (figure 15), demonstrating the exposure of phosphatidylserine, an early event of apoptosis. Cells in late apoptosis (Annexin/PI positives) or necrotic (PI positive cells) were negligible in both groups, control and treated cell populations. Our data is in agreement with those observed to Temporin-1CEa antimicrobial peptide, that induced apoptosis in MCF-7 and MDA-MB-231 breast cell lines through phosphatidylserine

externalization of cell surface confirmed by FITC-annexin V positive (Wang, E. et al, 2013). Similarity, LL-37 cationic peptide-induced apoptosis in Jurkat T leukemia cells characterized by DNA sub-diploid and internal cell surface reflection resulted in increasing of Annexin V staining (Mader, J. et al., 2009).

Neurotoxic risks can be evaluated using some cellular models in high throughput screening to evaluate cytotoxicity to neurons, such as SH-SY5Y neuroblastoma cells, LUHMES cells and Neural Stem Cells (from human fetal brain). These lineages display high sensitivity to identify toxicants, as previously described by Tong and collaborators (2017). The authors demonstrated that among these lineages, LUHMES cells exhibit a more favorable genetic profile and sensitivity for neurotoxicity detection. They tested several drugs, including doxorubicin that demonstrated cytotoxicity at a lower micro molar range. In a previous work, Krug and co-workers (2014) using neurite growth to compare toxicity of several chemicals to developing *versus* developed neurites found $EC_{50}$ values of a low micro molar range of anticancer drugs such as etoposide, cisplatin, and vincristine. LyeTx I_b peptide reduced the neurite growth and cell viability (Figure 11), and this effect resulted in LDH release and depletion of ATP and GSH (Figure 12) in consequence of the damage to the cell membrane. Despite those effect induced by peptide, the neurotoxic hazard to LUHMES was similar to some anticancer drugs used in clinics. Moreover, taxol, cisplatin, etoposide and methotrexate have all been implicated to have a percentage late-stage of safety-related clinical failures due to neurological side effects (Ivanov, D. P. et al., 2016 & James, S.E. et al., 2008).Therefore, the *in vitro* data demonstrated that the cationic antimicrobial peptide LyeTx I-b presents cytotoxicity against cancers cells. In addition, the peptide showed undesirable cytotoxicity such as neurotoxicity and immunotoxicity, but this was similar to other anticancer drugs used in clinic. Consequently, this deleterious effect cannot be considered as a restrictive reason to invalidate the antitumor potential of this peptide.

# Chapter 2

## Study of cell death mechanism induced by LyeTxI-b peptide in U-87 MG glioblastoma cells.

## Hypothesis

LyeTx I-b peptide possess cytotoxicity against glioblastoma U87 MG cells inducing a specific mechanism of cell death and could confer to it an anticancer potential as a prototype to develop a drug to treat Glioblastoma.

## 1. Material and Methods

The scheme 1A below summarizes the methodological strategies used to study the cell death triggered by LyeTx I-b in glioblastoma lineage U87 MG. In scheme 1B and C, morphological and biochemical studies strategies were also represented.

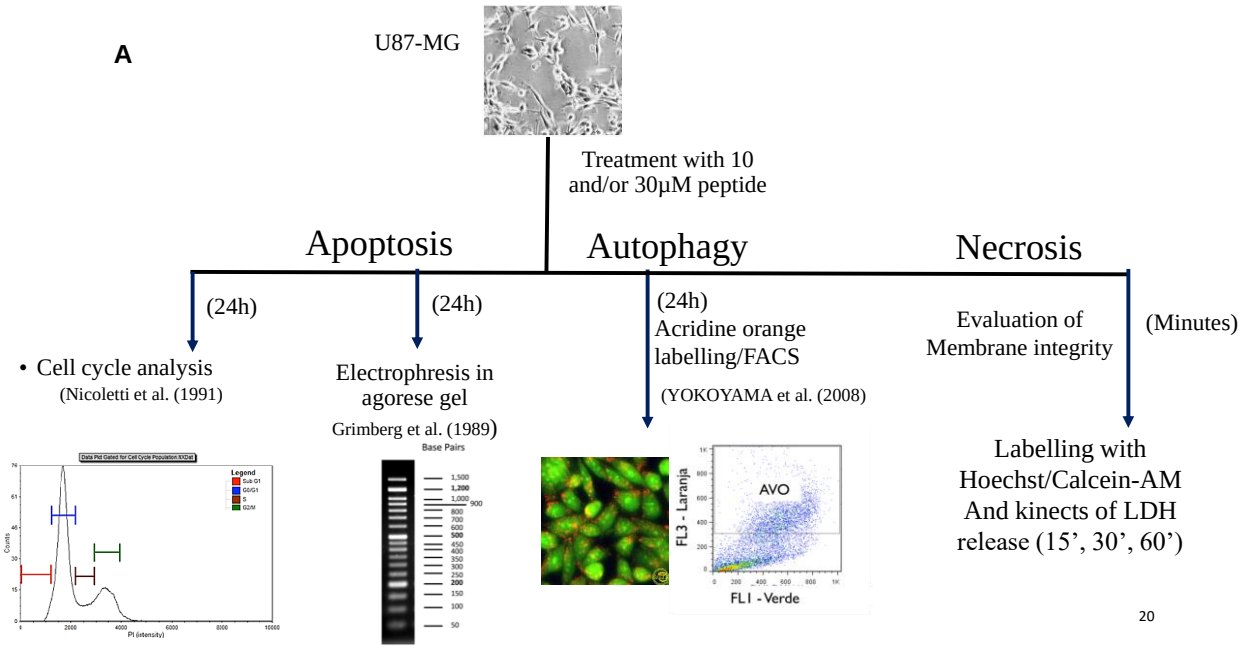


Scheme 3A. Methodological strategies for evaluation of the type of cell death induced by peptide. (A) Different assays to evaluate apoptosis, autophagy and necrosis

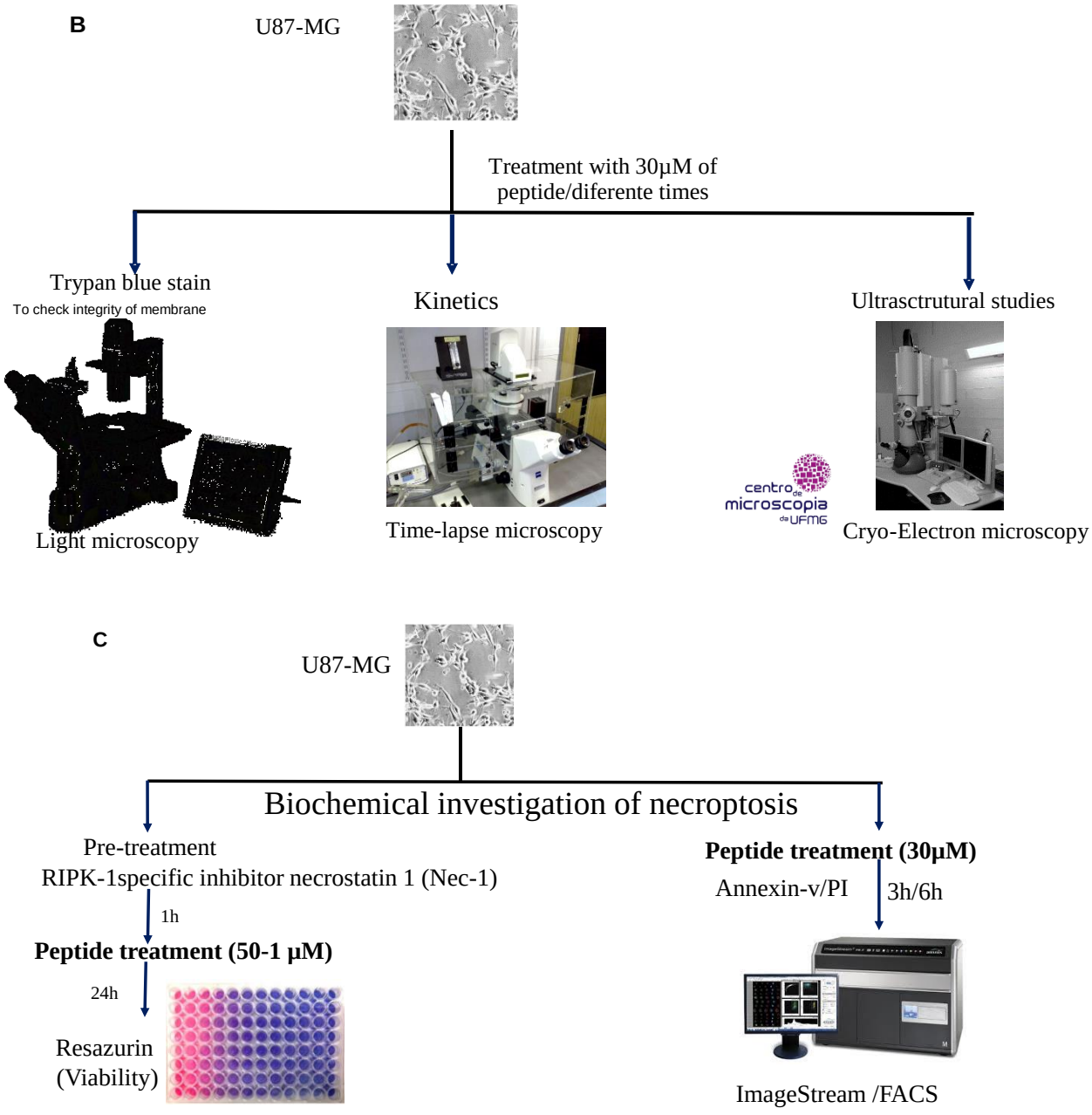


Scheme 3B and C. Methodological strategies for evaluation of the type of cell death induced by peptide. (B) morphological studies; (C) biochemical investigation of necroptosis. Two (morphological studies) or three independent experiments were performed in triplicate.

### 1.1. Evaluation of sub-diploid DNA content of U87 MG after treatment with peptde using flow cytometry.

Quantification of the DNA content and cell cycle analysis were performed by flow cytometry according to the method described by Nicolletti and co-workers (Nicoletti, Migliorati et al. 1991). U-87 MG cells were seeded in 24-well plates at confluence 200,000 cells/well and incubated overnight at 37 ° C for stabilization. Then U-87 MG cells were incubated with 30µM LyeTx I_b for 24 h. After treatment, the cells were transferred into 1 ml tubes and centrifuged at 10,000 rpm for 5 min in a microcentrifuge (Denver Instrument Company, USA). The supernatant was discarded and 300 µL of a Hypotonic Fluorochromic Solution (HFS) containing 50 µg / ml of Propidium Iodide - IP (Sigma, Saint Louis, Missouri USA) and 0.1% of Triton X-100 (Sigma, Saint Louis, Missouri USA) in 0.1% sodium citrate (Sigma, Saint Louis, Missouri USA). Plates were incubated for 4 h at 4° C. After incubation the samples were submitted to flow cytometry analysis. The FL2 voltage was adjusted so that the G0 / G1 and G2 / M phases formed peaks of values of 200 and 400, respectively, in FL2-A, The values of FSC-H, SSC-H, FL2-A and FL2-W were acquired for histograms and statistics analyzes in the FlowJo 7.6.4® program (Tree Star, Inc). At least, three independent experiments were performed in duplicate.

### 1.2. Profile of nuclear fragmentation of U87 MG cells after treatment with peptide by agarose gel electrophoresis

Profile of DNA fragmentation was verified by 1.5% agarose gel electrophoresis to observe the typical apoptosis profile with the formation of bands containing multiples of 180-200 ("ladder standard" or ladder) as prescribed by (Wlodkowic, S. et al. 2011). U-87 MG cells were grown in 6 well plate at 300,000 cells / well for 24 hours. 30µM LyeTx-1_b were added and the plate incubated again for 24 hours in a $CO_2$ incubator at 37 ° C. DNA extraction was performed after this treatment period as described in the well-established protocol (Grimberg, N. et al., 1989) and the DNA quantity was determined by reading absorbance at 260 nm in NanoDrop apparatus (Thermo Scientific). The electrophoresis was conducted in TAE-1X buffer at 100V and 500 mA and subsequently, the gel was stained with ethidium bromide solution (0.5 µg / mL) and photographed by trans-illuminator. At least three independent experiments were performed.

### 1.3. Quantification of acidic vesicles organelles (AVO) through staining with acridine orange

To evaluate autophagy induction, U-87 MG cells were labelled with acridine orange dye. Vital dyes such as acridine orange is commonly used to study autophagy. Acridine orange is a lysotropic dye that accumulates in acidic organelles in a pH-dependent manner. At a neutral pH, acridine orange is a hydrophobic green fluorescent molecule (FL1 in the histogram). However, within acidic vesicles, acridine orange becomes protonated and trapped within the organelle and forms aggregates that emit bright red fluorescence (FL3) and is associated with autophagy. The U-87 cells were plated at the density of 200,000 cells / well in 24-well plates and incubated at 37 ° C in an overnight $CO_2$ incubator. After this period, treatment with substances or negative control (PBS in medium) was performed for 24 h.

The Cells were washed with ice-cold PBS, then labelled with 10 µg / ml acridine orange solution (Sigma Aldrich) prepared in Milli-Q water. After 10 minutes of incubation at room temperature, the cells were taken for reading on a flow cytometer (FASCan, Becton Dickson). The cells were analyzed by FlowJo 7.6.4® program (Tree Star, Inc) (Kanematsu, U. et al., 2010).Three independent experiments in triplicates were performed

### 1.4. Evaluation of necrosis induced by LyeTx-I_b peptide in U-87 MG cells using lactate dehydrogenase enzyme activity.

U-87 MG cells were plated and the effect of the LyeTx I-b on the release of LDH enzyme was evaluated at 15, 30 and 60 minutes after treatment. Lactate production was determined by assaying the formation of NADH and pyruvate from lactate in the presence of excess NAD+ (Meira, M.C. et al., 2005). The reaction is catalyzed by lactate dehydrogenase, the lactate concentration being calculated from the extinction coefficient of NADH at 340 nm. 50 mM sodium phosphate buffer (pH 7.4) was prepared with 0.6 mM sodium pyruvate. 6.3 mM NADH solution was prepared at the time of use and protected from light and added immediately prior to reading. The LDH reaction was monitored after 30 minutes of reaction with reading absorbance at 340 nm in a Varioskan TM Flash spectrophotometer (Thermo Scientific). As a positive control, Triton X-100 (0.5%) was used, and ultra-pure water was as the negative control. For the calculation of the percentage

of lysis, cells treated with Triton X-100 were considered as 100% lysis (Chan, M/ et al., 2013).

## 1.5. Investigation of necroptosis mediated cytotoxicity of LyeTx-I_b peptide against U-87 cells

### 1.5.1. Quantification of the effect of Necrostatin-1 inhibitor on the viability of U-87 MG treated with the peptide.

Briefly, U-87 cells ($5 \times 10^3$/well) were seeded onto 96-well plates and pre-incubated with (100 µM) Necrostatin-1 for 1 hour. The peptide was added in different concentrations and Triton X-100 (0.1; 0.05 and 0.025% v/v), was used as a positive control (that induces necrosis). After 24 hours of treatment, cell viability was evaluated by Resazurin metabolism assay, as previously described by Gartlon et al. (2006). Three independent experiments were performed, in triplicate.

### 1.5.2. Cell death analysis with Imaging Flow Cytometry.

U-87 MG cells ($3 \times 10^5$ cells) were seeded into each well of a 6well/plate and cultured until reaching 80% confluence. Cell death was induced by adding LyeTx I-b for 3, 6 and 12 hours. Cells were trypsinized, carefully suspended in the medium, transferred to microfuge tubes, centrifuged at 1200 ×g for 5 min at 4°C and the supernatant then aspirated. Cells were washed with 1 ml PBS and resuspended in 100 µl staining buffer (BD Annexin V FITC Assay) by mixing 2.5 µl of Annexin-V and 2.5 µl propidium iodide (PI) in the incubation buffer according to manufacturer's instructions. The cells were incubated for 15 min at room temperature and protected from light. Samples were immediately analyzed by Amnis® Imaging Flow Cytometry according to Analysis of Apoptosis and Necroptosis by Fluorescence-Activated Cell Sorting (Wallberg, F. et al., 2016 & Pietkiewicz, M. et al., 2015).Three independent experiments were performed, in triplicate.

### 1.5.3. Evaluation of U-87 MG cell membrane integrity after treatment with the peptide using trypan blue exclusion.

Trypan blue is a dye that does not interact with cell unless the cell membrane is damaged. Healthy, undamaged cells exclude the dye. Damaged cells absorb the dye and become clearly visible under the microscope. After 15, 30, 60, 120 and 180 minutes of incubation with 30µM LyeTx-1_b, 20 µl of 0.2% trypan blue in PBS was added to the 96 well plate containing 1 × 104 cells per well and incubated for 5 min at room temperature. Then cells were examined under a microscope. Only dead cells would take up the dye and appear as darkly stained cells under the microscope as described by Simon (2003).Three independent experiments in triplicates were performed with count 20 to 50 cells per field.

### 1.6. Morphological studies

#### 1.6.1. Time-course using high-content automated imaging microscopy (Cellomics) to evaluate early events

The 24 h treatment period, cells were imaged using an Axio Observer.Z1 microscope (Zeiss, Oberkochen, Germany), equipped with an Axiocam MRm camera and an incubation system for constant temperature and $CO_2$. Phase contrast images of the migration zone were acquired every 10 min using a 20x objective. One experiment in triplicate was performed.

#### 1.6.2. Morphological alteration analysis using time lapse microscopy

Calcein/AM is a permeant dye can be used to determine cell viability in most eukaryotic cells. In live cells, the non-fluorescent calcein AM is converted to a green-fluorescent *calcein* after acetoxymethyl ester hydrolysis by intracellular esterase. U-87 cells were treated with peptide (10µM and 30µM) or Triton 0.1% (positive control of necrosis) for 15 minutes and, following labelled with Calcein/AM and Hoechst 3342 and analysis at Cellomics.

#### 1.6.3. Detection of nuclear and cytoskeleton alterations using confocal microscopy after labelling with TO-Pro-3 and Fluor 488 phalloidin

Using confocal microscopy LSM 510. The U-87 cells were stained with Fluor 488 phalloidin (Invitrogen) and TO-PRO-3 (Invitrogen), for F-actin and the nucleus, respectively According to Sung, Y. et al. (2011), 200.000 U-87 cells / well in 24-well plates and incubated

at 37 ° C in an overnight $CO_2$ incubator, After this period, treatment with 30µM of peptide substances or negative control was performed for 3h, 6h and overnight Then medium was removed and cells washed with PBS. U-87 cells were fixed with Paraformaldehyde and stained for actin and nucleic acid, with Alexa Fluor 488 phalloidin (green) and TO-PRO-3 (blue), respectively and analysed using a confocal microscopy (Zeiss, M510). Cell nuclei were classified as normal or condensed and/or fragmented and cell cytoskeleton as well. Two independent experiments in triplicates.

### 1.7.Ultra structure analysis of U-87 after treatment with LyeTx I_b peptide.

#### 1.7.1. Electron microscopic ultrastructural analysis of cryofixed, freeze-substituted cells

In order to U-87 MG detachment after peptide treatment, the control and treated cells were trypsinized, centrifuged at 960 xg at room temperature for 5 min, resuspended in DMEM medium supplemented with 0.1% FBS in microfuge tubes and then allowed to recover in the incubator for 2 h. The cells were centrifuged, resuspended in DMEM medium without serum and the cell count determined using a hemocytometer. The suspension was divided into 4 groups: one control, untreated group and three groups treated with LyeTx I-b for 30 min, 1 h and 3 h, respectively, in a water bath at 37°C. After each incubation period, cells were centrifuged at 960 xg at room temperature for 5 min, the supernatant was discarded, and 5 µL (~9000 cells) from the pellet of each group were immediately mixed with sterile PBS or cryo-protectant (20% dextran) and cryofixed by high-pressure freezing (HPF) in a Leica EM HPM100 (Leica Microsystems, Wetzlar, Germany). Ultra-rapid cryofixation methods were used in order to preserve the plasma membrane in as close to the native state as possible. Samples were also evaluated using standard EM fixatives and similar results were obtained (data not shown). Cryofixed samples were stored in liquid nitrogen (196ºC) overnight and then transferred to 2.0 ml cryo-tubes containing liquid nitrogen above a 1.0 ml frozen mixture of 1% osmium tetroxide in anhydrous acetone. Freeze substitution was carried out in a Leica EM AFS2, starting at -90ºC and slowly warming up to 20ºC over a 4 day period. During freeze-substitution, frozen water was removed from the samples by anhydrous acetone at a temperature low enough to prevent the cellular water from recrystallizing (Thompson, R.F. et al., 2016& Zabeo, D. et al., 2017). Samples were brought to room temperature and then processed for light, transmission and scanning electron microscopy using standard techniques.

### 1.7.2. Quantitative analyses of internal cell structures by high-resolution Light-field microscope (HRLM).

High-resolution images of 300-nm thick sections of cryo-fixed cells were captured at 1,000X using a Zeiss Axio Imager Z2 with Zen 2 Blue Edition V1.0 software (Carl Zeiss Microscopy GmbH, Jena, Germany). Images from different experiments (n=4) were randomly collected to distinguish the different cell death processes and then subjected to morphometric analyses. For each group, a total of 200 cells were counted. The identification of glioblastoma cells was based on the presence of typical cell features such as normal round euchromatic nucleus as well as intact plasma and nuclear membranes. Cell death processes were characterized as: a) apoptosis: clearly identified by its high toluidine blue affinity and morphological changes such as cell and nuclear shrinkage, chromatin condensation, membrane budding and apoptotic bodies formation; b) necroptosis: low toluidine blue affinity, swollen nucleus, increased cell volume, with intact or disarranged plasma and nuclear membranes; and c) necrosis: loss of plasma membrane integrity and consequent cytoplasmic content leakage.

### 1.7.3. Scanning Electron Microscope (SEM) Quantitative Analyses

Scanning electron micrographs of U-87 MG cells ranging in magnification from 10,000X to 20,000X and showing most of the cell surface were randomly taken from cryofixed, freeze-substituted samples and membrane structure alterations like slits, pores, or hole formations were analyzed.

### 1.7.4. Transmission electron microscopy (TEM) Quantitative Analyses

To study the cytoplasmic ultrastructural features of U-87 MG glioma cells and of the different cell death processes, a total of 80 U-87 MG electron micrographs ranging from 4,200X to 26,500X and showing the cell profile and nucleus were randomly taken from the cryofixed cells. The same characteristics as visualized in the high resolution light microscopy images were analyzed at the ultrastructural level, including the organelles organization within glioma cells.

### 1.8.Statistical analysis

The results were expressed as the mean ± standard deviation. Statistically significant or non-significant differences between the treatments and the controls were evaluated using Student's T-test or analysis of variance (ANOVA) and Turkey post-test using GraphPad Prism® program. $P<0.05$ were considered statistically significant. $IC_{50}$ values were determined by non-linear regression analysis of dose/response curves using GraphPad Prism 5.0. Data were expressed as geometric mean $IC_{50}$ plus 95% confidence interval.

## 2. Results

### 2.1. The increase of sub-diploid DNA content in glioblastoma cells, U87 MG, after exposed to LyeTx I-b peptide is not associated with apoptosis.

To gain insights into the mechanism of cell death induced by the peptide against U87 MG cells, different types of cell death mechanisms were investigated, including apoptosis, autophagy, necrosis and necroptosis. Despite the good cytotoxicity of peptide against the most of tumoral cell lines, the cell death mechanism was investigated in one cell lineage representative of brain tumor (U-87-MG), since this is common and very aggressive of human brain tumors, with few treatment options. Glioblastoma Multiform (GBM) is the most central nerve system malignant tumor with a high mortality (Wang, Y., et al., 2017). Cell death mechanisms involved in the cytotoxicity of many anticancer drugs include apoptosis, autophagy, necrosis and necroptosis among others. Then, apoptosis was the first mechanism that was addressed to investigate.

To understand the mechanism of cytotoxicity induced by LyeTx I-b against brain tumor cells in vitro, we investigated the effect of the peptide on U-87 MG cells. Cell death mechanisms involved in the cytotoxicity of many anticancer drugs include apoptosis, autophagy, necrosis and necroptosis among others. To evaluate if apoptosis was involved, the sub-diploid DNA content of U-87 MG cells treated with their $IC_{25}$ and $IC_{50}$ concentrations of peptide (10 and 30µM, respectively) was measured by flow cytometry after a 24h treatment. Cells undergoing apoptotic cell death display an increase of sub-diploid DNA content, which can be associated with the DNA fragmentation induced during late apoptosis or necrosis. The histograms in Figure 16A show a significant, concentration-dependent, increase in the percentage of sub-diploid (Sub-G1) content in U-87 MG cells after treatment with $IC_{50}$ concentrations of LyeTx I-b as compared with control (PBS). To confirm if the increase of the Sub-G1 DNA content correlated with DNA fragmentation, agarose gel electrophoresis was performed to evaluate genomic DNA. Results in Figure 16B display the profile of genomic DNA of U-87 MG cells after treatment with the $IC_{50}$ concentration (30 µM) of LyeTx I-b, and no DNA fragmentation ladder pattern was observed for treated or untreated control cells (i.e., DNA ladders of 180- to 200-bp oligomers are usually displayed in

apoptotic cells). This observation indicates that the DNA fragmentation observed in U-87 MG cells after treatment with LyeTx I-b was not associated to apoptosis.

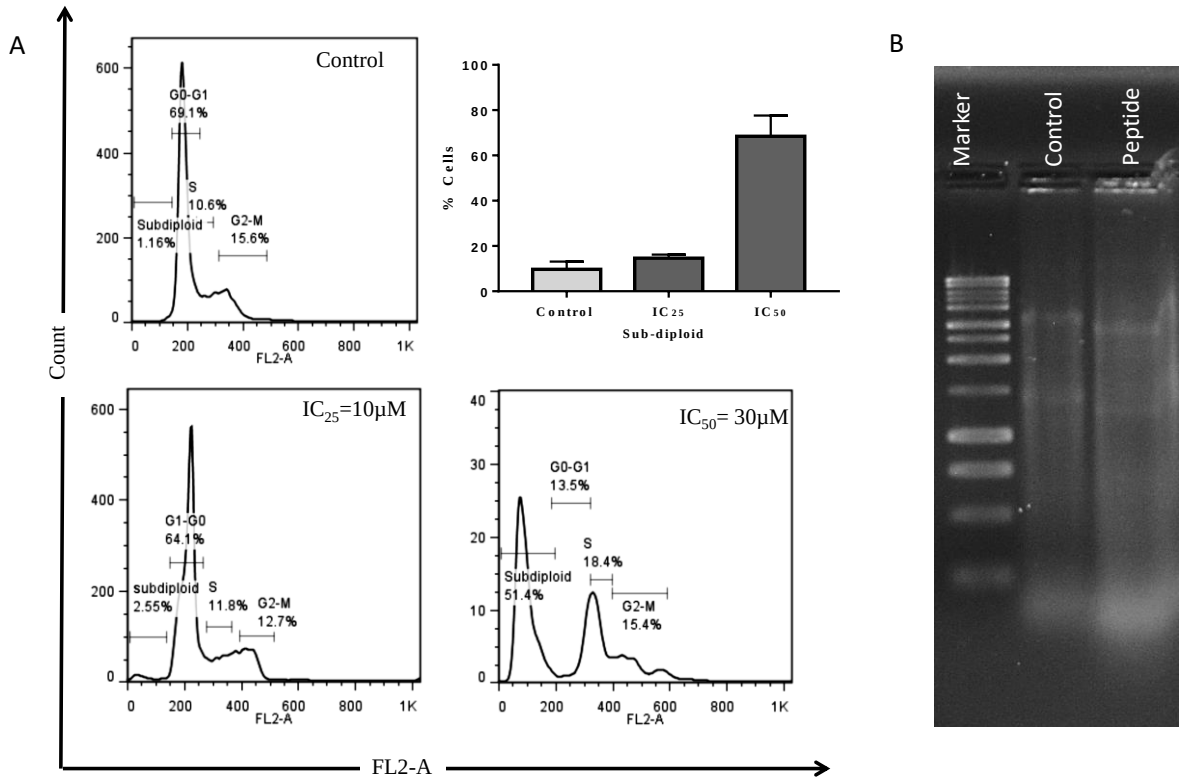


Figure 16. The increase of subdiploid DNA content in U-87 MG cells treated with LyeTx I-b is not associated with DNA fragmentation. Illustrative histograms showing cell cycle changes 24 hours after exposure to LyeTx I-b at $IC_{25}$ and $IC_{50}$ concentrations (10 and 30µM, respectively). Statistical analysis of independent triplicate experiments showed significant differences between the negative -control and the treated cells in terms of the subG1 (sub-diploid) population. (B) Analysis of U-87 MG cells genomic DNA treated with 30µM LyeTx I-b.. Note, no DNA fragmentation ladder laddering formation was obviously viewed on ethidium bromide-stained gels (2%) and photographed by UV illumination, when treated cells were compared with control (without treatment). Data shown are representative of three independent experiments.

## 2.2. Evaluation of autophagy induction by LyeTx I-b in U-87 MG cells by labelling with acridine orange

To identify if autophagy was involved in the toxicity of the peptide, the autophagic acidic cellular compartments were evaluated by FACS using acridine orange staining dye. The U-87 MG cells were treated with the same concentrations used to quantify the DNA content 10 and 30 µM LyeTx I-b. Flow cytometric analysis of untreated U-87 MG cells after acridine orange staining showed that most of the cells were labeled with green fluorescence,

and a minimal red fluorescence (8.1 %). Similarly, after treatment with the peptide, the cells still exhibited a green fluorescence comparable to the control, and showed a discreet increase in red fluorescence (12.7%), indicating presence of acidic vesicle organelles (AVO), which characterizes autophagy. These data suggest that this cell death is not the principal mechanism that contributes to the cytotoxicity of LyeTx I-b on U-87 MG cells (Figure 17).

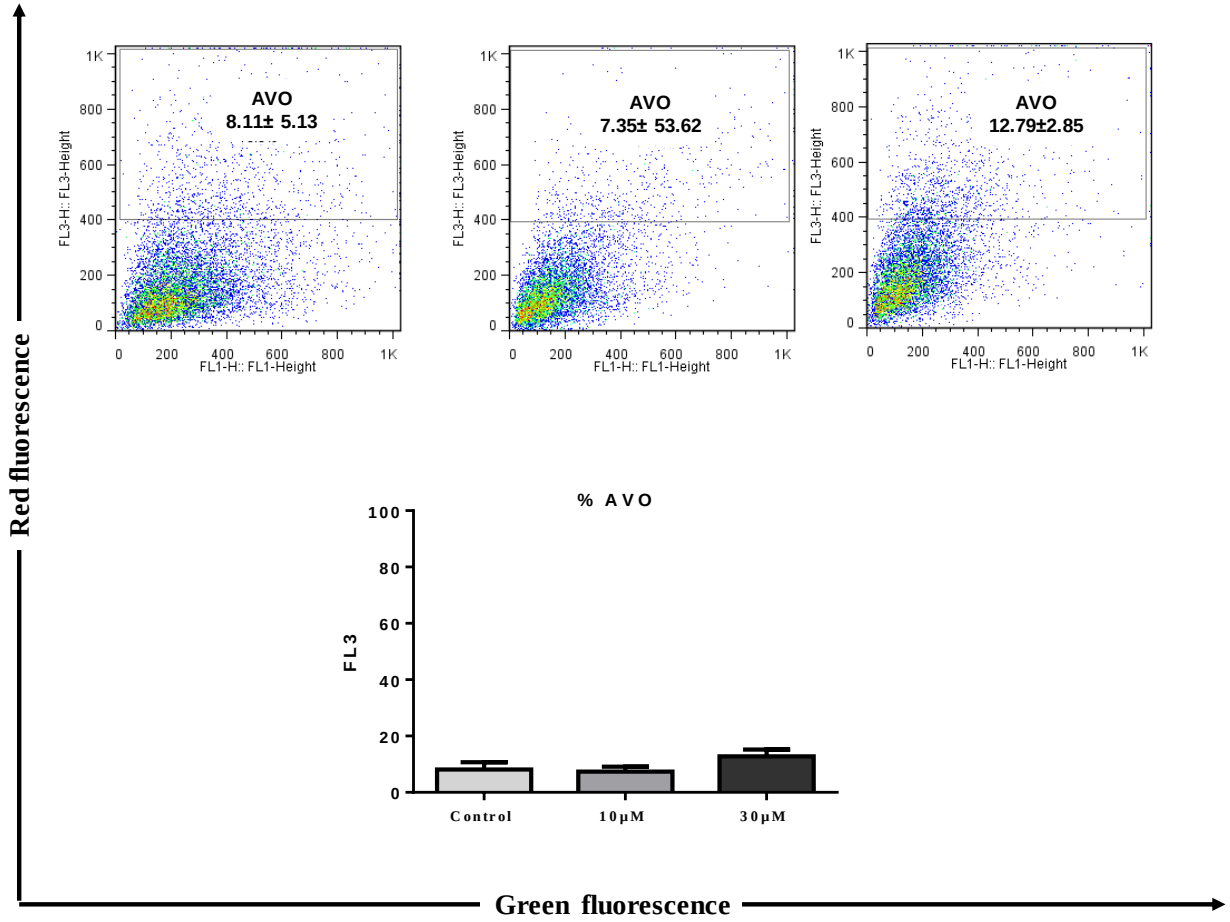


Figure 17. Representative images showing flow cytometric measurement of U-87 MG cells after exposed to LyeTx-I_b peptide for 24 hours and labeled with acridine orange. FL1-H indicates green color intensity, while FL3-H shows red color intensity (autophagy cells, AVO). Three independent experiments performed in duplicate.

## 2.3. LyeTx I-b peptide induces rapid loss of cell membrane integrity of U-87 MG cells associated with morphological alterations.

Since the results up to this point demonstrated that LyeTx I-b peptide does not induce apoptosis or autophagy on U-87 MG cells, we investigated the involvement of necrosis, in cell membrane integrity and cell morphology. For that, time kinetics experiments were performed by using MTT with $IC_{50}$ (30µM). The results in Figure 18A indicate that U-87 MG cells lose cell viability very quickly in the presence of 30µM LyeTx I-b (i.e., only after 15 min of treatment), as observed by LDH release. The increase in extracellular LDH levels indicates of cell membrane damage, and a reduction in cell viability was observed after 15 minutes, upon labeling with calcein-AM and Hoechst, as shown in Figure 18B. In control cultures, viable cells were labeled with both green calcein-AM and blue Hoechst after treatment with the peptide, the number of cells displaying green fluorescence decreased, while the number of blue nuclei became evident upon staining with Hoechst. Therefore, LyeTx I-b peptide induces damage in cell membrane integrity and concomitantly reduces the viability of U-87 MG cells in a time dependent-manner.

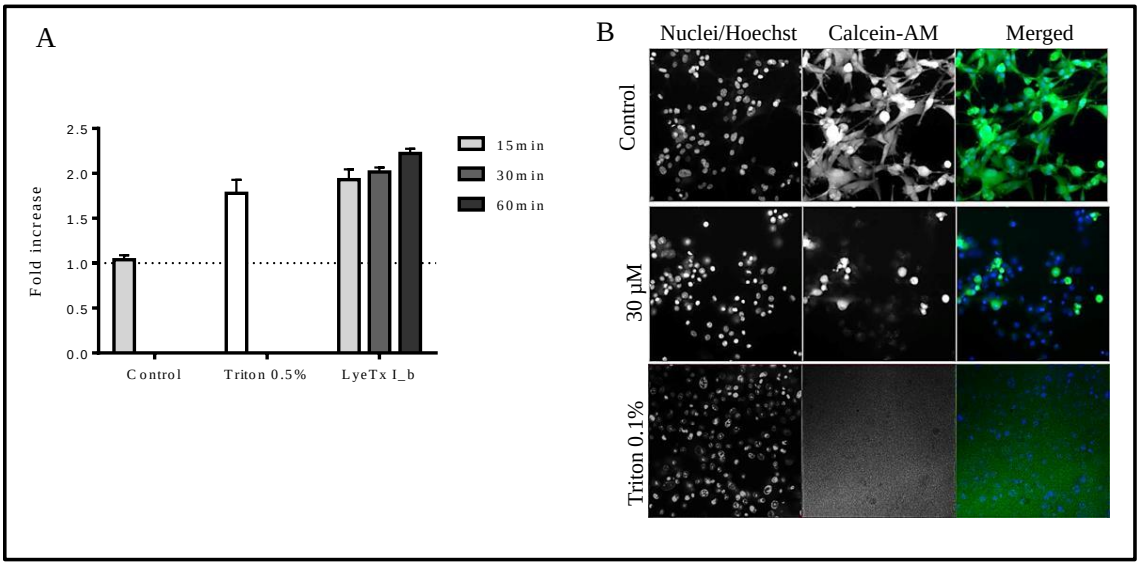


Figure 18. Effect of LyeTx I-b on LDH release and on the morphology of U-87 MG cells. (A) U-87 MG cells were treated with peptide (30µM) for 15, 30 and 60 min and LDH levels were evaluated (n=3). Triton X-100 (0.1%), a nonionic surfactant, was used as a positive control of cell membrane disruption. Relative LDH concentration was calculated as a % of the positive control. (B) U-87 MG cells were treated with peptide (30µM) for 15 minutes and then labelled with Calcein-AM and Hoeschst 3342. Double positive cells (green and blue) were counted as viable. The number of viable cells per field was detected using a high-content screening microscope (Scale bar, 50µm). At least 3 independent experiments were performed.

The morphological alterations were identified by light microscopy after stain with trypan blue (Figure 19A). Phase contrast microscopy confirmed the time-dependent morphological alterations observed with Calcein-AM and Hoechst labeling. Representative images of time-lapse analysis (Figure 19B) are corroborate with our previous findings, and show morphological alterations, including changes in cell shape, and reduction in cell size, probably due to depletion of intracellular constituents after plasma membrane damage (Figure 19B, arrows). The loss of membrane integrity was confirmed by scanning microscopy studies (Figure 20). Electron micrographs of control, untreated U-87 MG cells exhibited plasma membranes with a continuous, smooth, morphology, while cells exposed to 30 µM LyeTx I-b for 30, 60 and 180 minutes exhibited significant alterations in the cell membrane (Figure 19), including numerous cell membrane pores, holes and slits (Figure 5). These observations demonstrate that LyeTx I-b peptide is able to disrupt the plasma membrane, and suggests that necrotic cell death is the mechanism involved in the toxicity of peptide against U-87 MG cells.

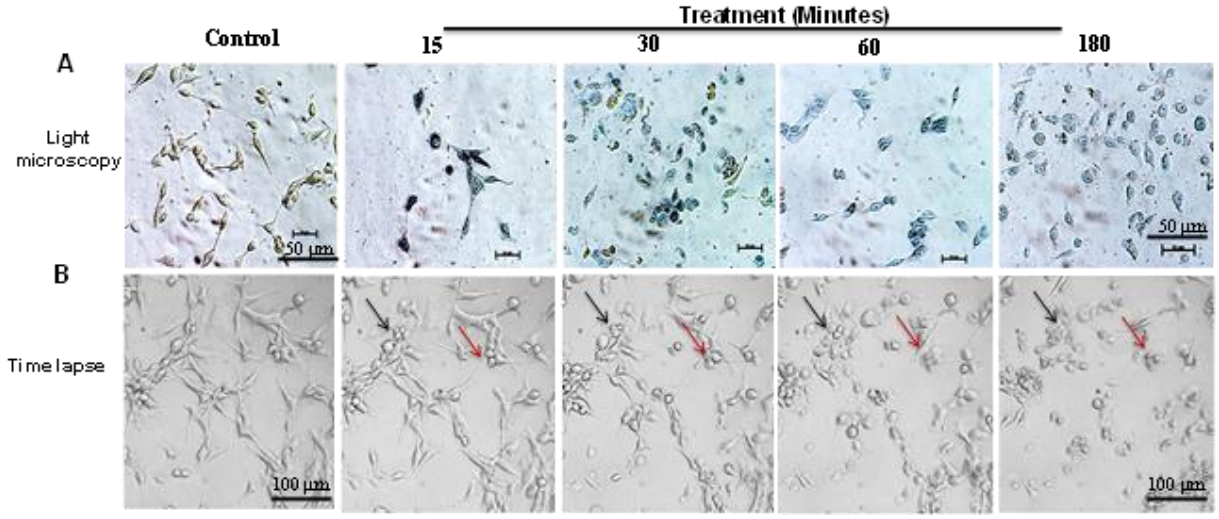


Figure 19. Partial disintegration of U-87 MG cell membranes after exposure to 30 µM LyeTx I-b. Control or treated cells were treated with the peptide for 0, 15, 30, 60, and 180 minutes, stained with trypan blue (A) and during time-lapse analysis (B). Red and black arrows represent alterations in both cells. Scale bars: (A) = 50 µm; (B) = 100 µm. Three independent experiments were done in duplicate for trypan blue, and time-lapse two experiments performed in triplicates.

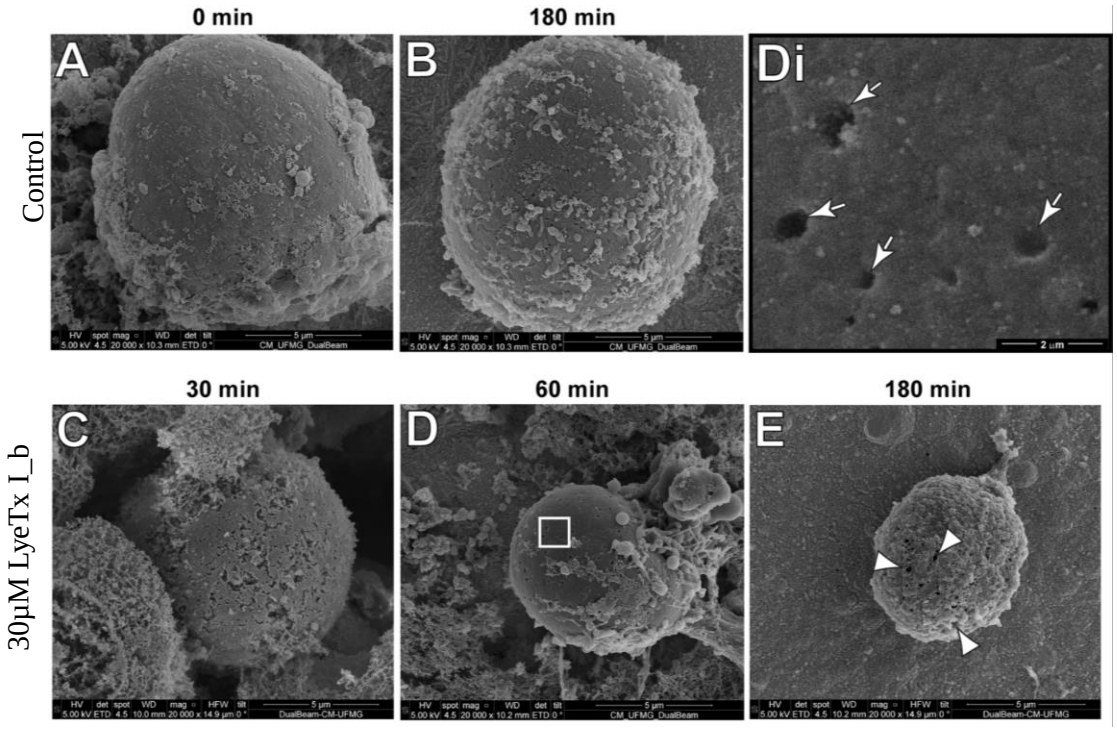


Figure 20. Ultrastructural changes on the U-87 MG cell surface exposed to 30 µM LyeTx I-b. (A, B) Control cells at 0 min and after 180 min of incubation respectively, displaying a smooth and homogeneous surface, with few membrane disruptions. (C, D, Di and E) After 30, 60 and 180 minutes of treatment with LyeTx I-b slits (C), pores (arrows) (Di) and hole (arrowheads) were detected in the plama membrane. (Di) is a higher magnification view of the white-boxed area in D. U-87 MG cells were cultured, fixed using high-pressure freezing (HPF), freeze-substituted and then processed for scanning electron microscopy (SEM). A total of 165 electron micrographs was randomly taken and analyzed at magnifications ranging from 10,000 to 20,000X. Bars: (A, B, C, D, E) = 5 µm; (Di) = 2 µm. Three independent experiments were performed, N=3.

All data presented until here suggested the induction of cell death by necrosis in U-87 after treatment with LyeTx-I_b peptide, and since was observed disruption of cell membrane, probably by pore formation. To evaluate other intracellular alterations at nuclei level, Topro-3 staining was used to detect possible nuclear alterations in the cells treated with peptide, after confocal analysis (figure 21). The nuclei of control stained uniformly with To-pro-3 whereas nuclei morphology of treated cells altered, showing the presence of chromatin condensation and swollen nucleus.

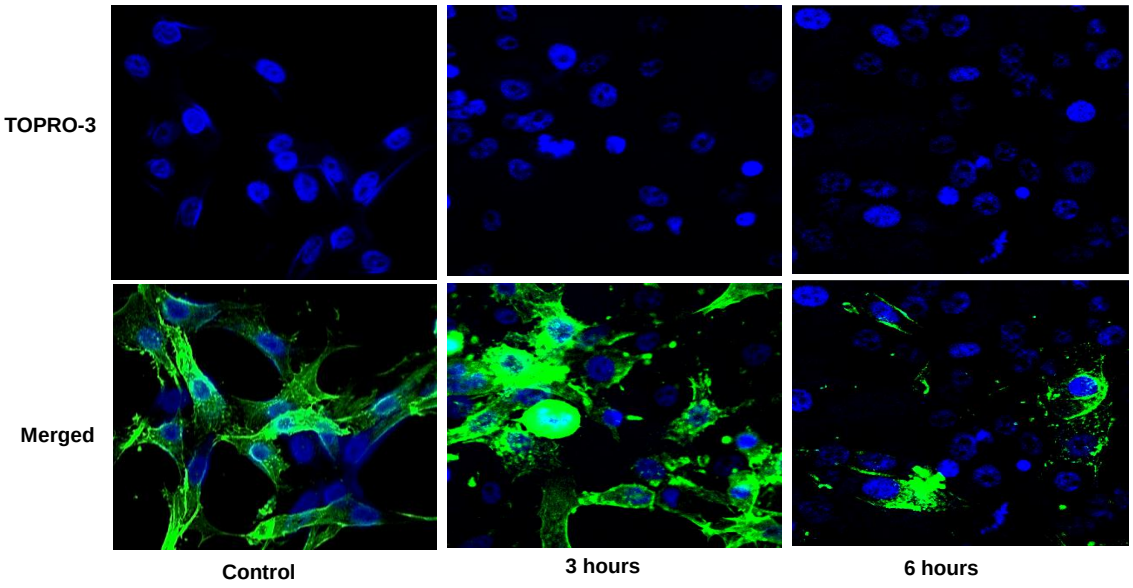


Figure 21. Confocal analysis of U-87 cells stained with TOPRO-3 was used for nuclear staining and Alexa Fluor 488 Phalloidin for cytoskeleton arrangements after exposure of U-87 to 30µM LyeTX-I_b peptide for 3 and 6 hours. Pictures were taken with Carl Zeiss LSM510 META confocal microscopy using 630 objective lens. Two independent experiments were performed.

Analysis of nuclear shape clearly demonstrated that no evidence for cell apoptosis occurred. However, it was observed DNA condensation that might result not only in necrosis, it may necroptosis effect due to nuclear translocation. In addition to Alexa flour 488 Phalloidin staining indicated that the F-actin filaments and cytoskeleton arranged regularly in the cytoplasm of normal cells. Whereas the cytoskeleton F-actin structure was disturbed in treated cells with peptide after exposure to 30 µM LyTx-I_b peptide for 3 and 6 hours (figure 21).

### 2.4. Pre-treatment with necrostatin-1 reduces loss of viability induced by the peptide on U-87 MG cells

To further confirm that necroptosis was involved in the cytotoxicity of the peptide against U-87 MG cells, assays with necrostatin-1, a specific inhibitor of necroptosis were performed. Triton-X 100 was used as a positive control. Pre-treatment of U87 cells with necrostatin-1 partially protected the cells from the toxicity of the peptide at 12.5, 25 and 50 µM, as observed by the higher values of resorufin fluorescence intensity, compared to the same treatment without necrostatin-1 (Figure 22).

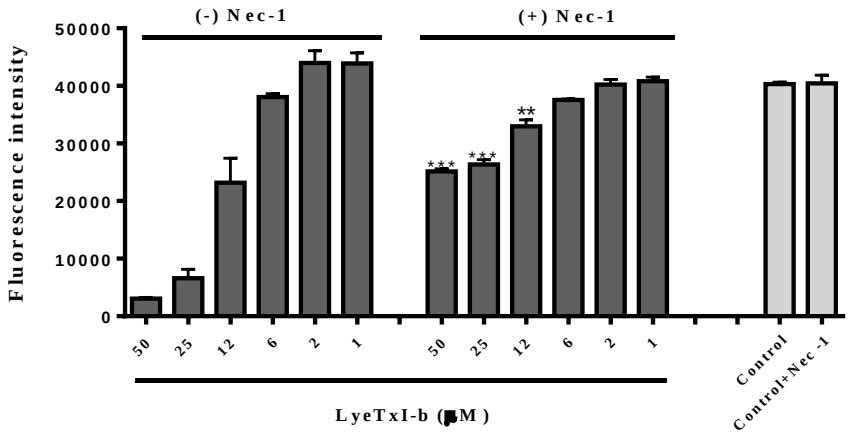


Figure 22. Effect of LyeTx I-b in cell membrane integrity and viability in the presence of necrostatin -1, a specific inhibitor of necroptosis. U-87 MG cells were pre-treated or not with 100 μM necrostatin -1 (nec-1) for 1h, followed by incubation with various concentrations of the peptide or Triton X100. Cell viability was measured by resazurin assay. The data shown here are representative of two experiments performed in triplicate. ***P <0.01, one-way ANOVA followed by Tukey Multiple Comparison test.

## 2.5. Electron microscopy studies displayed necrosis and regulated necrosis (necroptosis) as possible cell death processes involved with the LyeTx I-b peptide toxicity against U-87 MG cells.

To confirm that necrosis is induced by LyeTx I-b, a detailed ultrastructure study of cryofixed U-87 MG cells was carried out using transmission electron microscopy. Morphological structure alterations, indicating various cell death processes, were evaluated after 30, 60 and 180 min of 30μM peptide treatment. Transmission electron micrographs consistently displayed ultrastructure features that indicating a regulated necrosis process such as necroptosis as the principal findings in most of the observed fields. These characteristics include nuclei with mild DNA condensation, an increased cell volume with an electron-lucent nucleus and cytoplasm, and organelle vacuolization, but without rupture of nuclear or cell membranes (Figure 23C). In addition, a progression of the necroptotic process was clearly observed after 30 minutes of treatment, no plasmatic membrane alterations could be observed in the early stage (Figure 23C), and progressive enlargement of membrane pores could be observed from the intermediate late stages (Figure 23D, E). These findings suggest that the aggressive action of LyeTx I-b at 30μM concentration precludes these cells from undergoing a regulated apoptotic cell death process. Moreover, ultrastructural studies showed no morphological alterations indicating autophagy such

as presence of autophagosomes with intracellular organelles and disappearance of some cytoplasmic organelles, corroborating with the flow cytometry analysis.

Considering these data, the percentages of cells undergoing necroptosis, necrosis and apoptosis after treatment with LyeTx I-b were determined using high-resolution light microscopy (HRLM) morphometric analysis. The results confirmed necroptosis as the main cell death process while necrosis was measured as a minor proportion. The percentage of cells under apoptosis was similar to the control cells as shown in table 2. Apoptosis was identified by the chromatin condensation levels followed by nuclear and organelles shrinkage and the formation of apoptotic bodies (supplementary Figure 1A). Necrosis was best characterized by the huge plasma membrane rupture with extravasation of intracellular contents and organelles to the extracellular medium (supplementary Figure 1B).

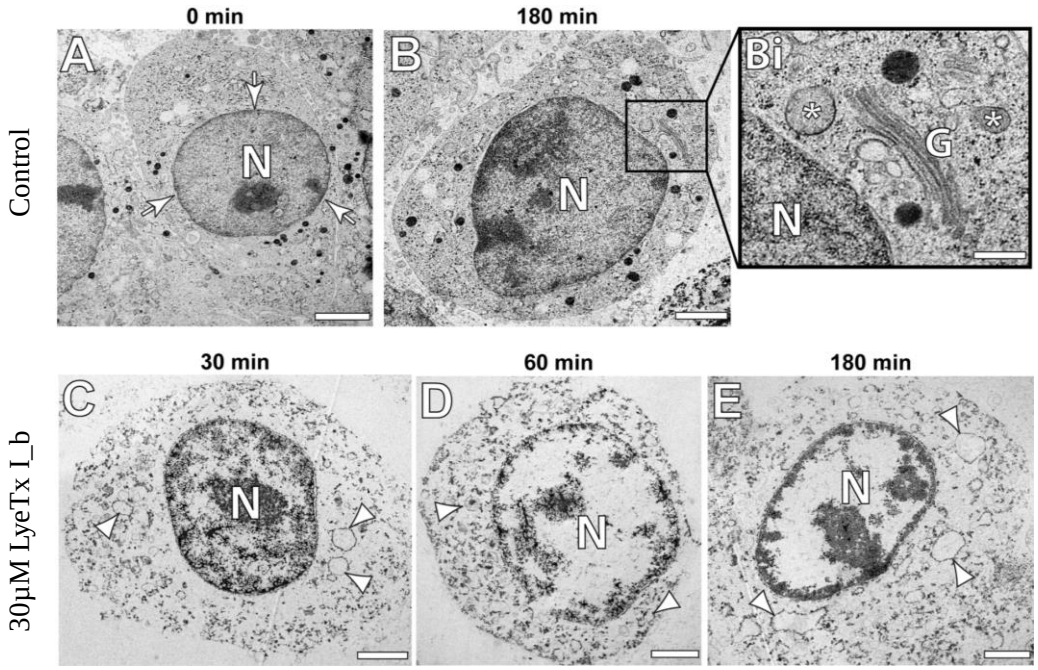


Figure 23. Intracellular ultrastructure of U-87 MG cells treated with 30 μM LyeTx I-b. (A, B) Control cells showing ultrastructural characteristics indicative of cellular activation such as the presence of a well round and central euchromatic nucleus (N) with fine distinction from the nuclear envelope (arrows). A higher magnification in (Bi) shows a prominent Golgi apparatus (G) and mitochondria (*). (C, D, E) Cells after 30 minutes of treatment, in different stages (early, intermediate, and late) of the necroptosis process, identified by the increase in the cell volume, swelling of the nucleus and cytoplasmic organelles (arrowheads), and electron lucent nucleus and cytoplasm. Differences in plasma membrane alterations ranging from membrane integrity maintenance (early stage) to the progressive membrane ruptures (middle to late stages) were detected. Human glioblastoma cells were cultivated and processed for transmission electron microscopy using high-pressure freezing and freeze-substitution. A total of 80 electron micrographs showing the entire cell profile and nucleus was randomly taken and analyzed at magnifications ranging from 4,200X to 26,500X. Bars: (A, B, C, D, E) = 2 μm; (Bi) = 500 nm. The micrographs shown here are representative of three experiments performed in triplicate.

Table 2. Morphometric analysis of transmission electron micrograph (TEM) of U-87 MG cell line after exposure to 30 µM LyeTx I-b for 30, 60 and 180 minutes.

| % | Normal | Apoptosis | Necroptosis | Necrosis |
|---|---|---|---|---|
| Control | 89.7 | 2.6 | 3.9 | 3.9 |
| 30 Minutes | 24.4 | 6.5 | 53.6 | 15.5 |
| 1 Hour | 5.7 | 1.9 | 64.2 | 28.3 |
| 3 Hours | 4.7 | 1.7 | 63.3 | 30.3 |

Note. The total count was at least 200 cells for each group.

### 2.6. LyeTx I-b peptide induction of necroptosis confirmed by Imaging Stream Flow Cytometry

Experiments using flow cytometric analyses were performed to differentiate between apoptosis, late apoptosis and necroptosis after treatment of U-87 MG with the peptide. Microscopy was combined with flow cytometry in one measurement to analyze morphological and biochemical features of cell death in a quantitative way, using classical annexin V/PI iodine staining to identify cells with phospholipids exposure and loss of membrane integrity. This strategy allowed classification of cells only labelled with annexin-V in early apoptosis, double positive cells (annexin-V and PI) in late apoptosis or necroptosis, and cells labelled only with PI in necrotic cells. To evaluate necroptotic cells, an image-based analysis was used to measure nuclear morphology, distinguishing cells with secondary necrosis due to late apoptosis and necroptosis, simultaneously (Pietkiewicz, S. et al., 2015). The results demonstrated that LyeTx I-b induced necroptotic death in U-87 MG cells after a 3 h treatment, observed by double positive staining with annexin V and PI, differently than observed in control cells. Control cells maintained a round shape and staining for either Annexin V or PI could not be detected (Figure 24A). Moreover, the number of double positive cells increased in correlation with increasing peptide concentration and time of incubation as observed in Figure 24B. After 3 hours of treatment with 30 µM LyeTx I-b, the percentage of double positive cells was 59.09 %, while after 6 hours it was 80.9% (Figure 24 C).

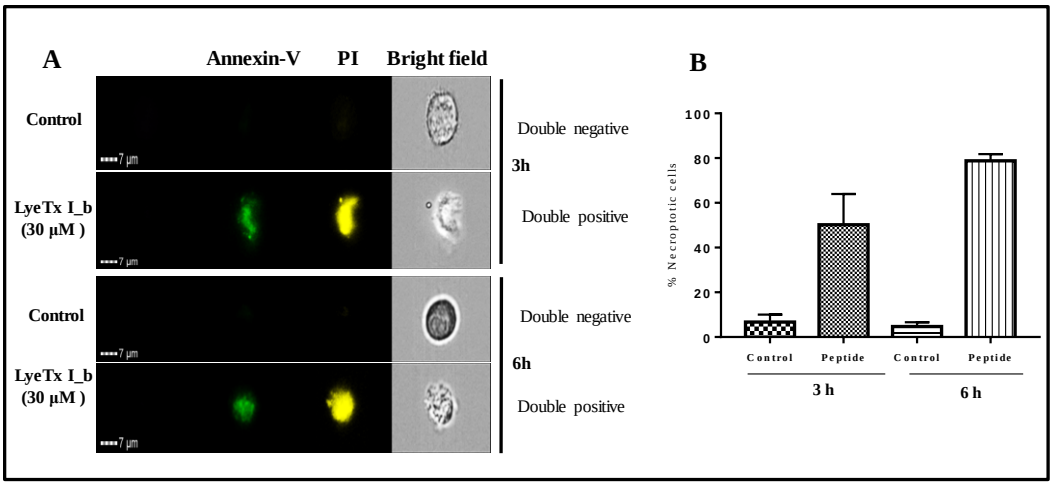


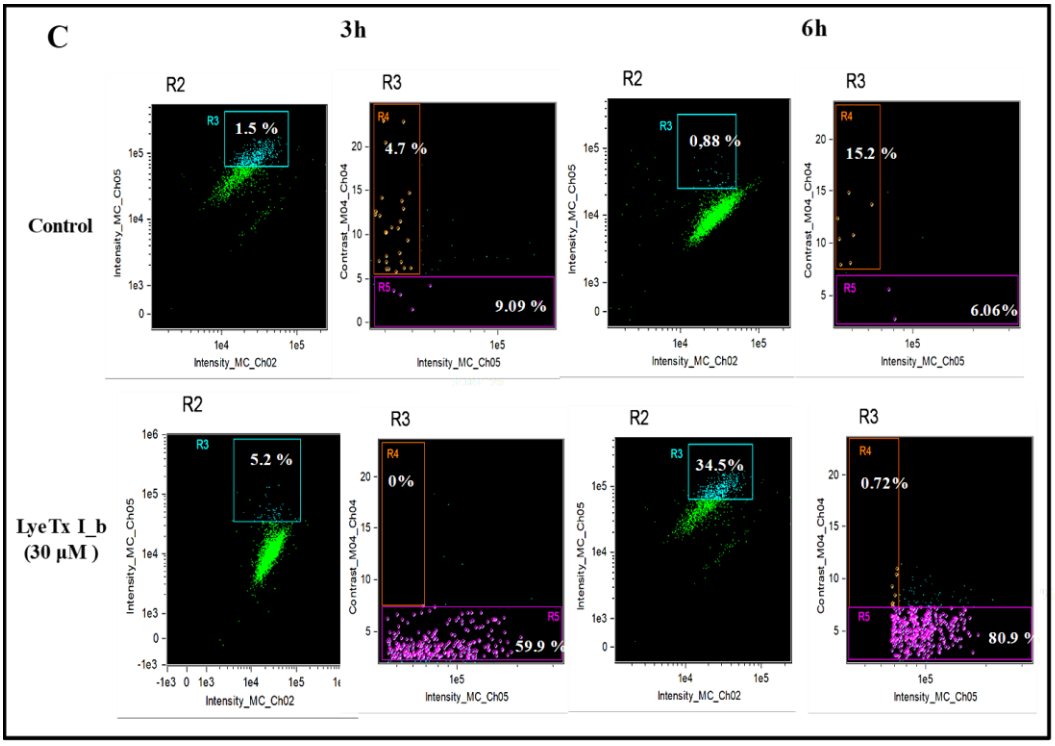


Figure 24. Imaging Stream Flow Cytometry of U-87 MG cells treated or not with LyeTx I-b. U-87 MG cells were treated with 30 µM peptide for 3 and 6 hours and labelled with Annexin-V (An) and propidium iodide (PI) and classified as live (double negative), early apopotic (An positive), late apoptotic (double positive) or necroptotic (double positive). Dots were constructed displaying intensity of Annexin, MC-Ch02; aspect ratio of PI stained nucleus , intensity of MC-Ch-05 and contrast morphology of PI, contrast MC_Ch04. (A) Representative images of U-87 MG, treated or not, acquired simultaneously with double negative and positive labelling (An+/PI+), as well as in bright field. (B) Percentage of necroptotic cells treated with 30 µM LyeTx I-b for 3 and 6h in two independent experiments. Graphs represent a different quantitative parameter that distinguishes between necroptosis and apoptosis.

## 3. Discussion

Cationic Antimicrobial Peptides (AMPs) are antimicrobial peptides that are able to stimulate innate immunity to fight against infections and have dual activities as anticancer and antimicrobial agent (Verano-Braga, T. et al., 2010 & Pane, K. et al., 2017). Glioma cell membrane contains high level from phospholipids like phosphatidylserine, sphingomyelin and phosphatidylethanolamine, which confers negative charges that allow them bind with the positive charges present in cationic peptides, increasing the selectivity of these peptides for cancer cells (Llado, V. et al., 2014 & Chen, C. et al., 2014). Furthermore, anticancer cationic peptides have many features such as mild toxicity without accumulation in different tissues and eventually selectivity and specificity for cancer targets and receptors (Deslouches, B. and Di, Y.P. 2017& Perez-Pitarch, A. et al., 2017). In this work, we focused on brain cancer cells, specifically in one representative lineage of glioblastoma multiform, U-87 MG cells as a model to understand the cytotoxic mechanism of LyeTx I-b peptide and evaluate it anticancer potential. This peptide displayed an excellent antimicrobial activities *in vitro* and *in vivo* (Dos Reis et al., 2018). The aggressive nature of this class of tumor and the poor prognosis of patients with GBM underscore the clear requirement for more precise and powerful treatments (Marqus, S. et al., 2017). U-87 MG, along with SK-MG-1 and U251-MG, cells were used by Bubien and coworkers (2004) to evaluate the activity and selectivity of Psalmotoxin 1 (PcTX-1), a peptide found in the venom of a West Indies tarantula that is able to inhibit the acid-sensing ion channels (ASIC). Authors have found that GBM cells have a unique profile of expressed cation channel that is different in normal human astrocytes, increasing the selectivity of Psalmotoxin 1 towards these tumor cells. PcTX-1 was also able to inhibit migration and proliferation in U87-MG and D54-MG cells, by inhibiting also the Deg/epithelial sodium channel (ENaC), along with ASIC. These authors concluded that cell migration and cycle progression processes in GBM cells seem to be regulated by cation conductance evoked by both acid-sensing ion channels and ENaC subunits (Rooj, A.K. et al., 2012). Also from arthropods, four mastoparan peptides isolated from wasps venoms (Anoplin and the mastoparans MP1, MPX, and HR1) were tested against T98G glioblastoma multiforme cells, an able to induce necrosis, most likely by membranolytic activity.

To elucidate the mechanism of cell death involved in the cytotoxic activity of LyeTx I-b against U-87 MG, classical cell death mechanisms such as apoptosis, necrosis and autophagy were investigated using flow cytometry and morphological studies. To evaluate apoptosis, cell cycle

analyses demonstrated an increase in the content of subdiploid DNA in U-87 MG cells after treatment with 30µM peptide (Figure 16A). Although this result indicates DNA fragmentation, agarose gel analyses clearly showed that the treatment of U-87 MG cells with the peptide did not induce apoptotic pattern of apoptosis, since no ladder was observed (Figure 16B). The cells undergoing apoptotic cell death exhibit different morphological and biochemical alterations such as DNA fragmentation due to endonucleases enzymes like caspase-3, that cleave the chromatin into fragments with 180 bp that appear after running the DNA in agarose gel, similarly to a "ladder" (Matassov, D. et al., 2004). These results were also supported by FACS analyses of one early apoptotic phenomena such as phosphatidylserine exposure since less than 15% of apoptotic cells, were detected in different times of incubation of U-87 MG cells with the peptide.

Furthermore, ultrastructural studies, this type of cell death usually demonstrates sequestration of cytoplasmic components within a double membrane structure called the autophagosome, followed by delivery to lysosomes for degradation. These lysosomes can be detected with acridine orange that can be quantified by flow cytometry (Gewirtz, D.A. et al., 2014) there was no indication of cells in autophagic process, since the presence of AVO was lower than 14%, comparing with the control (figure 17). Even considering that other markers of autophagy have not been investigated here, such as microtubule-associated protein LC3, which plays a key role for the formation of autophagosomes (Eum, M. and Lee, M. 2011 & Brauchle, B. et al., 2014). Morphological analysis using MET clearly demonstrated no signs of autophagy alterations such as the presence of double-membrane structure with undigested cytoplasmic organelles including mitochondria or endoplasmic reticulum as described by Mizushima and co-workers (2010). These results demonstrated that neither apoptosis nor autophagy were the main mechanisms triggered by the peptide on U-87 MG cells.

Most of the data presented here indicated that LyeTx I-b induced necrosis or a programmed necrosis through rapid cell membrane damage. Trypan blue uptake in U-87 MG cells occurred after 15 minutes incubation with 30µM LyeTx I-b, as well as, time-lapse studies showed cell membrane disruption (figure 19). This effect was in a concentration-dependents, confirmed by measurement of LDH release and calcein-AM (figure 18). Comparable data were observed by Burns and co-workers, who described the effect of pHLIP-KLAKLAK antimicrobial peptide on the integrity of MDA-MB-231 cell membrane (Burns, K. et al., 2016). They also showed trypan

blue uptake after treating with the toxic peptide, disruption and permeabilization of the cell membrane as a result of pore formation (Tran, S. et al., 2011).

Disruption of U-87 MG membrane after treatment with the peptide was confirmed herein by scanning microscopy studies. Our data suggest that LyeTx I-b was able to cause damage to the cell membrane after 30 minutes of treatment, forming "holes" after 180 minutes, leading to membrane destruction as shown in Figure 20. These findings suggested that LyeTx I-b can induce pores formation in the membrane of U-87 MG cells, in a time and dose-dependent way, leading to plasma membrane permeabilization and consequent cell degeneration. Scanning microscopy analyses of U-87 MG cells after treatment with the cationic anticancer peptide bacteriocin LS10 demonstrated cell membrane disintegration, similarly to our findings (Baindara, P. Et al., 2017). Lytic activities of peptides isolated from other venoms have been described. ABH3 peptide is a BCL-2 homologue artificial lytic peptide, which exhibits the ability to rapidly disrupt the cell membrane in different cancer cell lines HCT116, HeLa, U937, MCF-7 and MDA-MB-231 (Liu, Q. et al., 2016). A similar study, antimicrobial peptide temporin-1CEa, extracted from skin secretions of the Chinese brown frog demonstrated that temporin-1CEa able to disrupt cancer cell membranes, causing loss of membrane integrity due to the formation of transmembrane pores that allow an uptake of the peptide into the cytoplasmic compartment of the cancer cell (Wang, C. et al., 2013). However, we did not evaluate how the pores and were formed and their size in U-87 MG cells after treatment with the peptide in this approach.

Interesting finding observed after transmission electronic microscopy (TEM) and Ultra-structural analysis, suggested that the peptide at 30µM induced a regulated type of necrotic cell death in U-87 MG. Necrotic cells at the light of TEM studies have unique morphological features, such as swollen organelles, nuclear membrane dilatation, little chromatin condensation and breakdown of the plasma membrane due to oncosis, increasing the volume of cell membranes (Vandenabeele, P. et al., 2010). Necroptosis or regulated necrosis were frequently identified in most of the fields, characterized by swollen nuclei, vacuolization, increase of cell volume and integrity of cell membrane (Figure 8), in agreement with previously morphological alterations described this cell death process, like swollen nucleus, increased cell volume and mild chromatin condensation (Sun, Y. et al., 2018). We not only found cells with a necroptotic profile but also few cells in necrosis and apoptosis (nuclei with condensed chromatin and reduction of cell volume), at lower

frequencies. Morphometric analyses (table 2) demonstrated that after 30min, more than 50% of the cells were necroptotic, less than 20% were necrotic and less than 3% were apoptotic. These findings were time-dependent. TEM analysis characterize necroptotic cell death has been described in literature (Sun, W. et al., 2016). Our data demonstrated morphological necroptosis signs in U-87 MG cells after treating with 30µM LyeTx I-b, characterized by the swelling of nucleus and mitochondria, increase in cytoplasm volume, membrane disruption, cytoplasm vacuoles, and release of cellular content (figure 23). Other studies using TEM showed necroptosis signs after treatment with natural alkaloid compounds (martine) in cholangiocarcinoma cells (CCA) characterized by cytoplasmic vacuolation and extensive swelling of organelle and loss of plasma membrane integrity (Zhao, H. et al., 2016). As a consequence of cellular swelling and rupture of the plasma membrane, they also observed an extravasation of cellular components and increase in LDH, as observed in the present study (Tian, F. et al., 2016).

To better characterize the necroptotic death triggered by LyeTx I-b on U-87 MG, cells were pre-treated the cells with necrostatin-1 (Nec-1), which is a specific inhibitor of necroptosis (Xu, B. et al., 2017 & Melo-Lima, S. et al., 2014). As observed in figure 22, pre-treatment of U-87 MG cells with Nec-1 protected U-87 MG cells against the cytotoxicity induced by the peptide, observed by an increase in the number of viable cells, comparing with control. Flow cytometric studies (Figure 24) corroborate with these data, showing an increase in the number of necroptotic cells after 3h treatment, in a time and dose-dependent manner, 59.9% of cells were necroptotic, and after 6h, this number increasing to 80.9%. These data were in agreement with those observed after the morphometric analysis by TEM (table 2). Although other direct molecular markers of necroptosis (TNF-alpha receptor activation; MLKL phosphorylation, RIP3 involvement) have not been evaluated in this study, the use of the specific necroptosis inhibitor necrostatin, flow cytometry assays and ultrastructural studies clearly demonstrate that necroptosis is the main type of cell death induced by the peptide

In summary, we reported that the cationic antimicrobial peptide LyeTx I-b presents cytotoxicity against glioblastoma cells. This effect involves induction of necroptosis as the main cell death process.

# Chapter 3

## Anticancer potential of cationic antimicrobial peptide LyeTxI-b derived from *Lycosa erythrognatha* spider venom using the metastatic 4T1 triple-negative breast cancer murine model.

**Hypothesis**

LyeTx I-b peptide possess lower toxicity in healthy mice and reduces neoplastic development and migration by inhibiting the proliferation and inflammation processes in the metastatic 4T1 murine mammary carcinoma model, potential to confer anticancer drug.

## 1. Materials and Methods

Considering the cytotoxicity *in vitro* of peptide against breast cancer cells from human and mice, the in vivo experiments were performed using the metastatic 4T1 murine triple-negative breast cancer model, that mimetize this pathological process in human.

### 1.1. Animals

Females Balb/c mice (9-10 weeks old) were obtained from the animal housing facility from Universidade Federal de Minas Gerais (UFMG). The animals were housed in cages in temperature-controlled room, maintained on a 12 h light/dark cycle, and were provided with food and water ad libitum. Efforts were made to avoid any unnecessary distress to the animals. Animal procedures were conducted in accordance with the internationally accepted principles for Care and Use of Laboratory Animals and were approved by the Animal Ethics Committee of UFMG (CEUA protocol # 39/2018).

#### 1.1.1. Experimental tumor model

4T1 cells were detached from the T75 flask surface by 3 ml trypsin solution (0.05%), suspended in sufficient volume of DMEM medium to neutralize trypsin enzyme and then cells were centrifuged at 300 g for 5 minutes. After counting, the cells resuspended in PBS 1.5 $x10^6$ /100µL. To obtain the solid tumor, one-hundred microliters were injected subcutaneously in the posterior left flank of all animals (Paschall, A. & Liu, K. 2016).

### 1.2. *In Vivo* treatment design of Sub- acute toxicity:

Balb/c mice were randomly assigned to 2 groups: control (n=6) and treated (n=6). Animals were treated via i.p. with 100 µL of saline or peptide (5 mg/kg/day) (seven doses, 48 hours/apart) and were monitored for 15 days. The body animals weight were monitored three times a week and

tissues were collected for histopathological assess. Experimental strategy is represented below in scheme 4.

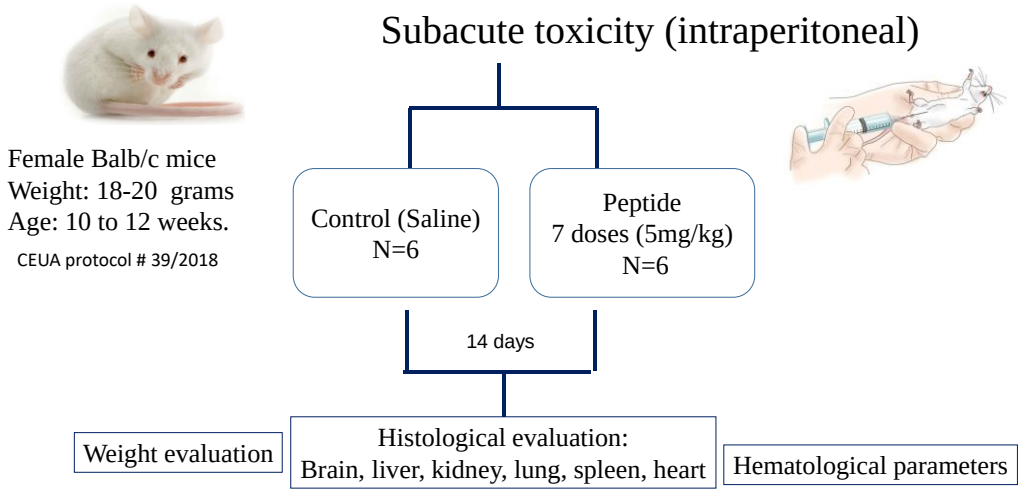


Scheme 4. Experimental design to evaluate the subacute toxicity of LyeTx I-b peptide in Balb/c mice.

**1.3. Evaluation of antitumor effect of LyeTxI-b in murine 4T1 mestastatic triplo-negative breast cancer.**

In order to study the potential anticancer effect of peptide, two strategies of administration (intratumoral and subcutaneous) were used as described in scheme 5.

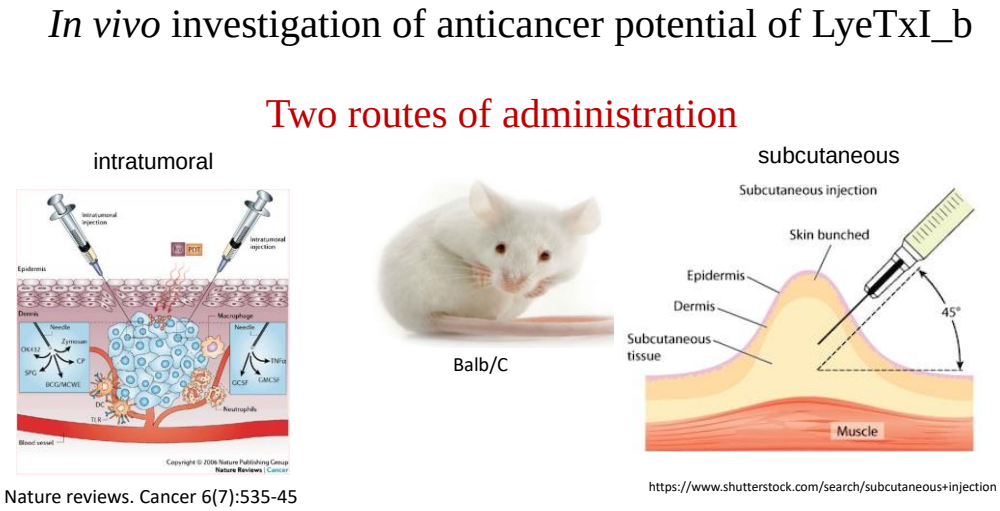


Scheme 5. Routes of administration to evaluate the anticancer potential of LyeTx I-b peptide using murine 4T1 breast cancer model.

### 1.3.1. Intratumoral drug administration

Female BALB/c mice (n = 21) were injected via Subcutaneous with 4T1 cells in the posterior left flank. After 10 days, when the tumor volume reached approximately 1.0 $cm^3$, animals were assigned to three groups: Control (treated with saline) (n =7), carboplatin (5mg/Kg), and LyeTxI-b peptide (5mg/kg) intratumorally. All animals received treatments for five subsequent times, 72 hours. Methodology is represented below in scheme 6.

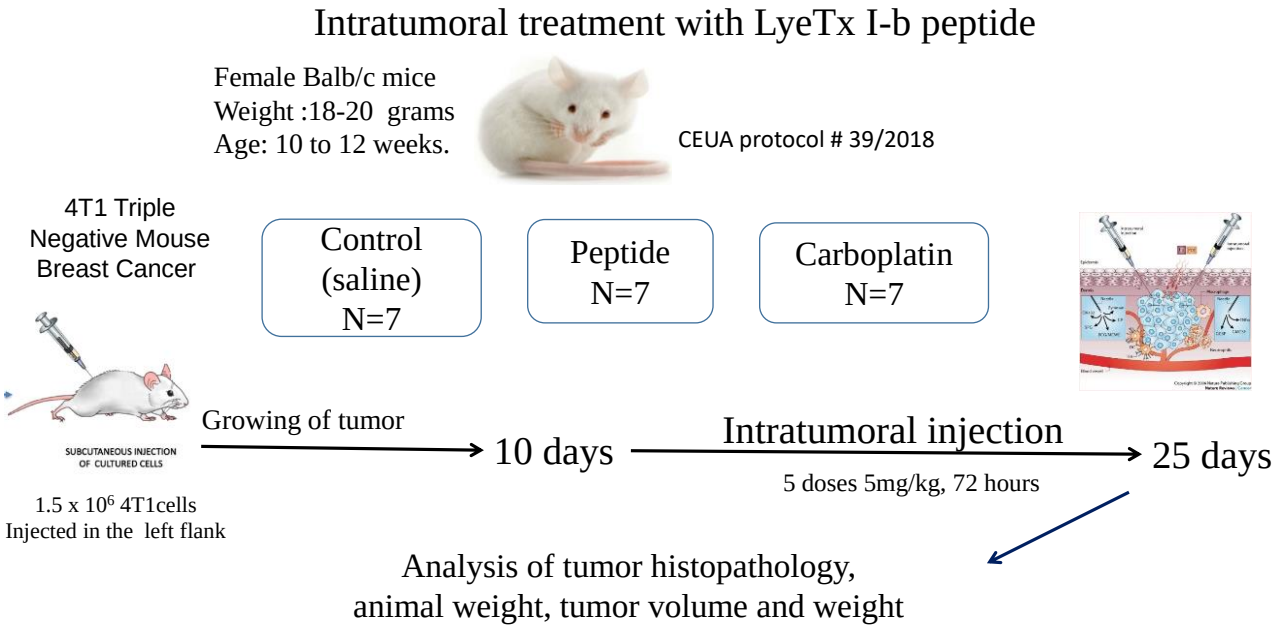


Scheme 6. Strategy used to evaluate the anticancer potential of the peptide in murine 4T1 breast cancer model using an intratumoral administration.

### 1.3.2. Subcutaneous drug administration

Eighteen females BALB/c mice were injected subcutaneously with 4T1 cells in the posterior left flank, after 5 days, when the tumor volume reached approximately 0,25 cm3, all animal were randomly assigned to main 3 groups: : saline (s.c.) (n = 6), carboplatin (s.c., 5 mg/Kg) (n =6) and LyeTxI-b peptide (s.c.; 5mg/kg)( n = 6). All animals received treatments for five subsequent times, every 72 hours. The body animal's weights and tumor volume were monitored every 3days. Signs of distress and pain were monitored daily (Szczepanski, C. et al., 2014). The measurement of tumor volume was calculated using the following equation: tumor volume ($mm^3$) = (length x $width^2$)/2, the length and width were expressed in mm (Fulzele, S. et al., 2006). Methodology is represented below in scheme 7.

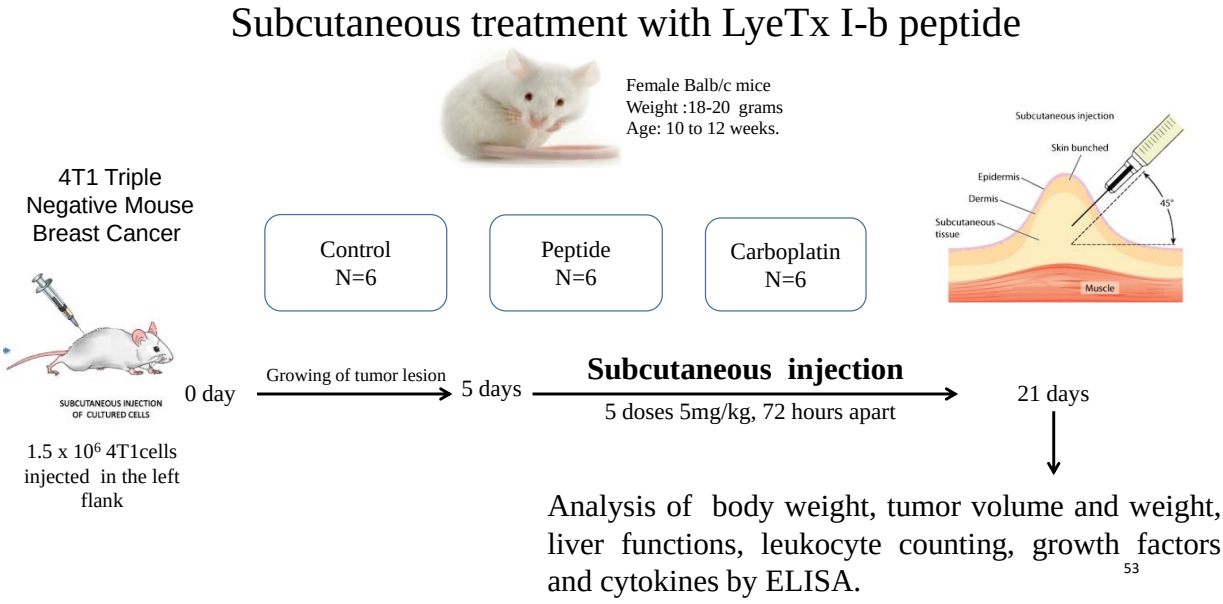


Scheme 7. Strategy used to evaluate the anticancer potential of the peptide in murine 4T1 breast cancer model using a subcutaneous administration.

### 1.4. LyeTx I_b peptide toxicity and tolerability

To examine LyeTx I_b peptide toxicity an tolerability on tissue, mice were anesthetized with a mixture of ketamine (150 mg/Kg) and xylazyne (10 mg/Kg), and perfused through the heart with 10% formalin. The tumor, spleen, lung, brain, kidney, and liver were quickly removed and fixed in 10% formalin for 48 h until subsequent histological analysis. Eighteen females BALB/c mice were used for this evaluation.

### 1.5. Histological analysis of tissue sections

According to tissue preparation for conventional histology protocol, after tumor and tissues fixation, transverse sections were obtained, embedded in paraffin, cut into 4µm sections and then stained with hematoxylin and eosin (H&E). The images were captured using light microscopy (Olympus), (plan apochromatic objective, 20x) (Hewitson, T. et al., 2010). All images were digitized by Spot Insight Color (SPOT® version 3.4.5.) A micro camera (Olympus Microscope, BX-40) mounted on the microscopy project the images to a monitor and images were analyzed by software. In order to evaluate the metastatic nodules, morphometric image analysis were performed using 40x objective (Dutra, A et al., 2008).

### 1.6. Evaluation of liver functions, glutamate-oxalacetic transaminase (GOT) and glutamate-pyruvic transaminase (GPT)

Acute and chronic hepatic impairment resulting an increase in serum aminotransferases enzymes activities. GPT, also known as alanine Aminotransferase (ALT), is an enzyme of predominantly hepatic origin, considered as sensitive marker of liver cell injury. GPT is often found in small amounts in the heart and skeletal muscles. GOT, also known as Aspartate Amino Transferase (AST), can be located in the liver, heart muscle, skeletal muscles, kidneys, pancreas, erythrocytes, and brain. In the context of tissues damage, GOT is released into the blood immediately (Giannini, E. et al., 2005). GOT and GPT are intracellular enzymes that catalyze the transfer of amine and alpha amino acid groups to alpha acetoacids, as demonstrated in the scheme below:

L- alanine + α-ketoglutarate $\longrightarrow$ L-Glutamate + Pyruvate

L-aspartate + α-ketoglutarate $\longrightarrow$ L- Glutamate + Oxalacetate

The pyruvate and oxalacetate amounts are proportional to the enzymatic activity and are quantified by formation of hydrazones, which are stained in an alkaline medium.

The quantification of GOT and GPT transaminases activity was performed by using the commercial colorimetric kit (Oliveira-Lima, O. et al., 2013). Mice were euthanized, blood samples were collected in a heparinized tube, and then centrifugated (5000 rpm / 10 min) in order to separate serum. For each sample, was prepared 200 µl of GOT substrate (0.2M L-aspartate, 0.002M alpha-ketoglutarate, and 0.1M phosphate buffer, pH 7.4), and 200µl GPT substrate (L-alanine O, 2M, 0.002M alpha-ketoglutarate, and 0.1M phosphate buffer pH7.4). After here, 25 µl of each sample was added to the GPT substrate, and 50 µl of each sample was added to the GOT substrate. The tubes were incubated in the dark at 37° C for 40 minutes. In the next step, 200 µl of the color reagent (0.001M 2, 4 Dinitrophenylhydrazine solution) was added to each tube at room temperature, for 20 minutes, and eventually, 2 ml of 0.4M sodium hydroxide was added to the tubes, for 2 minutes at room temperature. The absorbance measurement (540 nm) was performedt using spectrophotometer (BioTek, model Epoch). The zero was adjusted with distilled water. A calibration curve was used in order to calculate the values of GPT and GOT activities, expressed as unit per liter (U/mL).

### 1.7. Determination of Complete blood count (CBC).

A complete blood count (CBC) is a blood test used to measure several components and features of blood including, red blood cells, hematocrit, white blood cell, haemoglobin, platelets. Mice were euthanized, blood samples were collected in a heparinized tube, 100 µl of whole blood was submitted to ABCVet automatic blood analyzer for counting of red blood cells (RBC), hematocrit, hemoglobin, platelets, White blood cells (WBC), and also RBC parameters, mean cell volume (MCV), mean corpuscular hemoglobin (MCH), and mean corpuscular hemoglobin concentration (MCHC).

### 1.8. Quantification of differential circulating peripheral leukocytes populations.

Differential leukocytes counting determines a percentage of each type of white blood cell populations (Neutrophils, lymphocytes, monocytes, eosinophil, and basophil). Blood smears were made immediately after whole blood collection in 0.5 M sodium ethylenediaminetetraacetic acid (EDTA). EDTA was used in order to avoid plasma coagulation and platelet aggregation. In summary, two microscopic slides were used, one of them being used as a spreader slide. The edge of the slide spreader had been placing against the surface of the first blade at an angle of 30 to 45 degrees. After slide spreader contacted the drop of blood (30µl), using a smooth even motion, the slide spreader had been pushing forward. The blood had been spreading very quickly by capillary action within several millimeters of the edges of the slide. Blood film was stained with May-Grünwald's eosin methylene blue and Giemsa's azure eosin methylene blue, pH 6.4-7. Upon the coloration of differential leukocyte populations, the cells were counted by using a light microscope, 100 or 200 cells were counted either manually (Koepke, J. 1980). Santos and his collaborators have been described the normal hematological values of BALB/c mice using blood smear (Santos, E. et al., 2016).

### 1.9. ELISA: Quantification of cytokines and growth factors

Sandwich ELISA (enzyme-linked immunosorbent assay) is an efficient and sensitive technique to evaluate inflammatory cytokines and growth factor protein expressions in tumor tissues (Mathonnet, M. et al., 2006, Oliveira-Lima, O. et al., 2015). Cytokines and growth factors in the primary tumor, lung, spleen, and brain were determined using ELISA. Mice were anaesthetized and tissues were collected and preserved in -80$^{o}$ C until analysis. Each tissue (100 mg) was

homogenized in an extraction solution (containining 0.4 mol/L NaCl, 0.5% BSA, 0.1 mmol/L PMSF,, 0,1 mmol/L benzethonium chloride, 10 mmol/L EDTA and 20 KI aprotinin) using ultra-turrax machine of 1 ml contains 100 mg of tissue. The homogenates were centrifuged 3000 x g for 10 minutes at 4$^{o}$ C for 10 minutes, and supernatant (50 µl) was collected and stored at - 20$^{o}$ C. Samples were analyzed for VEGF, TGF-β, TNF-α, IL-1β, IL-10 and IL-6 using murine DuoSet ELISA kit (R&D Systems, USA). According to manufacturer's protocol, a capture murine monoclonal antibody against VEGF, TGF-β, TNF-α, IL-1β, IL-10 and IL-6 was added into 96-well polyvinylchloride microtiter plates and incubated overnight at room temperature. In the next day, plates were washed 3 times with washing buffer (phosphate buffered saline with Tween 20). A solution of 2% bovine serum albumin (BSA; 150 µL ) dissolved in PBS was added for 2 h at room temperature to block any nonspecific binding sites on the surface. Plates were rinsed twice with 0.1% BSA in PBS and 50 µL of the antigen solution (samples or standard) was added to the wells and incubated at least 2 h at room temperature. Next, 25 µL from detection antibody was added and incubated again for 2h at room temperature. After rinsing 3 times, 50 µL streptavidin conjugated to horseradish-peroxidase solution was added to each well and plates were incubated for 20 minutes at room temperature. Plates were washed and the substrate solution, OPD (ophenylendiamine, Sigma) diluted in 0.03M citrate buffer (pH 5.0) containing 0.02% $H_2O_2$ was added, followed by incubation in dark place at room temperature for 30 minutes. The reaction was stopped by adding 2N sulfuric acid (25 µl/ well) and the optical density of the color was measured immediately at 490 nm using ELISA reader (Spectramax-Molecular Devices®).The concentration of each molecule was calculated using a standard curve (range from 15 – 2000 pg/ml) and was expressed as pg/ml.

### 1.10. Evaluation of leukocyte-endothelial interactions by intravital microscopy

Intravital microscopy was used to evaluate leukocyte recruitment (rolling and adhesion steps) *in vivo* as previously described (dos Santos et al., 2008; Bernardes et al., 2013). Briefly, after 4T1 mammary carcinoma model induction, twenty four females BALB/c mice (9-10 weeks old) were randomly assigned to 4 groups: control (saline s.c.), 4T1 tumor-bearing treated withsaline, 4T1 tumor-bearing treated with LyeTxI-b peptide (5mg/kg), and LyeTxI-b peptide alone (5mg/kg). All animals received treatments for five subsequent times, every 72 hours. After 21 days from tumor inoculation, animals were anesthetized and hair of flank and back were removed and the body

sterilized with 70% alcohol. Next, retro-orbitall injection of rhodamine 6G (1 mg/ml) was performed for labelling platelets and leukocytes. Microvasculature of spinal cord (by laminectomy), flank and tumor were exposed to analyze in vivo leukocyte recruitment by intravital. After microcirculation exposure, animals were transferred to the microscope stage, and maintained at 37º C using a heating pad (Fine Sciences Tools Inc., Canada). To assess the leukocyte-recruitment interactions, fluorescent leukocytes were visualized under a fluorescence microscopy Zeiss Imager M.2 (20X long-distance objective lens; Gottingen, Germany) equipped with a fluorescent light source (epi-illumination at 510-560 nm, using 590 nm emission filter).Rolling leukocytes were defined as white cells moving at velocity less than erythrocytes. Cells were considered adherent when they remained stationary for at least 20 seconds, and results were expressed as leukocytes number leukocytes/20 seconds.The scheme 8 describes the resumed strategy of intravital studies.

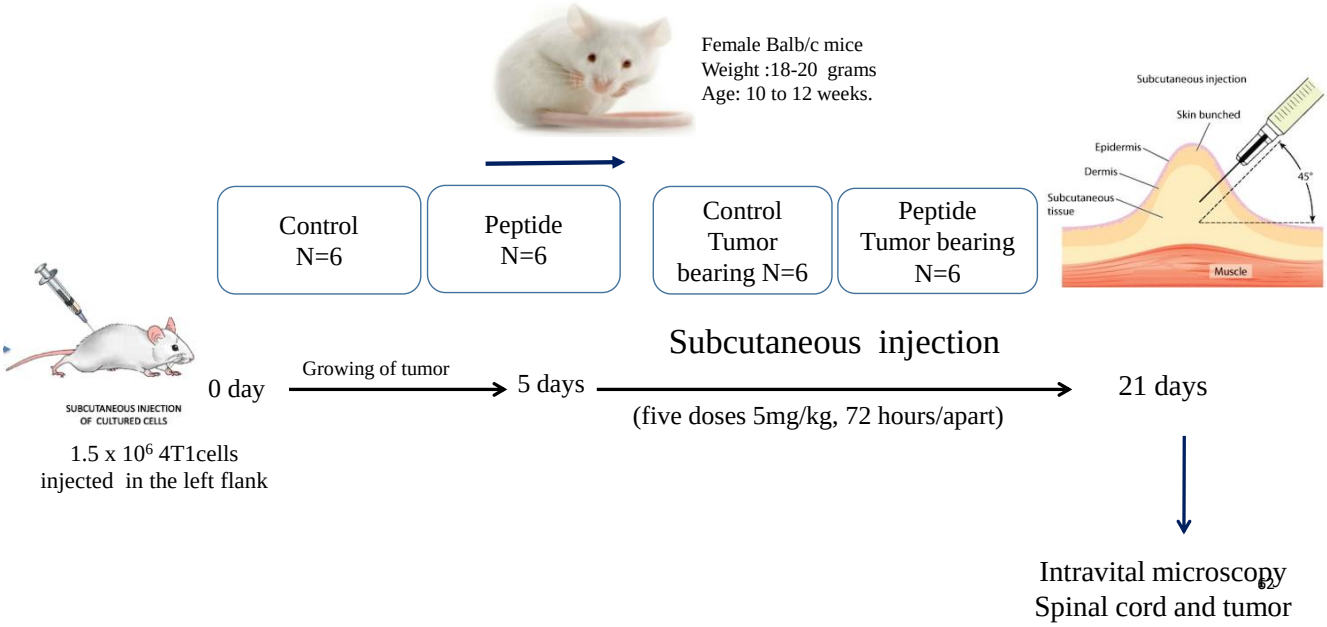


Scheme 8. Representative strategy used for the intravital studies to evaluate leukocyte recruitment.

## 2. Results

### 2.1. Sub-acute toxicity of LyeTx I_b peptide *in vivo*

In order to investigate *in vivo* sub-acute toxicity of LyeTx I_b peptide, female BALB/c mice were injected i.p. with of LyeTx I_b peptide (5 mg/kg) (seven doses, 48 hours/apart) and all animals were monitored for 14 days. Mortality, no signs of toxicity, skin ulcer, and diarrhea were not observed along time period assessed.

Body weight was evaluated along 14 days in animals treated with saline (control group) or treated with peptide (5 mg/Kg). No difference was observed in body weight between control and treated groups along time period assesses (figure 25A).

(A)

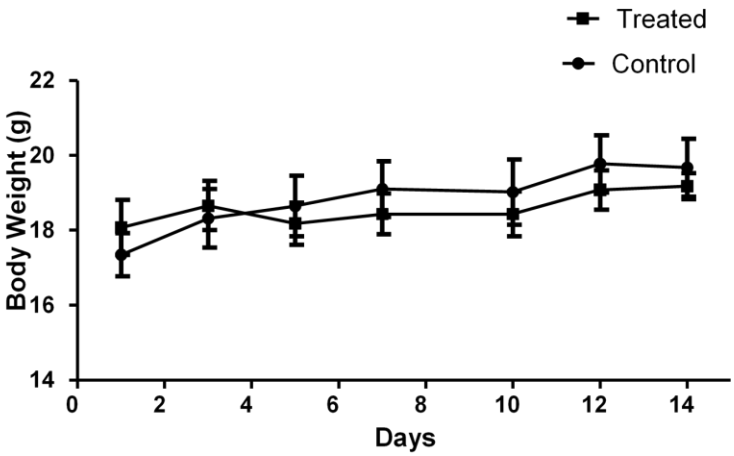


Figure 25A. Toxicity and tolerability of LyeTx I-b peptide (A) Effect of the peptide (5 mg/kg) on body weight Balb/C mice, along 14 days.

Histopathological and macroscopic analysis (lung, kidney, spleen, heart, brain, and liver) demonstrated that LyeTx I_b peptide did not reveal lesion or significant alterations in each organ. For instance, the examination of the renal cortex, the area of the Bowman's capsule, glomerulus and tubules were showed normal pattern compared to control. The lung histopathology was also preserved, without changes in alveoli, alveolar air spaces. The liver components i.e. parenchyma, hepatocytes, central vein, bile duct morphology were displayed normal pattern except that infiltrated mononuclear cells were noticed in one animal from treated group. The

histomorphometric parameters of spleen revealed well preserved white pulp, red pulp, central artery, and capsule. Moreover, the heart muscle fiber, intercalated disc and nuclei morphology were normal as well (Figures 25B and 25C).

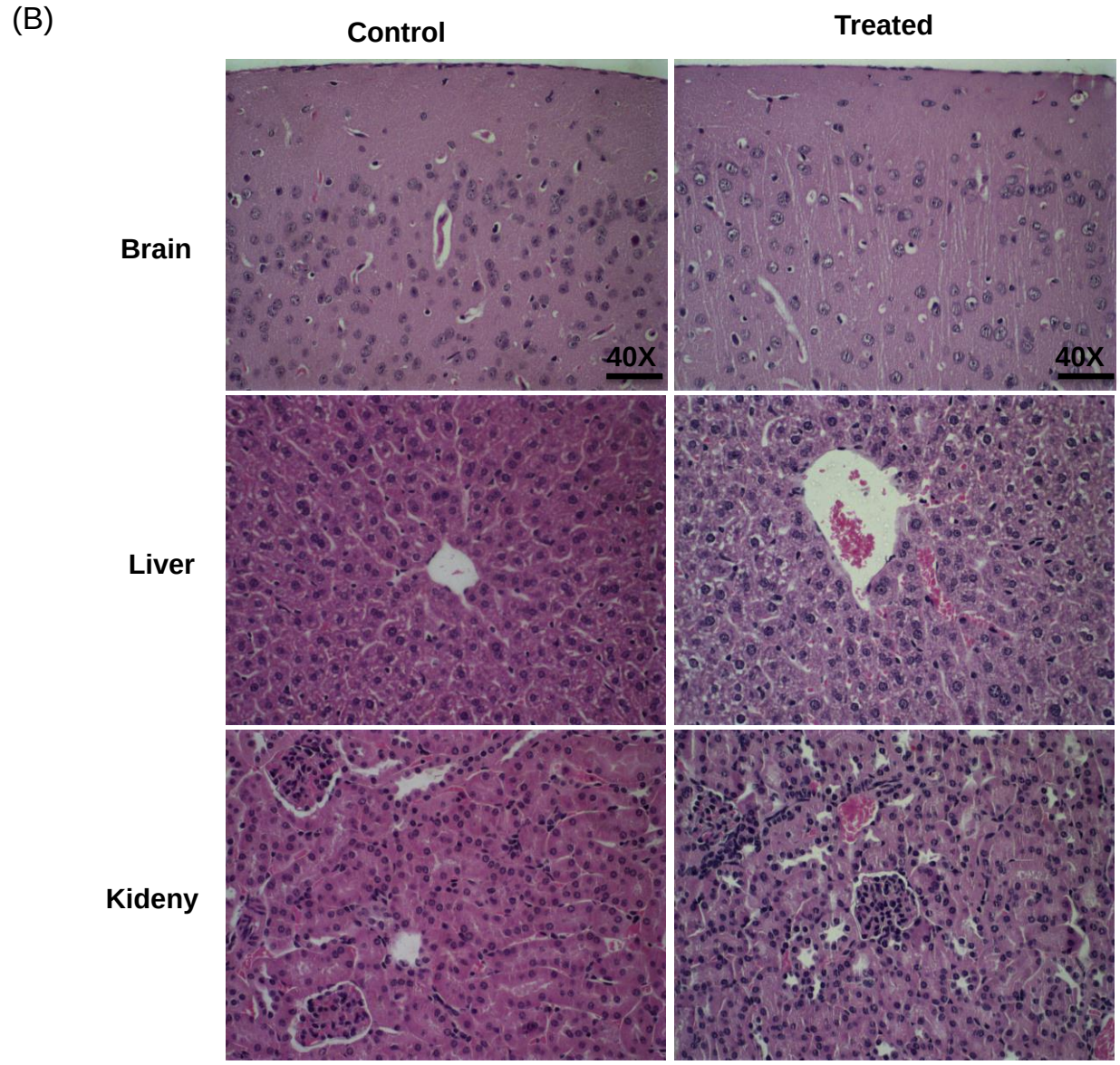


Figure 25B. Toxicity and tolerability of LyeTx I-b peptide. (B) Morphological analysis of brain, liver and kidney. Tissues were stained with hematoxylin and eosin. Objective 40X.

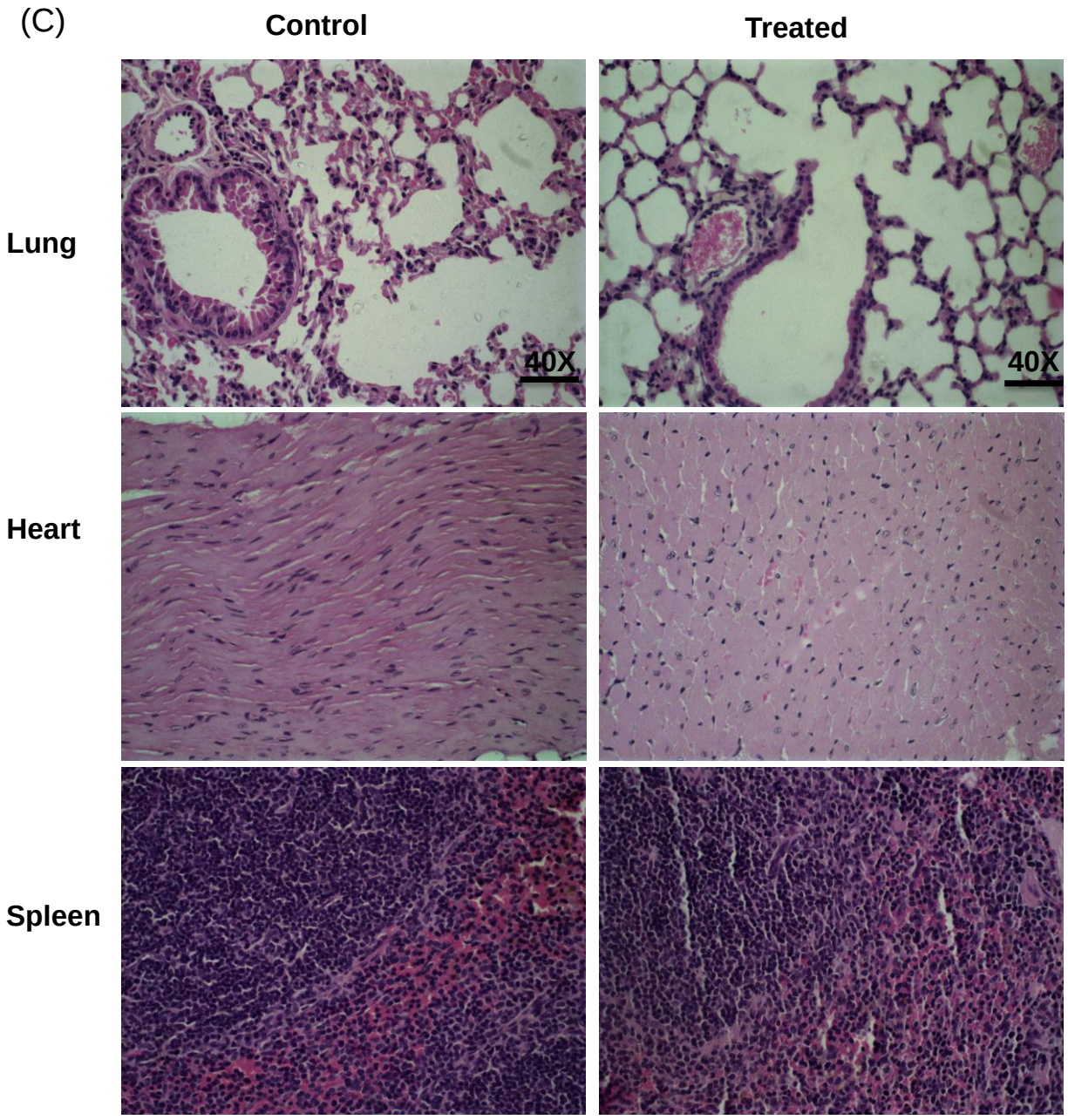


Figure 25C. Toxicity and tolerability of LyeTx I-b peptide. (C) Murine histopathological analyses after treatment with LyeTx I_b peptide (5mg/kg). Morphological analysis of Lung, spleen and heart. Tissues were stained with hematoxylin and eosin. Objective 40X.

Blood hematological values of control and treated groups did not show abnormal patterns generally including morphology and counts related to the age and sex, except the treated group with peptide displayed a mild reduction in platelets counts or thrombocytopenia. The white blood cells fractions exhibited an increase in lymphocytes counts related to the reduction of segmented neutrophils were included in both groups control and treated animals (table 3).

Table 3. Hematological values of Healthy BALB/C animals after systemic administration of 5mg/kg LyeTx I-b peptide (7 doses, 5mg/kg/ 48h in apart)

| Hematological parameter | Control | LyeTx I_b peptide | Reference Value |
|---|---|---|---|
| RBC ($x10^6/mm^3$) | 6.32 ±0.667 | 7.46 ±0.965 | 6.1 – 9.5 |
| Hb (g/dL) | 10.8 ± 2.66 | 12.9 ± 0.680 | 11.6 – 15.8 |
| Hematocrit | 38.9 ±8.66 | 39.4 ±2.56 | 37.4 – 51.7 |
| MCV(fL) | 61 ±7.57 | 48 ±4.50 | 41.5 – 57.4 |
| MCH (Pg) | 16.7 ±0.458 | 16.0 ±0.11 | 15.1 – 16 |
| MCHC % | 28.5 ±3.06 | 31.6 ±1.34 | 30.5 – 34.2 |
| WBC ($x10^3/mm^3$) | 2.3 ±2.26 | 4.1 ±0.70 | 1.5 – 4.8 |
| Lymphocytes | 91.7 ±5.13 | 89.2 ±4.03 | 55.5 - 83.82 |
| Monocytes | 4.3 ±1.556 | 4.1±1.553 | 3.75 - 7.26 |
| Neutrophils | 4 ±3.59 | 6.7 ±2.66 | 10.39 -17.8 |
| Platelets ($x10^3/mm^3$) | 443±73.6 | 278±80.0* | 325 – 888 |

RBC: erythrocytes, Hb: hemoglobin, WBC: leukocytes, MCV: mean cell volume, MCH: mean corpuscular Hemoglobin, and MCHC: mean corpuscular hemoglobin concentration. The results relate to average ± standard deviation. * Significant reduction. Santos et al., 2016.

### 2.2. Intratumoral administration of LyeTx I-b peptide decreases tumor volume *in vivo*

To assess antitumor activity of LyeTx I-b peptide, all animals were injected subcutaneously with 1.5 x $10^6$ 4T1 cells in the posterior left flank. On day 10 post-tumour inoculation when tumor volume reached 1000 $mm^3$ approximately, the animals were intratumorally injected with of LyeTx

I-b (100 µl) peptide, or carboplatin (5mg/kg), or saline (control group) (5 doses/72 h apart). Tumor volume analysis demonstrated that LyeTx I-b peptide could inhibit tumor growth significantly compared with aggressive tumor growth in carboplatin and control groups. At day 25 the animals treated with peptide, reached a mean inferred tumor volume of approximately1945 $mm^3$, while carboplatin and control groups reached 3309 and 4119 $mm^3$, respectively, as shown in figure 26 A. In addition, LyeTxI-b showed ability to reduce the weights of tumors (figure 26B). The mean tumor weight in the LyeTx I-b group was 2.14 g compared to control 3.07 g, and carboplatin 3.15 g. No difference was observed in the body weigh between control, LyeTx I-b and carboplatin groups (Figures 26C). Representative images of control animal and treated are shown in Figure 26D.

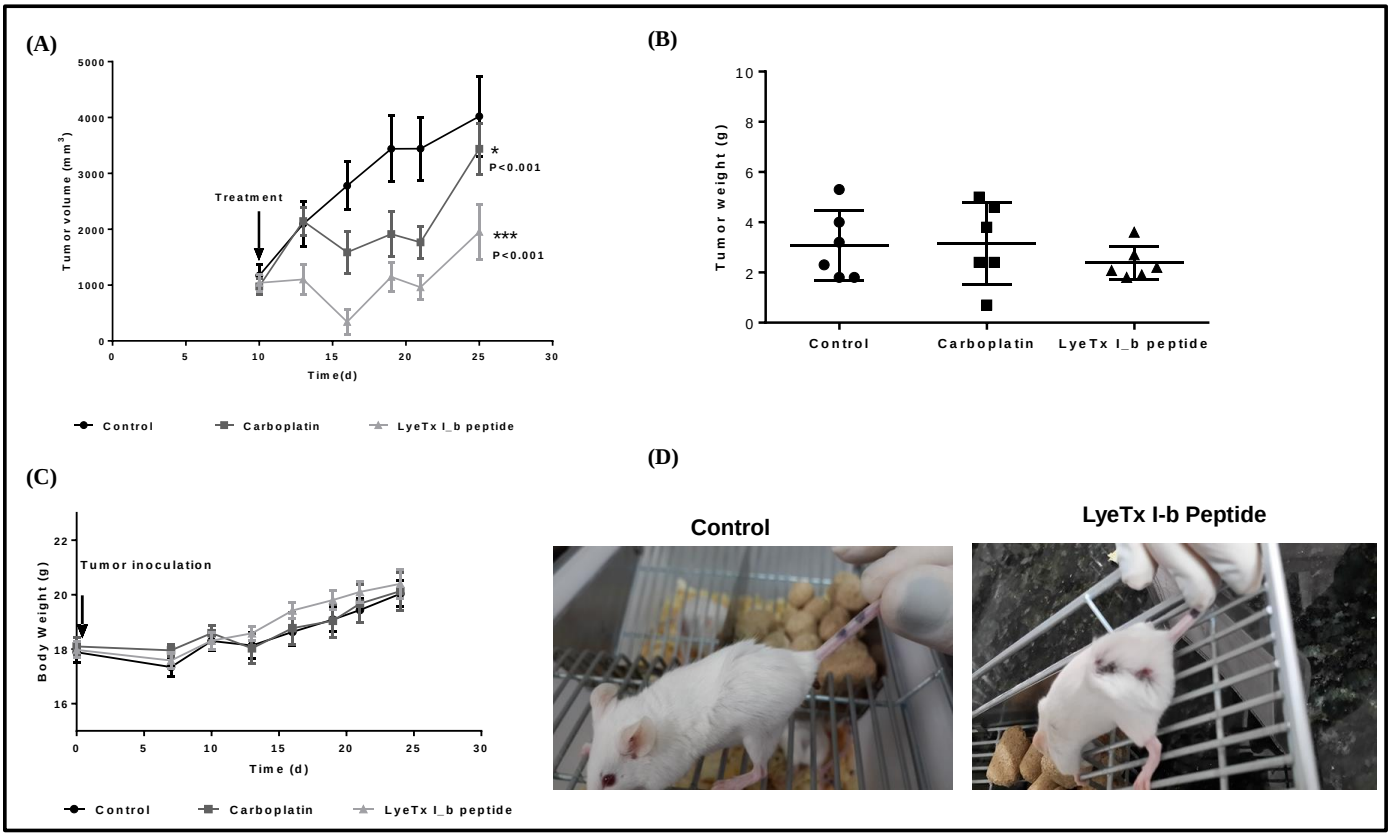


Figure 26. Effects of LyeTx I-b and carboplatin treatment of 4T1 murine mammary carcinoma with LyeTx I-b peptide on tumor volume, tumor weigh, and body volume. (A) LyeTx I-b peptide decreased tumor volume compared to control and Carboplatin groups. (B) No body weight differences along 25 days post-inoculation of 4T1 tumor, in control, LyeTx I-b peptide and carboplatin groups. (C) LyeTx I-b peptide reduced tumor weight. (D) representative images demonstrating reduction on size of tumor after treatment with peptide. Data represent means ±SD, One-way ANOVA followed by Tukey's multiple comparisons test, P< 0.001.

Qualitative histopathological analysis showed apparently that primary tumor from control group, presents an increase of infiltrated mononuclear inflammatory cells (lymphocytes and macrophages), which are associated with high growth of neoplastic cells and forming necrotic area (Figure 27). Moreover, extensive necrotic area was observed in a treated primary tumor.

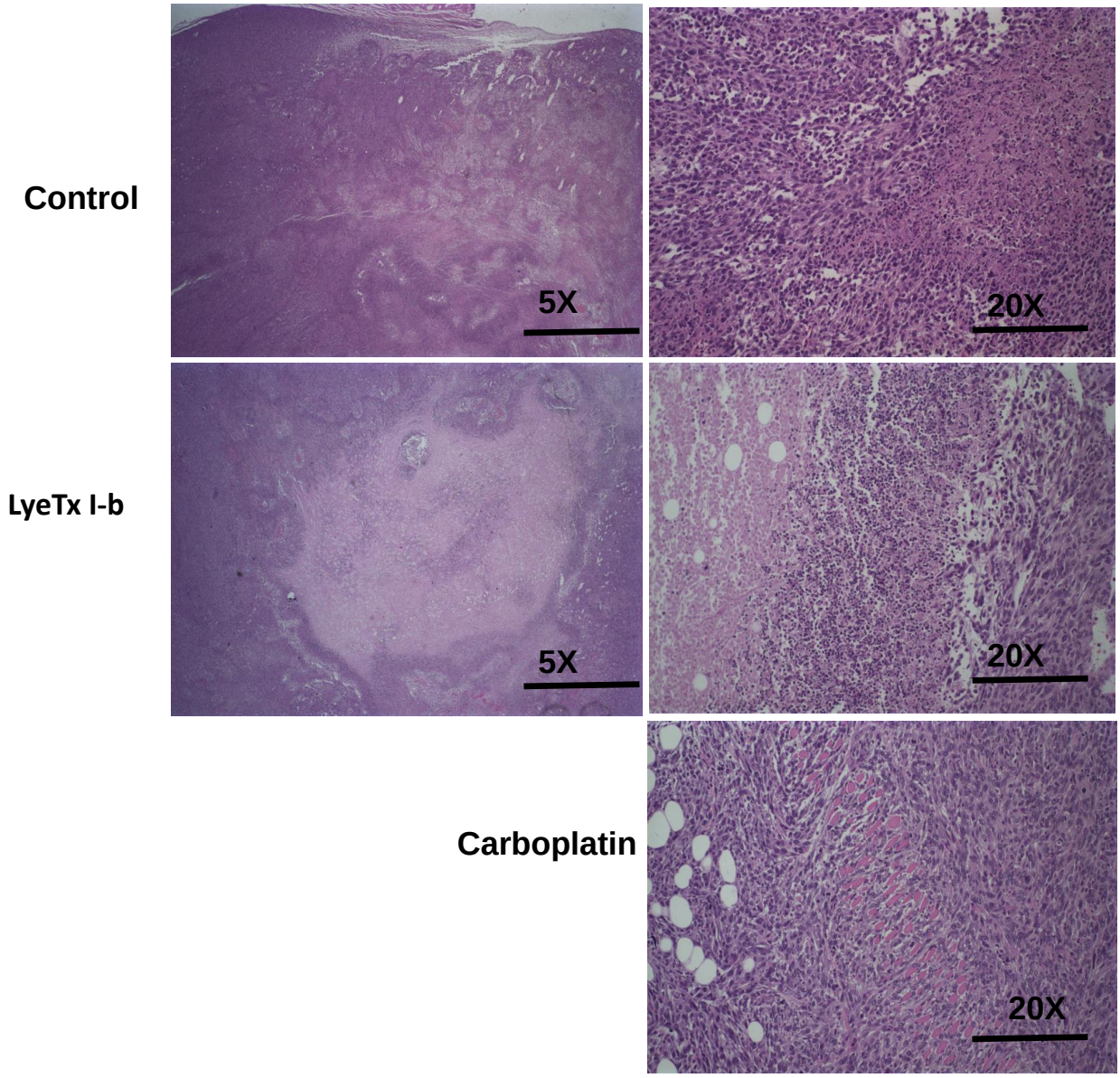


Figure 27. Morphological aspects of 4T1 murine primary tumor. Representative HE histology of low magnification, (5X) showed large necrosis area in LyeTx I-b peptide treated group compared with untreated group. In control group, infiltrated inflammatory, necrosis area and viable tumor cells, whereas the extensive necrotic area in treated group was characterized by the presence nucleus chromatin condensation accompanied by fragmented nuclei into various segments (karyorrhexis) H&E staining. Objectives 20X and 5X, Scale bars were 200 µm and 40 µm.

### 2.3. LyeTx I-b reduces the size and number of lung metastatic foci

The assessment of lung metastasis after 4T1 murine primary tumor induction has been done in control and carboplatin-treated groups. The total number of metastatic lesions were detected in control and treated group. LyeTx I-b diminished the number of metastatic foci significantly compared to carboplatin and control.The mean number of metastatic foci for peptide group was 1.66, carboplatin was 4.33 and control was 3.66. Moreover, LyeTx I-b peptide could be able to reduce the area of lesions (Figure 28).

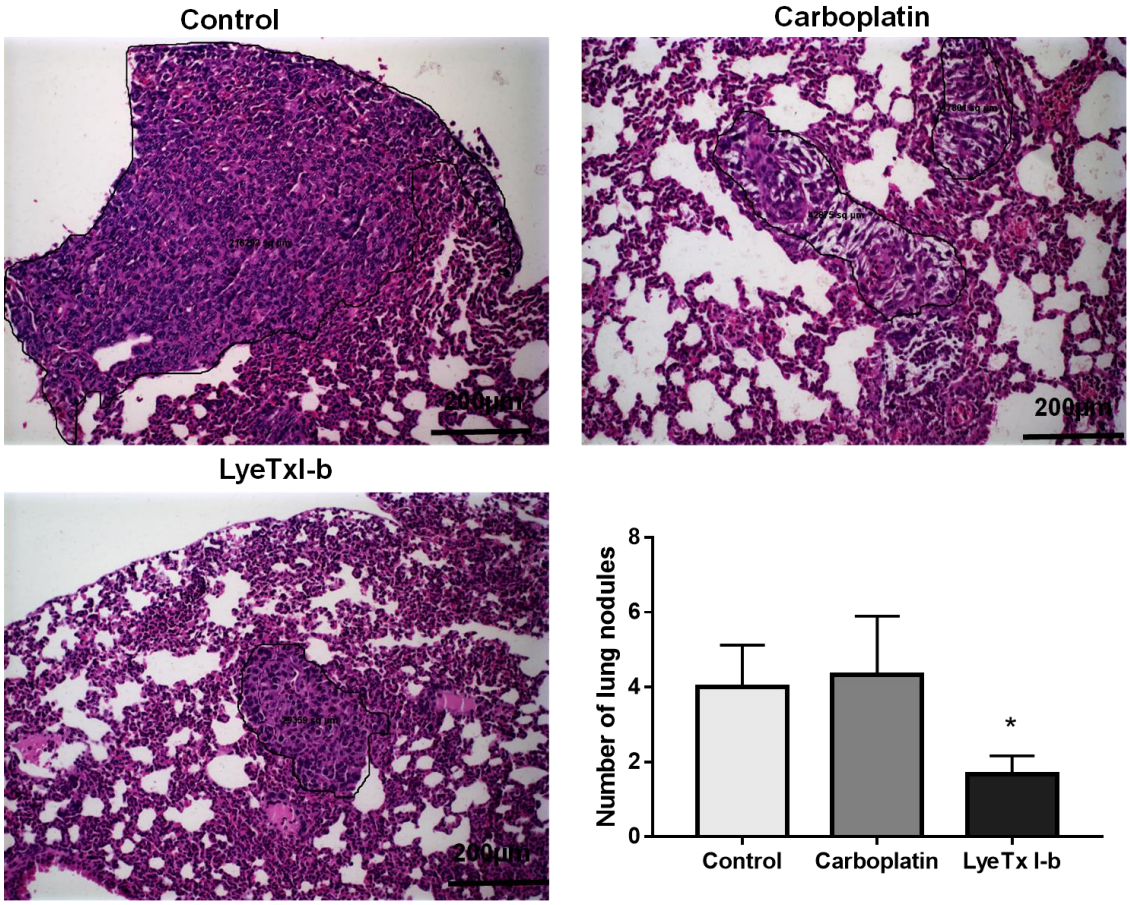


Figure 28. 4T1 metastasis in lung parenchyma. The significant reduction in the number of metastatic lesions of LyeTx I-b peptide group compared with carboplatin and control groups. Data represent mean ±SEM (*p<0.005, ANOVA one-way).

### 2.4. Subcutaneous administration of LyeTx I-b peptide reduces tumor volume in 4T1 tumor model

The subcutaneous administration of LyeTx I-b peptide was used in order to evaluate the efficacy of the peptide through lymphatic and vascular circulatory system. At day 5 post-tumour

inoculation, when tumor volume reached approximately 400 $mm^3$, animals received subcutaneous injections of LyeTx I-b peptide (100 µl), or carboplatin (5mg/kg), or saline (control group) (5 doses /72 hours in a part). The results demonstrated that LyeTx I-b peptide was able to reduce tumor volume and tumor weight significantly compared with control and carboplatin groups (figure 5 A and B). The average tumor weights of untreated, and carboplatin groups were 2.92g and 2.38g, respectively, while in the peptide group was 1.6 g. Furthermore, the average of tumor volume of LyeTx I-b peptide group was 1383 $mm^3$,while in the control group was 3236 $mm^3$, and carboplatin was 2513 $mm^3$ (Figure 29A). No difference was observed in the body weigh between control, LyeTx I-b and carboplatin groups (Figures 29C). Representative images of control animal and treated are shown in Figure 29D.

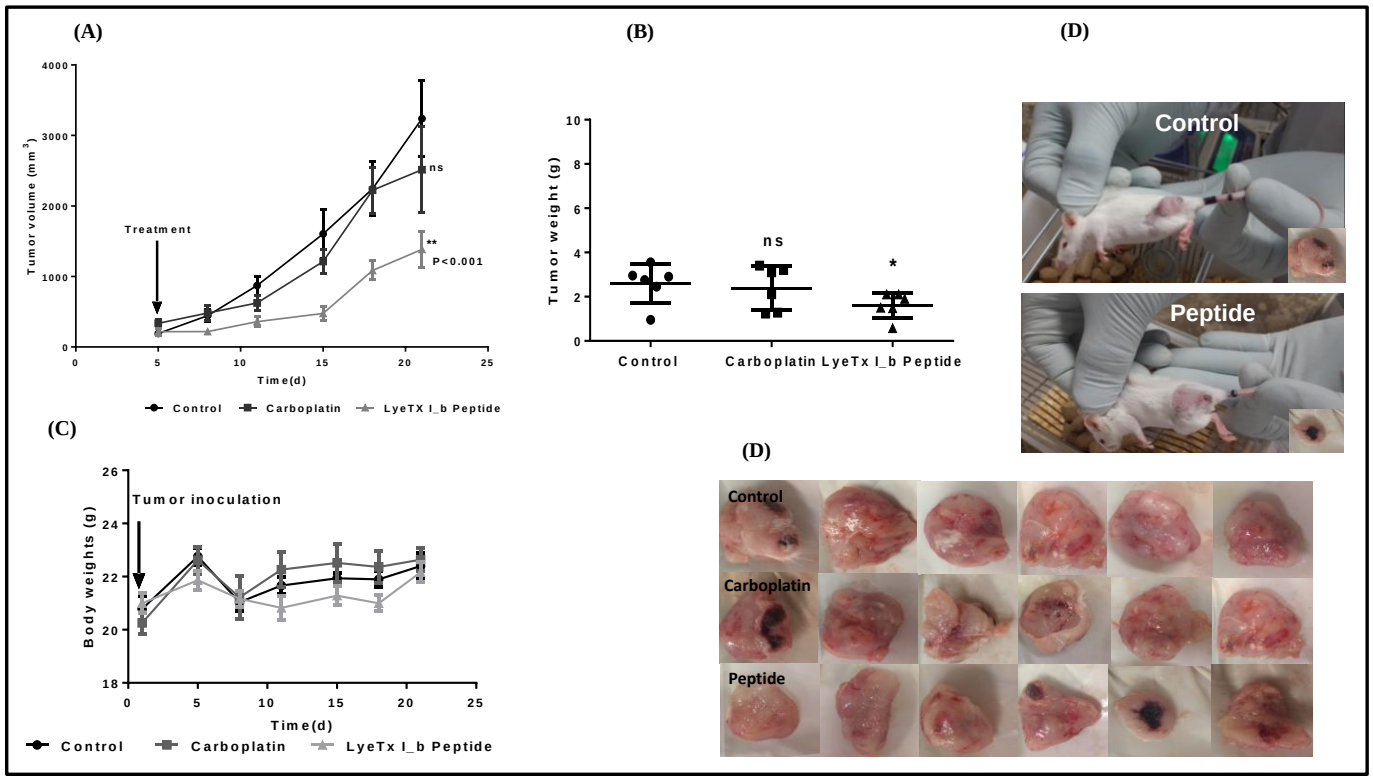


Figure 29. Effects of subcutaneous LyeTx I-b peptide treatment on tumor volume, tumor weight, and body weight after 4T1 murine mammary carcinoma induction. (A) LyeTx I-b peptide decreased tumor volume significantly compared to control and Carboplatin. (B) LyeTx I-b peptide reduced tumor weight compared to control and Carboplatin groups. (C) Influence of tumor induction and drug treatment on BALB/c body weight along 21 days post-inoculation of 4T1 tumor. . (D) representative images demonstrating reduction on size of tumor after treatment with peptide. Data represent means ±SD, One-way ANOVA followed by Tukey's multiple comparisons test, P< 0.001.

## 2.5. No liver function alteration induced by LyeTx I-b peptide treatment.

We further tested whether LyeTx I-b peptide could alter liver functions in 4T1 tumor-bearing animals. There was no alterations in serum ALT (alanine aminotransferase) level among all groups, whereas there was elevated serum AST (aspartate transaminase) level significantly associated with carboplatin treatment but not in animals treated with peptide (figure 30). Together, our data suggested that LyeTx I-b peptide treatment induced mild hepatotoxicity as 4T1 murine mammary carcinoma control group. The reference value of ALT enzymes in healthy females of Balb/c mice strain is 29.72 ± 4.40 U/ml, while the normal range of AST value is 71.32 ± 28.12 (Barbosa B.S. et al., 2017).

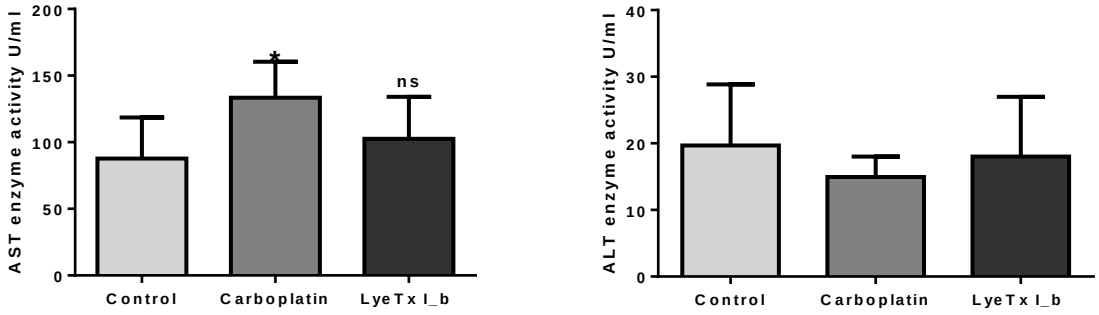


Figure 30. Liver functions in the serum of 4T1 tumor-bearing mice. Balb/c mice were injected subcutaneously 5 times during 15 days, with saline, LyeTx I-b peptide or carboplatin. Serum AST and ALT levels in control (saline), carboplatin and LyeTx I-b peptide groups were measured by using the colorimeter testing kit in triplicate, n=5. Data represent means ±SD, One-way ANOVA followed by Tukey's multiple comparisons test, P< 0.005.

## 2.6. LyeTx I-b peptide and carboplatin reduce total and differential Leukocyte Counts

Previous immunological studies have been carried out in order to evaluate the immunomodulation effects of chemotherapeutic agents. In fact, the aggressive 4T1 tumor growth and migration of tumor cells into spleen and liver resulted in increasing hematopoiesis activity, thus elevated circulating white blood cells (Tao, K. et al., 2008). Post-inoculation of 4T1 cells into Balb/c mice increased 3 fold of total leukocytes count at day 14, i.e. the beginning of the metastasis process corresponding with multiplying numbers of granulocytes, especially neutrophil and eosinophil counts due to changes of natural and acquired immunity during metastasis process (Jackson, W. et al., 2017).

In this study, we collected blood samples by cardiac puncture from anesthetized 4T1 tumor-bearing mice to determine counts of total and differential leukocytes count (Neutrophils,

lymphocytes, monocytes and eosinophils). We found that both drugs treatment, carboplatin, and LyeTx I-b peptide were able to decrease significantly total and differential number of peripheral blood leukocytes count compared with control group (Figure 31 A). Currently, the attractive target in the breast cancer murine models is depletion of tumor-infiltrating cells like neutrophils and monocytes that differentiate into metastasis-associated macrophages (Kitamura, T. et al., 2017). Our results showed that neutrophils and monocytes counts were reduced dramatically after treatment with LyeTx I-b peptide and carboplatin (Figure 31B). Eosinophils Peripheral blood count in breast cancer patients became an important indicator of primary tumor progress and prognosis, due eosinophil's crucial role in lung metastasis. (Szalayova, G. et al., 2016). We found that carboplatin and LyeTx I-b peptide diminished counts of eosinophil (figure 31B).

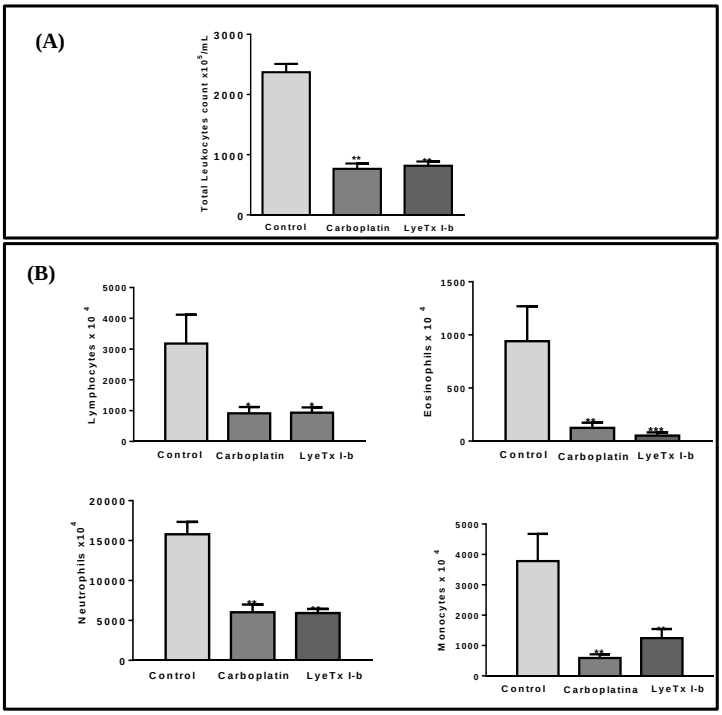


Figure 31. Leukogram of peripheral blood counts in 4T1 tumor-bearing mice, in control, carboplatin and LyeTx I-b (5mg/kg) groups. (A) Total leukocytes counts x $10^5$ (B) Differential leukocytes counts x $10^4$, monocytes, lymphocytes, eosinophils, neutrophils. LyeTx I-b and carboplatin induced leukopenia significantly in treated groups. Data are presented as mean ± SEM, ** P <0.001 compared with control group, n = 6 animals. Statistical analysis: One-way ANOVA followed by Newman-Keuls multiple comparison test.

## 2.7. LyeTx I-b peptide alters the amount of rolling and adhering leukocytes in 4T1 tumor-bearing mice by using the intravital microscopy *in vivo*.

Intravital microscopy is a technique used to visualize leukocyte-endothelial interaction *in vivo*. In order to quantify *in vivo* leukocyte recruitment (rolling and adhesion) in the spinal cord, tumor and

flank vessels during a metastatic stage, we have used intravital microscopy. Our results emphasized the remarkable increase of rolling leukocytes after treating with LyeTx I-b peptide in the spinal cord and tumor vessels compared to control group. In addition, we also observed a reduction in leukocyte adhesion into spinal cord and tumor microvessels from 4T1 tumor-bearing mice treated with the 4T1 tumor-bearing mice (Figure 32A, B, C, D).

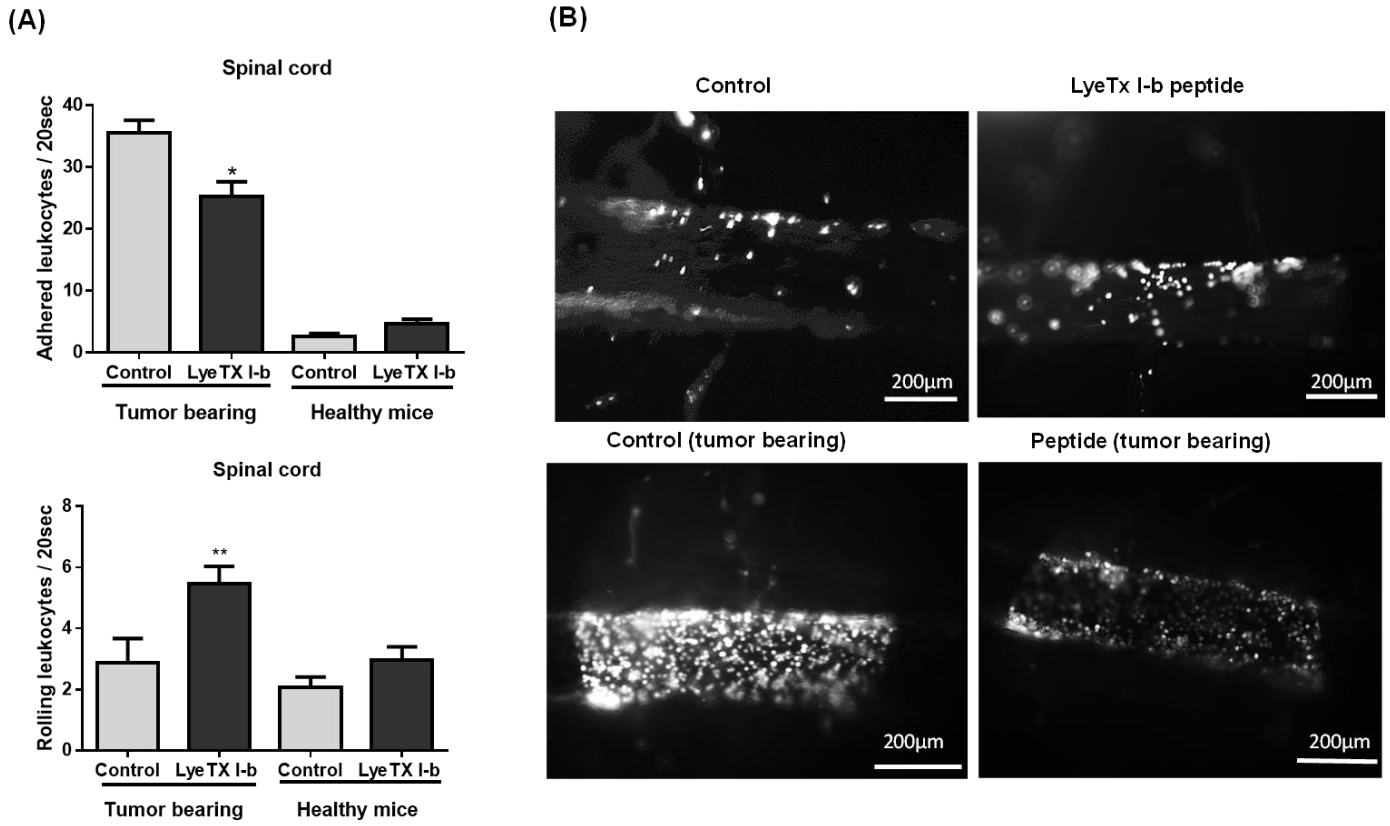


Figure 32 A and B. Intravital microscopy at 22 days post-inoculation of 4T1 tumor cells. (A) Number of leukocytes rolling and adherence. (B) Representative images of central venules from spinal cord showing the effect of LyeTx I-b treatment on leukocyte-endothelial interactions. Tumor vessels images. Statistical analysis: Data are presented as mean ± SD, ** P <0.001 compared with control group, n = 6 animals. One-way ANOVA followed by Tukey's multiple comparisons test.

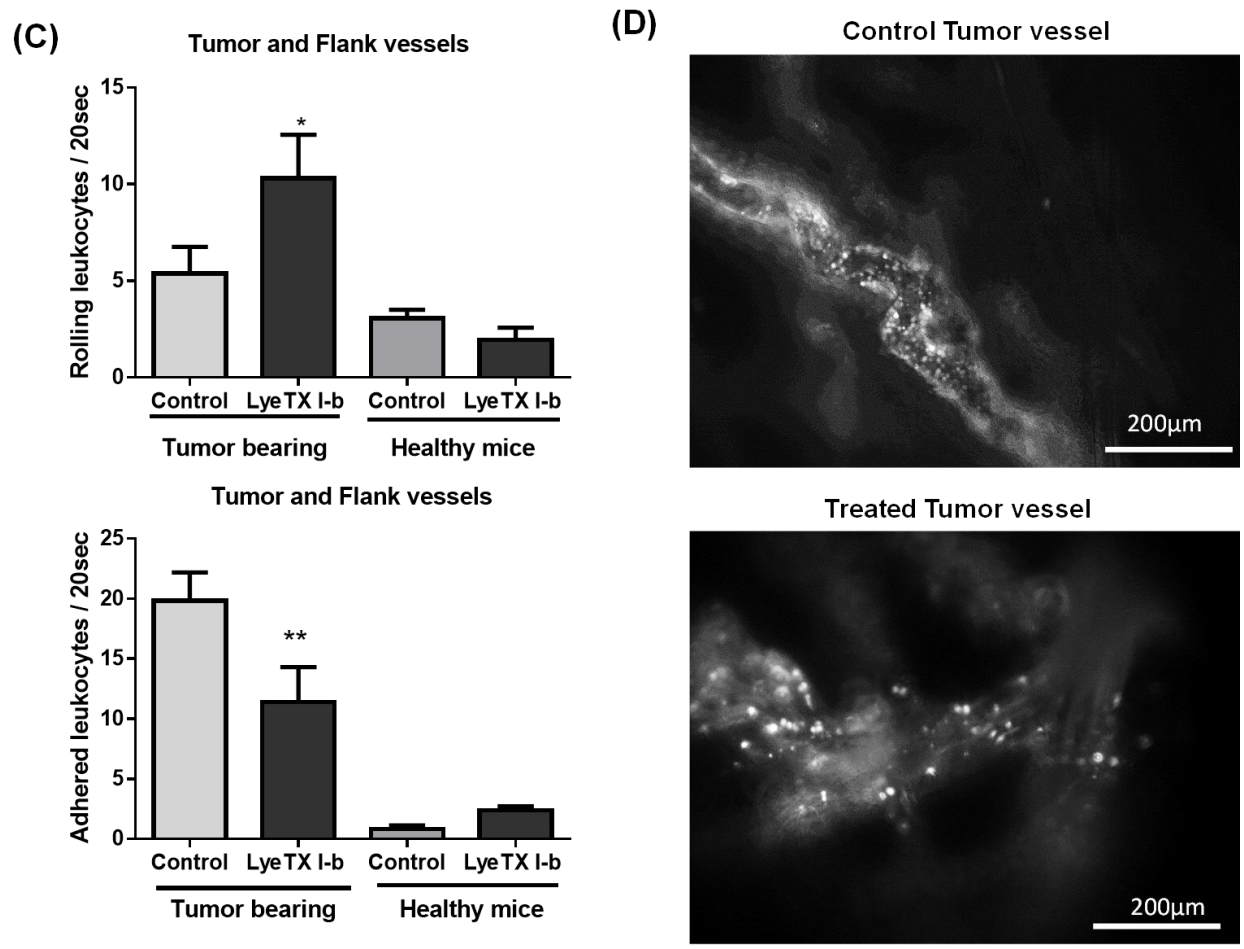


Figure 32 C and D. Intravital microscopy at 22 days post-inoculation of 4T1 tumor cells. (C) Number of leukocytes rolling and adhesion into tumor and normal flank vessels. (D). Tumor vessels images. Statistical analysis: Data are presented as mean ± SD, ** P <0.001 compared with control group, n = 6 animals. One-way ANOVA followed by Tukey's multiple comparisons test.

## 2.8. LyeTx I-b peptide changes protein expression of cancer receptor VEGF, TGF-β, and TNF-α in primary tumor and spleen.

Breast tumor microenvironment plays a critical role in invasion and metastasis. Overexpression of TGF-β (transforming growth factor), VEGF (Vascular endothelial growth factor), and TNF-α (Tumor necrosis factor) have been detected in murine 4T1 metastatic model and breast cancer patients as well, thus targeting these proteins leading reduces of metastasis incidence and increase patient survival rate (Buenrostro, D. et al., 2018). Several studies showed the proportional correlation between high levels of TGF- β and VEGF and early appearance of metastatic lesions. Moreover blocking of TGF- β and VEGF resulted in improves efficiency of chemotherapeutic

agents in 4T1 mammary tumor model and breast cancer patients through recruitment and normalizing of extracellular matrix, in particular, collagen coated matrices (Liu, J et al., 2012 &McEarchern, J. A. et al., 2001). Although TNF-α is utilizing cancer immunotherapy since last decades due to intratumoral injection of TNF-αinduced tumor regression, however recently several studies emphasized the ability of TNF-α to promote tumor progression and metastasis in many types of cancers through enhancing $T_{reg}$ cells and upregulation of VEGF receptor. In addition, TNF-α facilitating the proliferation of cancer cells in the immune microenvironment (Sheng, Y. et al., 2018 & Sasi, S. P. et al., 2014).

It is worthy to determine the expression of cytokines and tumor growth factors like VEGF, TGF-β, and TNF-α within the tumor microenvironment due to their roles in the regulation of tumor growth, tumorigenesis and metastasis. No statistically significant difference was found in VEGF concentration (Pg/ ml) from primary tumor and lung tissues comparing with LyeTx I-b peptide and carboplatin. (Figure 33A). In other hand, LyeTx I-b and carboplatin groups showed a significant reduction in TGF-β expression level in primary tumor and spleen compared with control (figure 33 B). Furthermore non-significant differences of TNF-α expression in primary tumor, whereas significant reduction in spleen was observed in both groups LyeTx I-b and carboplatin treated groups (Figure 33C).

Inflammatory cytokines have a dual role in tumor microenvironment based on the plasticity of immune cells. Our results displayed that LyeTx I-b and carboplatin treatments have suppressed proinflammatory IL-1 β expression in lung and primary tumor significantly (34 A). Moreover, the expression of anti-inflammatory IL-10 was increased in the primary tumor of LyeTx I-b group only (34 B) In the other hand, the proinflammatory IL-6 was elevated significantly in brain and spleen in peptide treated group (34 C).

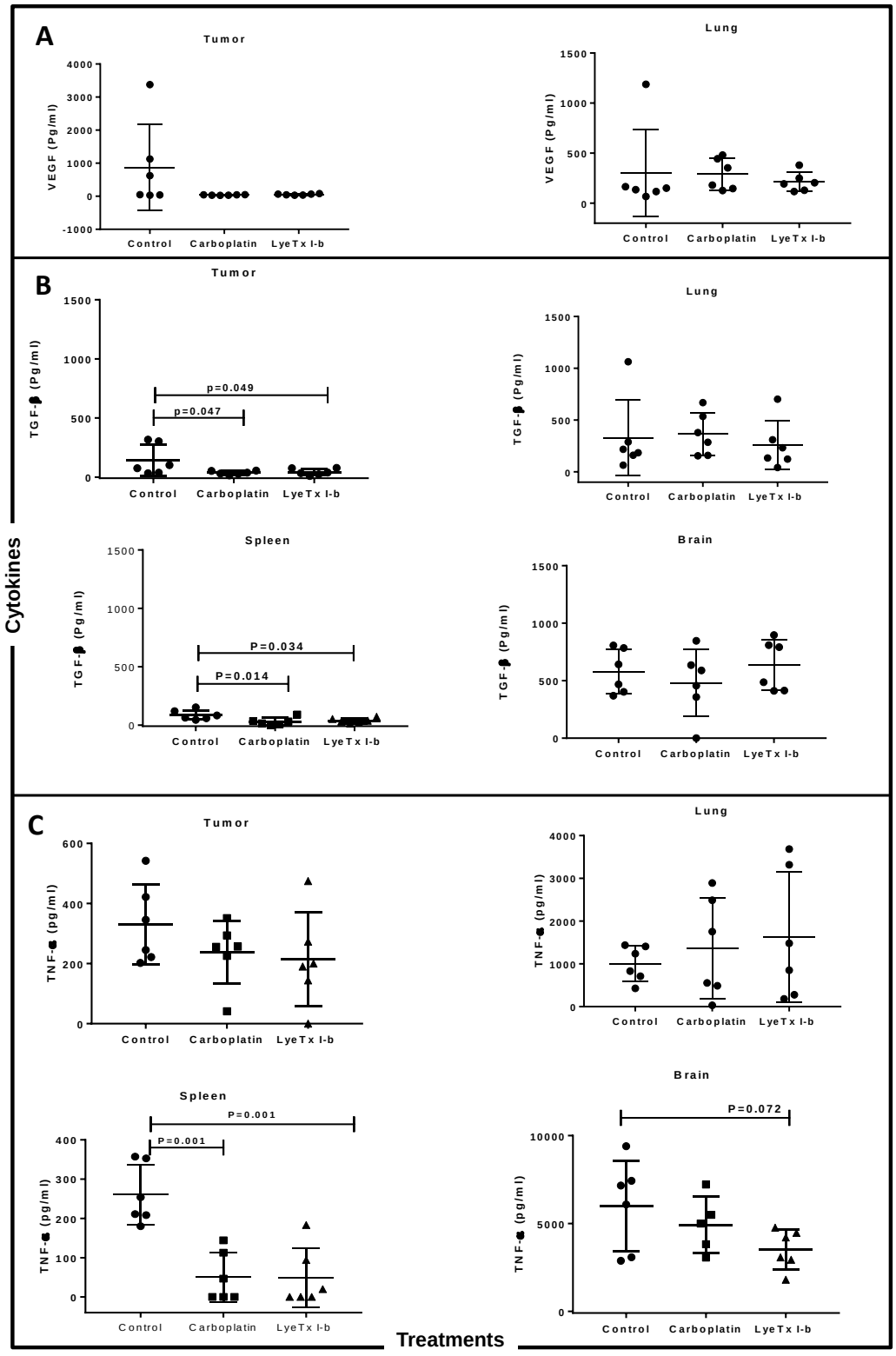


Figure 33. LyeTx I-b peptide attenuated VEGF, TGF-β and TNF-α expression in the tumor microenvironment. Individual values of mice (Pg/ml) presented in a dot plot with an average of each group (n=6). (A) Data correspond to VEGF levels in primary tumor and lung. (B, C) TGF-β and TNF-α levels in the primary tumor, brain, spleen, and lung. Statistical variation among groups was carried out in 6 animals of each group in duplicate using one-way ANOVA followed by Dunn's multiple comparisons test.

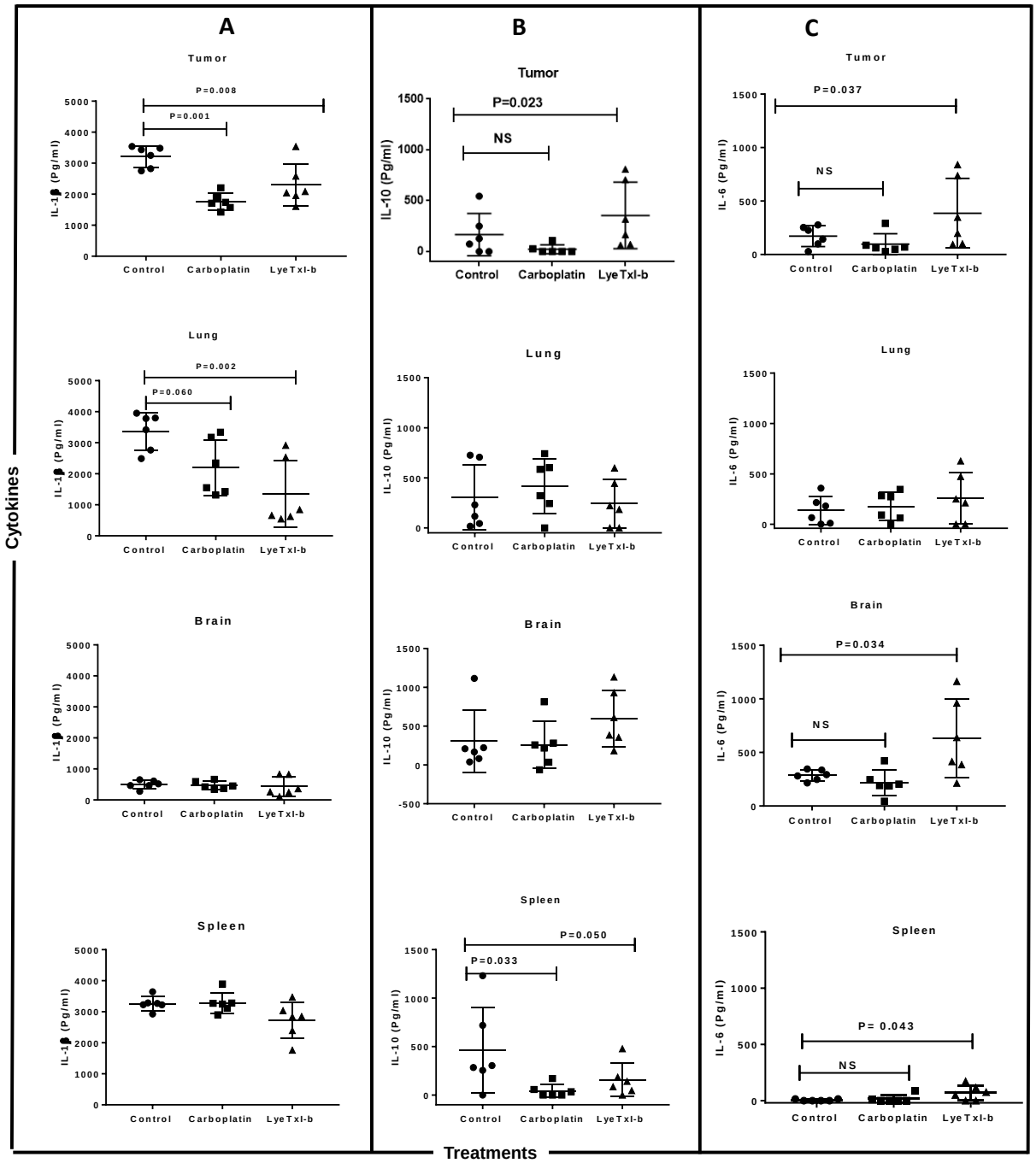


Figure 34. Expression IL-1β, IL-6 and IL-10 levels in the tumor microenvironment. Individual values of mice (Pg/ml) presented in a dot plot with an average of each group (n=6). (A) Data correspond to IL-1β found in the primary tumor, brain, spleen, and lung. (B, C) IL-10 and IL-6 values respectively. Statistical variation among using one-way ANOVA, followed by Dunn's multiple comparisons test. (n=6/group).

## 3. Discussion

Nowadays, chemotherapy based on biopharmaceutics like peptides became one of the favorable strategies to treat breast metastatic patients due to efficiency and mild adverse effects. To confirm the toxicity of LyeTx I-b cationic peptide *in vivo*, the systemic administration of peptide did not show signs of toxicity and no significant alterations were observed by histopathological and hematological analysis. These results corroborated findings of PFR peptide, which displayed the ability to inhibit tumor growth without toxic side effects (Lu, Y. et al., 2016).

The anticancer activity of LyeTx I-b peptide was examined in 4T1 metastatic breast cancer model. The intratumoral injection of LyeTx I-b peptide was able to suppress 52% of tumor growth (figure 26). Furthermore, we found a 61% reduction of pulmonary metastatic foci in comparison to control group. In a similar study, GK-1 peptide decreased tumor growth and a total number of metastatic nodules in the 4T1 murine model (Torres-García, D. et al., 2017). In order to confirm primary tumor death, the qualitative analysis of H&E stained images from tumor section has been done. The images showed a large necrosis area and pyknosis area in the treated group characterized by the occurrence of nuclei irreversible chromatin condensation and fragmentation (figure 27). Szczepanski and his colleagues (2014) reported that intratumoral administration of Cypep-1 peptide has induced tumor regression in the 4T1 murine model, as consequence of necrosis in a large area of the treated primary tumor. Moreover, local injection of L-K6 peptide induced nuclear fragmentation in the primary tumor of MCF-7 breast cancer xenograft model (Wang, C. et al., 2017). Furthermore, D-K6L9 peptide injected intratumorally, has inhibited tumor growth and recurrence in B16-F10 murine melanoma model, via necrosis in treated primary tumor (Cichon´, T. et al., 2014).

Currently, the subcutaneous (SC) is one of the favorable route of administration for biotherapeutics, due the ability to increase bioavailability of huge molecular weights (Richter, W. et al., 2012). It is an important route to deliver therapeutic peptide into the systemic circulation by the lymphatic system and blood capillaries depended on the molecular size and weight (Kagan, L. 2014). LyeTx I-b peptide was administered subcutaneously along 14 days, and our findings displayed a significant reduction of tumor growth by 58% compared to tumor-bearing control group (figure 29). Previous data showed that subcutaneous injection of Crotamine peptide delayed tumor growth significantly in the B16-F10 melanoma model (Pereira, A. et al., 2011).

Tumor cells in metastatic lesions utilize adhering leukocytes for extravasation into endothelium. The intravital microscope has been used for tracking remained primary tumor or metastatic lesion through visualization of rolling leukocytes on tumor vasculature endothelium (Palomba, R. et al., 2016). In our study, using intravital microscopy, we visualized rodhamine 6G fluorescent leukocyte rolling and adhesion into spinal cord and tumor microvessels after induction of metastatic 4T1 murine mammary carcinoma model. Our study evidenced that LyeTx I-b peptide treatment induced an increase of leukocytes rolling into spinal cord and tumor vessels from 4T1 tumor-bearing mice (figure 32A, B, C, D). Previous data have been showed that P-selectin expression on tumor cells correlated with cancer metastasis (Strell, C., & Entschladen, F. 2008). Rolling leukocytes is also mediated by L-selectin adhesion molecule, which is a key regulator of naive T-lymphocytes trafficking (Borsig, L. 2017). It is possible that LyeTx I-b peptide could be downregulated P-selectin expression on the surface of endothelial cells and tumor cells, or upregulating L-selectin on the surface of leukocytes. After quantified number of leukocyte adherent, we found that LyeTx I-b peptide promoted a decrease in leukocyte adhesion in the spinal cord and tumor microcirculation. We may speculate that LyeTx I-b peptide could be modulating integrins molecules on the surface of leukocytes, which are responsible for interaction with endothelium cells. Other mechanism that may decreasing leukocyte adhesion is the occurrence of a high and fast migration of leukocytes to surround parenchyma or distant organs. In order to elucidate potential mechanisms underline LyeTx I-b peptide effects, additional experiments will be necessary.

Innate immune systems during breast cancer play a vital role in tumor recurrence and relapse through activating transcription of genes encoding cytokines and chemokines (Standish, L. et al., 2008). Considering the aggressive tumor growth of 4T1 murine mammary carcinoma, previous studies reported that 4T1 is highly immunogenic model characterized by leukocytosis due to granulocytic hyperplasia of bone marrow (Dupre, S., & Hunter, K. 2007). All solid tumors including breast tumor contain large numbers of leukocytes that promote tumor migration and splenomegaly induced by tumor-infiltrating monocytes and neutrophils.Targeting spleen during cancer treatment is an urgent need for controlling tumor migration (Shand, F. et al., 2014). Some studies reported that immunosuppression caused by chemotherapy is beneficial because chemotherapeutic agent are killing immune cells like cytotoxic T-lymphocyte–associated antigen 4, and monocytes or macrophages , that promotes cancer metastasis (Janssen, L. et al., 2017 &

Naito, T. et al., 2015). Conventional chemotherapeutic agent not only induces cytotoxic effect but also prevent tumor development through a depletion of tumor-infiltrating immune cells (Galluzzi, L. et al., 2015). LyeTx I-b peptide revealed an immunomodulatory effect by attenuating counts of monocytes, lymphocytes, neutrophils, and eosinophil's in the 4T1 metastatic model (figure 31).

The role of TGF-β in breast cancer stages have been extensively studied, TGF-β contributes to breast cancer metastasis (Caja, F. & Vannucci, L. 2015). In addition, TGF-β is able to stimulate epithelial-to-mesenchymal transition (EMT), through upregulation of a transcription factor of EMT and E-cadherin that allows to breast cancer stem cells migration and invasion (Yin, X. et al., 2010). Using ELISA, our results demonstrated that LyeTx I-b peptide inhibited expression of TGF-β in primary tumor and spleen (figure 33). ).Tumor necrosis factor alpha (TNF-α) is an important inflammatory cytokine in breast cancer. It can activate nuclear factor kappa B (NF-κB) followed by promoting tumor microenvironment, that leading to tumor invasion and progression (Kamel, M. et al., 2012). Previous studies were indicated that TNF-α was promoted tumor progression and metastasis in the 4T1 murine model. The treatment of 4T1 tumor-bearing mice with carboplatin and thalidomide were able to decrease the level of TNF-α in the primary tumor (Souza, C et al., 2013 & De Souza, C. et al., 2014). Our findings in figure 33 showed that Carboplatin and LyeTx I-b peptide decreased production of TNF-α in the spleen, which is able to accumulate tumor-promoting immune cells responsible for metastatic process.

Immune cells and their inflammatory mediators such as cytokine and chemokine interfering with tumor microenvironment, give rise to tumor growth or regression depending on the type of inflammatory molecule produced by neutrophils, lymphocytes, and monocytes (Shrihari, T. 2017). Previous clinical study has been shown the dual role of cytokines in breast cancer microenvironment during tumor progression. VEGF, TNF-α, IL-1β, and IL-6 expression level have been increased in the biopsies tissues collected from breast cancer patients (Eftekhari, R. et al., 2017).

IL-1β expression plays an important role in tumor progression and metastasis as well. The IL-1β levels are associated with bad prognoses in several types of cancers such as breast, lung, prostate, neck, and head. It is worth mentioning that in our study LyeTx I-b peptide decreased significantly the expression of IL-1β in tumor and lung tissues (figure 34 A). Previous data demonstrated that inhibition of IL-1 receptor resulted in tumor regression of solid malignancies (Lewis, A. et al.,

2006). Similarity, blocking of the IL-1 receptor by Anakinra antagonist was demonstrated a significant reduction in breast cancer progression and bone metastasis in MCF-7 and MDA-MB-231 breast cancers model (Holen, I. et al., 2016).

The IL-10 is a cytokine that regulates angiogenesis and inhibits tumor migration and progression in early stage of breast cancer (Ahmed, N. et al., 2018). It is well known that overexpression IL-10 protected from carcinogenic and enhanced tumor immune surveillance through activation of intratumoral antigen-presenting molecules (APC), Cytotoxic CD8+ and IFN-ɣ (Mumm, J. et al., 2011). Interestingly, our data demonstrated that LyeTx I-b peptide has increased IL-10 anti-inflammatory cytokines level in primary tumor (figure 34 B). In contrast, LyeTx I-b peptide induced elevated levels of IL-6 proinflammatory cytokine in the brain, spleen and tumor. These results were consistent with previous study that LyeTxI-b decreased IL-1β level in the mice joint of septic arthritis model (Reis, P. et al., 2018). Interestingly, IL-6 production increased in tumor, spleen and brain (figure 34C), we assume that LyeTx I-b peptide does not induced sever inflammation in brain tissues. Despite, tumor inoculation of 4T1 cell line has generated greater levels of TNF-α, IL-1β, IL-6 in spleen, serum, primary tumor and liver, the IL-1β cytokine has increased only in cortex and hippocampus (Walker II, W.H. et al., 2017). Several studies have been shown that chemotherapy can activate toll-like receptors 4 (TLR4) which displayed increasing of proinflammatory IL-6 cytokine in blood and distant organs of tumor bearing animals and even breast cancer patients (Stojanovska, V. et al., 2018). Subsequently, widely used cytotoxic drugs such as 5-fluorouracil, doxorubicin and paclitaxel could be causing fatigue, cachexia and also may facilitating tumor progression in cancer survivors (Elsea, C. et al., 2015& Volk-Draper, L. et al., 2014& Stojanovska, V. et al., 2018 ).

In summary, our data suggested that one possible effect immunomodulatory effect of peptide was related with an increase of IL10 and decrease of TGF-β and IL1-β that can be associated with inhibiton of tumor invaniviness and cell migration as demonstrated in the model 1 of figure 35 below.

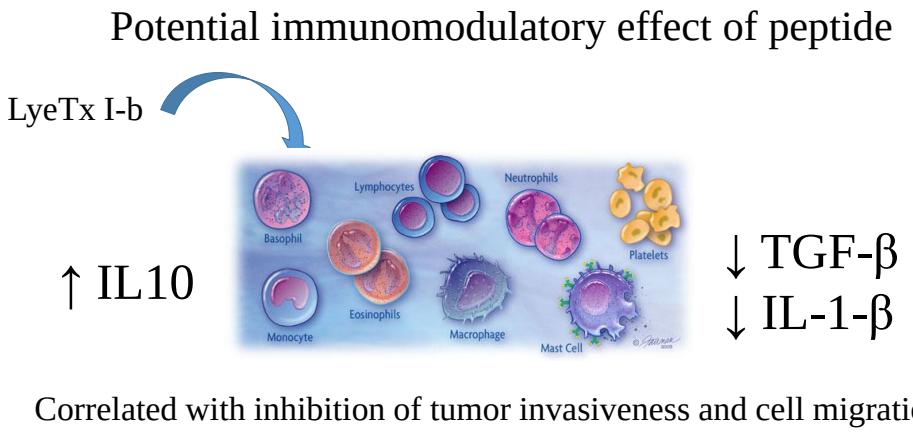


Figure 35. Illustrative model of the possible immunomodulatory effect of peptide on immune cells of 4T1 tumour-bearing mice.

Altogether, our data described for the first time the *in vitro* and *in vivo* effects of LyeTx I-b peptide in 4T1 mammary carcinoma model. *In vitro* evaluations showed that LyeTx I-b peptide was able to induce cytotoxicity and loss of viability of murine triple-negative 4T1 cell line. One possible mechanism can be apoptosis. In addition, LyeTx I-b was effective to suppress tumor growth and reduced lung metastasis in 4T1 highly aggressive and metastatic model through alterations in the cellular and molecular composition of tumor microenvironment, modulating neutrophils, lymphocytes, monocytes as well as production of TGF-β, TNF-α, IL-1β, IL-10 and IL-6.

## 4. Conclusion

*In vitro* data point out LyeTx I-b displayed cytotoxicity against human tumoral cells from solid tumor and leukemia, but with undesirable effect such as neurotoxicity and immunotoxicity. The cytotoxic effect against glioblastoma cells, resistant to anticancer drugs used in clinic, involves triggering cell death through necroptosis that is a promising strategy to overcome apoptosis resistance in cancer. The in vivo findings demonstrated that LyeTx I-b peptide reduced tumor growth, with anti-metastatic and immunomodulatory effects in 4T1 triple negative breast cancer murine model. Therefore, all results pointed out that this cationic antimicrobial peptide could be a potential immunomodulatory prototype to develop drugs for brain and breast cancer therapy to improve clinical outcome.

## 5. References


Aaron, S., Parkes, M., Atkin-Smith, G., Tixeira, I.,& Poon, I. (2017). Cell disassembly during apoptosis. WikiJournal of Medicine, 4(1):8. doi: 10.15347/wjm/2017.008.

Abe, H., Wada, H., Baghdadi, M., Nakanishi, S., Usui, Y., Tsuchikawa, T. & Seino, K.-I. (2016). Identification of a highly immunogenic mouse breast cancer sub cell line, 4T1-S. Human Cell, 29(2), 58–66. https://doi.org/10.1007/s13577-015-0127-1

Abulrob, A., Corluka, S., Blasiak, B., Gino Fallone, B., Ponjevic, D., Matyas, J., & Tomanek, B. (2017). LyP-1 Conjugated Nanoparticles for Magnetic Resonance Imaging of Triple Negative Breast Cancer. Molecular Imaging and Biology : MIB : The Official Publication of the Academy of Molecular Imaging. https://doi.org/10.1007/s11307-017-1140-4

Agarwal, S., et al. (2011). "Delivery of molecularly targeted therapy to malignant glioma, a disease of the whole brain." Expert Rev Mol Med 13: e17.

Agarwal, S., et al. (2013). "Function of the blood-brain barrier and restriction of drug delivery to invasive glioma cells: findings in an orthotopic rat xenograft model of glioma." Drug Metab Dispos 41(1): 33-39.

Aggarwal, B. B., Vijayalekshmi, R. V, & Sung, B. (2009). Targeting inflammatory pathways for prevention and therapy of cancer: short-term friend, long-term foe. Clinical Cancer Research: An Official Journal of the American Association for Cancer Research, 15(2), 425–430. https://doi.org/10.1158/1078-0432.CCR-08-0149

Ahles, T. A. and A. J. Saykin (2007). "Candidate mechanisms for chemotherapy-induced cognitive changes." Nat Rev Cancer**7** (3): 192-201.

Ahmad, N., Ammar, A., Storr, S. J., Green, A. R., Rakha, E., Ellis, I. O., & Martin, S. G. (2018). IL-6 and IL-10 are associated with good prognosis in early stage invasive breast cancer patients. Cancer Immunology, Immunotherapy, 67(4), 537–549. https://doi.org/10.1007/s00262-017-2106-8

Alameda J.P, Moreno-Maldonado, R. Navarro M. Bravo, A. Ramirez A, Page A, et al.,(2010). An inactivating CYLD mutation promotes skin tumor progression by conferring enhanced

proliferative, survival andangiogenic properties to epidermal cancer cells. Oncogene; 29(50):6522–32.

Amini, R.-M., Aaltonen, K., Nevanlinna, H., Carvalho, R., Salonen, L., Heikkilä, P., & Blomqvist, C. (2007). Mast cells and eosinophils in invasive breast carcinoma. BMC Cancer, 7, 165. https://doi.org/10.1186/1471-2407-7-165

Amulic, B., Cazalet, C., Hayes, G. L., Metzler, K. D., & Zychlinsky, A. (2012). Neutrophil function: from mechanisms to disease. Annual Review of Immunology, 30, 459–489. https://doi.org/10.1146/annurev-immunol-020711-074942

Baindara, P., Gautam, A., Raghava, G. P. S., & Korpole, S. (2017). Anticancer properties of a defensin like class IId bacteriocin Laterosporulin10. Scientific Reports, 7, 46541. Brauchle, E., Thude, S., Brucker, S. Y., & Schenke-Layland, K. (2014). Cell death stages in single apoptotic and necrotic cells monitored by Raman microspectroscopy. Sci Rep, 4, 4698. doi:10.1038/srep04698.

Barbosa, B.S., Praxedes, E.A., Lima, M.A. et al. (2017). Haematological and Biochemical Profle of Balb-c Mice. Acta Scientiae Veterinariae, 45: 1477. https://doi.org/10.22456/1679

Barbosa, I. R., D. L. B. de Souza, M. M. Bernal and C. C. Costa Í (2015). "Cancer mortality in Brazil: Temporal Trends and Predictions for the Year 2030." Medicine (Baltimore)94(16).

Basketter, D. A., Clewell, H., Kimber, I., Rossi, A., Blaauboer, B., Burrier, R., Hartung, T. (2012). A roadmap for the development of alternative (non-animal) methods for systemic toxicity testing - t4 report*. Altex, 29(1), 3-91.

Bell BD, Leverrier S, Weist BM, Newton RH,Arechiga AF, Luhrs KA, et al. (2008). FADD and caspase-8control the outcome of autophagic signaling in proliferating T cells. Proc Natl Acad Sci U S A.;105(43):16677–82.

Bernardes, D., Oliveira-Lima, O. C., Silva, T. V. da, Faraco, C. C. F., Leite, H. R., Juliano, M. A.,& Carvalho-Tavares, J. (2013). Differential brain and spinal cord cytokine and BDNF levels in experimental autoimmune encephalomyelitis are modulated by prior and regular exercise. Journal of Neuroimmunology, 264(1–2), 24–34. https://doi.org/10.1016/j.jneuroim.2013.08.014

Bhattacharjee, H. K., Bansal, V. K., Nepal, B., Srivastava, S., Dinda, A. K., & Misra, M. C. (2016). Is Interleukin 10 (IL10) Expression in Breast Cancer a Marker of Poor Prognosis? Indian Journal of Surgical Oncology, 7(3), 320–325. https://doi.org/10.1007/s13193-016-0512-6

Bhatti, J. S., S. Kumar, M. Vijayan, G. K. Bhatti and P. H. Reddy (2017). "Therapeutic Strategies for Mitochondrial Dysfunction and Oxidative Stress in Age-Related Metabolic Disorders." Prog Mol Biol Transl Sci146: 13-46.

Bhojwani, D., N. D. Sabin, D. Pei, J. J. Yang, R. B. Khan, J. C. Panetta, K. R. Krull, H. Inaba, J. E. Rubnitz, M. L. Metzger, S. C. Howard, R. C. Ribeiro, C. Cheng, W. E. Reddick, S. Jeha, J. T. Sandlund, W. E. Evans, C. H. Pui and M. V. Relling (2014). "Methotrexate-Induced Neurotoxicity and Leukoencephalopathy in Childhood Acute Lymphoblastic Leukemia." J Clin Oncol32(9): 949-959.

Bhowmik, A., et al. (2017). "Anti-SSTR2 peptide based targeted delivery of potent PLGA encapsulated 3,3'-diindolylmethane nanoparticles through blood brain barrier prevents glioma progression." Oncotarget 8(39): 65339-65358.

Bischofberger, M., et al. (2012). "Pathogenic pore-forming proteins: function and host response." Cell Host Microbe 12(3): 266-275.

Blot, E., Chen, W., Vasse, M., Paysant, J., Denoyelle, C., Pillé, J.-Y., … Soria, C. (2003). Cooperation between monocytes and breast cancer cells promotes factors involved in cancer aggressiveness. British Journal of Cancer, 88(8), 1207–1212. https://doi.org/10.1038/sj.bjc.6600872

Bonapace L. Bornhauser B.C. Schmitz M. Cario G.Ziegler U. Niggli FK, et al. (2010). Induction of autophagydependent necroptosis is required for childhoodacute lymphoblasti leukemia cells to overcome glucocorticoid resistance. J Clin Invest.;120(4):1310–23.

Borsig, L. (2017). Selectins in cancer immunity. Glycobiology. https://doi.org/10.1093/glycob/cwx105

Brauchle, E., Thude, S. S.Y. Brucker, Schenke-Layland, K (2014). Cell death stages in single apoptotic and necrotic cells monitored by Raman microspectroscopy., Sci. Rep. 4 (5) 4698. doi:10.1038/srep04698.

Bray, F., Ferlay, J., Soerjomataram, I., Siegel, R. L., Torre, L. A., & Jemal, A. (2018). Global cancer statistics 2018: GLOBOCAN estimates of incidence and mortality worldwide for 36 cancers in 185 countries. CA: A Cancer Journal for Clinicians, 68(6), 394–424. https://doi.org/10.3322/caac.21492

Brunetti, J., C. Falciani, G. Roscia, S. Pollini, S. Bindi, S. Scali, U. C. Arrieta, V. Gomez-Vallejo, L. Quercini, E. Ibba, M. Prato, G. M. Rossolini, J. Llop, L. Bracci and A. Pini (2016). "In vitro and in vivo efficacy, toxicity, bio-distribution and resistance selection of a novel antibacterial drug candidate." Sci Rep 6: 26077.

Bubien, K. , Ji, H.-L., G.Y. Gillespie, C.M. Fuller, J.M. Markert, T.B. Mapstone, Benos, D.J. (2004). Cation selectivity and inhibition of malignant glioma Na+ channels by Psalmotoxin 1. Am. J. Physiol. Cell Physiol. 287 (2) C1282-91. doi:10.1152/ajpcell.00077.2004.

Buenrostro, D., Kwakwa, K. A., Putnam, N. E., Merkel, A. R., Johnson, J. R., Cassat, J. E., & Sterling, J. A. (2018). Early TGF-beta inhibition in mice reduces the incidence of breast cancer induced bone disease in a myeloid dependent manner. Bone, 113, 77–88. https://doi.org/10.1016/j.bone.2018.05.008

Burns, K. E., McCleerey, T. P., & Thévenin, D. (2016). pH-Selective Cytotoxicity of pHLIPAntimicrobial Peptide Conjugates. Scientific Reports, 6, 28465. http://doi.org/10.1038/srep28465

Caja, F., & Vannucci, L. (2015). TGFβ: A player on multiple fronts in the tumor microenvironment. Journal of Immunotoxicology, 12(3), 300–307. https://doi.org/10.3109/1547691X.2014.945667

Carroll, C. (2016). The treatment of solid tumors with complete freund's adjuvant. Australian National University. PhD. Thesis

Carvalho-Tavares, J., Fox-Robichaud, A., & Kubes, P. (1999). Assessment of the mechanism of juxtacrine activation and adhesion of leukocytes in liver microcirculation. The American Journal of Physiology, 276(4 Pt 1), G828-34.

Carvalho-Tavares, J., Hickey, M. J., Hutchison, J., Michaud, J., Sutcliffe, I. T., & Kubes, P. (2000). A role for platelets and endothelial selectins in tumor necrosis factor-alpha-induced leukocyte recruitment in the brain microvasculature. Circulation Research, 87(12), 1141–1148.

Castañeda-Gill, J. M., & Vishwanatha, J. K. (2016). Antiangiogenic mechanisms and factors in breast cancer treatment. Journal of Carcinogenesis, 15, 1. https://doi.org/10.4103/1477-3163.176223

Chan, F. K., Moriwaki, K., & De Rosa, M. J. (2013). Detection of necrosis by release of lactate dehydrogenase activity. Methods Mol Biol, 979, 65-70. doi:10.1007/978-1-62703-290-2_7 Carvalho, C., R. X. Santos, S. Cardoso, S. Correia, P. J. Oliveira, M. S. Santos and P. I. Moreira (2009). "Doxorubicin: the good, the bad and the ugly effect." Curr Med Chem**16**(25): 3267-3285.

Chatterjee, S., A. Chattopadhyay, S. N. Senapati, D. R. Samanta, L. Elliott, D. Loomis, L. Mery and P. Panigrahi (2016). "Cancer Registration in India - Current Scenario and Future Perspectives." Asian Pac J Cancer Prev17(8): 3687-3696.

Chen, C., Hu, J., Zeng, P., Pan, F., Yaseen, M., Xu, H., & Lu, J. R. (2014). Molecular mechanisms of anticancer action and cell selectivity of short alpha-helical peptides. Biomaterials, 35(5), 15521561. doi:10.1016/j.biomaterials.2013.10.082

Chen, D., J. Yu and L. Zhang (2016). "Necroptosis: an alternative cell death program defending against cancer." Biochim Biophys Acta1865 (2): 228-236.

Cho, Y., McQuade, T., Zhang, H., Zhang, J., & Chan, F. K. (2011). RIP1-dependent and independent effects of necrostatin-1 in necrosis and T cell activation. PLoS One, 6(8), e23209. Consuegra, J., et al. (2013). "Peptides: beta-cyclodextrin inclusion compounds as highly effective antimicrobial and anti-epithelial proliferation agents." J Periodontol 84(12): 1858-1868.

Chu, H.-L., Yip, B.-S. K.-H. Chen, H.-Y. Yu, Y.-H. Chih, H.-T. Cheng, Y.-T. Chou, Cheng, J.-W (2015). Novel Antimicrobial Peptides with High Anticancer Activity and Selectivity, PLoS One. 10 (5) e0126390. doi:10.1371/journal.pone.0126390.

Cichoń, T., Smolarczyk, R., Matuszczak, S., Barczyk, M., Jarosz, M., & Szala, S. (2014). D-K(6)L(9) Peptide Combination with IL-12 Inhibits the Recurrence of Tumors in Mice. Archivum Immunologiae et Therapiae Experimentalis, 62(4), 341–351. https://doi.org/10.1007/s00005-014-0268-z

Cook, G. J. R. (2010). PET and PET/CT imaging of skeletal metastases. Cancer Imaging, 10(1), 153–160. https://doi.org/10.1102/1470-7330.2010.0022

Crowley, L. C., Marfell, B. J., Scott, A. P., & Waterhouse, N. J. (2016). Quantitation of Apoptosis and Necrosis by Annexin V Binding, Propidium Iodide Uptake, and Flow Cytometry. Cold Spring Harbor Protocols, 2016(11), pdb.prot087288. https://doi.org/10.1101/pdb.prot087288

Cruz Olivo, E. A., Santos, D., Elena de Lima, M., Dos Santos, V. L., Sinisterra, R. D., & Cortes, M. E. (2016). Antibacterial Effect of Synthetic Peptide LyeTxI and LyeTxI/betaCD Association Compound against Planktonic and Multispecies Biofilms of Periodontal Pathogens. J Periodontol, 1-16.

Dalzini, A., Bergamini, C., Biondi, B., De Zotti, M., Panighel, G., Fato, R., … Maniero, A. L. (2016). The rational search for selective anticancer derivatives of the peptide Trichogin GA IV: a multi-technique biophysical approach. Scientific Reports, 6, 24000. https://doi.org/10.1038/srep24000

Dardevet, L., D. Rani, T. A. Aziz, I. Bazin, J. M. Sabatier, M. Fadl, E. Brambilla and M. De Waard (2015). "Chlorotoxin: a helpful natural scorpion peptide to diagnose glioma and fight tumor invasion." Toxins (Basel)**7**(4): 1079-1101.

Darzynkiewicz, Z. (2010). Critical Aspects in Analysis of Cellular DNA Content. Current Protocols in Cytometry / Editorial Board, J. Paul Robinson, Managing Editor ... [et Al.], CHAPTER, Unit7.2-Unit7.2. https://doi.org/10.1002/0471142956.cy0702s52

Davitt, K., B. D. Babcock, M. Fenelus, C. K. Poon, A. Sarkar, V. Trivigno, P. A. Zolkind, S. M. Matthew, N. Grin'kina, Z. Orynbayeva, M. F. Shaikh, V. Adler, J. Michl, E. Sarafraz-Yazdi, M. R. Pincus and W. B. Bowne (2014). "The anti-cancer peptide, PNC-27, induces tumor cell necrosis of a poorly differentiated non-solid tissue human leukemia cell line that depends on expression of HDM-2 in the plasma membrane of these cells." Ann Clin Lab Sci44(3): 241-248.

De Souza, C. M., Araujo e Silva, A. C., de Jesus Ferraciolli, C., Moreira, G. V., Campos, L. C., dos Reis, D. C., … Cassali, G. D. (2014). Combination therapy with carboplatin and thalidomide suppresses tumor growth and metastasis in 4T1 murine breast cancer model. Biomedicine & Pharmacotherapy = Biomedecine & Pharmacotherapie, 68(1), 51–57. https://doi.org/10.1016/j.biopha.2013.08.004

de Vries, S. J., Rey, J., Schindler, C. E. M., Zacharias, M., & Tuffery, P. (2017). The pepATTRACT web server for blind, large-scale peptide-protein docking. Nucleic Acids Research, 45(W1), W361–W364. https://doi.org/10.1093/nar/gkx335

Delp, J. Gutbier, Klima , S. Hoelting, S. , L., Pinto-Gil, K., Hsieh, J.-H., … Leist, M. (2018). A high-throughput approach to identify specific neurotoxicants/ developmental toxicants in human neuronal cell function assays. ALTEX. https://doi.org/10.14573/altex.1712182

Deslouches, B., Di, Y.P. (2014). Antimicrobial peptides with selective antitumor mechanisms: prospect for anticancer applications., Oncotarget. 8 (6) 46635–46651. doi:10.18632/oncotarget.16743.

Di Carlo, D. T., Cagnazzo, F., Benedetto, N., Morganti, R., & Perrini, P. (2017). Multiple high-grade gliomas: epidemiology, management, and outcome. A systematic review and meta-analysis. Neurosurgical Review. https://doi.org/10.1007/s10143-017-0928-7

Di Cesare Mannelli, L., E. Lucarini, L. Micheli, I. Mosca, P. Ambrosino, M. V. Soldovieri, A. Martelli, L. Testai, M. Taglialatela, V. Calderone and C. Ghelardini (2017). "Effects of natural and synthetic isothiocyanate-based H2S-releasers against chemotherapy-induced neuropathic pain: Role of Kv7 potassium channels." Neuropharmacology121: 49-59.

Do Nascimento, T. G., de Andrade, M., de Oliveira, R. A., de Almeida, A. M., & Gozzo, T. de O. (2014). Neutropenia: occurrence and management in women with breast cancer receiving chemotherapy. Revista Latino-Americana de Enfermagem, 22(2), 301–308. https://doi.org/10.1590/0104-1169.3305.2416

Dos Reis, P. V. M, Boff. D, Rodrigo. M. V., de Melo-Braga. M.V, Cortés. M.E, dos Santos. D.M, de Castro Pimenta. A.M, da Amaral. F.A., Resende. J.M., de Lima. M.E (2018) LyeTxI-b, a

Synthetic Peptide Derived From Lycosa erythrognatha Spider Venom, Shows Potent Antibiotic Activity in Vitro and in Vivo., Front. Microbiol. 667 (6) 1-12. doi:10.3389/fmicb.2018.00667

Dos Santos, A. C., Roffe, E., Arantes, R. M. E., Juliano, L., Pesquero, J. L., Pesquero, J. B., … Carvalho-Tavares, J. (2008). Kinin B2 receptor regulates chemokines CCL2 and CCL5 expression and modulates leukocyte recruitment and pathology in experimental autoimmune encephalomyelitis (EAE) in mice. Journal of Neuroinflammation, 5, 49. https://doi.org/10.1186/1742-2094-5-49

Douglas, S., Hoskin, D. W., & Hilchie, A. L. (2014). Assessment of antimicrobial (host defense) peptides as anti-cancer agents. Methods in Molecular Biology (Clifton, N.J.), 1088, 159–170. https://doi.org/10.1007/978-1-62703-673-3_11

Drappatz, J., et al. (2013). "Phase I study of GRN1005 in recurrent malignant glioma." Clin Cancer Res 19(6): 1567-1576.

Drechsel, D. A., Liang, L. P., & Patel, M. (2007). 1-methyl-4-phenylpyridinium-induced alterations of glutathione status in immortalized rat dopaminergic neurons. Toxicol Appl Pharmacol, 220(3), 341-348. doi:10.1016/j.taap.2007.02.002

Duffner, P. K., F. D. Armstrong, L. Chen, K. J. Helton, M. L. Brecher, B. Bell and A. R. Chauvenet (2014). "Neurocognitive and neuroradiologic central nervous system late effects in children treated on Pediatric Oncology Group (POG) P9605 (standard risk) and P9201 (lesser risk) acute lymphoblastic leukemia protocols (ACCL0131): a methotrexate consequence? A report from the Children's Oncology Group." J Pediatr Hematol Oncol36(1): 8-15.

Dupre, S., & W Hunter, K. (2007). Murine mammary carcinoma 4T1 induces a leukemoid reaction with splenomegaly: Association with tumor-derived growth factors. Experimental and molecular pathology (Vol. 82). https://doi.org/10.1016/j.yexmp.2006.06.007

Dutra, A.P., Azevedo Júnior, G.M., Schmitt, F.C., & Cassali, G.D.. (2008). Assessment of cell proliferation and prognostic factors in canine mammary gland tumors. Arquivo Brasileiro de Medicina Veterinária e Zootecnia, 60(6), 1403-1412. https://dx.doi.org/10.1590/S0102-09352008000600015

Eftekhari, R., Esmaeili, R., Mirzaei, R., Bidad, K., de Lima, S., Ajami, M., … Majidzadeh-A, K. (2017). Study of the tumor microenvironment during breast cancer progression. Cancer Cell International, 17, 123. https://doi.org/10.1186/s12935-017-0492-9

Ejlertsen, B. (2016). Adjuvant chemotherapy in early breast cancer. Danish Medical Journal, 63(5).

Elsea, C. R., Kneiss, J. A., & Wood, L. J. (2015). Induction of IL-6 by Cytotoxic Chemotherapy Is Associated With Loss of Lean Body and Fat Mass in Tumor-free Female Mice. Biological Research for Nursing, 17(5), 549–557. https://doi.org/10.1177/1099800414558087

Esquivel-Velázquez, M., Ostoa-Saloma, P., Palacios-Arreola, M. I., Nava-Castro, K. E., Castro, J. I., & Morales-Montor, J. (2015). The Role of Cytokines in Breast Cancer Development and Progression. Journal of Interferon & Cytokine Research, 35(1), 1–16. https://doi.org/10.1089/jir.2014.0026

Ethier, J.-L., Desautels, D., Templeton, A., Shah, P. S., & Amir, E. (2017). Prognostic role of neutrophil-to-lymphocyte ratio in breast cancer: a systematic review and meta-analysis. Breast Cancer Research : BCR, 19, 2. https://doi.org/10.1186/s13058-016-0794-1

Eum, K.-H., & Lee, M. (2011). Targeting the Autophagy Pathway Using Ectopic Expression of Beclin 1 in Combination with Rapamycin in Drug-Resistant v-Ha-ras-Transformed NIH 3T3 Cells. Molecules and Cells, 31(3), 231–238. http://doi.org/10.1007/s10059-011-0034-6

Felicio, M. R., Silva, O. N., Goncalves, S., Santos, N. C., & Franco, O. L. (2017). Peptides with Dual Antimicrobial and Anticancer Activities. Front Chem, 5, 5. doi:10.3389/fchem.2017.00005.

Ferrari, G., Cook, B. D., Terushkin, V., Pintucci, G., & Mignatti, P. (2009). TRANSFORMING GROWTH FACTOR-BETA 1 (TGF-β1) INDUCES ANGIOGENESIS THROUGH VASCULAR ENDOTHELIAL GROWTH FACTOR (VEGF)-MEDIATED APOPTOSIS. Journal of Cellular Physiology, 219(2), 449–458. https://doi.org/10.1002/jcp.21706

Fishel, M. L., M. R. Vasko and M. R. Kelley (2007). "DNA repair in neurons: so if they don't divide what's to repair?" Mutat Res614(1-2): 24-36.

Floeter, A. E., A. Patel, M. Tran, M. C. Chamberlain, P. C. Hendrie, A. K. Gopal and R. D. Cassaday (2017). "Posterior Reversible Encephalopathy Syndrome Associated With Dose-

adjusted EPOCH (Etoposide, Prednisone, Vincristine, Cyclophosphamide, Doxorubicin) Chemotherapy." Clin Lymphoma Myeloma Leuk17(4): 225-230.

Fosgerau, K. and T. Hoffmann (2015). "Peptide therapeutics: current status and future directions." Drug Discov Today20(1): 122-128.

Franken, N. A. P., Rodermond, H. M., Stap, J., Haveman, J., & van Bree, C. (2006). Clonogenic assay of cells in vitro. Nature Protocols, 1, 2315. Retrieved from http://dx.doi.org/10.1038/nprot.2006.339

Fulzele, S. V, Chatterjee, A., Shaik, M. S., Jackson, T., & Singh, M. (2006). Inhalation delivery and anti-tumor activity of celecoxib in human orthotopic non-small cell lung cancer xenograft model. Pharmaceutical Research, 23(9), 2094–2106. https://doi.org/10.1007/s11095-006-9074-6

Fuscaldi, L. L., dos Santos, D. M., Pinheiro, N. G. S., Araújo, R. S., de Barros, A. L. B., Resende, J. M., Cardoso, V. N. (2016). Synthesis and antimicrobial evaluation of two peptide LyeTx I derivatives modified with the chelating agent HYNIC for radiolabeling with technetium-99m. The Journal of Venomous Animals and Toxins Including Tropical Diseases, 22, 16.

Galluzzi, L., Buque, A., Kepp, O., Zitvogel, L., & Kroemer, G. (2015). Immunological Effects of Conventional Chemotherapy and Targeted Anticancer Agents. Cancer Cell, 28(6), 690–714. https://doi.org/10.1016/j.ccell.2015.10.012

Galluzzi, L., et al. (2011). "Programmed necrosis from molecules to health and disease." Int Rev Cell Mol Biol 289: 1-35.

Galluzzi, L., Vitale, I., Vacchelli, E., & Kroemer, G. (2011). Cell death signaling and anticancer therapy. Front Oncol, 1, 5.

Gao, H., Z. Yang, S. Cao, Y. Xiong, S. Zhang, Z. Pang and X. Jiang (2014). "Tumor cells and neovasculature dual targeting delivery for glioblastoma treatment." Biomaterials35(7): 23742382.

Garcia-Lora, A., Algarra, I., & Garrido, F. (2003). MHC class I antigens, immune surveillance, and tumor immune escape. Journal of Cellular Physiology, 195(3), 346–355. https://doi.org/10.1002/jcp.10290

Gartlon, J., Kinsner, A., Bal-Price, A., Coecke, S., & Clothier, R. H. (2006). Evaluation of a proposed in vitro test strategy using neuronal and non-neuronal cell systems for detecting neurotoxicity. Toxicol In Vitro, 20(8), 1569-1581. doi:10.1016/j.tiv.2006.07.009

Gaspar, D., A. S. Veiga and M. A. Castanho (2013). "From antimicrobial to anticancer peptides. A review." Front Microbiol4: 294.

Gaspar, D., A.S. Veiga, and M.A. Castanho (2013). From antimicrobial to anticancer peptides. A review. Front Microbiol,. 4: p. 294.

Geserick, P., et al. (2015). "Absence of RIPK3 predicts necroptosis resistance in malignant melanoma." Cell Death Dis 6: e1884.

Gewirtz, D. A. (2014). An autophagic switch in the response of tumor cells to radiation and chemotherapy. Biochem Pharmacol, 90(3), 208-211. doi:10.1016/j.bcp.2014.05.016

Ghoncheh, M., Pournamdar, Z., & Salehiniya, H. (2016). Incidence and Mortality and Epidemiology of Breast Cancer in the World. Asian Pacific Journal of Cancer Prevention : APJCP, 17(S3), 43–46.

Giannini, E. G., Fasoli, A., Borro, P., Botta, F., Malfatti, F., Fumagalli, A., … Testa, R. (2005). 13C-galactose breath test and 13C-aminopyrine breath test for the study of liver function in chronic liver disease. Clinical Gastroenterology and Hepatology, 3(3), 279–285. https://doi.org/10.1016/S1542-3565(04)00720-7

Gilbert, Mark R. et al. “Cilengitide in Patients with Recurrent Glioblastoma: The Results of NABTC 0302, a Phase II Trial with Measures of Treatment Delivery.” Journal of neuro-oncology 106.1 (2012): 147–153.

Gilchrist, L. S., L. R. Tanner and K. K. Ness (2017). "Short-term recovery of chemotherapy-induced peripheral neuropathy after treatment for pediatric non-CNS cancer." Pediatr Blood Cancer64(1): 180-187.

Girardi, F., Barnes, D. R., Barrowdale, D., Frost, D., Brady, A. F., Miller, C., Henderson, A., Donaldson, A., Murray, A., Brewer, C., Pottinger, C., Evans, D. G., Eccles, D., EMBRACE, Lalloo, F., Gregory, H., Cook, J., Eason, J., Adlard, J., Barwell, J., Ong, K. R., Walker, L., Izatt, L., Side, L. E., Kennedy, M. J., Tischkowitz, M., Rogers, M. T., Porteous, M. E., Morrison, P. J., Eeles, R., Davidson, R., Snape, K., Easton, D. F., … Antoniou, A. C. (2018). Risks of breast or ovarian cancer in BRCA1 or BRCA2 predictive test negatives: findings from the EMBRACE

study. Genetics in medicine : official journal of the American College of Medical Genetics, 10.1038/gim.2018.44. Advance online publication. doi:10.1038/gim.2018.44

Goldberg, J. E., & Schwertfeger, K. L. (2010). Proinflammatory cytokines in breast cancer: mechanisms of action and potential targets for therapeutics. Current Drug Targets, 11(9), 1133–1146.

Golovtchenko, A. M., & Raichvarg, D. (1975). [Lymphocytes. Roles in cellular immunity and humoral immunity]. Annales de biologie clinique, 33(2), 63–74.

Gomes, J. A., Bahia-Oliveira, L. M., Rocha, M. O., Martins-Filho, O. A., Gazzinelli, G., & CorreaOliveira, R. (2003). Evidence that development of severe cardiomyopathy in human Chagas' disease is due to a Th1-specific immune response. Infect Immun, 71(3), 1185-1193.

Gong, Y., Chippada-Venkata, U. D., & Oh, W. K. (2014). Roles of matrix metalloproteinases and their natural inhibitors in prostate cancer progression. Cancers, 6(3), 1298–1327. https://doi.org/10.3390/cancers6031298

Grimberg, J., Nawoschik, S., Belluscio, L., McKee, R., Turck, A., & Eisenberg, A. (1989). A simple and efficient non-organic procedure for the isolation of genomic DNA from blood. Nucleic Acids Res, 17(20), 8390.

Grisold, W., G. Cavaletti and A. J. Windebank (2012). "Peripheral neuropathies from chemotherapeutics and targeted agents: diagnosis, treatment, and prevention." Neuro Oncol14 Suppl 4: iv45-54.

Grivennikov, S. I., Greten, F. R., & Karin, M. (2010). Immunity, inflammation, and cancer. Cell, 140(6), 883–899. https://doi.org/10.1016/j.cell.2010.01.025

Guo, Z., H. Peng, J. Kang and D. Sun (2016). "Cell-penetrating peptides: Possible transduction mechanisms and therapeutic applications." Biomed Rep4(5): 528-534.

Guo, Z., Peng, H., Kang, J., & Sun, D. (2016). Cell-penetrating peptides: Possible transduction mechanisms and therapeutic applications. Biomedical reports, 4(5), 528-534.

Gupta, G. P., & Massague, J. (2006). Cancer metastasis: building a framework. Cell, 127(4), 679–695. https://doi.org/10.1016/j.cell.2006.11.001

Hamed, E. A., Zakhary, M. M., & Maximous, D. W. (2012). Apoptosis, angiogenesis, inflammation, and oxidative stress: basic interactions in patients with early and metastatic breast cancer. Journal of Cancer Research and Clinical Oncology, 138(6), 999–1009. https://doi.org/10.1007/s00432-012-1176-4

Hamidullah, Changkija, B., & Konwar, R. (2012). Role of interleukin-10 in breast cancer. Breast Cancer Research and Treatment, 133(1), 11–21. https://doi.org/10.1007/s10549-011-1855-x

Han W, Li L, Qiu S, Lu Q, Pan Q, Gu Y, et al.(2007). Shikonin circumvents cancer drug resistance byinduction of a necroptotic death. Mol Cancer Ther.;6(5):1641–9.

Han, Jeonghun et al. "Rapid Emergence and Mechanisms of Resistance by U-87 Glioblastoma Cells to Doxorubicin in an in Vitro Tumor Microfluidic Ecology." Proceedings of the National Academy of Sciences of the United States of America 113.50 (2016): 14283–14288. PMC. Web. 1 July 2017.

Hanahan, D., & Weinberg, R. A. (2000). The hallmarks of cancer. Cell, 100(1), 57–70.

Hanahan, D., & Weinberg, R. A. (2018). Hallmarks of Cancer: The Next Generation. Cell, 144(5), 646–674. https://doi.org/10.1016/j.cell.2011.02.013

Harrison, H., Bennett, G., Blakeley, D., Brown, A., Campbell, S., Chen, L., … Lee, K. (2017). Abstract 5144: BT1718, a novel bicyclic peptide-maytansinoid conjugate targeting MT1-MMP for the treatment of solid tumors: Design of bicyclic peptide and linker selection. Cancer Research, 77(13 Supplement), 5144 LP-5144. https://doi.org/10.1158/1538-7445.AM2017-5144

Hassan, M. S. U., Ansari, J., Spooner, D., & Hussain, S. A. (2010). Chemotherapy for breast cancer (Review). Oncology Reports, 24(5), 1121–1131.

He, S., L. Wang, L. Miao, T. Wang, F. Du, L. Zhao and X. Wang (2009). "Receptor interacting protein kinase-3 determines cellular necrotic response to TNF-alpha." Cell 137(6): 1100-1111.

Herr, N., Mauler, M., Bode, C., & Duerschmied, D. (2015). Intravital Microscopy of Leukocyte-endothelial and Platelet-leukocyte Interactions in Mesenterial Veins in Mice. Journal of Visualized Experiments : JoVE, (102), e53077. https://doi.org/10.3791/53077

Herr, N., Mauler, M., Bode, C., & Duerschmied, D. (2015). Intravital Microscopy of Leukocyte-endothelial and Platelet-leukocyte Interactions in Mesenterial Veins in Mice. Journal of Visualized Experiments : JoVE, (102), 53077. Advance online publication. http://doi.org/10.3791/53077

Heulot, M., N. Chevalier, J. Puyal, C. Margue, S. Michel, S. Kreis, D. Kulms, D. Barras, A. Nahimana and C. Widmann (2016). "The TAT-RasGAP317-326 anti-cancer peptide can kill in a caspase-, apoptosis-, and necroptosis-independent manner." Oncotarget7(39): 64342-64359.

Hewitson, T. D., Wigg, B., & Becker, G. J. (2010). Tissue preparation for histochemistry: fixation, embedding, and antigen retrieval for light microscopy. Methods in Molecular Biology (Clifton, N.J.), 611, 3–18. https://doi.org/10.1007/978-1-60327-345-9_1

Holen, I., Lefley, D. V, Francis, S. E., Rennicks, S., Bradbury, S., Coleman, R. E., & Ottewell, P. (2016). IL-1 drives breast cancer growth and bone metastasis in vivo. Oncotarget, 7(46), 75571–75584. https://doi.org/10.18632/oncotarget.12289

Hon, G. M., Hassan, M. S., van Rensburg, S. J., Abel, S., Erasmus, R. T., & Matsha, T. (2011). Peripheral blood mononuclear cell membrane fluidity and disease outcome in patients with multiple sclerosis. Indian journal of hematology & blood transfusion : an official journal of Indian Society of Hematology and Blood Transfusion, 28(1), 1-6.

Hong, S. H., Ren, L., Mendoza, A., Eleswarapu, A., & Khanna, C. (2012). Apoptosis resistance and PKC signaling: distinguishing features of high and low metastatic cells. Neoplasia (New York, N.Y.), 14(3), 249-58.

Hou, L., Liu, K., Li, Y., Ma, S., Ji, X., & Liu, L. (2016). Necrotic pyknosis is a morphologically and biochemically distinct event from apoptotic pyknosis. Journal of Cell Science, 129(16), 3084–3090. https://doi.org/10.1242/jcs.184374

Huang, Y. C., S. Ming, P. C. Hsieh, J. H. Shih, W. Tsu-Shing, Y. C. Wang, T. H. Lin and S. H. Wang (2017). "Galangin ameliorates cisplatin-induced nephrotoxicity by attenuating oxidative stress, inflammation and cell death in mice through inhibition of ERK and NF-kappaB signaling." Toxicol Appl Pharmacol.

Huang, Y., Huang, J., & Chen, Y. (2010). Alpha-helical cationic antimicrobial peptides: relationships of structure and function. Protein & Cell, 1(2), 143–152. https://doi.org/10.1007/s13238-010-0004-3

Huang, Y.-B., Wang, X.-F., H.-Y. Wang, Y. Liu, Chen, Y. (2011). Studies on mechanism of action of anticancer peptides by modulation of hydrophobicity within a defined structural framework., Mol. Cancer Ther. 10 (11) 416–426. doi:10.1158/1535-7163.MCT-10-0811.

Iadocicco, K., Monteiro, L. H. A., & Chaui-Berlinck, J. G. (2002). A theoretical model for estimating the margination constant of leukocytes. BMC Physiology, 2, 3. Retrieved from http://www.ncbi.nlm.nih.gov/pmc/articles/PMC100780/

Hughes, J. P., Rees, S., Kalindjian, S. B., & Philpott, K. L. (2011). Principles of early drug discovery. British Journal of Pharmacology, 162(6), 1239–1249. https://doi.org/10.1111/j.1476-5381.2010.01127.x

Idris, A., Ghazali, N. B., & Koh, D. (2015). Interleukin 1β—A Potential Salivary Biomarker for Cancer Progression? Biomarkers in Cancer, 7, 25–29. https://doi.org/10.4137/BIC.S25375

Inoue, K., & Fry, E. A. (2016). Novel Molecular Markers for Breast Cancer. Biomarkers in Cancer, 8, 25–42. https://doi.org/10.4137/BIC.S38394

Instituto Nacional de Câncer (INCA). ‘’Câncer de mama’’ https://www.inca.gov.br/tipos-de-cancer/cancer-de-mama.

Ivanov, D. P., Al-Rubai, A. J., Grabowska, A. M., & Pratten, M. K. (2016). Separating chemotherapyrelated developmental neurotoxicity from cytotoxicity in monolayer and neurosphere cultures of human fetal brain cells. Toxicol In Vitro, 37, 88-96. doi:10.1016/j.tiv.2016.09.007

Iwasaki, T., J. Ishibashi, H. Tanaka, M. Sato, A. Asaoka, D. Taylor and M. Yamakawa (2009). "Selective cancer cell cytotoxicity of enantiomeric 9-mer peptides derived from beetle defensins depends on negatively charged phosphatidylserine on the cell surface." Peptides30 (4): 660-668.

Jackson, W. 3rd, Sosnoski, D. M., Ohanessian, S. E., Chandler, P., Mobley, A., Meisel, K. D., & Mastro, A. M. (2017). Role of Megakaryocytes in Breast Cancer Metastasis to Bone. Cancer Research, 77(8), 1942–1954. https://doi.org/10.1158/0008-5472.CAN-16-1084

Jacotot, E., A. Deniaud, A. Borgne-Sanchez, Z. Touat, J. P. Briand, M. Le Bras and C. Brenner (2006). "Therapeutic peptides: Targeting the mitochondrion to modulate apoptosis." Biochim Biophys Acta1757 (9-10): 1312-1323.

Jain, P., S. Gulati, R. Seth, S. Bakhshi, G. S. Toteja and R. M. Pandey (2014). "Vincristine-induced neuropathy in childhood ALL (acute lymphoblastic leukemia) survivors: prevalence and electrophysiological characteristics." J Child Neurol29(7): 932-937.

Jakel, C. E., et al. (2012). "Efficacy of a proapoptotic peptide towards cancer cells." In Vivo 26(3): 419426.

James, S. E., Burden, H., Burgess, R., Xie, Y., Yang, T., Massa, S. M., Lu, Q. (2008). Anti-cancer drug induced neurotoxicity and identification of Rho pathway signaling modulators as potential neuroprotectants. Neurotoxicology, 29(4), 605-612.

Janssen, L. M. E., Ramsay, E. E., Logsdon, C. D., & Overwijk, W. W. (2017). The immune system in cancer metastasis: friend or foe? Journal for Immunotherapy of Cancer, 5, 79. https://doi.org/10.1186/s40425-017-0283-9

John, T., N. Lomeli and D. A. Bota (2017). "Systemic cisplatin exposure during infancy and adolescence causes impaired cognitive function in adulthood." Behav Brain Res319: 200-206.

Jones, G. B., Collins, D. S., Harrison, M. W., Thyagarajapuram, N. R., & Wright, J. M. (2017). Subcutaneous drug delivery: An evolving enterprise. Science Translational Medicine, 9(405). https://doi.org/10.1126/scitranslmed.aaf9166

Jordan, V. C. (1993). Fourteenth Gaddum Memorial Lecture. A current view of tamoxifen for the treatment and prevention of breast cancer. British Journal of Pharmacology, 110(2), 507–517. Retrieved from http://www.ncbi.nlm.nih.gov/pmc/articles/PMC2175926/

Juang, V., Lee, H.-P., Lin, A. M.-Y., & Lo, Y.-L. (2016). Cationic PEGylated liposomes incorporating an antimicrobial peptide tilapia hepcidin 2–3: an adjuvant of epirubicin to overcome multidrug resistance in cervical cancer cells. International Journal of Nanomedicine, 11, 6047–6064.

Kagan, L. (2014). Pharmacokinetic Modeling of the Subcutaneous Absorption of Therapeutic Proteins. Drug Metabolism and Disposition, 42(11), 1890 LP-1905. Retrieved from http://dmd.aspetjournals.org/content/42/11/1890.abstract

Kamel, M., Shouman, S., El-Merzebany, M., Kilic, G., Veenstra, T., Saeed, M., … Salama, S. (2012). Effect of Tumour Necrosis Factor-Alpha on Estrogen Metabolic Pathways in Breast Cancer Cells. Journal of Cancer, 3, 310–321. https://doi.org/10.7150/jca.4584

Kandoth, C., McLellan, M. D., Vandin, F., Ye, K., Niu, B., Lu, C., … Ding, L. (2013). Mutational landscape and significance across 12 major cancer types. Nature, 502(7471), 333–339. https://doi.org/10.1038/nature12634

Kandoth, C., McLellan, M. D., Vandin, F., Ye, K., Niu, B., Lu, C., … Ding, L. (2013). Mutational landscape and significance across 12 major cancer types. Nature, 502(7471), 333–339. https://doi.org/10.1038/nature12634

Kandula, M., Chennaboina, K. K., Ys, A. R., & Raju, S. (2013). Phosphatidylinositol 3-kinase (PI3KCA) oncogene mutation analysis and gene expression profiling in primary breast cancer patients. Asian Pacific Journal of Cancer Prevention: APJCP, 14(9), 5067–5072.

Kanematsu, S., Uehara, N., Miki, H., Yoshizawa, K., Kawanaka, A., Yuri, T., & Tsubura, A. (2010). Autophagy inhibition enhances sulforaphane-induced apoptosis in human breast cancer cells. Anticancer Res, 30(9), 3381-3390.

Karpel-Massler, G., U. Schmidt, A. Unterberg and M. E. Halatsch (2009). "Therapeutic inhibition of the epidermal growth factor receptor in high-grade gliomas: where do we stand?" Mol Cancer Res7(7): 1000-1012.

Kawamoto, M., T. Horibe, M. Kohno and K. Kawakami (2011). "A novel transferrin receptor-targeted hybrid peptide disintegrates cancer cell membrane to induce rapid killing of cancer cells." BMC Cancer11: 359.

Khanna, C., & Hunter, K. (2005). Modeling metastasis in vivo. Carcinogenesis, 26(3), 513–523. https://doi.org/10.1093/carcin/bgh261

Kikuchi, O., S. Ohashi, T. Horibe, M. Kohno, Y. Nakai, S. Miyamoto, T. Chiba, M. Muto and K. Kawakami (2016). "Novel EGFR-targeted strategy with hybrid peptide against oesophageal squamous cell carcinoma." Sci Rep 6: 22452.

Kim, H., Park, H., & Lee, S. J. (2017). Effective method for drug injection into subcutaneous tissue. Scientific Reports, 7, 9613. https://doi.org/10.1038/s41598-017-10110-w

Kitamura, T., Doughty-Shenton, D., Cassetta, L., Fragkogianni, S., Brownlie, D., Kato, Y., … Pollard, J. W. (2017). Monocytes Differentiate to Immune Suppressive Precursors of Metastasis-Associated Macrophages in Mouse Models of Metastatic Breast Cancer. Frontiers in Immunology, 8, 2004. http://doi.org/10.3389/fimmu.2017.02004

Knieke, K., Lingel, H., Chamaon, K., & Brunner-Weinzierl, M. C. (2012). Migration of Th1 Lymphocytes Is Regulated by CD152 (CTLA-4)-Mediated Signaling via PI3 Kinase-Dependent Akt Activation. PLoS ONE, 7(3), e31391. https://doi.org/10.1371/journal.pone.0031391

Kocatürk, B., & Versteeg, H. H. (2015). Orthotopic Injection of Breast Cancer Cells into the Mammary Fat Pad of Mice to Study Tumor Growth. Journal of Visualized Experiments : JoVE, (96), 51967. https://doi.org/10.3791/51967

Koepke, J. A. (1980). Standardization of the Manual Differential Leukocyte Count. Laboratory Medicine, 11(6), 371–375. Retrieved from http://dx.doi.org/10.1093/labmed/11.6.371

Kohrmann, A., Kammerer, U., Kapp, M., Dietl, J., & Anacker, J. (2009). Expression of matrix metalloproteinases (MMPs) in primary human breast cancer and breast cancer cell lines: New findings and review of the literature. BMC Cancer, 9, 188. https://doi.org/10.1186/1471-2407-9-188

Kondo, E., K. Saito, Y. Tashiro, K. Kamide, S. Uno, T. Furuya, M. Mashita, K. Nakajima, T. Tsumuraya, N. Kobayashi, M. Nishibori, M. Tanimoto and M. Matsushita (2012). "Tumour lineage-homing cell-penetrating peptides as anticancer molecular delivery systems." Nat Commun3: 951.

Krug, A. K., Balmer, N. V., Matt, F., Schonenberger, F., Merhof, D., & Leist, M. (2013). Evaluation of a human neurite growth assay as specific screen for developmental neurotoxicants. Arch Toxicol, 87(12), 2215-2231.

Krug, A. K., Gutbier, S., Zhao, L., Poltl, D., Kullmann, C., Ivanova, V. . Leist, M. (2014). Transcriptional and metabolic adaptation of human neurons to the mitochondrial toxicant MPP(+). Cell Death Dis, 5, e1222.

Kubowitz F & Ott P (1943). Isolation and crystallization of a fermenting ferment from tumors. Biochemical Journal,314: 94-117.

KUMAR, V., ABBAS, A. K., FAUSTO, N. & ASTER, J. C. 2014. Robbins and Cotran pathologic basis of disease, Elsevier Health Sciences.

Labbe, C. M., Rey, J., Lagorce, D., Vavrusa, M., Becot, J., Sperandio, O., … Miteva, M. A. (2015). MTiOpenScreen: a web server for structure-based virtual screening. Nucleic Acids Research, 43(W1), W448-54. https://doi.org/10.1093/nar/gkv306

Laffon, B., N. Fernandez-Bertolez, C. Costa, E. Pasaro and V. Valdiglesias (2017). "Comparative study of human neuronal and glial cell sensitivity for in vitro neurogenotoxicity testing." Food Chem Toxicol102: 120-128.

Lakomska, I., Hoffmann, K., Wojtczak, A., Sitkowski, J., Maj, E., & Wietrzyk, J. (2014). Cytotoxic malonate platinum(II) complexes with 1,2,4-triazolo[1,5-a]pyrimidine derivatives: structural characterization and mechanism of the suppression of tumor cell growth. Journal of Inorganic Biochemistry, 141, 188–197. https://doi.org/10.1016/j.jinorgbio.2014.08.005

Lalaoui, N. and G. Brumatti (2017). "Relevance of necroptosis in cancer." Immunol Cell Biol 95(2): 137-145.

Lambert, A. W., Wong, C. K., Ozturk, S., Papageorgis, P., Raghunathan, R., Alekseyev, Y., … Thiagalingam, S. (2016). Tumor Cell-Derived Periostin Regulates Cytokines That Maintain Breast Cancer Stem Cells. Molecular Cancer Research : MCR, 14(1), 103–113. https://doi.org/10.1158/1541-7786.MCR-15-0079

Lapin, N. A., Krzykawska-Serda, M., Ware, M. J., Curley, S. A., & Corr, S. J. (2016). Intravital microscopy for evaluating tumor perfusion of nanoparticles exposed to non-invasive radiofrequency electric fields. Cancer Nanotechnology, 7, 5. http://doi.org/10.1186/s12645-016-0016-7

Lau, J. L., & Dunn, M. K. (2018). Therapeutic peptides: Historical perspectives, current development trends, and future directions. Bioorganic & Medicinal Chemistry, 26(10), 2700–2707. https://doi.org/10.1016/j.bmc.2017.06.052

Laubli, H., & Borsig, L. (2010). Selectins promote tumor metastasis. Seminars in Cancer Biology, 20(3), 169–177. https://doi.org/10.1016/j.semcancer.2010.04.005

Le Joncour, V., & Laakkonen, P. (2017). Seek & Destroy, use of targeting peptides for cancer detection and drug delivery. Bioorganic & Medicinal Chemistry. https://doi.org/https://doi.org/10.1016/j.bmc.2017.08.052

Lechner, M. G., Karimi, S. S., Barry-Holson, K., Angell, T. E., Murphy, K. A., Church, C. H., … Epstein, A. L. (2013). Immunogenicity of murine solid tumor models as a defining feature of in vivo behavior and response to immunotherapy. Journal of Immunotherapy (Hagerstown, Md. : 1997), 36(9), 477–489. https://doi.org/10.1097/01.cji.0000436722.46675.4a

Lee, S.-H., & Nam, H.-S. (2008). TNF alpha-induced down-regulation of estrogen receptor alpha in MCF-7 breast cancer cells. Molecules and Cells, 26(3), 285–290.

Lee, T.G., Jeong, E.H., Kim, S.Y., Kim, H.R., Kim, C.H. (2015). The combination ofirreversible EGFR TKIs and SAHA induces apoptosis and autophagymediated cell death to overcome acquired resistance in EGFR T790Mmutated lung cancer. Int J Cancer;136(11):2717–2729.

Leveque, D. (2014). Subcutaneous administration of anticancer agents. Anticancer Research, 34(4), 1579–1586.

Lewis, A. M., Varghese, S., Xu, H., & Alexander, H. R. (2006). Interleukin-1 and cancer progression: the emerging role of interleukin-1 receptor antagonist as a novel therapeutic agent in cancer treatment. Journal of Translational Medicine, 4, 48. https://doi.org/10.1186/1479-5876-4-48

Li, Y., H. Xiong and D. Q. Yang (2012). "Functional switching of ATM: sensor of DNA damage in proliferating cells and mediator of Akt survival signal in post-mitotic human neuron-like cells." Chin J Cancer31(8): 364-372.

Linkermann, A., & Green, D. R. (2014). Necroptosis. N Engl J Med, 370(5), 455-465.

Liu, J., Liao, S., Diop-Frimpong, B., Chen, W., Goel, S., Naxerova, K., … Xu, L. (2012). TGF-beta blockade improves the distribution and efficacy of therapeutics in breast carcinoma by normalizing the tumor stroma. Proceedings of the National Academy of Sciences of the United States of America, 109(41), 16618–16623. https://doi.org/10.1073/pnas.1117610109

Liu, Q., Zhao, H., Jiang, Y., Wu, M., Tian, Y., Wang, D., … Li, Z. (2016). Development of a lytic peptide derived from BH3-only proteins. Cell Death Discovery, 2, 16008.

Liu, Q., Zhao, H., Jiang, Y., Wu, M., Tian, Y., Wang, D.,… Li, Z. (2016). Development of a lytic peptide derived from BH3-only proteins. Cell Death Discovery, 2, 16008

Liu, S., H. Yang, L. Wan, J. Cheng and X. Lu (2013). "Penetratin-mediated delivery enhances the antitumor activity of the cationic antimicrobial peptide Magainin II." Cancer Biother Radiopharm28(4): 289-297.

Liu, S., Yang, H., Wan, L., Cai, H., Li, S., Li, Y., … Lu, X. (2011). Enhancement of cytotoxicity of antimicrobial peptide magainin II in tumor cells by bombesin-targeted delivery. Acta Pharmacologica Sinica, 32(1), 79–88. https://doi.org/10.1038/aps.2010.162

Liu, Y., L. Mei, C. Xu, Q. Yu, K. Shi, L. Zhang, Y. Wang, Q. Zhang, H. Gao, Z. Zhang and Q. He (2016). "Dual Receptor Recognizing Cell Penetrating Peptide for Selective Targeting, Efficient Intratumoral Diffusion and Synthesized Anti-Glioma Therapy." Theranostics6(2): 177-191.

Llado, V., Lopez, D.J., Ibarguren, M., M. Alonso, J.B. Soriano, P. V Escriba, Busquets, X. (2014). Regulation of the cancer cell membrane lipid composition by NaCHOleate: effects on cell signaling and therapeutical relevance in glioma., Biochim. Biophys. Acta. 1838 (5) 1619–1627. doi:10.1016/j.bbamem.2014.01.027.

Longatto Filho, A., Lopes, J. M., & Schmitt, F. C. (2010). Angiogenesis and Breast Cancer. Journal of Oncology, 2010, 576384. https://doi.org/10.1155/2010/576384

Lu, Y., T. F. Zhang, Y. Shi, H. W. Zhou, Q. Chen, B. Y. Wei, X. Wang, T. X. Yang, Y. E. Chinn, J. Kang and C. Y. Fu (2016). "PFR peptide, one of the antimicrobial peptides identified from the derivatives of lactoferrin, induces necrosis in leukemia cells." Sci Rep6: 20823.

Lu, Y., Zhang, T. F., Shi, Y., Zhou, H. W., Chen, Q., Wei, B. Y., . . . Fu, C. Y. (2016). PFR peptide, one of the antimicrobial peptides identified from the derivatives of lactoferrin, induces necrosis in leukemia cells. Sci Rep, 6, 20823.

Lu, Y., Zhang, T.-F., Shi, Y., Zhou, H.-W., Chen, Q., Wei, B.-Y., … Fu, C.-Y. (2016). PFR peptide, one of the antimicrobial peptides identified from the derivatives of lactoferrin, induces necrosis in leukemia cells. Scientific Reports, 6, 20823. https://doi.org/10.1038/srep20823

Mader, J. S., Mookherjee, N., Hancock, R. E. W., & Bleackley, R. C. (2009). The human host defense peptide LL-37 induces apoptosis in a calpain- and apoptosis-inducing factor-dependent manner involving Bax activity. Molecular Cancer Research : MCR, 7(5), 689–702. https://doi.org/10.1158/1541-7786.MCR-08-0274

Madsen, C. D., & Sahai, E. (2010). Cancer Dissemination—Lessons from Leukocytes. Developmental Cell, 19(1), 13–26. https://doi.org/https://doi.org/10.1016/j.devcel.2010.06.013

Makarov, R., et al. (2013). "Cell death in the skin: how to study its quality and quantity?" Methods Mol Biol 961: 201-218.

Mariathasan, S., Newton, K., Monack, D. M., Vucic, D., French, D. M., Lee, W. P., … Dixit, V. M. (2004). Differential activation of the inflammasome by caspase-1 adaptors ASC and Ipaf. Nature, 430, 213. Retrieved from http://dx.doi.org/10.1038/nature02664

Mariotto, A. B., Etzioni, R., Hurlbert, M., Penberthy, L., & Mayer, M. (2017). Estimation of the Number of Women Living with Metastatic Breast Cancer in the United States. Cancer Epidemiology Biomarkers & Prevention, 26(6), 809 LP-815. Retrieved from http://cebp.aacrjournals.org/content/26/6/809.abstract.

Marqus, S., Pirogova, E., & Piva, T. J. (2017). Evaluation of the use of therapeutic peptides for cancer treatment. Journal of Biomedical Science, 24, 21.

Marqus, S., Pirogova, E., & Piva, T. J. (2017). Evaluation of the use of therapeutic peptides for cancer treatment. Journal of Biomedical Science, 24(1), 21. https://doi.org/10.1186/s12929-017-0328-x

Massagué, J. (2012). TGFβ signalling in context. Nature Reviews Molecular Cell Biology, 13, 616. Retrieved from http://dx.doi.org/10.1038/nrm3434

Massodi, I. et al.( 2010). Inhibition of ovarian cancer cell proliferation by a cell cycleinhibitory peptide fused to a thermally responsive polypeptide carrier. Int J Cancer;126(2):533–44.

Matassov, D., et al. (2004). "Measurement of apoptosis by DNA fragmentation." Methods Mol Biol 282: 1-17.

Mathonnet, M., Descottes, B., Valleix, D., Labrousse, F., Truffinet, V., & Denizot, Y. (2006). Quantitative analysis using ELISA of vascular endothelial growth factor and basic fibroblast growth factor in human colorectal cancer, liver metastasis of colorectal cancer and hepatocellular carcinoma. World Journal of Gastroenterology : WJG, 12(23), 3782–3783. http://doi.org/10.3748/wjg.v12.i23.3782

McEarchern, J. A., Kobie, J. J., Mack, V., Wu, R. S., Meade-Tollin, L., Arteaga, C. L., … Akporiaye, E. T. (2001). Invasion and metastasis of a mammary tumor involves TGF-beta signaling. International Journal of Cancer, 91(1), 76–82.

Meira, D. D., Marinho-Carvalho, M. M., Teixeira, C. A., Veiga, V. F., Da Poian, A. T., Holandino, C., . . . Sola-Penna, M. (2005). Clotrimazole decreases human breast cancer cells viability through alterations in cytoskeleton-associated glycolytic enzymes. Mol Genet Metab, 84(4), 354-362.

Mellinghoff, I. K. and R. J. Gilbertson (2017). "Brain Tumors: Challenges and Opportunities to Cure." J Clin Oncol 35(21): 2343-2345.

Melo-Lima, S., Celeste Lopes, M., & Mollinedo, F. (2014). Necroptosis is associated with low procaspase-8 and active RIPK1 and -3 in human glioma cells. Oncoscience, 1(10), 649-664.

Mitri, Z., Constantine, T., & O'Regan, R. (2012). The HER2 Receptor in Breast Cancer: Pathophysiology, Clinical Use, and New Advances in Therapy. Chemotherapy Research and Practice, 2012, 743193. https://doi.org/10.1155/2012/743193

Mizushima, N., Yoshimori, T., Levine, B. (2010). Methods in mammalian autophagy research. Cell, 140(3), 313–326. https://doi.org/10.1016/j.cell.2010.01.028

Monks, A., Scudiero, D., Skehan, P., Shoemaker, R., Paull, K., Vistica, D., et al. (1991). Feasibility of a high-flux anticancer drug screen using a diverse panel of cultured human tumor cell lines. J Natl Cancer Inst, 83(11), 757-766.

Monks, A., Scudiero, D., Skehan, P., Shoemaker, R., Paull, K., Vistica, D., et al. (1991). Feasibility of a high-flux anticancer drug screen using a diverse panel of cultured human tumor cell lines. J Natl Cancer Inst, 83(11), 757-766.

Mosmann, T. (1983). Rapid colorimetric assay for cellular growth and survival: application to proliferation and cytotoxicity assays. J Immunol Methods, 65(1-2), 55-63.

Mourtada, R., Fonseca, S. B., Wisnovsky, S. P., Pereira, M. P., Wang, X., Hurren, R., Parfitt, J., Larsen, L., Smith, R. A., Murphy, M. P., Schimmer, A. D., … Kelley, S. O. (2013). Re-directing an alkylating agent to mitochondria alters drug target and cell death mechanism. PloS one, 8(4), e60253. doi:10.1371/journal.pone.0060253

Mrugala, M. M. (2013). "Advances and challenges in the treatment of glioblastoma: a clinician's perspective." Discov Med15(83): 221-230.

Mumm, J. B., Emmerich, J., Zhang, X., Chan, I., Wu, L., Mauze, S., … Oft, M. (2011). IL-10 elicits IFNgamma-dependent tumor immune surveillance. Cancer Cell, 20(6), 781–796. https://doi.org/10.1016/j.ccr.2011.11.003

Naito, T., Baba, T., Takeda, K., Sasaki, S., Nakamoto, Y., & Mukaida, N. (2015). High-dose cyclophosphamide induces specific tumor immunity with concomitant recruitment of LAMP1/CD107a-expressing CD4-positive T cells into tumor sites. Cancer Letters, 366(1), 93–99. https://doi.org/10.1016/j.canlet.2015.06.009

Nicoletti, I., Migliorati, G., Pagliacci, M. C., Grignani, F., & Riccardi, C. (1991). A rapid and simple method for measuring thymocyte apoptosis by propidium iodide staining and flow cytometry. J Immunol Methods, 139(2), 271-279.

Nicoletti, I., Migliorati, G., Pagliacci, M. C., Grignani, F., & Riccardi, C. (1991). A rapid and simple method for measuring thymocyte apoptosis by propidium iodide staining and flow cytometry. J Immunol Methods, 139(2), 271-279.

Oberoi, R. K., et al. (2016). "Strategies to improve delivery of anticancer drugs across the blood-brain barrier to treat glioblastoma." Neuro Oncol 18(1): 27-36.

Oberst, A. (2013). Autophagic cell death RIPs into tumors. Cell Death and Differentiation, 20(9), 1131– 1132.

O'Brien, J., Wilson, I., Orton, T., & Pognan, F. (2000). Investigation of the Alamar Blue (resazurin) fluorescent dye for the assessment of mammalian cell cytotoxicity. Eur J Biochem, 267(17), 5421-5426.

Oh, B., H. Song, D. Lee, J. Oh, G. Kim, S. H. Ihm and M. Lee (2017). "Anti-cancer effect of R3V6 peptide-mediated delivery of an anti-microRNA-21 antisense-oligodeoxynucleotide in a glioblastoma animal model." J Drug Target25 (2): 132-139.

Ohtake, J., Ohkuri, T., Togashi, Y., Kitamura, H., Okuno, K., & Nishimura, T. (2014). Identification of novel helper epitope peptides of Survivin cancer-associated antigen applicable to developing helper/killer-hybrid epitope long peptide cancer vaccine. Immunology Letters, 161(1), 20–30. https://doi.org/https://doi.org/10.1016/j.imlet.2014.04.010

Ojha, R., Bhattacharyya, S., & Singh, S. K. (2015). Autophagy in Cancer Stem Cells: A Potential Link between Chemoresistance, Recurrence, and Metastasis. Biores Open Access, 4(1), 97-108.

Oliveira-Lima, O. C., Bernardes, D., Xavier Pinto, M. C., Esteves Arantes, R. M., & Carvalho-Tavares, J. (2013). Mice lacking inducible nitric oxide synthase develop exacerbated hepatic inflammatory responses induced by Plasmodium berghei NK65 infection. Microbes and Infection, 15(13), 903–910. https://doi.org/10.1016/j.micinf.2013.08.001

Oliveira-Lima, O. C., Pinto, M. C. X., Duchene, J., Qadri, F., Souza, L. L., Alenina, N., … Carvalho-Tavares, J. (2015). Mas receptor deficiency exacerbates lipopolysaccharide-induced cerebral and systemic inflammation in mice. Immunobiology, 220(12), 1311–1321. https://doi.org/10.1016/j.imbio.2015.07.013

Ousingsawat, J., Cabrita, I., Wanitchakool, P., Sirianant, L., Krautwald, S., Linkermann, A., Kunzelmann, K. (2017). Ca2+ signals, cell membrane disintegration, and activation of TMEM16F during necroptosis. Cell Mol Life Sci, 74(1), 173-181.

Ozkok, A., K. Ravichandran, Q. Wang, D. Ljubanovic and C. L. Edelstein (2016). "NF-kappaB transcriptional inhibition ameliorates cisplatin-induced acute kidney injury (AKI)." Toxicol Lett240 (1): 105-113.

Palomba, R., Parodi, A., Evangelopoulos, M., Acciardo, S., Corbo, C., de Rosa, E., … Tasciotti, E. (2016). Biomimetic carriers mimicking leukocyte plasma membrane to increase tumor

vasculature permeability. Scientific Reports, 6, 34422. Retrieved from http://dx.doi.org/10.1038/srep34422

Pane, K., Durante, L., Crescenzi, O., Cafaro, V., Pizzo, E., Varcamonti, M., . . . Notomista, E. (2017). Antimicrobial potency of cationic antimicrobial peptides can be predicted from their amino acid composition: Application to the detection of "cryptic" antimicrobial peptides. J Theor Biol, 419, 254-265.

Papo, N. and Y. Shai (2003). "New lytic peptides based on the D, L-amphipathic helix motif preferentially kill tumor cells compared to normal cells." Biochemistry 42(31): 9346-9354. Pasparakis, M. and P. Vandenabeele (2015). "Necroptosis and its role in inflammation." Nature 517(7534): 311-320.

Papo, N., D. Seger, A. Makovitzki, V. Kalchenko, Z. Eshhar, H. Degani and Y. Shai (2006). "Inhibition of tumor growth and elimination of multiple metastases in human prostate and breast xenografts by systemic inoculation of a host defense-like lytic peptide." Cancer Res66 (10): 5371-5378.

Paschall, A. V, & Liu, K. (2016). An Orthotopic Mouse Model of Spontaneous Breast Cancer Metastasis. Journal of Visualized Experiments: JoVE, (114), 10.3791/54040. https://doi.org/10.3791/54040

Paschall, A. V, & Liu, K. (2016). An Orthotopic Mouse Model of Spontaneous Breast Cancer Metastasis. Journal of Visualized Experiments : JoVE, (114), 10.3791/54040. https://doi.org/10.3791/54040

Pennarun, B., Gaidos, G., Bucur, O., Tinari, A., Rupasinghe, C., Jin, T., Khosravi-Far, R. (2013). KillerFLIP: a novel lytic peptide specifically inducing cancer cell death. Cell Death & Disease, 4(10), e894.

Pereira, A., Kerkis, A., Hayashi, M. A. F., Pereira, A. S. P., Silva, F. S., Oliveira, E. B., … Kerkis, I. (2011). Crotamine toxicity and efficacy in mouse models of melanoma. Expert Opinion on Investigational Drugs, 20(9), 1189–1200. https://doi.org/10.1517/13543784.2011.602064

Perez-Pitarch, A., Guglieri-Lopez, B., A. Nacher, V. Merino, Merino-Sanjuan, M. (2017). Impact of Undernutrition on the Pharmacokinetics and Pharmacodynamics of Anticancer Drugs: A Literature Review., Nutr. Cancer. 69 (10) 555–563. doi:10.1080/01635581.2017.1299878.

Pietkiewicz, S., et al. (2015). "Quantification of apoptosis and necroptosis at the single cell level by a combination of Imaging Flow Cytometry with classical Annexin V/propidium iodide staining." J Immunol Methods 423: 99-103.

Pietras, K., & Östman, A. (2010). Hallmarks of cancer: Interactions with the tumor stroma. Experimental Cell Research, 316(8), 1324–1331. https://doi.org/https://doi.org/10.1016/j.yexcr.2010.02.045

Pillai, R. K. and K. Jayasree (2017). "Rare cancers: Challenges & issues." Indian J Med Res145(1): 17-27.

Poltl, D., Schildknecht, S., Karreman, C., & Leist, M. (2012). Uncoupling of ATP-depletion and cell death in human dopaminergic neurons. Neurotoxicology, 33(4), 769-779.

Ponnusamy, L., Mahalingaiah, P. K. S., & Singh, K. P. (2016). Chronic Oxidative Stress Increases Resistance to Doxorubicin-Induced Cytotoxicity in Renal Carcinoma Cells Potentially Through Epigenetic Mechanism. Molecular Pharmacology, 89(1), 27–41. https://doi.org/10.1124/mol.115.100206

Poon, I., A. A. Baxter, F. T. Lay, G. D. Mills, C. G. Adda, J. A. Payne, T. K. Phan, G. F. Ryan, J. A. White, P. K. Veneer, N. L. van der Weerden, M. A. Anderson, M. Kvansakul and M. D. Hulett (2014). "Phosphoinositide-mediated oligomerization of a defensin induces cell lysis." Elife3: e01808.

Prasad, S., Mathur, A., Sharma, R. (2006). Octapeptide Analogs of Somatostatin Containing α,α-Dialkylated Amino Acids with Potent Anticancer Activity. Int J Pept Res Ther, 12(179). https://doi.org/10.1007/s10989-005-9005-0

Puduvalli, V. K., R. Chaudhary, S. G. McClugage and J. Markert (2017). "Beyond Alkylating Agents for Gliomas: Quo Vadimus?" Am Soc Clin Oncol Educ Book37: 175-186.

Pulaski, B. A., & Ostrand-Rosenberg, S. (2001). Mouse 4T1 breast tumor model. Current Protocols in Immunology, Chapter 20, Unit 20.2.https://doi.org/10.1002/0471142735.im2002s39

Radisky, E. S., & Radisky, D. C. (2015). Matrix metalloproteinases as breast cancer drivers and therapeutic targets. Frontiers in Bioscience (Landmark Edition).

Rafehi, H., Orlowski, C., Georgiadis, G. T., Ververis, K., El-Osta, A., & Karagiannis, T. C. (2011). Clonogenic Assay: Adherent Cells. Journal of Visualized Experiments : JoVE, (49), 2573. Advance online publication. http://doi.org/10.3791/2573

Ramalingayya, G. V., S. P. Cheruku, P. G. Nayak, A. Kishore, R. Shenoy, C. M. Rao and N. Krishnadas (2017). "Rutin protects against neuronal damage in vitro and ameliorates doxorubicin-induced memory deficits in vivo in Wistar rats." Drug Des Devel Ther11: 1011-1026.

Rasul, R., G. Harper, M., & Rajaram, N. (2018). Intravital imaging of tumor bioenergetics in metastatic and nonmetastatic breast cancer. https://doi.org/10.1117/12.2289621

Ravelli, A., Roviello, G., Cretella, D., Cavazzoni, A., Biondi, A., Cappelletti, M. R., … Generali, D. (2017). Tumor-infiltrating lymphocytes and breast cancer: Beyond the prognostic and predictive utility. Tumor Biology, 39(4), 1010428317695023. https://doi.org/10.1177/1010428317695023

Reinhardt, A. and I. Neundorf (2016). "Design and Application of Antimicrobial Peptide Conjugates." Int J Mol Sci17(5).

Reis, D., Maria de Souza, C., Cunha Campos, L., Silva, A., paz lopes, M., Cassali, G., & Ferreira, E. (2014). Thalidomide promotes leukocytosis in mice inoculated with 4T1 mammary carcinoma. Jornal Brasileiro de Patologia e Medicina Laboratorial (Vol. 50). https://doi.org/10.1590/S1676-24442014000100009

REIS, P. V. M. D. (2015). Peptídeos sintéticos antimicrobianos, derivados da Toxina LyeTx I da peçonha da aranha Lycosa erithrognatha. Master UNIVERSIDADE FEDERAL DE MINAS GERAIS.

Reis, P. V. M., Boff, D., Verly, R. M., Melo-Braga, M. N., Cortés, M. E., Santos, D. M., … de Lima, M. E. (2018). LyeTxI-b, a Synthetic Peptide Derived From Lycosa erythrognatha Spider Venom, Shows Potent Antibiotic Activity in Vitro and in Vivo. Frontiers in Microbiology, 9, 667. https://doi.org/10.3389/fmicb.2018.00667

Ren, S. X., Shen, J., Cheng, A. S. L., Lu, L., Chan, R. L. Y., Li, Z. J., … Cho, C. H. (2013). FK-16 Derived from the Anticancer Peptide LL-37 Induces Caspase-Independent Apoptosis and Autophagic Cell Death in Colon Cancer Cells. PLoS ONE, 8(5), e63641.

Repsold, L., et al. (2017). "An overview of the role of platelets in angiogenesis, apoptosis and autophagy in chronic myeloid leukaemia." Cancer Cell Int 17: 89.

Richter, W. F., Bhansali, S. G., & Morris, M. E. (2012). Mechanistic determinants of biotherapeutics absorption following SC administration. The AAPS Journal, 14(3), 559–570. https://doi.org/10.1208/s12248-012-9367-0

Riedl, S., D. Zweytick and K. Lohner (2011). "Membrane-active host defense peptides--challenges and perspectives for the development of novel anticancer drugs." Chem Phys Lipids164 (8): 766-781.

Rivera, E., & Gomez, H. (2010). Chemotherapy resistance in metastatic breast cancer: the evolving role of ixabepilone. Breast Cancer Research: BCR, 12 Suppl 2, S2. https://doi.org/10.1186/bcr2573.

Rivera-Franco, M. M., & Leon-Rodriguez, E. (2018). Delays in Breast Cancer Detection and Treatment in Developing Countries. Breast Cancer : Basic and Clinical Research, 12, 1178223417752677. http://doi.org/10.1177/1178223417752677

Rizvi, W., Truong, P., & Truong, Q. (2017). Metastatic Breast Cancer with BRCA Mutation Discovered By Next-Generation Sequencing Responding to Olaparib. Cureus, 9(6), e1337. doi:10.7759/cureus.1337

Rogers, Kara, ed. (2011), "Leukocytosis definition", Blood: Physiology and Circulation, Chicago: Britannica Educational Publishing, p. 198, ISBN 978-1-61530-250-5, retrieved 12 November 2011

Rooj, A.K., McNicholas, C.M., R. Bartoszewski, Z. Bebok, D.J. Benos, Fuller, C.M (2012). Glioma-specific cation conductance regulates migration and cell cycle progression., J. Biol. Chem. 287 (8) 4053–4065. doi:10.1074/jbc.M111.311688.

Sah, N. K., Khan, Z., Khan, G. J., & Bisen, P. S. (2018). Structural, functional and therapeutic biology of survivin. Cancer Letters, 244(2), 164–171. https://doi.org/10.1016/j.canlet.2006.03.007

Sa-nguanraksa, D., & O-charoenrat, P. (2012). The Role of Vascular Endothelial Growth Factor A Polymorphisms in Breast Cancer. International Journal of Molecular Sciences, 13(11), 14845–14864. https://doi.org/10.3390/ijms131114845

Santos, D. M., R. M. Verly, D. Pilo-Veloso, M. de Maria, M. A. de Carvalho, P. S. Cisalpino, B. M. Soares, C. G. Diniz, L. M. Farias, D. F. Moreira, F. Frezard, M. P. Bemquerer, A. M. Pimenta and M. E. de Lima (2010). "LyeTx I, a potent antimicrobial peptide from the venom of the spider Lycosa erythrognatha." Amino Acids39 (1): 135-144.

Santos, E., Cunha de Oliveira, D., Hastreiter, A., Batista da Silva, G., Beltran, J., Tsujita, M., … Borelli, P. (2016). Hematological and biochemical reference values for C57BL/6, Swiss Webster and BALB/c mice. Brazilian Journal of Veterinary Research and Animal Science (Vol. 53). https://doi.org/10.11606/issn.1678-4456.v53i2p138-145

Sasi, S. P., Bae, S., Song, J., Perepletchikov, A., Schneider, D., Carrozza, J., … Goukassian, D. A. (2014). Therapeutic non-toxic doses of TNF induce significant regression in TNFR2-p75 knockdown Lewis lung carcinoma tumor implants. PloS One, 9(3), e92373. https://doi.org/10.1371/journal.pone.0092373

Sasser, A. K., Sullivan, N. J., Studebaker, A. W., Hendey, L. F., Axel, A. E., & Hall, B. M. (2007). Interleukin-6 is a potent growth factor for ER-alpha-positive human breast cancer. FASEB Journal : Official Publication of the Federation of American Societies for Experimental Biology, 21(13), 3763–3770. https://doi.org/10.1096/fj.07-8832com

Sato, H., & Feix, J. B. (2006). Peptide-membrane interactions and mechanisms of membrane destruction by amphipathic alpha-helical antimicrobial peptides. Biochim Biophys Acta, 1758(9), 12451256. doi:10.1016/j.bbamem.2006.02.021

Schildknecht, S., Poltl, D., Nagel, D. M., Matt, F., Scholz, D., Lotharius, J. Leist, M. (2009). Requirement of a dopaminergic neuronal phenotype for toxicity of low concentrations of 1methyl-4-phenylpyridinium to human cells. Toxicol Appl Pharmacol, 241(1), 23-35.

Schneble, E., Jinga, D.-C., & Peoples, G. (2015). Breast Cancer Immunotherapy. Mædica, 10(2), 185–191. Retrieved from http://www.ncbi.nlm.nih.gov/pmc/articles/PMC5327815/

Schrijver, W. A. M. E., Suijkerbuijk, K. P. M., van Gils, C. H., van der Wall, E., Moelans, C. B., & van Diest, P. J. (2018). Receptor Conversion in Distant Breast Cancer Metastases: A Systematic Review and Meta-analysis. Journal of the National Cancer Institute. https://doi.org/10.1093/jnci/djx273

Schweizer, F. (2009). "Cationic amphiphilic peptides with cancer-selective toxicity." Eur J Pharmacol625(1-3): 190-194.

Shand, F. H. W., Ueha, S., Otsuji, M., Koid, S. S., Shichino, S., Tsukui, T., … Matsushima, K. (2014). Tracking of intertissue migration reveals the origins of tumor-infiltrating monocytes. Proceedings of the National Academy of Sciences of the United States of America, 111(21), 7771–7776. https://doi.org/10.1073/pnas.1402914111

Sheikhpour, E., Noorbakhsh, P., Foroughi, E., Farahnak, S., Nasiri, R., & Neamatzadeh, H. (2018). A Survey on the Role of Interleukin-10 in Breast Cancer: A Narrative. Reports of Biochemistry & Molecular Biology, 7(1), 30–37. Retrieved from https://www.ncbi.nlm.nih.gov/pubmed/30324115

Sheng, Y., Li, F., & Qin, Z. (2018). TNF Receptor 2 Makes Tumor Necrosis Factor a Friend of Tumors. Frontiers in Immunology, 9, 1170. https://doi.org/10.3389/fimmu.2018.01170

Shrihari, T. G. (2017). Dual role of inflammatory mediators in cancer. Ecancermedicalscience, 11, 721. https://doi.org/10.3332/ecancer.2017.721

Simon LP. Viable cell counting using trypan blue, Cancer cell culture methods and Protocols. Simon P, editor. Langdon: Humana press; 2004. pp. 26.

Souza, C. M. de, Gamba, C. de O., Campos, C. B. de, Lopes, M. T. P., Ferreira, M. A. N. D., Andrade, S. P., & Cassali, G. D. (2013). Carboplatin delays mammary cancer 4T1 growth in mice. Pathology, Research and Practice, 209(1), 24–29. https://doi.org/10.1016/j.prp.2012.10.003

Standish, L. J., Sweet, E. S., Novack, J., Wenner, C. A., Bridge, C., Nelson, A., … Torkelson, C. (2008). Breast Cancer and the Immune System. Journal of the Society for Integrative Oncology, 6(4), 158–168. Retrieved from http://www.ncbi.nlm.nih.gov/pmc/articles/PMC2845458/

Stewart, T. J., & Abrams, S. I. (2008). How tumours escape mass destruction. Oncogene, 27(45), 5894–5903. https://doi.org/10.1038/onc.2008.268

Stiegler, N. V., Krug, A. K., Matt, F., & Leist, M. (2011). Assessment of chemical-induced impairment of human neurite outgrowth by multiparametric live cell imaging in high-density cultures. Toxicol Sci, 121(1), 73-87.

Stojanovska, V., McQuade, R. M., Fraser, S., Prakash, M., Gondalia, S., Stavely, R., … Nurgali, K. (2018). Oxaliplatin-induced changes in microbiota, TLR4+ cells and enhanced HMGB1 expression in the murine colon. PloS One, 13(6), e0198359. https://doi.org/10.1371/journal.pone.0198359

Strell, C., & Entschladen, F. (2008). Extravasation of leukocytes in comparison to tumor cells. Cell Communication and Signaling : CCS, 6, 10. https://doi.org/10.1186/1478-811X-6-10

Strell, C., & Entschladen, F. (2008). Extravasation of leukocytes in comparison to tumor cells. Cell Communication and Signaling : CCS, 6, 10. https://doi.org/10.1186/1478-811X-6-10

Su, Z., Yang, Z., Xie, L., DeWitt, J. P., & Chen, Y. (2016). Cancer therapy in the necroptosis era. Cell Death and Differentiation, 23(5), 748–756. https://doi.org/10.1038/cdd.2016.8

Sullivan, N. J., Sasser, A. K., Axel, A. E., Vesuna, F., Raman, V., Ramirez, N., … Hall, B. M. (2009). Interleukin-6 induces an epithelial-mesenchymal transition phenotype in human breast cancer cells. Oncogene, 28(33), 2940–2947. https://doi.org/10.1038/onc.2009.180

Sun, W., et al. (2016). "2-Methoxy-6-acetyl-7-methyljuglone (MAM), a natural naphthoquinone, induces NO-dependent apoptosis and necroptosis by H2O2-dependent JNK activation in cancer cells." Free Radic Biol Med 92: 61-77.

Sun, Y., Zhai, L., Ma, S., Zhang, C., Zhao, L., Li, N., Zhao, X. (2018). Down-regulation of RIP3 potentiates cisplatin chemoresistance by triggering HSP90-ERK pathway mediated DNA repair in esophageal squamous cell carcinoma. Cancer Letters. https://doi.org/10.1016/j.canlet.2018.01.022

Sung, J. H., Yu, J., Luo, D., Shuler, M. L., & March, J. C. (2011). Microscale 3-D hydrogel scaffold for biomimetic gastrointestinal (GI) tract model. Lab Chip, 11(3), 389-392.

Suryadinata, R. Sadowski. M. Sarcevic, B. (2010). Control of cell cycle progression byphosphorylation of cyclin-dependent kinase (CDK) substrates. Biosci Rep.; 30(4):243–55.

Swartz, A.M., et al. (2015). Peptide vaccines for the treatment of glioblastoma. J Neurooncol,: 123(3): p. 433-40.

Szalayova, G., Ogrodnik, A., Spencer, B., Wade, J., Bunn, J., Ambaye, A., … Rincon, M. (2016). Human breast cancer biopsies induce eosinophil recruitment and enhance adjacent cancer cell proliferation. Breast Cancer Research and Treatment, 157(3), 461–474. https://doi.org/10.1007/s10549-016-3839-3

Szczepanski C, Tenstad O, Baumann A, Martinez A, Myklebust R, Bjerkvig R et al.(2014).“Identification of a novel lytic peptide for the treatment of solid tumours”. GenesCancer; 5: 186–200.

Szczepanski, C., Tenstad, O., Baumann, A., Martinez, A., Myklebust, R., Bjerkvig, R., & Prestegarden, L. (2014). Identification of a novel lytic peptide for the treatment of solid tumours. Genes & Cancer, 5(5–6), 186–200.

Tan, H., et al. (2017). "Spider Toxin Peptide Lycosin-I Functionalized Gold Nanoparticles for in vivo Tumor Targeting and Therapy." Theranostics 7(12): 3168-3178.

Tao, K., Fang, M., Alroy, J., & Sahagian, G. G. (2008). Imagable 4T1 model for the study of late stage breast cancer. BMC Cancer, 8, 228. https://doi.org/10.1186/1471-2407-8-228

Taylor, T. E., F. B. Furnari and W. K. Cavenee (2012). "Targeting EGFR for treatment of glioblastoma: molecular basis to overcome resistance." Curr Cancer Drug Targets12 (3): 197-209.

Thompson, R.F., Walker, M., Siebert, C.A., et al (2016) An introduction to sample preparation and imaging by cryo-electron microscopy for structural biology. Methods (San Diego, Calif) 100:3–15. doi: 10.1016/j.ymeth.2016.02.017

Tian, F., et al. (2016). "5-Aminolevulinic Acid-Mediated Sonodynamic Therapy Inhibits RIPK1/RIPK3Dependent Necroptosis in THP-1-Derived Foam Cells." Sci Rep 6: 21992.

Tian, K. Ruiming, Z. & Xia, W. (2017). Association of interleukin-10 polymorphisms and haplotypes with the risk of breast cancer in northern China. Int J Clin Exp Pathol, 10(6), 6989–6996.

Tjensvoll, K., Oltedal, S., Heikkila, R., Kvaloy, J. T., Gilje, B., Reuben, J. M.… Nordgard, O. (2012). Persistent tumor cells in bone marrow of non-metastatic breast cancer patients after primary surgery are associated with inferior outcome. BMC Cancer, 12, 190. https://doi.org/10.1186/1471-2407-12-190

Tong, Z.-B., Hogberg, H., D. Kuo, S. Sakamuru, M .Xia, L.Smirnova, Gerhold, D. (2017). Characterization of three human cell line models for high-throughput neuronal cytotoxicity screening. Journal of Applied Toxicology, JAT, 37(2), 167–180. doi.org/10.1002/jat.3334

Tran, S.-L., Puhar, A., Ngo-Camus, M., & Ramarao, N. (2011). Trypan Blue Dye Enters Viable Cells Incubated with the Pore-Forming Toxin HlyII of Bacillus cereus. PLoS ONE, 6(9), e22876. https://doi.org/10.1371/journal.pone.0022876

Udi, Y., Fragai, M., Grossman, M., Mitternacht, S., Arad-Yellin, R., Calderone, V., … Sagi, I. (2013). Unraveling hidden regulatory sites in structurally homologous metalloproteases. Journal of Molecular Biology, 425(13), 2330–2346. https://doi.org/10.1016/j.jmb.2013.04.009

Uhm, T. G., Kim, B. S., & Chung, I. Y. (2012). Eosinophil Development, Regulation of Eosinophil-Specific Genes, and Role of Eosinophils in the Pathogenesis of Asthma. Allergy Asthma Immunol Res, 4(2), 68–79. Retrieved from http://synapse.koreamed.org/DOIx.php?id=10.4168%2Faair.2012.4.2.68

Vaidya, J. S., Massarut, S., Vaidya, H. J., Alexander, E. C., Richards, T., Caris, J. A., … Tobias, J. S. (2018). Rethinking neoadjuvant chemotherapy for breast cancer. BMJ, 360. Retrieved from http://www.bmj.com/content/360/bmj.j5913.abstract

Van de Ven, A. L., Kim, P., Ferrari, M., & Yun, S. H. (2013). Real-time intravital microscopy of individual nanoparticle dynamics in liver and tumors of live mice. Protocol Exchange, 2013. https://doi.org/10.1038/protex.2013.049

Van Keymeulen, A., Lee, M. Y., Ousset, M., Brohee, S., Rorive, S., Giraddi, R. R. … Blanpain, C. (2015). Reactivation of multipotency by oncogenic PIK3CA induces breast tumour heterogeneity. Nature, 525(7567), 119–123. https://doi.org/10.1038/nature14665

Van Lint, P., & Libert, C. (2007). Chemokine and cytokine processing by matrix metalloproteinases and its effect on leukocyte migration and inflammation. Journal of Leukocyte Biology, 82(6), 1375–1381. https://doi.org/10.1189/jlb.0607338

Van Tellingen, O., B. Yetkin-Arik, M. C. de Gooijer, P. Wesseling, T. Wurdinger and H. E. de Vries (2015). "Overcoming the blood–brain tumor barrier for effective glioblastoma treatment." Drug Resistance Updates19: 1-12.

Vanden Berghe, T., et al. (2010). "Necroptosis, necrosis and secondary necrosis converge on similar cellular disintegration features." Cell Death Differ 17(6): 922-930.

Vandenabeele P, Galluzzi L, Vanden Berghe T, Kroemer G. (2010). Molecular mechanisms of necroptosis: an ordered cellular explosion. Nat Rev Mol Cell Biol.; 11(10):700–714.

Venturi, G. M., Tu, L., Kadono, T., Khan, A. I., Fujimoto, Y., Oshel, P., … Tedder, T. F. (2003). Leukocyte migration is regulated by L-selectin endoproteolytic release. Immunity, 19(5), 713–724.

Verano-Braga, T., Figueiredo-Rezende, F., Melo, M.N., R.Q. Lautner, E.R.M. Gomes, L.T. Mata-Machado, A. Murari, C. Rocha-Resende, M. Elena de Lima, S. Guatimosim, R.A.S. Santos, Pimenta, A.M.C. (2010). Structure-function studies of Tityus serrulatus Hypotensin-I (TsHpt-I): A new agonist of B(2) kinin receptor., Toxicon., (56)1162–1171. doi:10.1016/j.toxicon.2010.04.006.

Verma, S., Miles, D., Gianni, L., Krop, I. E., Welslau, M., Baselga, J., … Group, for the E. S. (2012). Trastuzumab Emtansine for HER2-Positive Advanced Breast Cancer. The New England Journal of Medicine, 367(19), 1783–1791. https://doi.org/10.1056/NEJMoa1209124

Verstappen, C. C., J. J. Heimans, K. Hoekman and T. J. Postma (2003). "Neurotoxic complications of chemotherapy in patients with cancer: clinical signs and optimal management." Drugs63(15): 1549-1563.

Volk-Draper, L., Hall, K., Griggs, C., Rajput, S., Kohio, P., DeNardo, D., & Ran, S. (2014). Paclitaxel therapy promotes breast cancer metastasis in a TLR4-dependent manner. Cancer Research, 74(19), 5421–5434. https://doi.org/10.1158/0008-5472.CAN-14-0067

Vonderheide, R. H., Domchek, S. M., & Clark, A. S. (2017). Immunotherapy for breast cancer: what are we missing? Clinical Cancer Research : An Official Journal of the American Association for Cancer Research, 23(11), 2640–2646. https://doi.org/10.1158/1078-0432.CCR-16-2569

Walker II, W. H., Borniger, J. C., Surbhi, Zalenski, A. A., Muscarella, S. L., Fitzgerald, J. A., … DeVries, A. C. (2017). Mammary Tumors Induce Central Pro-inflammatory Cytokine Expression, but Not Behavioral Deficits in Balb/C Mice. Scientific Reports, 7, 8152. https://doi.org/10.1038/s41598-017-07596-9

Wallberg, F., et al. (2016). "Analysis of Apoptosis and Necroptosis by Fluorescence-Activated Cell Sorting." Cold Spring Harb Protoc 2016(4): pdb.prot087387.

Wallberg, F., et al. (2016). "Analysis of Apoptosis and Necroptosis by Fluorescence-Activated Cell Sorting." Cold Spring Harb Protoc 2016(4): pdb.prot087387.

Wang, C., Dong, S., Zhang, L., Zhao, Y., Huang, L., Gong, X., … Shang, D. (2017). Cell surface binding, uptaking and anticancer activity of L-K6, a lysine/leucine-rich peptide, on human breast cancer MCF-7 cells. Scientific Reports, 7(1), 8293. https://doi.org/10.1038/s41598-017-08963-2

Wang, C., Tian, L.-L., Li, S., Li, H.-B., Zhou, Y., Wang, H. Shang, D.-J. (2013). Rapid Cytotoxicity of Antimicrobial Peptide Tempoprin-1CEa in Breast Cancer Cells through Membrane Destruction and Intracellular Calcium Mechanism. PLoS ONE, 8(4), e60462.

Wang, C., Tian, L.-L., Li, S., Li, H.-B., Zhou, Y., Wang, H., … Shang, D.-J. (2013). Rapid cytotoxicity of antimicrobial peptide tempoprin-1CEa in breast cancer cells through membrane destruction and intracellular calcium mechanism. PloS One, 8(4), e60462. https://doi.org/10.1371/journal.pone.0060462

Wang, S., Zhang, H., Cheng, L., Evans, C., & Pan, C.-X. (2010). Analysis of the cytotoxic activity of carboplatin and gemcitabine combination. Anticancer Research, 30(11), 4573–4578.

Wang, X. and Z. Guo (2015). "Chlorotoxin-conjugated onconase as a potential anti-glioma drug." Oncol Lett 9(3): 1337-1342.

Wang, Y., et al. (2017). "MicroRNA-613 is downregulated in HCMV-positive glioblastoma and inhibits tumour progression by targeting arginase-2." Tumour Biol 39(7): 1010428317712512.

Wang, Y., Wang, L., Yang, H., Xiao, H., Farooq, A., Liu, Z., Shi, X. (2016). The Spider Venom Peptide Lycosin-II Has Potent Antimicrobial Activity against Clinically Isolated Bacteria. Toxins, 8(5), 119.

Wanjale, M. V. and G. S. Kumar (2016). "Peptides as a therapeutic avenue for nanocarrier-aided targeting of glioma." Expert Opin Drug Deliv.

Ward, R., Sims, A. H., Lee, A., Lo, C., Wynne, L., Yusuf, H., … Lamb, R. (2015). Monocytes and macrophages, implications for breast cancer migration and stem cell-like activity and treatment. Oncotarget, 6(16), 14687–14699. Retrieved from http://www.ncbi.nlm.nih.gov/pmc/articles/PMC4546497/

Watt, H. L., Kharmate, G., & Kumar, U. (2008). Biology of somatostatin in breast cancer. Molecular and Cellular Endocrinology, 286(1), 251–261. https://doi.org/https://doi.org/10.1016/j.mce.2008.01.006

Wei, J. W., J. Q. Cai, C. Fang, Y. L. Tan, K. Huang, C. Yang, Q. Chen, C. L. Jiang and C. S. Kang (2017). "Signal Peptide Peptidase, Encoded by HM13, Contributes to Tumor Progression by Affecting EGFRvIII Secretion Profiles in Glioblastoma." CNS Neurosci Ther 23(3): 257-265.

Weingart, S. N., Zhang, L., Sweeney, M., & Hassett, M. (2018). Chemotherapy medication errors. The Lancet Oncology, 19(4), e191–e199. https://doi.org/10.1016/S1470-2045(18)30094-9

Wlodkowic, D., Skommer, J., & Darzynkiewicz, Z. (2011). Rapid quantification of cell viability and apoptosis in B-cell lymphoma cultures using cyanine SYTO probes. Methods Mol Biol, 740, 81-89.

Xiao, Z., S. L. Morris-Natschke and K. H. Lee (2016). "Strategies for the Optimization of Natural Leads to Anticancer Drugs or Drug Candidates." Med Res Rev 36(1): 32-91.

Xie, F., Ling, L., van Dam, H., Zhou, F., & Zhang, L. (2018). TGF-beta signaling in cancer metastasis. Acta Biochimica et Biophysica Sinica, 50(1), 121–132.m https://doi.org/10.1093/abbs/gmx123

Xu, B., et al. (2017). "Matrine induces RIP3-dependent necroptosis in cholangiocarcinoma cells." Cell Death Discov 3: 16096.

Yang, L., T. Horibe, M. Kohno, M. Haramoto, K. Ohara, R. K. Puri and K. Kawakami (2012). "Targeting interleukin-4 receptor alpha with hybrid peptide for effective cancer therapy." Mol Cancer Ther 11(1): 235-243.

Yang, M. and C. Moon (2013). "Neurotoxicity of cancer chemotherapy." Neural Regen Res 8(17): 16061614.

Yang, M., J. Kim, S. H. Kim, J. S. Kim, T. Shin and C. Moon (2012). "Temporal profiles of synaptic plasticity-related signals in adult mouse hippocampus with methotrexate treatment." Neural Regen Res 7(21): 1651-1658.

Yang, M., J. S. Kim, J. Kim, S. H. Kim, J. C. Kim, J. Kim, H. Wang, T. Shin and C. Moon (2011). "Neurotoxicity of methotrexate to hippocampal cells in vivo and in vitro." Biochem Pharmacol 82(1): 72-80.

Yin, X., Wolford, C. C., Chang, Y.-S., McConoughey, S. J., Ramsey, S. A., Aderem, A., & Hai, T. (2010). ATF3, an adaptive-response gene, enhances TGF{beta} signaling and cancer-initiating cell features in breast cancer cells. Journal of Cell Science, 123(Pt 20), 3558–3565. https://doi.org/10.1242/jcs.064915

Yoon, S., Bogdanov, K., Kovalenko, A., & Wallach, D. (2016). Necroptosis is preceded by nuclear translocation of the signaling proteins that induce it. Cell Death and Differentiation, 23(2), 253–260.

Yu, T., Malugin, A., & Ghandehari, H. (2011). Impact of silica nanoparticle design on cellular toxicity and hemolytic activity. ACS Nano, 5(7), 5717-5728.

Zabeo, D., Cvjetkovic. A., Lässer, C., et al (2017) Exosomes purified from a single cell type have diverse morphology. Journal of Extracellular Vesicles 6:1329476. doi: 10.1080/20013078.2017.1329476.

Zhang, H., Lu, H., Xiang, L., Bullen, J. W., Zhang, C., Samanta, D.,… Semenza, G. L. (2015). HIF-1 regulates CD47 expression in breast cancer cells to promote evasion of phagocytosis and maintenance of cancer stem cells. Proceedings of the National Academy of Sciences of the United States of America, 112(45), E6215–E6223. https://doi.org/10.1073/pnas.1520032112

Zhang, L., Blackwell, K., Workman, L.M., et al. (2015). RIP1 cleavage in the kinase domain regulates TRAIL-induced NF-kappaB activation and lymphoma survival. Mol Cell Biol. ;35(19):3324– 3338.

ZHANG, M. E. I. H., MAN, H. T. A. O., ZHAO, X. D. A. N., DONG, N. I., & MA, S. H. I. L. (2014). Estrogen receptor-positive breast cancer molecular signatures and therapeutic potentials (Review). Biomedical Reports, 2(1), 41–52. https://doi.org/10.3892/br.2013.187

Zhang, M., Lee, A. V, & Rosen, J. M. (2017). The Cellular Origin and Evolution of Breast Cancer. Cold Spring Harbor Perspectives in Medicine, 7(3), a027128. https://doi.org/10.1101/cshperspect.a027128

Zhang, W., J. Li, L. W. Liu, K. R. Wang, J. J. Song, J. X. Yan, Z. Y. Li, B. Z. Zhang and R. Wang (2010). "A novel analog of antimicrobial peptide Polybia-MPI, with thioamide bond substitution, exhibits increased therapeutic efficacy against cancer and diminished toxicity in mice." Peptides 31(10): 1832-1838.

Zhang, X.-Y., & Lu, W.-Y. (2014). Recent advances in lymphatic targeted drug delivery system for tumor metastasis. Cancer Biology & Medicine, 11(4), 247–254. https://doi.org/10.7497/j.issn.2095-3941.2014.04.003

Zhao, H., et al. (2016). "Pristimerin triggers AIF-dependent programmed necrosis in glioma cells via activation of JNK." Cancer Lett 374(1): 136-148.

Zheng, C., C. Ma, E. Bai, K. Yang and R. Xu (2015). "Transferrin and cell-penetrating peptide dualfunctioned liposome for targeted drug delivery to glioma." Int J Clin Exp Med 8(2): 1658-1668.

Zhou, H., Forveille, S., Sauvat, A., Yamazaki, T., Senovilla, L., Ma, Y., … Kroemer, G. (2016). The oncolytic peptide LTX-315 triggers immunogenic cell death. Cell Death & Disease, 7, e2134. https://doi.org/10.1038/cddis.2016.47

Zhu, C., Martinez, A. F., Martin, H. L., Li, M., Crouch, B. T., Carlson, D. A., … Ramanujam, N. (2017). Near-simultaneous intravital microscopy of glucose uptake and mitochondrial membrane potential, key endpoints that reflect major metabolic axes in cancer. Scientific Reports, 7(1), 13772. https://doi.org/10.1038/s41598-017-14226-x

Zips, D., Thames, H. D., & Baumann, M. (2005). New anticancer agents: in vitro and in vivo evaluation. In Vivo (Athens, Greece), 19(1), 1–7.

Zu, X., Zhang, Q., Cao, R., Liu, J., Zhong, J., Wen, G., & Cao, D. (2012). Transforming growth factor-beta signaling in tumor initiation, progression and therapy in breast cancer: an update. Cell and Tissue Research, 347(1), 73–84. https://doi.org/10.1007/s00441-011-1225-3

**SUPPLEMENTARY**

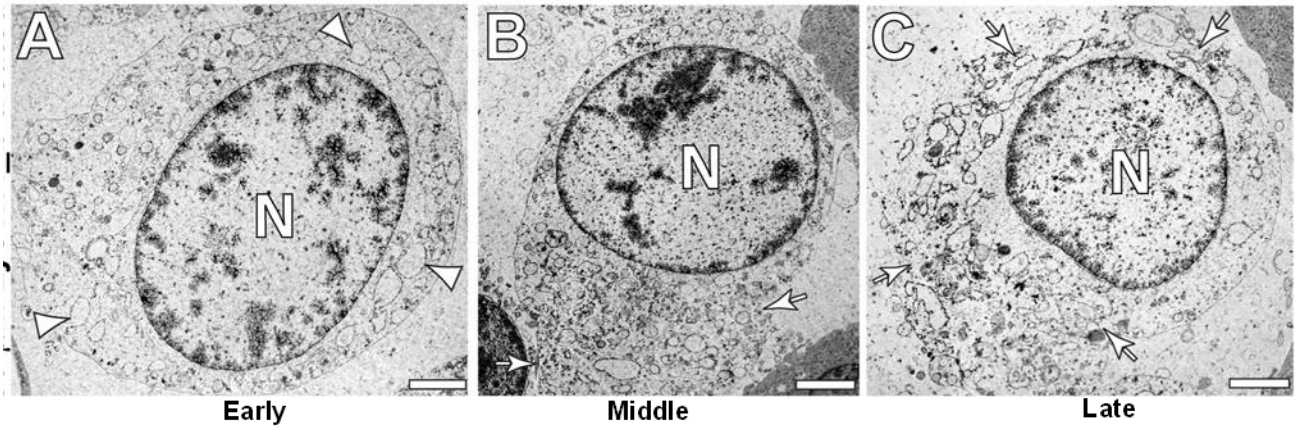


Supplementary Figure 1. Intracellular ultrastructure of the human Glioblastoma multiform (GBM) cells treated with 30 μM LyeTx I_b. (A, B, C) Cells after 30 minutes of treatment, in different stages (early, intermediate, and late) of the necroptosis process, identified by the increase in the cell volume, swelling of the nucleus and cytoplasmic organelles (arrowheads), and electron lucent nucleus and cytoplasm. Differencs in plasma membrane alterations ranging from membrane integrity maintenance (early stage) to the progressive membrane ruptures (middle to late stages) were detected. Human glioblastoma cells were cultivated and processed by high-pressure freezing (HPF) and transmission electron microscopy (TEM). A total of 80 electron micrographs showing the entire cell profile and nucleus was randomly taken and analyzed at a magnification ranging from 4,200X to 26,500X. Bars: (A) = 1 μm; (B) = 2 μm

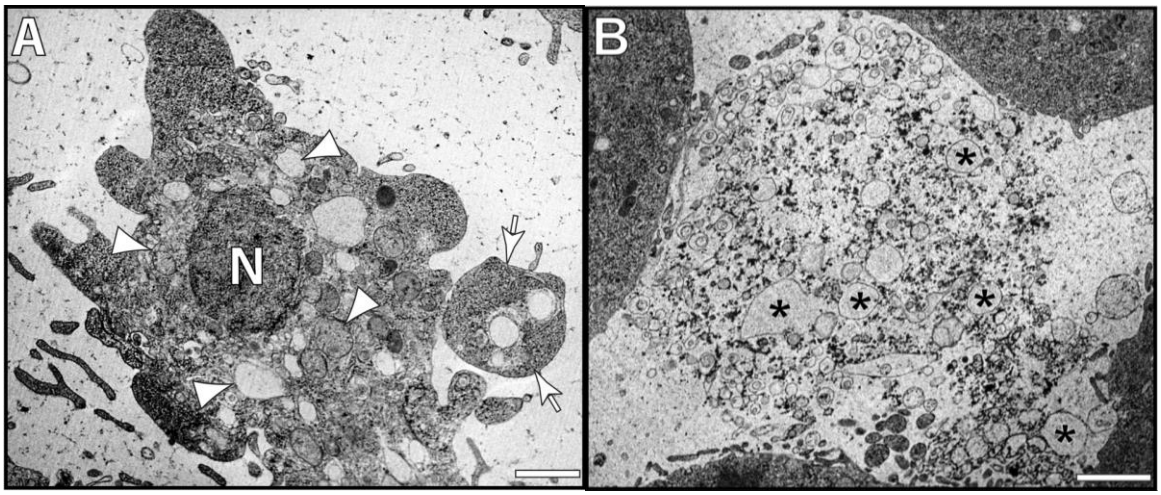


Supplementary Figure 2. Intracellular ultrastructure of human Glioblastoma multiform (GBM) cells treated with 30 μM LyeTx I_b. (A) Apoptosis was identified by the chromatin condensation levels followed by nuclear and organelle shrinkage and the formation of apoptotic bodies (B) Necrosis was best characterized by the huge plasma membrane rupture with extravasation of intracellular contents and organelles to the extracellular medium.

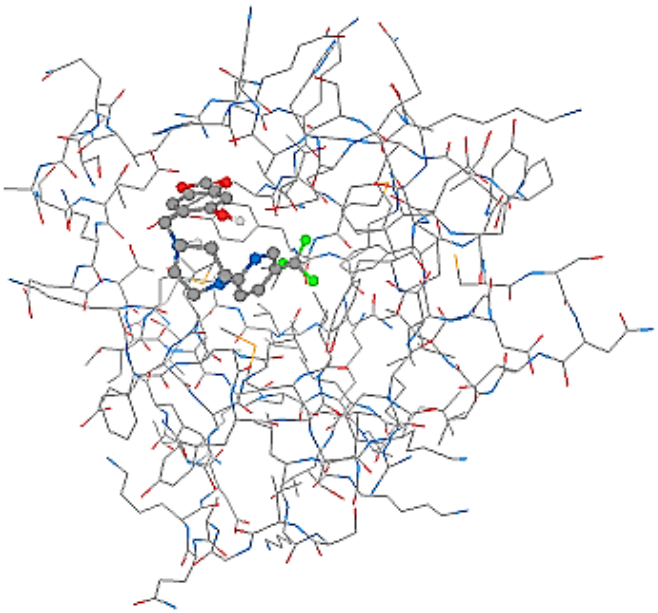

Supplementary Figure 3. MTiOpenScreen interactive results, Moleucular docking of Human RIP1 Kinase domain protein structure (PDB ID: 4ITH) in Complex with LyeTx I_b Peptide. Ligand correspond to the PubChem SID name was accepted with energy equal -8.390 and High-quality prediction, RMSD < 1.5 A .

As mentioned previously that Nec-1 was able to significantly increase cell survival, in presence of 50 µM LyeTx I-b peptide, the next step was to investigate the protein and LyeTx I-b peptide interaction, in silico. For this purpose, we used free virtual screening web server MTiOpenScreen (http://bioserv.rpbs.univ-paris-diderot.fr/services/MTiOpenScreen/). According to the protocol of protein-peptide docking, the prediction of output through using autodock vina, the results displayed ability of LyeTx I-b peptide to interact with Human RIP1 Kinase domain protein, in high quality with energy equal -8.390, and the docking performance RMSD was less than 1.5 A ° as shown in supplementary figure 5 (Labbe, C.M. et al., 2015& de Vries, S.J. et al., 2017).

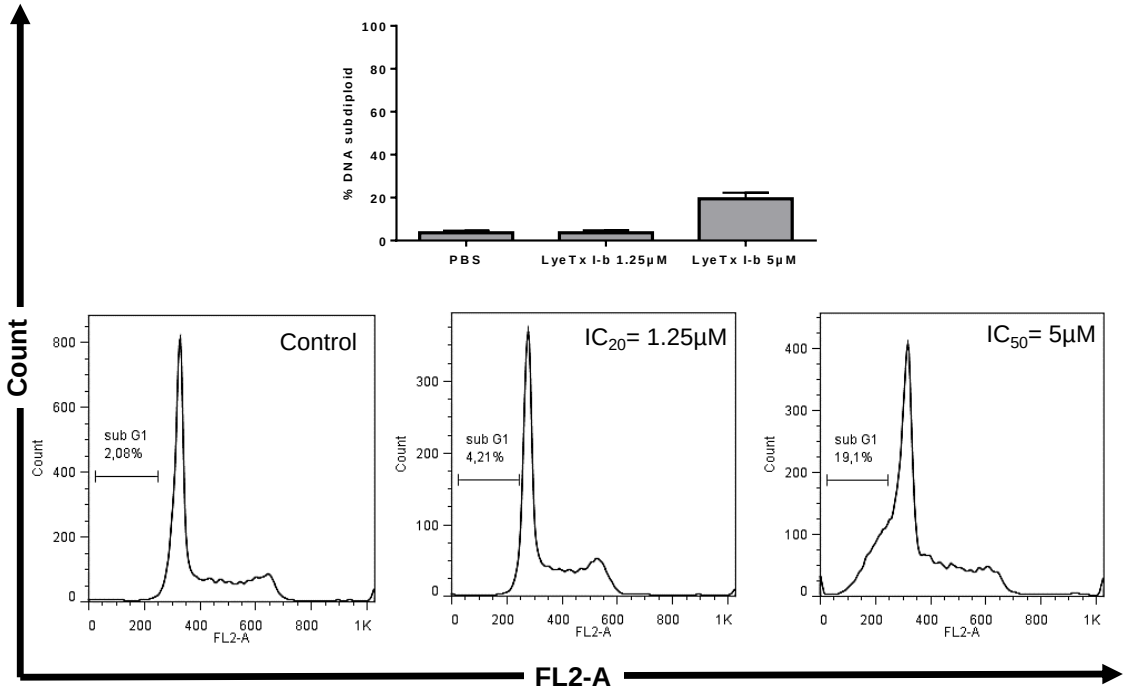


Supplementary Figure 6. Cell cycle changes after exposure MCF-7 breast adenocarcinoma cells to 1.25and 5µM LyeTx-I_b peptide. An illustrative case showing cell cycle changes 24 hours after exposure to LyeTx-I_b peptide. Two independent experiments were performed.

Approval sheet of animal ethics committee at Federal University of Minas Gerias.

UFMG

**UNIVERSIDADE FEDERAL DE MINAS GERAIS**

**CEUA**
COMISSÃO DE ÉTICA NO USO DE ANIMAIS

Prezado(a):

Esta é uma mensagem automática do sistema Solicite CEUA que indica mudança na situação de uma solicitação.

**Protocolo CEUA:** 39/2018
**Título do projeto:** Avaliação de efeitos antitumorais, anti-metastáticos e anti-inflamatórios do peptídeo LyeTx I-b em modelo de câncer murino de mama induzido por células 4T1.
**Finalidade:** Pesquisa
**Pesquisador responsável:** Juliana Carvalho Tavares
**Unidade:** Instituto de Ciencias Biologicas
**Departamento:** Departamento de Fisiologia e Biofisica

**Situação atual:** Decisão Final - Aprovado

Aprovado COM RECOMENDAÇÃO na reunião do dia 18/06/2018. Validade: 18/06/2018 à 17/06/2023 RECOMENDAÇÃO: Prezado pesquisador, o biotério onde sua pesquisa será realizada não está com cadastro e credenciamento finalizado no novo site do CIUCA/CONCEA. Solicitamos informar ao responsável pelo biotério para concluir o cadastro, porque em breve somente poderemos aprovar os que estiverem devidamente cadastrados e credenciados.
Belo Horizonte, 19/06/2018.

Atenciosamente,

Sistema Solicite CEUA UFMG
https://aplicativos.ufmg.br/solicite_ceua/

Universidade Federal de Minas Gerais
Avenida Antônio Carlos, 6627 – Campus Pampulha
Unidade Administrativa II – 2º Andar, Sala 2005
31270-901 – Belo Horizonte, MG – Brasil
Telefone: (31) 3409-4516
www.ufmg.br/bioetica/ceua - cetea@prpq.ufmg.br

Amino Acids
https://doi.org/10.1007/s00726-018-2678-4

ORIGINAL ARTICLE

# The synthetic peptide LyeTxI-b derived from Lycosa erythrognatha spider venom is cytotoxic to U-87 MG glioblastoma cells

Mostafa A. L. Abdel-Salam[1] · Juliana Carvalho-Tavares[1] · Kamila Sousa Gomes[2] · Andrea Teixeira-Carvalho[3] · Gregory T. Kitten[4,6] · Johanna Nyffeler[5] · Felipe F. Dias[6] · Pablo V. Mendes dos Reis[2] · Adriano M. C. Pimenta[2] · Marcel Leist[5] · Maria Elena de Lima[2,7] · Elaine Maria de Souza-Fagundes[1]

Received: 13 August 2018 / Accepted: 8 November 2018


## Abstract

Antimicrobial peptides present a broad spectrum of therapeutic applications, including their use as anticancer peptides. These peptides have as target microbial, normal, and cancerous cells. The oncological properties of these peptides may occur by membranolytic mechanisms or non-membranolytics. In this work, we demonstrate for the first time the cytotoxic effects of the cationic alpha-helical antimicrobial peptide LyeTx I-b on glioblastoma lineage U87-MG. The anticancer property of this peptide was associated with a membranolytic mechanism. Loss of membrane integrity occurred after incubation with the peptide for 15 min, as shown by trypan blue uptake, reduction of calcein-AM conversion, and LDH release. Morphological studies using scanning electron microscopy demonstrated disruption of the plasma membrane from cells treated with LyeTx I-b, including the formation of holes or pores. Transmission electron microscopy analyses showed swollen nuclei with mild DNA condensation, cell volume increase with an electron-lucent cytoplasm and organelle vacuolization, but without the rupture of nuclear or plasmatic membranes. Morphometric analyses revealed a high percentage of cells in necroptosis stages, followed by necrosis and apoptosis at lower levels. Necrostatin-1, a known inhibitor of necroptosis, partially protected the cells from the toxicity of the peptide in a concentration-dependent manner. Imaging flow cytometry confirmed that 59% of the cells underwent necroptosis after 3-h incubation with the peptide. It is noteworthy that LyeTx I-b showed only mild cytotoxicity against normal fibroblasts of human and monkey cell lines and low hemolytic activity in human erythrocytes. All data together point out the anticancer potential of this peptide.

**Keywords** Glioblastoma multiform · U-87 MG cells · Anticancer peptide · LyeTx I-b

## Abbreviations

| | |
|---|---|
| Cryo-EM | Cryo-electron microscopy |
| TEM | Transmission electron microscope |
| SEM | Scanning electron microscope |
| Nec-1 | Necrostatin |
| GBM | Glioblastoma multiform |

Handling Editor: G. J. Peters.

Electronic supplementary material The online version of this article (https://doi.org/10.1007/s00726-018-2678-4) contains supplementary material, which is available to authorized users.

✉ Elaine Maria de Souza-Fagundes
elainefagundes@gmail.com; elainefagundes@ufmg.br

[1] Departamento de Fisiologia e Biofísica, Instituto de Ciências Biológicas, Universidade Federal de Minas Gerais, Belo Horizonte, Brazil

[2] Departamento de Bioquimia e Imunologia, Instituto de Ciências Biológicas, Universidade Federal de Minas Gerais, Belo Horizonte, Brazil

[3] Laboratório de Biomarcadores de Diagnóstico e Monitoramento, Centro de Pesquisas René Rachou, Belo Horizonte, Brazil

[4] Departamento de Morfologia, Instituto de Ciências Biológicas, Universidade Federal de Minas Gerais, Belo Horizonte, Brazil

[5] In Vitro Toxicology and Biomedicine, Department of Biology, University of Konstanz, Konstanz, Germany

[6] Centro de Microscopia, Uniersidade Federal de Minas Gerais, Belo Horizonte, Brazil

[7] Programa de Pós-graduação em Ciências da Saúde, Biomedicina e Medicina, Instituto de Ensino e Pesquisa da Santa Casa de Belo Horizonte, Grupo Santa Casa de Belo Horizonte, Belo Horizonte, MG, Brazil